Influence of biocompatible ionic liquids on the structure and stability of proteins and organic solvents

KIRAN KUMAR PANNURU
Orcid.org 0000-0001-8757-7002

Thesis accepted in fulfilment of the requirements for the degree *Doctor of Philosophy in Chemistry* at the North-West University

Promoter: Prof Indra Bahadur

Co-promoter: Prof Eno. E. Ebenso

Graduation: April 2019

Student number: 28383753

DECLARATION

I hereby declare that the thesis entitled “Influence of Biocompatible Ionic Liquids on the Structure and Stability of Proteins and Organic Solvents” submitted to the Department of Chemistry, North-West University, Mafikeng Campus for the fulfilment of the degree of Doctor of Philosophy in Chemistry is a faithful record of original research work carried out by me under the guidance and supervision of Prof Indra Bahadur and Prof Eno. E. Ebenso. No part of this work has been submitted by any other researcher or students. Sources of my information have been properly acknowledged in the reference pages.

Signature..... Date.....

Kiran Kumar Pannuru

Signature..... Date.....

Prof Indra Bahadur

Signature..... Date.....

Prof Eno. E. Ebenso

DEDICATION

Dedicated to My Parents

ACKNOWLEDGEMENTS

I offer my obeisance to the almighty of **Lord Venkateswara** for completing my studies successfully and present this piece of work for which I am extremely indebted.

First and foremost, I wish to express my sincere and deepest gratitude to my Supervisors **Prof. Indra Bahadur** and **Prof. Eno. E. Ebenso** for their impetus, inspiring guidance and valuable suggestions throughout the course of the present work. In this span of three years apart from being supervisors they had been my well-wishers, who had inculcated in me values, discipline, critical thinking, patience and scientific abilities. They had always provided me opportunities to explore new ideas and encouraged me to work on them. I am highly honoured to have them as my guides.

This project would not have been completed without the assistance of **North-West University**, **South Africa**. I am very much grateful to the **Dean, Head of Department, Academic, Materials Science Innovation and Modelling (MaSIM) staff as well as the support staff in the Chemistry Department** for giving me the opportunity to do my doctoral studies. I sincerely and heart fully thank the Department of Chemistry of **University of Delhi** where I carried out some experimental part of this project.

I am also very thankful to, **Mr. Ronewa Phadagi, Ms. Kgomotso Masilo, Ms. Sinethemba Manquthu, Mr. Peter Mandla Mahlangu, Mr. Taiwo Quadri, Mr. Kagiso Mokalane, Dr.Varadhi Govinda, Dr. Srinivasulu, Dr. Chandrabhan Verma, Dr. Raphael, Dr. Ganesh, Dr. Sangeeta Singh, Dr. Lukman Olasunkanmi and Dr. Ajay Kumar** who assisted me and encouraged me throughout my research.

I would like to express my heartfelt gratitude to **Prof. P. Venkatesu,** Department of Chemistry, University of Delhi, India, for his valuable suggestions, for spending time to collaboration research work. I would like to thank his students **Dr. Indrani Jha, Dr. Anjeeta**

Rani, Dr. Umapathi Redicherla, Dr. Meena Bisht, Dr. Naveen Mogha, Mr. Sumith, Mr. Krishan, Ms. Payal, Ms. Kavya, Ms. Ritu and Ms. Anamika, for their valuable suggestions and help.

I would like to thank my parents for their understanding, endless love and encouragement, especially to my mother **Smt. Pannuru Lakshmi**, my father **Shri. Pannuru Ramaiah Shetty**, My loving brother **Pannuru Lokanadham (Lokesh Kumar)** for who has always stood behind me with his best support for my success. I am wholeheartedly thankful to my uncle and aunty **Pannuru Geetha Venkatesu**, who always loved me more than my parents, and also their motivation and encouragement, priceless moral support throughout my studies.

I would like to thank my beloved family members, especially to my grandfather Shri. **Pannuru Kalappa Shetty**, grandmother **Smt. Pannuru Alivelamma** my family members: **Mr. and Mrs. Manjula Kumar, Dr. Pavani, Ms. Bhavya Latha, Ms. Jaahnavi, Mr. Bhargava, Mr. Chaitanya Sai, Mr. Sonith Kumar, Mr. Shashank, Mr. Uttej, Mr. Manoj Kumar, Mr. Pavan Kumar, Mr. Neeraj Kumar and Ms Pavitra,** for their constant encouragement and patient endurance which made this venture possible.

I am thankful to my friends **Mr. Prakash, Mr. Noor Mohammad, Mr. Munaf, Mr. Abdulla, Mr. Anil and Mr. Saravana Kumar** who have been good friends over the years, for keeping me sane, giving me perspective and who have made the time more enjoyable.

ABSTRACT

In protein science, ionic liquids (ILs) have a great influence on the structure, stability, and functional groups of protein. In addition, ILs has received extensive attention in protein assays due to their novel and highly efficient reaction medium as well as also active participants in different biological processes. The present thesis explains the role of ILs (particularly imidazolium and cholinium based) on the protein folding/unfolding studies.

Therefore, in this work, it has been explored the structure, stability and activity of stem bromelain (BM) in the presence of different ILs such as imidazolium and choline-based, namely: 1-butyl-3-methylimidazolium chloride ([Bmim][Cl]), 1-butyl-3-methylimidazolium bromide ([Bmim][Br]), 1-butyl-3-methylimidazolium iodide ([Bmim][I]), 1-butyl-3-methylimidazolium hydrogen sulphate ([Bmim][HSO_4]), 1-butyl-3-methylimidazolium acetate ([Bmim][CH_3COO]), 1-butyl-3-methylimidazolium nitrate ([Bmim][NO_3]), choline chloride ([Ch][Cl]), choline acetate ([Ch][Ac]), choline dihydrogen phosphate ([Ch][Dhp]), choline bitartrate ([Ch][Bit]), choline iodide ([Ch][I]) and choline hydroxide ([Ch][OH]) by using various spectroscopic and dynamic light scattering (DLS) measurement techniques. All of these imidazolium based ILs acted as destabilizer for the native structure of BM except concentrations of (such as 0.01 and 0.05 M). Evidently, the stability of series of Hofmeister ions are found to be in the trend of HSO_4^- > CH_3COO^- > NO_3^- > Cl^- > Br^- > I^-. In the case of choline based ILs the ([Ch][Cl]) is the best stabilizer, whereas ([Ch][OH]) is the strongest destabilizer among all studied ILs for BM structure. The overall stability order of BM in the presence of choline based ILs follow the trend: [Cl] > [Ac] > [Dhp] > [I]) > [Bit] > [OH]. Finally, it has been concluded that the stability of protiens is dependent on the nature of the ILs and their concentrations.

In addition to above, the thermophysical properties such as density (ρ), sound velocity (u), viscosity (η) and refractive indice (n_D) of binary mixtures of ammonium based ILs, namely tetrapropylammonium hydroxide (TPAOH), tetraethylammonium hydroxide (TEAOH) and tetrabutylammonium hydroxide (TBAOH) with N,N-dimethylacetamide (DMA) over the whole range of composition at different temperatures from 25 to 40 ^{0}C under atmospheric pressure have been also reported. The derived properties such as deviation in isentropic compressibilities ($\Delta\kappa_s$), excess molar volumes (V^E), deviation in viscosities ($\Delta\eta$) and deviation in refractive indices (Δn_D) were calculated from experimental values and correlated by Redlich-Kister polynomial type equations. It has been observed the strength of intermolecular interactions such as ion-ion pair interactions, hydrogen bonding and induced dipole interactions between the ions of ammonium-based ILs with DMA.

Futhermore, the solute-solvent interactions of binary mixtures containing 1-methyl-1-propyl pyrrolidinium tetrafluoroborate ([MPpyr][BF_4]) with water, alcohols (methanol and ethanol) at various temperatures from 25 to 40 ^{0}C under atmospheric pressure have been also studied. Derived properties such as apparent molar volume (V_φ), limiting apparent molar volumes (V_φ^0), the limiting apparent molar expansibility (E_φ^0), and thermal expansion coefficients (α_P) were evaluated from experimental density data. The parameters correlated using to the Redlich–Mayer type equation. The obtained results were discussed in terms of the effect of temperature as well as concentration on specific solute-solvent interactions that prevail in the presence of IL solution.

CONTENT

Declaration i

Dedication ii

Acknowledgments iii

Abstract v

Contents vii

List of Tables xiii

List of Figures xv

List of symbols xxii

List of abbreviations xxvi

CHAPTER 1: INTRODUCTION 1

1.1 History of ionic liquid 2

1.1.1 Classification of ILs based on their relevant physical properties 3

1.1.2 The potential application of ionic liquids 5

1.2. Introduction to proteins 6

1.2.1 Protein structural arrangements 7

1.2.2 Classification of protein structures 9

1.2.2.1 Primary structure 9

1.2.2.2 Secondary structure 10

1.2.2.3 Tertiary structure 11

1.2.2.4. Quaternary structure 13

1.3 Protein folding and unfolding 14

1.4 Effect of co-solvents on the protein structure and stability 16

1.5 The importance of thermophysical and thermodynamic properties 18

1.6 Scope of the present study 23

1.6.1 The study of protein folding/unfolding in the presence of Different ILs 23

1.6.2 Excess/apparent properties binary mixtures 24

1.7 Research aim and objectives 24

1.8 Outline of the thesis 26

CHAPTER 2: LITERATURE REVIEW 27

2.1 Structure and stability of proteins/enzymes in the presence of various ionic liquids 28

2.1.1 The influence of imidazolium-based ionic liquids on the stability and activity of various proteins 30

2.1.2 The conformation structure and stability of various proteins in the presence of Choline based ionic liquids 41

2.1.3 The conformation structure and stability of proteins in the presence of some other ILs 45

2.1.4 The protein stability in Hofmeister series of ionic liquids 48

2.2 A review of the thermophysical properties of binary mixtures 51

2.2.1 Excess molar properties 51

2.2.2 Apparent molar properties 61

CHAPTER 3: EXPERIMENTAL METHODS & THEORETICAL FRAME WORK 68

3.1 Materials and Sample preparation 69

3.1.1 Materials 69

3.1.2 Structure of stem bromelain (BM) used in the present work 71

3.2 Sample preparation 72

3.3 Experimental methods 73

3.3.1 Spectroscopic techniques 73

3.3.1.1 UV-visible spectroscopy 73

3.3.1.2 Enzymatic activity of bromelain protein 75

3.3.1.3 Fluorescence spectroscopy 75

3.3.1.3.1 Thermodynamics analysis of protein unfolding using Fluorescence spectroscopy 78

3.3.1.4 Circular dichroism (CD) spectroscopy 81

3.3.1.4.1 Analysis of the secondary structure of a protein using CD 82

3.3.1.4.2 Analysis of the tertiary structure of a protein using CD 83

3.3.1.5 Dynamic light scattering (DLS) 85

3.3.2 Measurement of excess molar volumes and apparent molar volumes 87

3.3.2.1 The vibrating tube densitomer (Anton paar DMA 4500 M) 87

3.3.2.2 Ultrasonic interferometer 88

3.3.2.3 Viscosity measurement 90

3.3.2.4 Refractive Index Measurement 91

3.4 Theoretical study of thermophysical properties 91

3.4.1 Density (ρ) 91

3.4.2 Excess and apparent molar volumes (V^E and V_φ) 92

3.4.3 Sound velocity (u) 93

3.4.4 Deviation in Isentropic Compressibilities ($\Delta\kappa_s$) 94

3.4.5 Viscosity (η) 94

3.4.6 Deviation in viscosity ($\Delta\eta$) 96

3.4.7 Refractive index (n_D) 96

3.4.8 Refractive index deviation (Δ_{nD}) 97

CHAPTER 4:RESULTS & DISCUSSION 98

4.1 Investigation of structure and stability of bromelain (BM) in the presence of [Bmim][Cl], [Bmim][Br] and [Bmim][I] using spectroscopic studies 99

4.2 Influence of imidazolium-based ionic liquids on the structure and stability of stem bromelain (BM) 99

4.2.1 Absorption spectroscopy of BM in Imidazolium-Based ILs 99

4.2.2. Analysis of BM structure and stability with the aid of fluorescence spectroscopy 101

4.2.3. Thermal stability of BM in ILS 103

4.2.4. Changes in the secondary structure of BM in the presence of imidazolium-based ILs 105

4.2.5 Changes in the tertiary structure of BM in the presence of imidazolium-based ILs 107

4.2.6 Exploration of hydrodynamic diameter of BM in the presence of imidazolium-based ILs 108

4.3 Influence of choline-based ionic liquids on the structure, stability and activity of stem bromelain (BM) 114

4.3.1 Absorption spectroscopy analysis for BM in choline-based ILs 115

4.3.2 Analysis of steady-state fluorescence of BM in choline-based ILs 117

4.3.3 Thermal stabilization of BM in presence of choline-based ILs 118

4.3.4 CD spectral analysis for BM in presence of choline-based ILs 120

4.3.5 Influence of choline-based ILs on the hydrodynamic diameter (d_H) of BM by by dynamic light scattering (DLS) measurements 123

4.3.6 Evaluation of activity of BM in the presence of choline-based ILs 125

4.4 Studies on thermodynamic properties of binary mixtures of ammonium based ionic liquids containing different anions with N,N-dimethylacetamide (DMA) 128

4.5 Studies on apparent molar properties of binary mixtures of 1-methyl-1-propylpyrrolidinium tetrafluoroborate ([MPpyr][BF_4]) with water and alcohols 129

4.5.1. Density values for binary mixtures 129

4.5.2 Apparent molar volumes 132

CHAPTER 5: CONCLUSION 138

REFERENCES 143

APPENDIX I 184

List of publications 184

APPENDIX II 186

Suplementary figures and tables for 4.1 186

APPENDIX III 193

Suplementary figures and tables for 4.4 193

LIST OF TABLES

Table 2.1 The influence of various ILs on the stability and activity of proteins.

Table 2.2 Summary of the binary systems from literature is given below.

Table 3.1 A division into groups of chemical compounds: Ionic liquids, proteins, solvents.

Table 4.1A Transition temperature (T_m) of the BM in different concentrations of ILs.

Table 4.2A Hydrodynamic diameter (d_H) of BM in different concentrations of ILs.

Table 4.3 Transition temperatures (T_m) of the BM in the presence of different concentrations of ILs.

Table 4.4 Hydrodynamic diameter (d_H) of BM in different concentrations of ILs.

Table 4.5 The T_m values of BM in the presence of PBS and various concentrations of ILs.

Table 4.6 Hydrodynamic diameter (d_H) of BM in buffer and various concentrations of choline based ILs.

Table 4.7A Molecular mass (MW), solvent purity, density (ρ), speed of sound (u), viscosity (η) and refractive index (nD) for ammonium-based ILs and DMA at T = 30 °C.

Table 4.8A Mole fraction (x_1) of ILs, Density (ρ), Ultrasonic Sound Velocity (u), Viscosity (η), Refractive Index (n_D), Excess Molar Volumes (V^E), Isentropic Compressibility(κ_s), Deviation in Isentropic Compressibility ($\Delta\kappa_s$), Deviation in Viscosity ($\Delta\eta$) and Deviation in Refractive Index (Δn_D) for TEAH, TPAH and TBAH with DMA system at different temperatures.

Table 4.9A Estimated Parameters of Redlich-Kister equation and standard deviation, (σ) for the systems of ammonium-based ILs with DMA at different temperatures.

Table 4.10 Molality (m), densities (ρ) and apparent molar volumes (V_φ) for ([MPpyr][BF_4] + water or methanol or ethanol) at 25, 30, 35 and 40 °C.

Table 4.11 Limiting apparent molar volumes (V_φ^0), and fitting parameters (S_V and B_V) and standard deviation (σ), of IL (solute) in water or Methanol or Ethanol (solvent) at 25, 30, 35 and 40 °C.

Table 4.12 The limiting apparent molar expansibility (E_φ^0) and isobaric thermal expansion Coefficients (α_p).

LIST OF FIGURES

Figure 1.1 Various cation and anion used for the preparation of ILs.

Figure 1.2 Numerous applications of ILs in different scientific fields.

Figure 1.3 Schematic diagram of amino acid.

Figure 1.4 A sequence of AAs in a primary structure of the protein.

Figure 1.5 (a) α-helix and (b) β-sheet structures in a protein. The hydrogen bonds between the AA residues are presented by dashed yellow lines.

Figure 1.6 Tertiary structure of a protein with ionic, H-bond, disulfide bond and polypeptide backbone.

Figure 1.7 Quaternary structure of protein with polypeptide chains.

Figure 1.8 Schematic representation of unfolded state of protein structure in the presence of some physiological stress.

Figure 1.9 Classification of thermophysical and thermodynamic properties.

Figure 2.1 The stability of a protein in presence of co-solvents.

Figure 2.2 A number of publications regarding protein stability in ILs as a function of the year based on our own literature survey up to June 2018.

Figure 2.3 The stability order of anions of Hofmeister series.

Figure 3.1 A division into groups of chemical compounds: Ionic liquids, proteins, solvents.

Figure 3.2 Schematic representation of the structure of BM.

Figure 3.3 The possible electronic transitions in UV-vis spectroscopy.

Figure 3.4 UV-visible spectrophotometer.

Figure 3.5 Schematic representation of a Jablonski diagram (energy diagram) representing fluorescence mechanism.

Figure 3.6 Varian cary eclipse fluorescence spectrophotometer.

Figure 3.7 Schematic representation of two-state unfolding transitions in a protein as a function of temperature.

Figure 3.8 The analysis of α-helix, β-sheet and random coil using CD spectroscopy.

Figure 3.9 Circular dichroism (CD).

Figure 3.10 Dynamic light scattering (DLS).

Figure 3.11 Anton-Paar densitometer 4500 M.

Figure 3.12 Mittal-ultrasonic Interferometer model F-05.

Figure 3.13 Diagram of interferometer cell.

Figure 3.14 Sine-wave vibro viscometer.

Figure 3.15 Illustration of abbe digital refractometer.

Figure 4.1A UV–vis spectra analysis of BM in buffer (black) and in (a) [Bmim][Cl] with red (0.01M), green (0.05M), blue (0.10 M), cyan (0.50 M), magenta (1.0M), yellow (1.5 M) at 25 ^{o}C (b) [Bmim][Br] with red (0.01 M), green (0.05 M), blue (0.10 M), cyan (0.50 M), magenta (1.0 M), yellow (1.5 M) and (c) [Bmim][I] with red (0.01 M), green (0.05 M), blue (0.10 M), cyan (0.50 M), magenta (1.0 M), yellow (1.5 M) at 25 ^{o}C.

Figure 4.2A Fluorescence spectra analysis of BM in buffer (black) and in (a) [Bmim][Cl] with red (0.01 M), green (0.05 M), blue (0.10M), cyan (0.50M),magenta (1.0

M), yellow(1.5 M) at 25 ^{o}C (b) [Bmim][Br]with red (0.01M), green (0.05M), blue (0.10 M), cyan (0.50 M), magenta (1.0 M), yellow (1.5 M) and (c) [Bmim][I] with red (0.01 M), green (0.05 M), blue (0.10 M), cyan (0.50 M), magenta (1.0 M), yellow (1.5 M) at 25 ^{o}C.

Figure 4.3A The variation in T_m values of BM in buffer (black) with [Bmim][Cl] (red),[Bmim][Br] (green) and [Bmim][I] (blue)which is obtained from fluorescence analysis.

Figure 4.4A Influence of [Bmim][Cl], [Bmim][Br] and [Bmim][I]on the structure of BM in buffer (black), from far-UV CD analysis with red (0.01 M), green (0.05 M), blue (0.10 M), cyan (0.50 M), magenta (1.0 M), yellow (1.5 M) at 25 ^{o}C.

Figure 4.5A Influence of [Bmim][Cl], [Bmim][Br] and [Bmim][I]on the structure of BM in buffer (black), from near-UV CD analysis with red (0.01M), green(0.05 M), blue (0.10 M), cyan (0.50 M), magenta (1.0 M), yellow (1.5 M) at 25 ^{o}C.

Figure 4.6A Hydrodynamic diameter (d_H) obtained from the intensity distribution graph for BM in buffer with [Bmim][Cl] (red), [Bmim][Br] (green) and [Bmim][I] (blue) at different concentrations.

Figure 4.7 UV-vis spectra analysis of BM in buffer (black) and in (a) [Bmim][HSO_4] with 0.01 M (red), 0.05 M (green), 0.10 M (blue), 0.50 M (cyan), 1.0 M (magenta), 1.5 M (yellow) at 25 ^{o}C (b) [Bmim][CH_3COO] with 0.01 M (red), 0.05 M (green), 0.10 M (blue), 0.50 M (cyan), 1.0 M (magenta), 1.5 M (yellow) at 25 ^{o}C and (c) [Bmim][NO_3] with 0.01 M (red), 0.05 M (green), 0.10 M (blue), 0.50 M (cyan), 1.0 M (magenta), 1.5 M (yellow) at 25 ^{o}C.

Figure 4.8 Fluorescence spectra analysis of BM in buffer (black) and in (a) [Bmim] [HSO_4] with red 0.01 M (red), 0.05 M (green), 0.10 M (blue), 0.50 M

(cyan), 1.0 M (magenta), 1.5 M (yellow) at 25 ^{o}C (b) [Bmim][CH_3COO] with 0.01 M (red), 0.05 M (green), 0.10 M (blue), 0.50 M (cyan), 1.0 M (magenta), 1.5 M (yellow) at 25 ^{o}C and (c) [Bmim][NO_3] with red 0.01 M (red), 0.05 M (green), 0.10 M (blue), 0.50 M (cyan), 1.0 M (magenta), 1.5 M (yellow) at 25 ^{o}C.

Figure 4.9 The variation in T_m values of BM in buffer (black) with red ([Bmim][HSO_4]), green ([Bmim][CH_3COO]) and blue ([Bmim][NO_3]) which is obtained from fluorescence analysis.

Figure 4.10 Influence of (a) [Bmim][HSO_4], (b) [Bmim][CH_3COO] and (c) [Bmim][NO_3] on the structure of BM in buffer (black), from far-UV CD analysis with 0.01 M (red), 0.05 M (green), 0.10 M (blue), 0.50 M (cyan), 1.0 M (magenta), 1.5 M (yellow) at 25 ^{o}C.

Figure 4.11 Influence of (a) [Bmim][HSO_4], (b) [Bmim][CH_3COO] and (c) [Bmim][NO_3] on the structure of BM in buffer (black), from near-UV CD analysis with 0.01 M (red), 0.05 M (green), 0.10 M (blue), 0.50 M (cyan), 1.0 M (magenta), 1.5 M (yellow) at 25 ^{o}C.

Figure 4.12 Hydrodynamic diameter (d_H) obtained from the intensity distribution graph for BM in buffer with red ([Bmim][HSO_4]), green ([Bmim][CH_3COO]) and blue ([Bmim][NO_3]) at different concentrations.

Figure 4.13 UV-visible absorption spectra of BM at 25 ^{o}C in PBS and varying concentrations of ILs.

Figure 4.14 Fluorescence spectra of BM at 25 ^{o}C in the presence of PBS and varying concentrations of ILs.

Figure 4.15 The variation in Tm values of BM in the presence of PBS and varying concentrations of ILs.

Figure 4.16 UV CD (Far) spectra of BM at 25 ^{o}C in the presence of PBS and varying concentrations of ILs.

Figure 4.17 Hydrodynamic diameter (d_H) of BM in the presence of PBS and various concentration of ILs.

Figure 4.18 Relative proteolytic activity measurements of BM in PBS and in presence of ILs at 25 ^{o}C.

Figure 4.19A Plots of densities (ρ) for the mixtures of ILs with DMA vs. mole fraction (x_1) of IL for (a) TEAH (b) TPAH or (c) TBAH + DMA (x_2) at different temperatures, 25 ^{o}C (□), 30 ^{o}C (○), 35 ^{o}C (△) and 40 ^{o}C (■).The solid lines represent the smoothness of the data.

Figure 4.20A Plots of ultrasonic sound velocities (u) for the mixtures of ILs with DMA vs. mole fraction (x_1) of IL for (a) TEAH (b) TPAH or (c) TBAH + DMA (x_2) at different temperatures, 25 ^{o}C (□), 30 ^{o}C (○), 35 ^{o}C (△) and 40 ^{o}C (■).The solid lines represent the smoothness of the data.

Figure 4.21A Plots of viscosities (η) for the mixtures of ILs with DMA vs. mole fraction (x_1) of IL for (a) TEAH (b) TPAH or (c) TBAH + DMA (x_2) at different temperatures, 25 ^{o}C (□), 30 ^{o}C (○), 35 ^{o}C (△) and 40 ^{o}C (■). The solid lines represent the smoothness of the data.

Figure 4.22A Plots of refractive indices (n_D) for the mixtures of ILs with DMA vs. mole fraction (x_1) of IL for (a) TEAH (b) TPAH or (c) TBAH + DMA (x_2) at

different temperatures, 25 ^{o}C (□), 30 ^{o}C (○), 35 ^{o}C (△) and 40 ^{o}C (■).The solid lines represent the smoothness of the data.

Figure 4.23A Plots of (a) densities (ρ) (b) ultrasonic sound velocities (u) (c) viscosities (η) (d) refractive indices (n_D) for the mixtures of ILs + DMA as function of the mole fraction (x_1) of IL; (□) TEAH; (○) TPAH and (Δ) TBAH at 25 ^{o}C. The solid lines represent the smoothness of the data.

Figure 4.24A Plots of excess molar volumes (V^E) for the mixtures of ILs with DMA vs. mole fraction (x_1) of IL for (a) TEAH (b) TPAH or (c) TBAH + DMA (x_2) at different temperatures, 25 ^{o}C (□), 30 ^{o}C (○), 35 ^{o}C (△) and 40 ^{o}C (■).The solid (–) lines correlated by Redlich–Kister equation.

Figure 4.25A Plots of deviation in isentropic compressibilities ($\Delta\kappa_s$) for the mixtures of ILs with DMA vs. mole fraction (x_1) of IL for (a) TEAH (b) TPAH or (c) TBAH + DMA (x_2) at different temperatures, 25 ^{o}C (□), 30 ^{o}C (○), 35 ^{o}C (△) and 40 ^{o}C (■). The solid (–) lines correlated by Redlich-Kister equation.

Figure 4.26A Plots of deviation in viscosities ($\Delta\eta$) for the mixtures of ILs with DMA vs. mole fraction (x_1) of IL for (a) TEAH (b) TPAH or (c) TBAH + DMA (x_2) at different temperatures, 25 ^{o}C (□), 30 ^{o}C (○), 35 ^{o}C (△) and 40 ^{o}C (■).The solid (–) lines correlated by Redlich-Kister equation.

Figure 4.27A Plots of deviation in refractive indices (Δn_D) for the mixtures of ILs with DMA vs. mole fraction (x_1) of IL for (a) TEAH (b) TPAH or (c) TBAH + DMA (x_2) at different temperatures, 25 ^{o}C (□), 30 ^{o}C (○), 35 ^{o}C (△) and 40 ^{o}C (■).The solid (–) lines correlated by Redlich–Kister equation.

Figure 4.28A Plots of (a) excess molar volumes (V^E) (b) deviations in isentropic compressibilities ($\Delta\kappa_s$) (c) deviations in viscosities ($\Delta\eta$) (d) deviations in refractive indices (Δn_D) for the mixtures of ILs + DMA as function of the mole fraction (x_1) of IL; (□) TEAH; (○) TPAH and (Δ) TBAH at 25 ^oC. The solid (–) lines correlated by Redlich-Kister equation.

Figure 4.29 Density (ρ), for the mixtures of (a) IL + Water, (b) IL + Methanol and (c) IL + Ethanol at 25 ^oC (■),30 ^oC (◆), 35 ^oC (▲) and 40 ^oC (▼).

Figure 4.30 Apparent molar volume (V_φ) for the mixtures of (a) IL + Water, (b) IL + Methanol and (c) IL + Ethanol at 25 ^oC (■),30 ^oC (◆), 35 ^oC (▲) and 40 ^oC (▼).

List of symbols

ρ	Density
u	Ultrasonic sound velocity
η	Viscosity
n_D	Refractive indices
V^E	Excess molar volumes
$\Delta\kappa s$	Deviation in isentropic compressibilities
$\Delta\eta$	Deviation in viscosities
Δn_D	Deviation in refractive indices
κ_s	Isentropic compressibility of mixture
V_φ	Apparent molar volume
V_φ^0	Limiting apparent molar volumes
E_φ^0	Limiting apparent molar expansibility
α_P	Thermal expansion coefficients
S_v	Empirical parameter for apparent molar volume
B_v	Empirical parameter for apparent molar volume
S_k	Empirical parameter for apparent adiabatic compressibility
B_k	Empirical parameter for apparent adiabatic compressibility

m	Molality
M	Molar mass
T_{m}	Transition temperature
ΔG	Free energy change
ΔH	Enthalpy changes
ΔC_p	Heat capacity changes
Y_f	Pre-transition region
Y	Transition region
$\mathrm{Y_u}$	Post-transition region
f_u	Fraction of unfolded protein
Y_f	Measured intensity of the folded state
Y_u	Measured intensity of the unfolded state
ΔG_u	Free energy change of unfolding
ΔS_u	Entropy change of unfolding
ΔH_u	Enthalpy change of unfolding
θ	Ellipticity in degrees
L	Optical path length
M	Molecular weight
N	Number of residues in the protein
C	Concentration

d_H	Hydrodynamic diameter
D	Translational diffusion coefficient
K	Boltzmann's constant
x_1	Mole fraction of the 1st component
x_2	Mole fraction of the 2nd component
M_1	Molar mass of ionic liquid
M_2	Molar mass of solvent
ρ_{mix}	Density of the mixture
K	Equilibrium constant
R	Gas constant
λ	Wavelength
f	Frequency
T_K	Absolute Temperature
K	Kelvin
V	Total volume of assay
ν_1	Volume of enzyme
ν_2	Volume of sample
I_{max}	Fluorescence intensities
λ_{max}	Emission wavelength
T	Temperature

n	Number of experimental point
K	Number of coefficients used in the Redlich–Kister equation

List of Abbreviations

ILs	Ionic liquids
FTIR	Fourier transform infrared spectroscopy.
DLS	Dynamic light scattering
UV-Vis	Ultraviolet visible spectra
CDS	Circular dichroism spectroscopy
VOCs	Volatile organic compounds
RTILs	Room temperature ionic liquids
PILs	Protic ionic liquids
AAs	Amino acids
PBS	Phosphate buffer solution
FDA	Food and drug administration
H_2O	Water
CH_3OH	Methanol
C_2H_5OH	Ethanol
MEA	Monoethanolamine
BM	Bromelain
Cyt C	Cytochrome C
Lyz	Lysozyme
CT	α-Chymotrypsin

HAS	Human serum albumin
BSA	Bovine serum albumin
Mb	Myoglobin
Hb	Haemoglobin
RHIL-2	Recombinant human interleukin-2
DNA	Deoxyribonucleic acid
RNA	Ribo Nucleic acid
Ty	Tyrosinase
PPL	Photinus pyralisluciferase
ADH	Alcohol dehydrogenase

Ionic Liquids Abbreviations

DMA	N,N-dimethylacetamide
DMF	N,N-dimethylformamide
DMSO	Dimethyl sulfoxide
DCM	Dichloromethane
DEOAN	Diethanolammonium nitrate
DEAA	Diethyl ammonium acetate
DEAF	Diethyl ammonium formate
DEAB	Diethyl ammonium butanoate

DEAP	Diethyl ammonium propionate
DEAS	Diethyl ammonium hydrogen sulphate
DMEG	N,N-dimethylethanolammonium glycolate
DEEAP	Diethylethanolammonium propionate
EA	Ethyl acetate
EAN	Ethyl ammonium nitrate
EAF	Ethyl ammonium formate
EAMs	Ethyl ammonium methanesulfonate
EAA	Ethyl ammonium acetate
EAP	Ethyl ammonium pivalate
EATfA	Ethylammoniumtrifluoroacetate
EOAN	Ethanolammonium nitrate
EAPP	Ethyl ammonium propionate
EPEP	Ethyl phosphonium diethyl phosphate
MOEAF	2-Methoxyethylammoniumformate
NMP	N-methyl-2-pyrrolidone
[BHEAA]	Bis (2-hydroxyethyl) ammonium acetate
[BDMAH]	Benzyldimethylammonium hexanoate
[BDMAP]	Benzyldimethylammonium propionate
[BDMAA]	Benzyldimethylammonium acetate

[BMAH]	Benzylmethylammonium hexanoate
[BMAP]	Benzylmethylammonium propionate
[OHEAA]	2- Hydroxyl ethyl ammonium acetate
[OHEAP]	2-Hydroxy ethyl ammonium pentanoate
[OHEAB]	2-Hydroxy ethylammonium butanoate
[OHDEAH]	2-Hydroxy diethyl ammonium hexanoate
[OHEAH]	2-Hydroxy ethyl ammonium hexanoate
[N_4BAO]	N-butyl ammonium oleate
[N_4NO_3]	N-butyl ammonium nitrate
[N_4 Ac]	N-butyl ammonium acetate
[N_4Ac]	N-butylammonium acetate
[N_4Pro]	N-butyl ammonium propanoate
[N_4Hex]	N-butyl ammonium hexanoate
[N_4Dec]	N-butylammonium decanoate
PAF	Propyl ammonium formate
TEAOH	Tetraethyl ammonium hydroxide
TPAOH	Tetra propyl ammonium hydroxide
TBAOH	Tetra butyl ammonium hydroxide
TMAOH	Tetramethylammonium hydroxide
TEAP	Triethylammonium phosphate

TEAAc	Triethylammonium acetate
TEAS	Triethylammonium hydrogen sulphate
TMAS	Trimethylammonium hydrogen sulfate
TMAAc	Trimethylammonium acetate
TMAP	Trimethylammonium dihydrogen phosphate
TBPMS	Tributyl methyl phosphonium methyl sulfate
TEOAN	Triethanolammoniumnitrate
[Amim][Cl]	1-Allyl-3- methylimidazolium chloride
[APy][Cl]	N-alkyl pyridinium chlorides
[Bmim][Cl]	1-Butyl-3-methylimidazolium chloride
[Bmim][Br]	1-Butyl-3-methylimidazolium bromide
[Bmim][I]	1-Butyl-3-methylimidazolium iodide
[Bmim][HSO_4]	1-Butyl-3-methylimidazolium hydrogen sulphate
[Bmim][Ac]	1-Butyl-3-methylimidazolium acetate
[Bmim][NO_3]	1-Butyl-3-methylimidazolium nitrate
[Bmim][SCN]	1-Butyl-3-methyl imidazolium thiocyanate
[Bmim][BF_4]	1-Butyl-3-methylimidazolium tetra fluoroborate
[Bmim][PF_6]	1-Butyl-3-methylimidazolium hexafluorophosphate
[Bmim][Gly]	1-Butyl-3-methylimidazolium glycine
[Bmim][I]	1,3-Dimethylimidazolium iodine

[Bmim][OS]	1-Butyl-3-methylimidazolium octyl sulfate
[Bmim][DHP]	1-Butyl-3-methylimidazolium dihydrogen phosphate
[Bmim][$MeSO_3$]	1-Butyl-3-methylimidazolium methane sulfonate
[Bmim][lac]	1-Butyl-3-methylimidazolium lactate
[BHEA][A]	N-butyl-2-hydroxyethyl ammonium acetate
[BHEA][For]	N-butyl-2-hydroxyethyl ammonium formate
[BZmim][Cl]	1-Benzyl-3-methylimidazolium chloride
[BZmim][BF_4]	1-Benzyl-3-methylimidazolium tetra fluoroborate
[BPy][Cl]	Butylpyridinium chloride
[BMPY][Cl]	1-Butyl-4-methylpyridinium chloride
[BMPYR][Cl]	1-Butyl-1-methylpyrrolidinium chloride
[BMPYR][TF]	1-Butyl- 1- methylpyrrolidinium trifluoromethanesulfonate
[BPYM][BF_4]	1-Butylpyridinium tetra fluoroborate
[BMPYR][Br]	N-butyl-N-methyl-2-oxopyrrolidinium bromide
[Bmim][OTf]	1-Butyl-3-methylimidazolium trifluoromethanesulfonate
[Bmim][$FeCl_4$]	1-Butyl-3-methylimidazolium tetrachloroferrate
[Bmim][NTf_2]	1-Butyl-3-methylimidazoliumbis (trifluoromethylsulfonyl)imide
[Ch][Cl]	Choline chloride
[Ch][Ac]	Choline acetate
[Ch][Dhp]	Choline dihydrogen phosphate

[Ch][Bit]	Choline bitartrate
[Ch][I]	Choline iodide
[Ch][OH]	Choline hydroxide
[Ch][Dhc]	Choline dihydrogen citrate
[Ch][TMA]	Choline trimethylacetate
[Ch][Prop]	Choline propionate
[Ch][Hex]	Choline hexanoate
[Ch][Lac]	Choline lactate
[Ch][DMP]	Choline dimethyl phosphate
[Ch][TFMS]	Choline trifluoromethane sulfonate
[Ch][TF_2N]	Choline bis(trifluoromethylsulfonyl)amide
[Ch][Glu]	Choline glutarate
[Ch][C_1SO_3]	Choline methane sulfonate
[C_{14}mim][Br]	1-Tetradecyl-3-methylimidazolium bromide
[DMP][I]	N, N-dimethyl-2-oxopyrrolidinium iodide
[Dmim][Cl]	1-Decyl-3-methylimidazolium chloride
[DBmim][Cl]	Dibutylimidazolium chloride
[DMSCA][Tos]	N, N-dimethyl-N-(3-sulfopropyl) cyclohexylammonium tosylate
[Emim][Cl]	1-Ethyl-3-methylimidazolium chloride

[Emim][Br]	1-Ethyl-3-methyl-imidazolium bromide
[Emim][BF_4]	1-Ethyl-3-methylimidazolium tetra fluoroborate
[Emim][$EtSO_4$]	1-Ethyl-3-methylimidazolium ethylsulfate
[Emim][FSI]	1-Ethyl-3-methylimidazolium bis(fluorosulfonyl)imide
[Emim][PF_6]	1-Ethyl-3-methylimidazolium hexafluorophosphate
[Emim][NO_3]	1-Ethyl-3-methyl imidazolium nitrate
[Emim][DMP]	1-Ethyl-3-methylimidazolium dimethyl phosphate
[Emim][SCN]	1-Ethyl-3-methyl imidazolium thiocyanate
[Emim][DCA]	1-Ethyl-3-methyl imidazolium dicyanamide
[Emim][$MeSO_3$]	1-Ethyl-3-methylimidazolium methanesulfonate
[Emim][$MeSO_4$]	1-Ethyl-3-methylimidazolium methyl sulfate
[Emim][TFMS]	1-Ethyl-3-methylimidazolium trifluoromethane sulfonate
[EMPY][I]	1-Ethyl-1-methyl pyrrolidinium iodide
[Emim][Tf_2N]	1-Ethyl-3-methylimidazolium bis [(trifluoromethyl)sulfonyl] imide
[Emim][NTf_2]	1-Ethyl-3-methylimidazoliumbis(trifluoromethylsulfonyl) imide
[EPMPYR][Cl]	N-methyl-N-(2′, 3′-epoxypropyl)-2-oxopyrrolidinium chloride
[Hmim][Cl]	1-Hexyl-3-methyl-imidazolium chloride
[Hmim][Br]	1-Hexyl-3-methyl-imidazolium bromide

[Hmim][PF_6]	1-Hexyl-3-methylimidazolium hexafluorophosphate
[Hmim][$FeCl_4$]	1-Hexyl-3-methylimidazolium tetrachloroferrate
[HPy][Cl]	Hexylpyridinium chloride
[Hmim][NTf2]	1-Hexyl-3-methylimidazo-lium bis(trifluoromethylsulfonyl)-imide
[Hmim][TfO]	1-Hexyl-3-methylimidazolium trifluoromethanesulfonate
[Mmim][CH_3SO_4]	1,3-Dimethylimidazolium methyl sulfate
[MPy][Cl]	Methyl pyridinium chloride
[MPpyr][BF_4]	1-Methyl-1-propyl pyrrolidinium tetrafluoroborate
[MeOEA][Ac]	Bis (2-methoxyethyl) ammonium acetate
[MTOA][NTf_2]	Methyl trioctyl ammonium bis (trifluoromethyl) sulfonyl amide
[MPiC_6Py][NTf_2]$_2$	1-(1-Methypiperidinium-1-yl) hexane-(1-pyridinium) bis (trifluoromethanesulfonyl) imide
[NMP][HSO_4]	N-methyl pyrrolidonium bisulfate
[OPy][Cl]	Octylpyridinium chloride
[Omim][Cl]	1-Methyl-3-octylimidazolium chloride
[Omim][Br]	1-Octyl-3-methylimidazolium bromide
[Omim][PF_6]	1-Methyl-3-octylimidazolium hexafluorophosphate
[Omim][$FeCl_4$]	1-Octyl-3-methylimidazolium tetrachloroferrate

[OH-Pmim][Cl]	N-(3-hydroxypropyl)-N-methylimidazolium chloride
[OH-Emim][Cl]	N-(2-hydroxyethyl)-N-methylimidazolium chloride
[PY][HSO_4]	Pyrrolidinium bisulfate
[PMPY][I]	1- Methyl-1-propyl pyrrolidinium iodide
[TBP][Br]	Tetra-butyl phosphonium bromide
[TBA][PF_6]	Tetrabutylammonium hexafluorophosphate
[TMG][Pro]	Tetramethylguanidine propionate
[TMG][Lac]	Tetramethylguanidine lactate

CHAPTER 1

INTRODUCTION

1.1 History of ionic liquid

The ionic liquids (ILs) have gained much attention as a novel class of materials with the majority of applications in an extensive variety of disciplines and are increasing rapidly because of their tuneable and unique properties [1–3]. Due to these characteristics, ILs are proving to be promising as a ‘‘green solvents’’ alternative to conventional volatile organic compounds (VOCs) mostly in terms of their low vapour pressure that reduces their inhalatory exposure as well as accounts for nearly 67% of all industrial emissions [4,5]. ILs is a particular class of salts which entirely composed of ions with the melting temperature lower than the boiling point of water (< 100 ^{0}C temperature). Most of the salts identified in the literature as ILs are liquid at room temperature can be labeled as room-temperature ionic liquids (RTILs) [6–8]. Nowadays, ILs are an important part of academic research because of their different specific chemical and physical properties. RTILs are usually molten or fused salts composed of asymmetric organic cations and various inorganic anions. They are also called as ‘designer green solvents’ because of their physical properties, including viscosity, density, miscibility, and polarity that can be tuned as according to the requirement by suitable choice of appropriate cations and anions species. By the alteration of the structures of the anion or cation, we can create the several kinds of ILs, which make them “designer solvents” [7,8]. Furthermore, ILs are attaining a wide range of great attention earned in the field of protein folding/ unfolding, since, ILs attend as active participants in various biological processes [1,9–11].

In the specific situation, ILs are established as a novel class of solvents considerably for the substitution of standard VOCs in the optimization of biochemical processes to decrease environmental pollution [1,2,9,12]. In history, the first RTIL namely, ethylammonium nitrate ($[C_2H_5NH_3][NO_3]$, EAN) with a melting point of 12 ^{0}C was reported by Paul Walden in 1914 [13]. At that period, Paul Walden never assumed that ILs would turn into a main scientific field

after around one century. After some few decades, in 1951 Hurley and Wier at Rice University were industrialised low melting salts using chloroaluminate ions for low-temperature plating of aluminum chloride ($AlCl_3$) [14]. During the period of the 1970s and 1980s, these ILs were studied mostly used for electrochemical applications [14,15]. In the early 1980s, low melting point ILs were recommended for organic synthesis as solvents by Fry and Pienta [16] and Boon et al. [15] Alkyl imidazolium salts $(C_nmim)^+$ were also testified in the mid-1980's [17] . John S. Wilkes has presented an admirable small history of the birth of introduction of ILs, which covers the key moments of research area [18]. Later, in the year of 1990s, molten or fused salts are having melting point lower than 100 ^oC that generated a novel exclusive media for biochemical reactions. After that, several researchers from different areas are extensively used [1,18,19].

1.1.1. Classification of ILs based on their relevant physical properties

As ILs are composed entirely of ions (such as cations and anions), their bulk and interfacial performance is complex and is governed by dipole-dipole, van der Waals, Coulombic, solvophobic forces and hydrogen-bonding [20,21]. While IL is made by adding a strong base with a strong acid, the proton is normally expected to be placed very strongly on the base. In this condition, the IL is mostly composed solely of ions [22]. Based on experimental results, a high majority of the ILs with different assortments of the cation along with the anions have been classified as protic ionic liquids (PILs) and aprotic ionic liquids (APILs) based on their relevant physical properties to deprotonate/protonate in solvent media [23]. A comprehensive analysis dealing with a systematic investigation and evaluation of the stability of different biomolecules in presence of APILs and PILs containing aqueous media is still lacking. The reason for this difference is that PILs are volatile through their nature because of the most acidic proton can be distracted by the simple anion at room temperature. The acid-base

chemical equilibrium for the abstraction reaction permits the development of neutral molecular chemical species that promptly vanish [24].

ILs are implied and are usually composed entirely of ions, mainly derived from large asymmetric organic cations such as imidazolium, ammonium, cholinium, phosphonium, pyridinium, sulfonium, guanidinium, pyrrolidinium with long alkyl chain substituent with variety of anions such as bromide, chloride, iodide, nitrate, acetate, hydrogen sulphate, tetrafluoroborate, hexafluorophosphate, trifluoromethanesulfonyl, alkylsulfate, dicyanamide and *bis*(trifluoromethanesulfonyl)imide [9,25,26]. These ILs are attracting much interest due to their many unique properties, such as low vapour pressures, broad liquid range, non-flammability, non-volatile, outstanding solvent ability, thermal stability, chemical stability, tuneable nonexplosive viscosity, nonexplosive reaction media, wide electrochemical potential window, ionic conductivity, reusability and recyclability [27–29]. Due to these properties, ILs are promising materials which used in many fields such as in electrochemical devices, engineering fluids, and replacements of solvent for numerous organic reactions. All of these potential characters of ILs turn into clear applicants for "environmental-friendly or greener solvents" [30]. Organic cations and coordinating anions that are commonly used in recent generations of ILs are depicted in Figure 1.1.

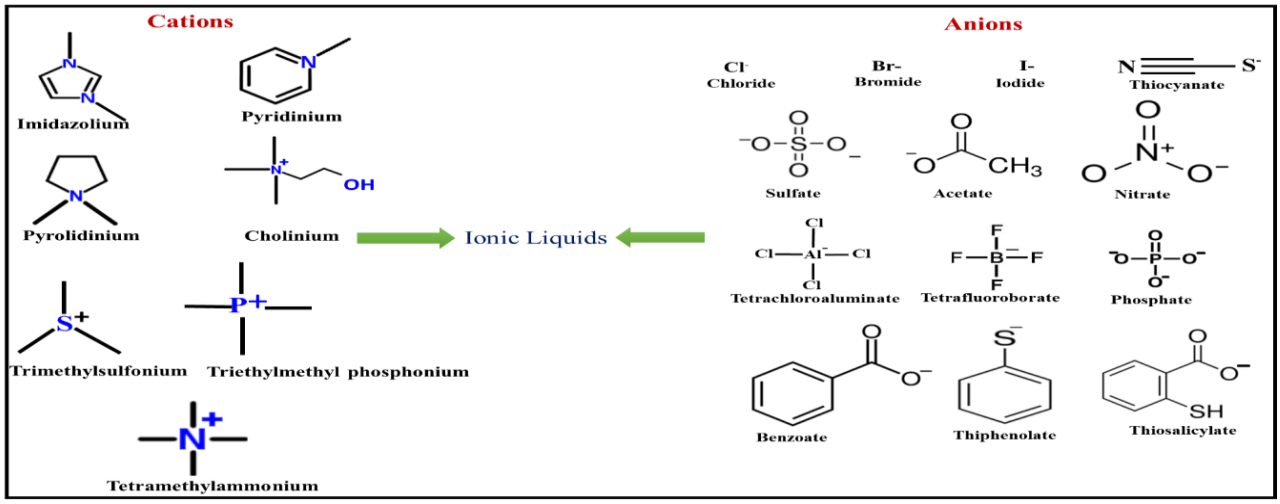

Figure 1.1: Various cation and anion used for the preparation of ILs.

1.1.2. The potential application of ionic liquids

For the past two decades, ILs as innovative fluids has been gained great attention as neoteric solvents in several scientific applications. Moreover, the application of ILs have shown great promising prospect in sample preparation. The benefits of utilizing ILs in enzymatic biocatalysis, as equated to VOCs, are improvement in the solubility of products or substrates without inactivation of the proteins/enzymes, great conversion values and high stability as well as activity of proteins [31–34]. A multidisciplinary study on ILs is developing, including chemistry, electrochemistry, biochemistry, biotechnology, chemical engineering, materials science, medical science, pharmaceutical, environmental science and food industries [35–37]. In several chemical reaction processes, ILs are used as catalysts, stoichiometric organic synthesis solvents and reagents. Combinations of ILs have been proposed for many applications in different fields such as lubricants, battery electrolytes, homogeneous and heterogeneous catalyst, for extraction, removing of metal ions, purification of gases, gas absorption agents, biomass conversion, solar and thermal energy conversion, sensors, treatment of high-level nuclear waste plasticisers, nuclear fuel processing, matrices for mass spectroscopy, biological and medical procedures, development of drug delivery systems and others [31–37]. Such incredible developments in many areas have been obviously confirmed by growing interest and publication activity, which still displays outstanding growth of ILs [5,38–45]. Moreover, tremendous applications include its uses in the laboratory settings, analytical methods, purification of biomaterials, purification in refineries, cyclic voltammetry, ultrasound-promoted, microwave-promoted, the manufacture of Deoxyribonucleic acid (DNA) oligonucleotides and manufacturing of drug materials and various useful products, photographic flicks and smart functional materials amongst others [46–48]. A special issue of ILs on several scientific applications was published [49] which shows that ILs offer new potential possibilities of application from solvent engineering field

to enzymatic processes. In the last two decades, ILs have attracted much attention as conventional reaction media for enzymes in solvent media with some extraordinary results [9]. The several applications of ILs in different fields are growing rapidly, which is schematically represented in Figure 1.2.

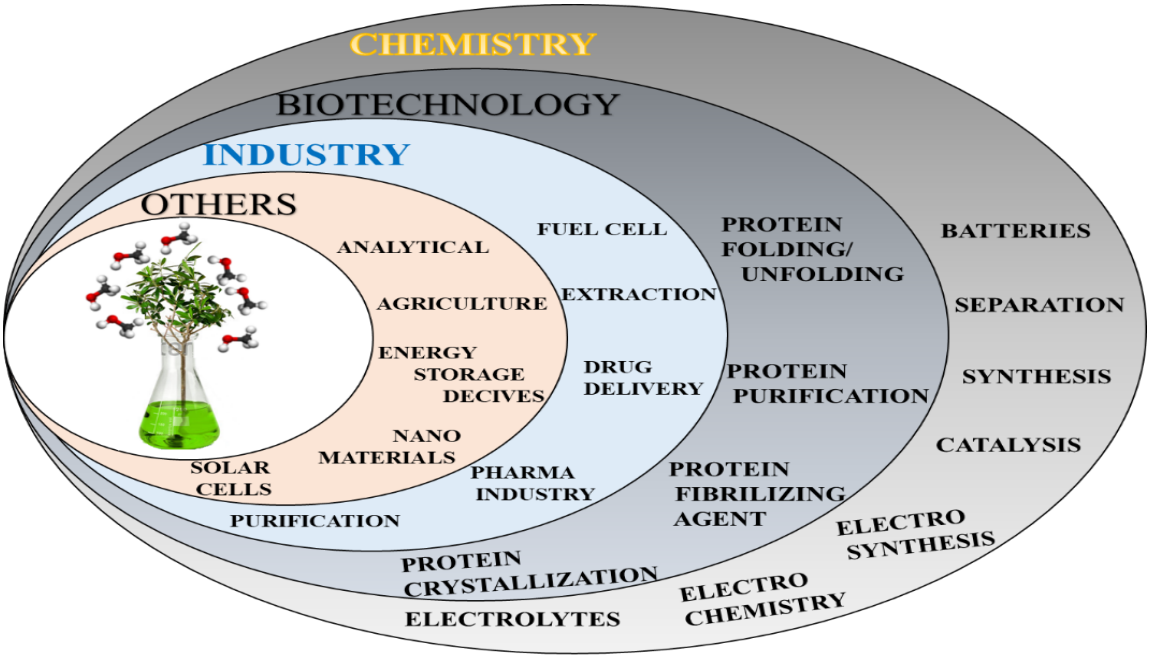

Figure 1.2: Numerous applications of ILs in different scientific fields.

1.2. Introduction to proteins

Proteins are one of the most essential biological-macromolecules in living organisms and which are made up of one or more polypeptide chain of amino acid (AA) residues. Proteins gained great importance in biological processes namely: stability, protein kinetics and activity are mainly influenced by the various chemical and physical properties of co-solvent, additives, environmental condition and others [50]. Proteins are the major structural fragments of the blood cells, enzymes, nerve tissues, hormones, muscles, bone, skin, ligament, hair, and all other organs which help us in body growth and development [51–54]. Moreover, they are also existing in plants to provide the structure and biological activity [55]. Proteins are involved in nearly every aspect of living beings and clearly, without protein, all living things

would not exist. Proteins are linear polypeptide chains of amino acids (AA_s) and have the ability to form a unique three-dimensional structure in their folded or native state [56,57]. Chemically, a definite three-dimensional shape is meaningfully fascinating and exciting that associations the features of biophysical properties, structural aspects and the conformation of certain AAs functional states of proteins [58–60]. The structural multiplicities seem necessary for different proteins to complete various biological roles which directly depending on their natural form. The change in their functional properties designates and the conformational variations within the molecule, which can be essentially carried out around by the modification in the native structure environment [61,62].

Especially, in the body each protein depends on its specific function of AA sequences. There are incredibly useful biological functions of proteins that form the basis for cellular life. Inside and outside cells, proteins achieve a numerous of functions, for example, structural roles (cytoskeleton), as hormones (enzymes), transporting molecules from one location to another membrane. They help in the full functioning of the body, few of them, such as catalyzing metabolic reactions, responding to stimuli, DNA replication, include various enzymatic and chemical reactions in the body. Furthermore, the three-dimensional structure of a protein arises particularly because of the sequences in AA_s of the protein polypeptide chains fold to produce compact solid domains. Nature selected only those AA_s sequences that can fold powerfully and form single equilibrium structures [63–65].

1.2.1 Protein structural arrangements

Proteins are macromolecules, linear polymers and genetically building blocks of biological macromolecules and comprised of 20 different naturally occurring AA residues associated by non-repetitive peptide covalent bonds (-CO-NH-) into a linear polypeptide chain [66,67]. Each of the amino acid (AA) is mainly composed of one central carbon atom attached to four dissimilar chemical groups which are a hydrogen atom, an amino group ($–NH_3^+$), a carboxyl

group ($–COO^-$) and a variable residue (side chain) denoted as –R group [60,63,67]. The schematic diagram of AA is displayed in Figure 1.3. The arrangement of these 20 different AA_s makes a protein distant beyond those of simpler macromolecule.

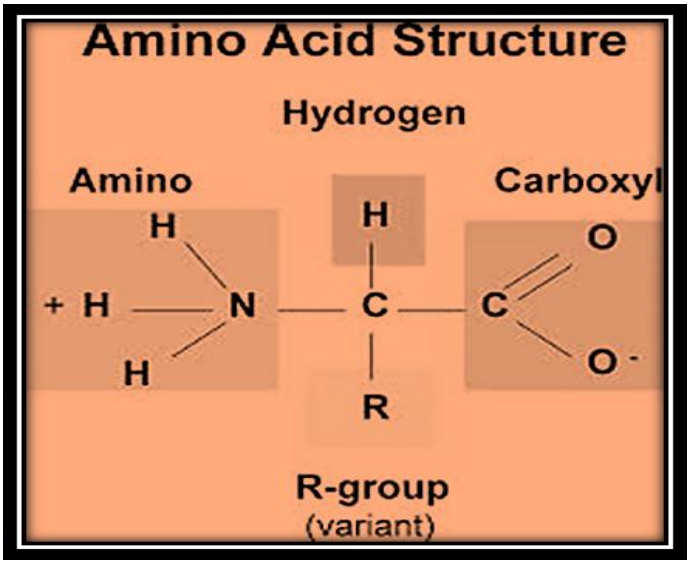

Figure 1.3: Schematic diagram of amino acid.

Naturally, there is covalent linking between α-carboxyl groups of one AA with the α-amino group of other molecule and there is a loss of water molecule through the formation of a peptide bond. All of AAs found in proteins have the basic structure, differing only in the structure of the R-group [66,68]. More than 700 amino acids occur naturally, however, 20 of them are essentially important AAs, which include histidine (His), lysine (Lys), threonine (Thr), isoleucine (Ile), methionine (Met), leucine (Leu), tryptophan (Trp), tyrosine (Tyr), phenylalanine (Phe), valine (Val), serine (Ser), asparagine (Asp), glutamic acid (Glu), aspartic acid (Asp), glycine (Gly), alanine (Ala), arginine (Arg), cysteine (Cys), proline (Pro), and glutamine (Glu) [60,62,64]. Moreover, the nature and the sequence of the AA chain along with the protein peptide backbone are responsible for the specific characteristics of the biomolecules, and it has been predictable that complete information relating to the proteins are implied in the AA arrangement. The ability of AA_s to form a three-dimensional protein shape is essentially motivating and fascinating that combines the facets of biophysical properties,

specific structural arrangements and conformation of some functional groups of macromolecules [60,66].

1.2.2 Classification of protein structures

Danish protein chemist K. U. Lindersrøm-Lang explained three different levels of protein structure: primary, secondary and tertiary. Likewise, another chemist J. D. Bernal included the quaternary structure in which the protein is made up of more than one domain [65].

1.2.2.1 Primary structure

The primary structure is referred to the number and sequence of AAs residues that make up a linear polypeptide chain in proteins. Beginning with the free amino group and retained by the polypeptide bonds attaching every AA to the next sequence. Likewise, the primary structure of a protein is described beginning from the amino group-terminal (N) end to the carboxyl group-terminal (C). Obviously, the specific combination of AAs in a protein, positive intra– and inter chain cross-links assuming any, as known as the primary structure [62,65]. Figure. 1.4, represents the sequence of AAs in the primary structure of the protein [62-63].

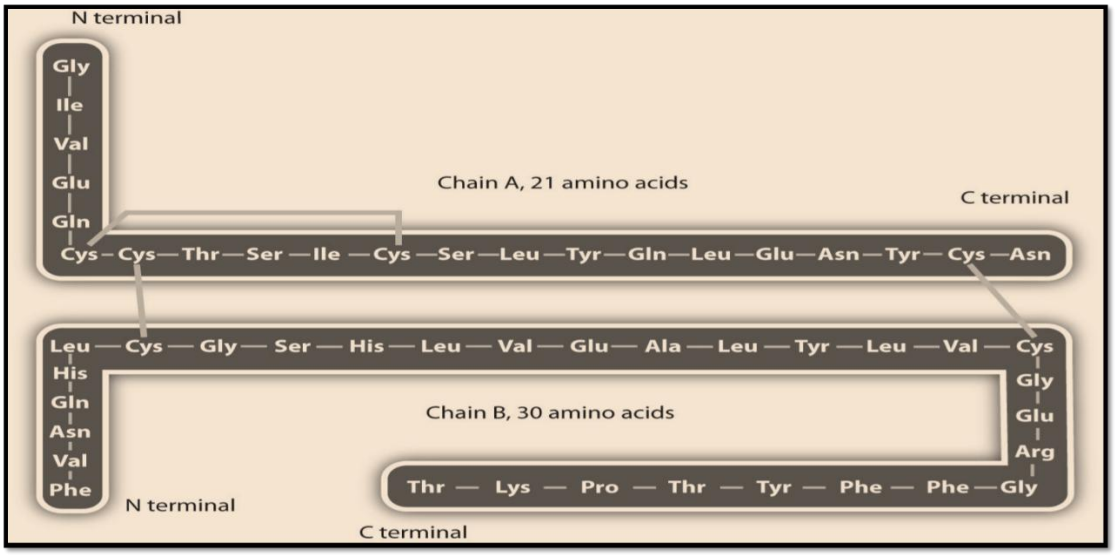

Figure 1.4: A sequence of AAs in a primary structure of the protein.

1.2.2.2 Secondary structure

The Secondary structure refers to especially stable arrangements of AA residues giving rise to a structural pattern. It is the most important level in the hierarchical classification and responsible feature of the protein's structure and it is used to recognize protein structures for fold recognition. The secondary structure of polypeptide chain occurs particularly as α-helices and β- pleated sheets [62–64]. The secondary structure take place because of the hydrogen bonding interaction between the N–H (amino groups) and C=O (carbonyl groups) groups of the AA_s in the polypeptide backbone or main chain which is represented in Figure 1.5 [62-63]. However, the arrangement of secondary structure in a native state of the polypeptide backbone is to some extent influenced by the primary structure of protein [64,69,70]. Specifically, the side-chain substituent of the AA groups in the α-helix extends to the outside. Hydrogen bonds formation between the oxygen of the carbonyl group and the hydrogen of the amino group of the peptide bond four AA_s below in the helix. The structural geometry of proteins especially combining regions of the α-helical secondary structure is also mainly influenced by necessities for effective packing between the helices [70–72]. The formation of hydrogen bonds makes the α-helix structure particular more stable (Figure 1.5a). Obviously, α-helices are formed from a successive set of residues in the AA sequences of the polypeptide chain.

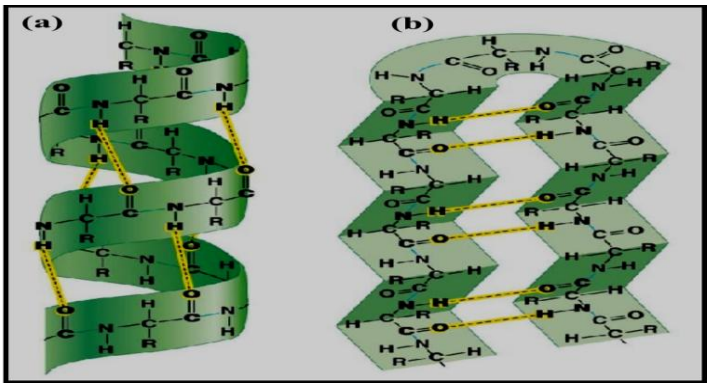

Figure 1.5: (a) α-helix and (b) β-sheet structures in a protein. The hydrogen bonds between the AA residues are presented by dashed yellow lines.

On other hand, the hydrogen bonding in a β-sheet is between strands (inter-strand) as opposed to inside strands. In β- pleated sheet secondary structure, the segments of the main chain interact by adjacent hydrogen bonds. All β-sheets form the middle core of several globular proteins. Variations in the direction of β-sheets are attained by the structure called as a β-turn or β-bend that frequently attaches the ends of two lateral strands of anti-parallel β- pleated sheets. As represented in Figure 1.5 b, the sheet compliance consists of sets of strands deceiving one next to the other. The carbonyl oxygen group in one strand is hydrogen bonded with the amino hydrogen group of the lateral strand. These two adjacent strands can be either parallel sheets or anti-parallel sheets depending on whether the strand directions are the similar or inverse [61,63,65,66].

1.2.2.3 Tertiary structure

The tertiary structure contains the high information contents of the overall, unique, three dimensional folding of a polypeptide protein. As shown in Figure 1.6 [63], the tertiary structure of a protein describes the folding of its structural features and identifies the different positions of each molecule in the protein, containing those of its side chains. The tertiary structure rises due to the mutual effects of different type's interactions between the polypeptide chains and AA_s within a protein atom [62–64,70,73]. Furthermore, the tertiary structure of protein molecule is generally stabilized by different kinds of interactions such as ionic bonding, hydrogen bonding, disulfide bonds and hydrophobic interactions (van der Waals interactions) takes place between different AA residues (Figure 1.6).

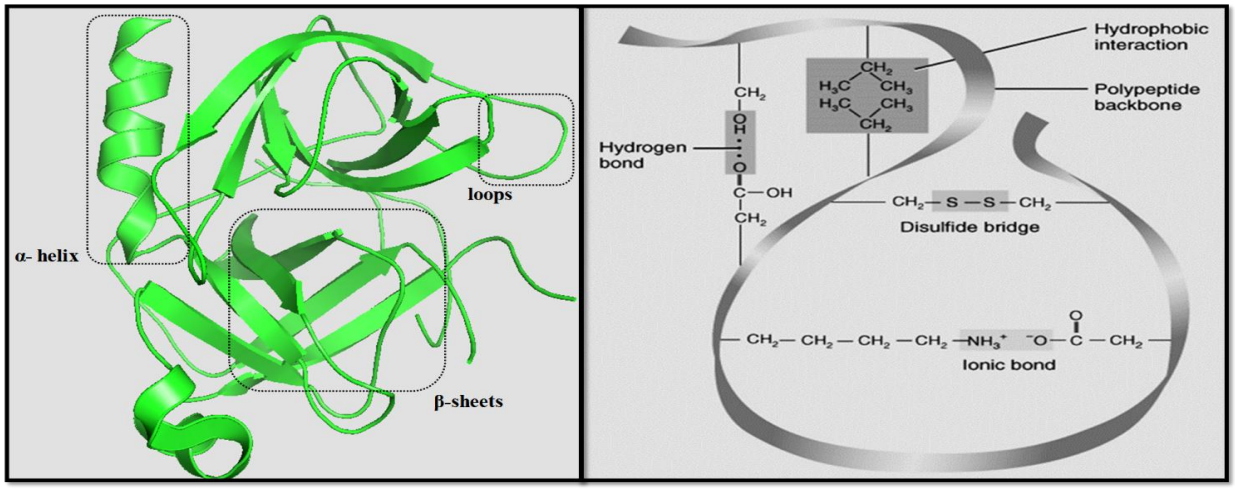

Figure 1.6: Tertiary structure of a protein with ionic, H-bond, disulfide bond and polypeptide backbone.

Almost, under physiological conditions, the hydrophobic AA_s such as Phe and Ile or Trp have a tendency to burry in the interior of the molecule of protein thereby escaping away from the aqueous environment [63]. On the other hand, the hydrophilic AA_s residues such as Asp, Glu and Ser are usually found on the outside surface of the protein, where they are able to interact with water. The polypeptide chain bends and coils in such a way as to attain extreme stability or lowest energy state [66]. Though the three-dimensional structure of a protein appears asymmetrical and random, it is twisted by various stabilizing forces owing to interaction bonds between the polypeptide side-chain groups of the AA residues. Likewise, in the tertiary structure, disulfide bonds play a vital role in the folding and greater stability of proteins, normally secreted in the extracellular environment. Different chains in the tertiary structure of protein molecules are held together through disulfide bonds between the Cys groups inside the polypeptide chains. The formation of disulfide bonds of the sulfhydryl groups on Cys is an essential part of the stabilization of tertiary structure of the protein, permitting several parts of the polypeptide chain to be held together covalently.

1.2.2.4. Quaternary structure

Maximum proteins, mainly those with molecular weight > 100 kD, contains more than one polypeptide chain in the structural arrangement. These polypeptides units associated with a specific structural geometry of proteins. The three-dimensional arrangement of these subunits is known as a protein's quaternary structure. The quaternary structure is a greater assembly of many molecules or polypeptide chains, usually known as subunits. The assembly of two or more polypeptides (i.e. multiple subunits) is known as multimers. If it contains two or three or four subunits are called as dimer, trimer and a tetramer. Figure 1.7 [62-63], illustrates the protein quaternary structure is an assembly of several peptide chains in single function of integral structure, the arrangement of peptide chain which gives rise to a stable structure of the protein. Moreover, the stability of the quaternary structure depends upon the non-covalent interactions and disulfide bonds of the tertiary structure of the protein. Also, the assembling of these polypeptide sub-units decreases the exposure of hydrophobic side chains to the solvent medium.

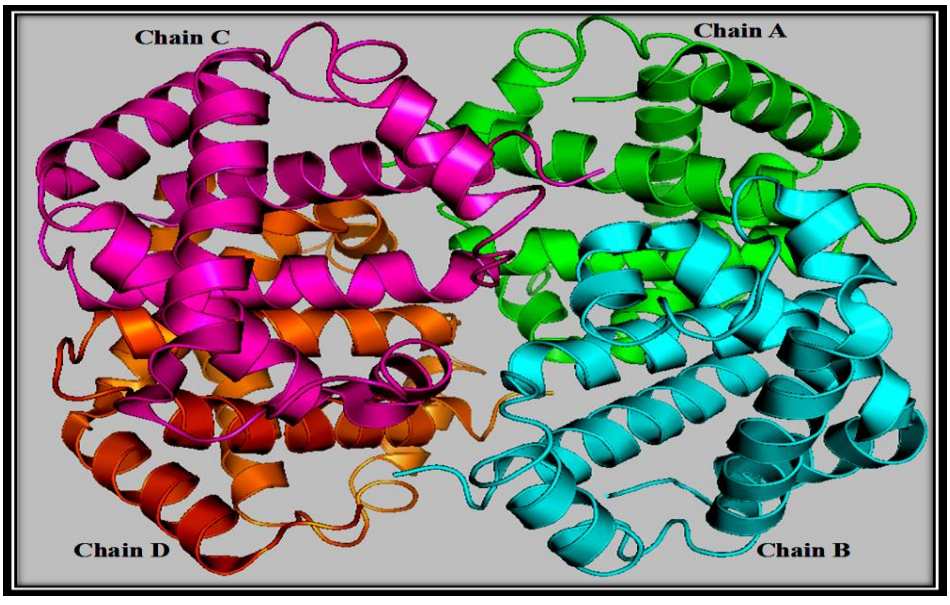

Figure 1.7: Quaternary structure of protein with polypeptide chains.

1.3 Protein folding and unfolding

Most of the proteins found in the environment have to receive a particular three-dimensional conformation, termed as folded or native state for suitable functioning, which is important for performing their different biological functions and activities. Basically, the understanding of biological phenomenon depends on the single way or another on molecular recognition, and in the arrangement of macromolecular complexes, is depending on protein folding. As discussed in the previous sections, the physical process by which a polyamino acids or lypeptide chain obtains its specific native three-dimensional structures to achieve the functionally and biologically active native state is known as protein folding [61]. Generally, the native state of proteins is called a folded state, whereas the denatured or the inactive state of proteins is termed as an unfolded state. A complete loss of organized structures (such as secondary, tertiary or quaternary structures) of proteins due to exposure to some kind of pressure is called as unfolding or misfolding [74]. However, proteins can lose their native structure by insignificant changes in the physiological environment, such as pH, temperature, pressure, ionic strength, extreme cold, and mechanical stresses or by the addition of co-solvents [74–78]. These slight changes in the environmental surroundings may influence the selection between folding and unfolding or misfolding. The active state of a globular protein is necessary for its bio-catalytic function; however, it is slightly stable opposed to unfolding state. Protein can present in two different states, the active state having a compact native (folded) conformation and denatured (unfolded) state that is schematically presented in Figure 1.8.

Protein folding is a reversible transition state of a protein made up of AA residues that are in prompt symmetry between its well-ordered and disordered states [75–77]. Furthermore, protein folding is of specific disquiet in the production of industrial biocatalysis as well as for storage

purpose, whereas the biomolecules are frequently inactive because of unfolding. The structure and stability of a protein replicate the range to which its conformation resists change when subject to pressure [79]. Accepting the protein folding process encourages us to understand the performance of the protein is pose tremendous challenges in both present pharmaceutical and biophysical environments. The absolute consequences of protein folding, and so, mirrors the involvement of various interdependent impacts that lead to structures of intra-molecular or increasing complexity as in protein folding [80,81]. Protein stability and associations totally depend on the result of complex interactions such as ionic interactions, electrostatic, van der Waals, hydrophobic, hydrogen bonds and steric interactions amongst themselves and with other solvent molecules [82].

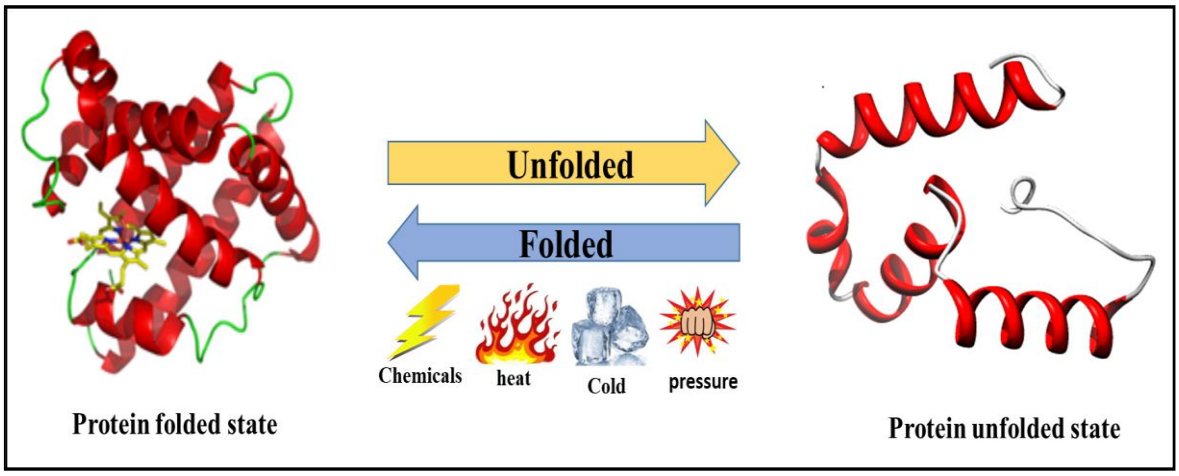

Figure 1.8: Schematic representation of unfolded state of protein structure in the presence of some physiological stress.

The unfolding process can be carried about not only by heat and pH but also through surface action, ultraviolet light, high pressure and by addition of co-solvents etc. Denaturation process is a slightly non-proteolytic alteration of the single structure of a native protein, gives rise to certain modifications in chemical, physical, or biological properties." Denaturation might carry [75],

(a) The decrease in the solubility

(b) Loss of biological activity

(c) Loss of crystallizing ability

(d) Increased reactivity of the constituent groups

(e) Changes in the molecular shape of the protein.

Particularly, protein unfolding/ denaturation is not only limited to industrial and biological process but also protein unfolding can be resulted in many diseases such as Alzheimer, Parkinson and Huntington's disease, sickle cell disease, Creutzfeldt–Jakob disease, cystic fibrosis as well as degenerative and neurodegenerative disorders [83–85]. This gives rise to totally irreversible thermal denaturation and insolubility. Native structure of biomolecules parallels to the particular structure that is thermodynamically more stable conformation under physiological environments [86]. The fundamental principles of protein folding stability have been a theme of impassioned study over the past several decades and remain one of the boundless mysteries currently [87,88].

1.4 Effect of co-solvents on the protein structure and stability

In general, most of the proteins are sensitive and highly functional complex systems, exhibiting a considerable amount of structural instability in their folded state. The structure and stability of biomolecules in the co-solvent conditions are dependent on the natural surroundings of the co-solvent, which can change a protein physical properties and structural arrangements through molecular interactions amongst its functional groups and the solvent particles [89–91]. Moreover, within the sight of co-solvents, the variances among a remarkable number of folded and unfolded compliances take place by means of a wide range of pathways, then again, proteins can be stabilized or destabilized. Thermodynamic point of view, a protein in a solution exists in equilibrium between the folded and the misfolded states (Figure 1.8) [78].

The protein molecule surface is basically answerable for the interaction with co-solvents that provides to the protein stability. The support of a protein's structure depends on the great number of interactions made with the solvent condition [89,90]. Essentially, the co-solvents that change the equilibrium towards folded state are called as protectants while those that favor the unfolded/misfolded state are called as denaturants [75].

The use of proteins in co-solvents has comprehensive useful applications and permitted the combinations of biologically active materials, which are challenging to achieve with conventional biochemical catalytic agents. Several biophysical studies have been done in enhancing the protein stability in the presence of co-solvents and it has been recognized that the protein stability is stable between the intra-molecular interaction of protein functional groups and their interaction with Co-solvent molecules environment conditions [92,93]. The hydrophobic interactions with AA residues play a key role in various biological processes such as membrane, protein interactions and protein stability. Proteins in aqueous solution, particularly for polypeptides, the condition is even more difficult than just specified, for the reason that water changes its atmosphere as a function of temperature [94,95]. The stability of proteins is elevated by the protectants that are not interfering functional activity of the proteins, while the stability of proteins is compact by denaturants, which ultimately destabilizes the activity, as well as function sites, and changes the structure of the proteins. Small changes in the native surrounding environment of a protein molecule can reason structural modifications leading to the development of different conformations, and thus, disturbing the actual functional shape of the protein. More essentially, deserts inactive native state protein folding might be the molecular basis for an extensive variety of human genetic conditions. Luckily, the environment has provided a shield of ensuring co-solvents to avoid this disorder in biomolecules. Biologically, these rapid physiological stresses and disorder in biomolecules overcome in the presence of biocompatible ILs that slightly represents a different class of

environment-friendly compound. Since, ILs because of their specific nature, size, and desirable physical properties play a pivotal role in the folding/unfolding states of proteins. Consequently, in order to found the advantage of drug-based ILs for FDA, and also it is very important and interesting to see the overall effects of the different types of ILs on the structure and stability of various proteins [3,96–98].

1.5 The importance of thermophysical and thermodynamic properties

Thermophysical properties of pure solvents or mixed solvents are having much attention in phase equilibria that can be parameter for the design of various technological processes and many tremendous applications. These properties are the assets of a substance or material which influence the mass transfer and storage of heat, they may change with the composition temperature, and pressure of the mixture [99–102]. The investigations of composition requirement of the thermophysical properties are of great significance and most essential in many facets for the scientific communities, which can be an effective source of information with respect to the visible impacts of the different types of intermolecular forces (such as electrostatic, induction, dispersion and chemical forces) which are available in liquid mixtures [103–105]. These molecular interactions provide specific information on how the thermodynamic properties like entropy (*S*), energy (*U*), enthalpy (*H*), helmholtz free energy (*A*) and gibb's free energy (*G*) will be changing with pressure, density and temperature [106–108]. Subsequently, volumetric properties of liquids are frequently communicated by equations of state which are more suitable to ascertain thermodynamic/thermophysical properties related to the independent factors or volume (*V*) and temperature (*T*).

To better understanding of the molecular interactions between the liquids and the liquid mixture, a detailed knowledge of thermodynamic and thermophysical properties of liquids and their liquid mixtures are essentially required. Moreover, experimental measurements data

of thermophysical and thermodynamic properties of fluids and liquid mixtures are interesting and of high essential, empirical significance for the chemical industry [109–111]. In spite of the fact that a qualitative association between the microscopic and macroscopic features are important to both academic research and chemical industry communities [112–114]. The requirement for specific properties of thermodynamic/thermophysical information is winding up progressively imperative for industrial applications. Although, the understanding of thermophysical data of binary liquid mixtures of ILs with other organic solvents is vital for improvement of particular chemical processes [115,116].

In the present situation there has been an extraordinary growth in thorough thermodynamic properties of binary liquid mixtures not only because of industrial importance but also on the source that they lead to a good understanding of the molecular interaction between (solute-solvent) the liquid mixture and the continuation of solution theories [117–121]. When two fluids are combined together, the consequential changes in thermophysical and thermodynamic properties can be considered as an amount of any contributions in terms of change in energy, change in free volume, molecular alignment, change in nature of molecular interactions and stearic prevention [119,120]. Excess and apparent thermodynamic properties of binary mixtures are more useful for obtaining the molecular interactions and in terms of molecular size, shape, polarity, nature of component molecules and also structural changes [121,122].

The better understanding of thermophysical properties of liquids and their liquid mixtures have a lot of essential to the chemists and chemical engineers several approaches in terms of the applicability theories of liquids and their mixtures will helpful in the assessment of mixtures of similar nature,

- to elucidate, compare and predict thermodynamic properties via molecular thermophysical considerations,
- to find the applicability theories of fluids and to expect the properties of mixtures of similar nature,
- to understand the intermolecular interactions between different kinds of solutions,
- further, these volumetric properties are useful for designing the industrial equipment with better precision, thus reducing the capital costs, pipelines and pumps with better precision,
- volumetric measurement studies of liquids mixtures are useful from petrochemistry to pharmaceutical industries,
- to examine the present theories of solutions due to their sensitivity to the distinction in sign and magnitude of excess and apparent thermodynamic functions and geometry of the component molecules,
- to test the present theories of solutions due to their sensitivity to the variance in sign and magnitude of excess thermodynamic functions and geometry of the component particles.

The excess and apparent properties are widely used to study the difference of a specific liquid mixture from ideality of solution [123–125]. Moreover, the formation of hydrogen bond interactions between the molecules of a binary liquid mixture is an additional mutual chemical effect influence the thermodynamic properties or result to a greater extent than other specific and physical interactions of liquid mixtures [126–131]. These interactions clearly reveal that the scope of intermolecular interaction and self-association between unlike molecules fluctuate with the composition of the mixture.

The complex nature of the molecular interactions presently in the liquid stage creates the assignment of predicting thermodynamic measures problematic [132–135]. However, thermophysical information is in helpful industry, for the optimization of the development of many industrial processes such as heat transfer, pipeline systems, surface facilities, oil recovery mass transfer, oil and gas for flow assurance, fluid flow, biomedical research as well as pharmaceutical, polymer for solvent emission and selection [109,123,129]. The understanding of thermodynamic/thermophysical properties of the ILs mixture with other solvents are helpful for the development of particular technological processes of a reaction and chemical processes [130]. Evidently, thermophysical information of methods are used to determine the thermophysical properties which are most important to designing advance future developments and tools involving chemical and chemical engineering processes. These thermophysical properties, containing activity coefficients of coponents at infinite dilution and excess molar volumes and apparent molar volume are also very useful for the design of predictive models for systems having ILs mixtures [131]. The classification of thermophysical and transport properties is shown in Figure 1.9.

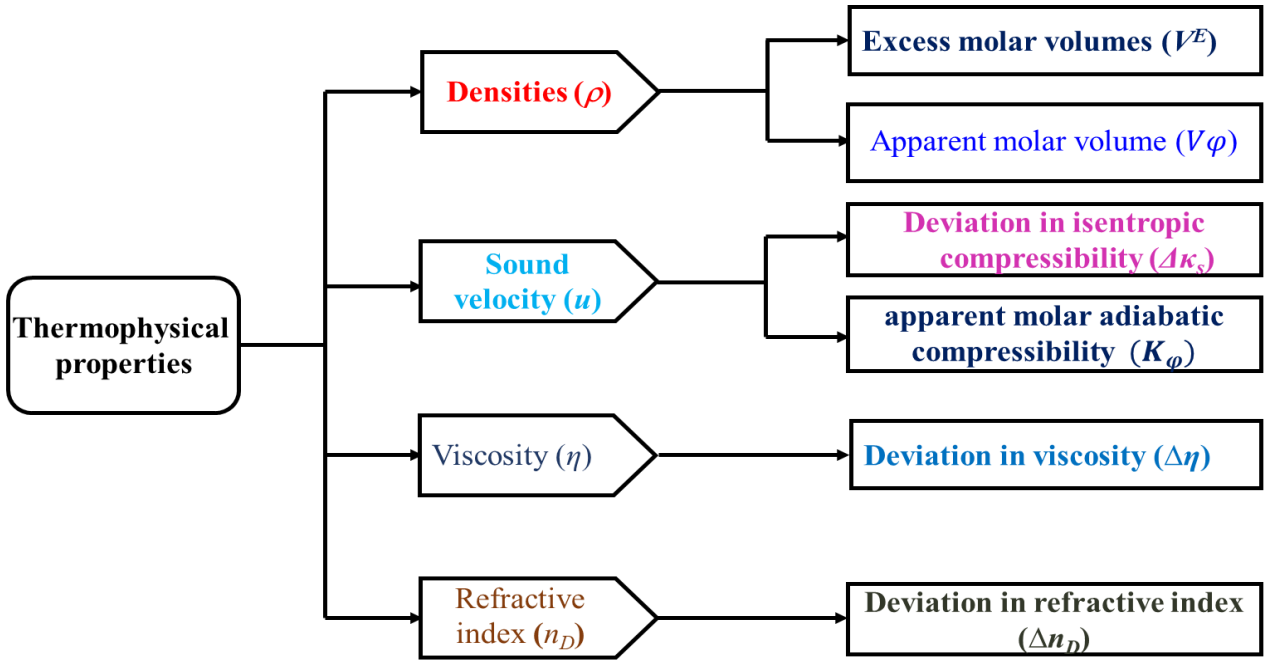

Figure 1.9: Classification of thermophysical and thermodynamic properties.

To this end, a database of anion and cation of ILs and thermophysical properties must be helpful and partial volumes at infinite dilution (V_{mi}^{∞}) can be utilized as a basis for the understanding of the molecular interactions namely dispersion forces, hydrogen bonding interactions in liquid mixtures. Correspondingly, thermophysical data provide useful information and very interesting to understand the intra- and intermolecular interactions in between the component particles in the mixtures and are also used to easily reveal the solute-solute, solvent-solvent and solute-solvent structural interactions between the ions of ILs and solvent molecules of liquid mixtures which is an essential aspect of the scientific community [104,132–134]. Mainly, the objective of investigating thermophysical properties of binary liquid mixtures of ILs is to provide to a database of thermodynamic properties of liquid mixtures containing components efficient of undergoing particular interactions and to explore the relationship between ionic structures of the IL. And also establish the principles for the molecular arrangements, molecular design, geometrical effects and molecular modelling of suitable ILs for chemical separation processes [121,132,135,136].

Therefore, an industrial scale point of view to design any chemical process containing an IL it is essential to recognize the thermodynamic properties such as density, sound velocity as well as activity coefficients at infinite dilution [137]. These ILs have received, over the past decade, much attention as environmentally-benign substitutes to conservative organic solvents [19,138,139]. Till to date, ILs characteristically consist of minor anions and large cations such as pyridinium, imidazolium, cholinium, quaternary ammonium, and phosphonium. Nevertheless, the intermolecular interactions between ions so weak as compared to coulombic interaction between dipolar molecules that atomic behavior of ILs is different from that of conservative dipolar liquids. In contrast to the strong electrostatic interaction between ions, the steric effect of the big size of cations inhibits ILs from getting solidified at room temperature as take place in common salts. Finally, attending to the scarce

of experimental works corresponding to an ionic liquid containing mixtures, further research is essentially important to understand their internal association and developed models for expectation.

1.6 Scope of the present study

The thesis is divided mainly into two parts.

1.6.1 The study of protein folding/unfolding in the presence of different class of ILs

The structure and stability of proteins in the presence of ILs has been of considerable due to their biotechnological and pharmaceutical applications. Various studies have been carried out by many research groups on this protein science field, since a complete understanding of the unsolved puzzle of protein folding will certainly result in obvious biotechnological and medical applications. Attractively, biocompatibility has been attained for a number of these ILs in recent decades. Moreover, the biomolecular mechanisms of Hofmeister anion series of imidazolium and cholinium-based ILs special effects on different biomolecules have not been clearly explained. Therefore, we have taken this opportunity to study the effect of structure and stability of proteins in imidazolium and choline-based ILs. Consequently, in order to improve our understanding of the effect of Hofmeister series, studies on the anions of different ILs on the structure, stability and activity of BM protein has been carried out in the present thesis work.

Therefore, the present studied reported the structural stability and activity of BM in the presence of choline and imidazolium-based ILs such as ([Bmim][Cl]), ([Bmim][Br]), ([Bmim][I]), ([Bmim][HSO_4]), ([Bmim][CH_3COO]), ([Bmim][NO_3]), ([Ch][Ac]), ([Ch][Dhp]), ([Ch][Cl]), ([Ch][Bit]), ([Ch][OH]) and ([Ch][I]) by using UV–visible spectroscopy, dynamic light scattering (DLS), steady-state and thermal fluorescences, circular dichroism techniques.

1.6.2 Excess/apparent properties of binary mixtures

As a part of this study, thermodynamic properties such as excess molar volumes (V^E), deviation in viscosities ($\Delta\eta$), deviation in isentropic compressibilities (ΔKs) and deviation in refractive indices (Δ_{nD}) were calculated from experimental densities (ρ), viscosities (η), sound velocities (u) and refractive indices (n_D) values for the ammonium-based ILs with N, N-dimethylacetamide (DMA) at various temperatures from 25 to 40 ^{o}C and atmospheric pressure. The calculated thermophysical properties (V^E, ΔKs, $\Delta\eta$, Δ_{nD}) were correlated with the Redlich-Kister polynomial type equation to confirm the accuracy of measurement data of different binary systems.

Furthermore, it has been explored using apparent properties for the binary mixtures containing IL 1-methyl-1-propyl pyrrolidinium tetrafluoroborate [MPpyr][BF_4] and solvents water, alcohols (methanol and ethanol) at different temperatures. The apparent molar volume (V_φ) have been calculated from the experimental density data, respectively. Limiting apparent molar volumes (V_φ^0), the limiting apparent molar expansibility (E_φ^0) and thermal expansion coefficients α_p were also calculated using Redlich–Mayer type equation.

1.7. Research aim and objectives

The aim of the present research is to explore the role of biocompatible ILs on the protein folding/unfolding studies as well as to enhance the structure, stability and activity of BM in the presence of different (cations and anions) biocompatible ILs. In addition,

- To identify the anion effect of biocompatible ILs on protein structure
- Identification of suitable co-solvent for a particular protein,
- To see the concentration effect of biocompatible ILs on protein stability,
- To see whether Hofmeister series of anion is followed or not.

Furthermore, measure the thermophysical properties of different concentrations of ILs and their derivatives in organic solvents at various temperatures and under atmospheric pressure and study the alkyl chain length of cation/anion of ILs effect on the organic solvents interactions of the liquid mixtures. The present study will also focus on excess and apparent properties of binary mixtures containing specific and non-specific interactions.

The objectives below will be achieved in the following steps:

- To explore protein folding/unfolding in the presence of different ILs.
- To study the effect of Hofmeister anion series of ILs on protein folding studies.
- To interpret temperature effect on the molecular interactions between ammonium based ILs and N, N-dimethylacetamide (DMA) molecule as well as solute-solvent interactions between 1-methyl-1-propyl pyrrolidinium tetrafluoroborate [MPpyr] [BF_4] with water or alcohols.
- To understand the molecular interactions between the DMA with ammonium group of binary mixtures of ILs.
- To understand the solute-solvent interactions between the pyrrolidinium-based ionic liquid with water and alcohols.
- In the current study, it has been explored various thermodynamic properties such as V^E, κ_s, $\Delta\kappa_s$, $\Delta\eta$ and Δn_D for the binary mixtures of DMA + ILs of quaternary ammonium salt as well as V_φ for the binary systems of [MPpyr] [BF_4] + water or alcohols.
- These thermodynamic properties (V^E, κ_s, $\Delta\kappa_s$, $\Delta\eta$, Δn_D and V_φ) actively using in solution chemistry to know the various solvent and solution properties.
- To investigate the effect of temperature on these properties and their derived properties.

1.8 Outline of the thesis

The outline of this thesis is as follows:

Chapter 1 gives an introduction to the study of proteins, folding/unfoding, ILs and thermophysical properties of ILs mixtures.

Chapter 2 delineates the detailed review of the literature on protein structure and stability of imidazolium and choline based ILs. Chapter 2 also gives a summary of the literature on thermophysical properties of binary mixtures containing ILs.

Chapter 3 mainly describes the materials and experimental techniques used throughout the research for carrying in this present thesis.

Chapter 4 presents the obtained results and discussions on study of proteins folding/unfoding in presence of ILs and thermophysical properties of ILs with aquous and organic mixtures.

Chapter 5 presents the conclusions of the work carried out in the thesis.

CHAPTER 2

LITERATURE REVIEW

2.1 Structure and stability of proteins/enzymes in the presence of various ionic liquids

Varieties of proteins/enzymes are present in the environment and are the important molecules in the processes of a life cycle. They all belong to a class of biomolecules, which means that they contain evidently, and often especially, long polypeptide chains of amino acids. One of the major challenges in protein science has been the ability to protect the three-dimensional protein structure [140,141]. Though, the maintenance of a protein structure in its active native state is one of main significance for its biological functions and activities. In the present situation, the stability and biological activity of proteins in the presence of ILs have been an area for dynamic research due to their biomedical, biological, food fields, biotechnological and pharmaceutical applications [142–144]. Moreover, the physical and chemical properties, folding, unfolding, stability, the activity of a protein depends on the sequence of amino acids residues and also in the presence of co-solvents [50,57,145]. The equilibrium between the stability and destability of proteins can be perturbed by the addition of co-solvents. For the sake of clarity, it has been presented the equilibrium between the unfolded and folded the states of proteins Figure 2.1.

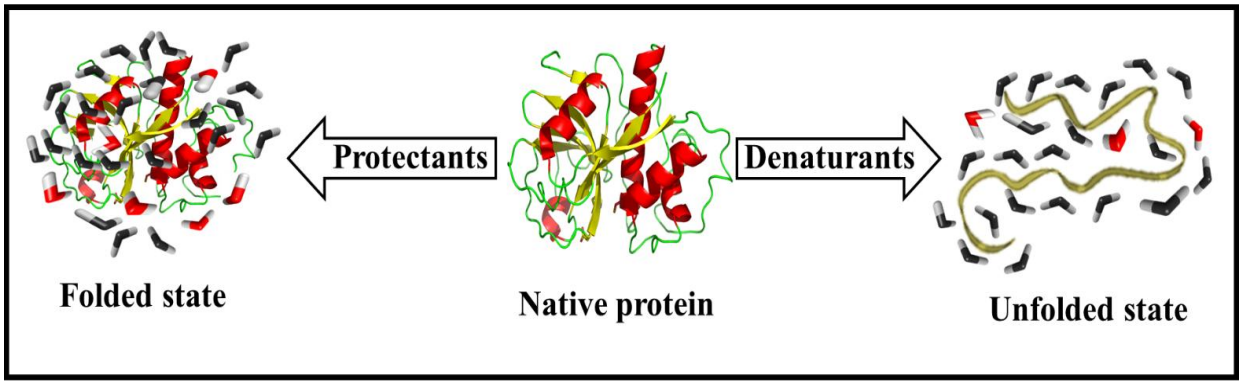

Figure 2.1: The stability of a protein in presence of co-solvents.

Basically, all biological processes depend on molecular recognition, which either is intermolecular as in ligand binding macromolecule complexes, or intramolecular between protein functional groups. Therefore, it is very essential for a protein to be in its native state (folded state) to accomplish several biological functions. Consequently, plenty of work has been done on the structure and stability of different proteins in ILs. Figure 2.2 signifies the year-wise journals straightly dealing with the stability of proteins/enzymes in the presence of different combination of ILs. However, medium-induced proteins stability using ILs are likely to be used progressively more in a valuable approach for enhancing the performance of enzymes/proteins.

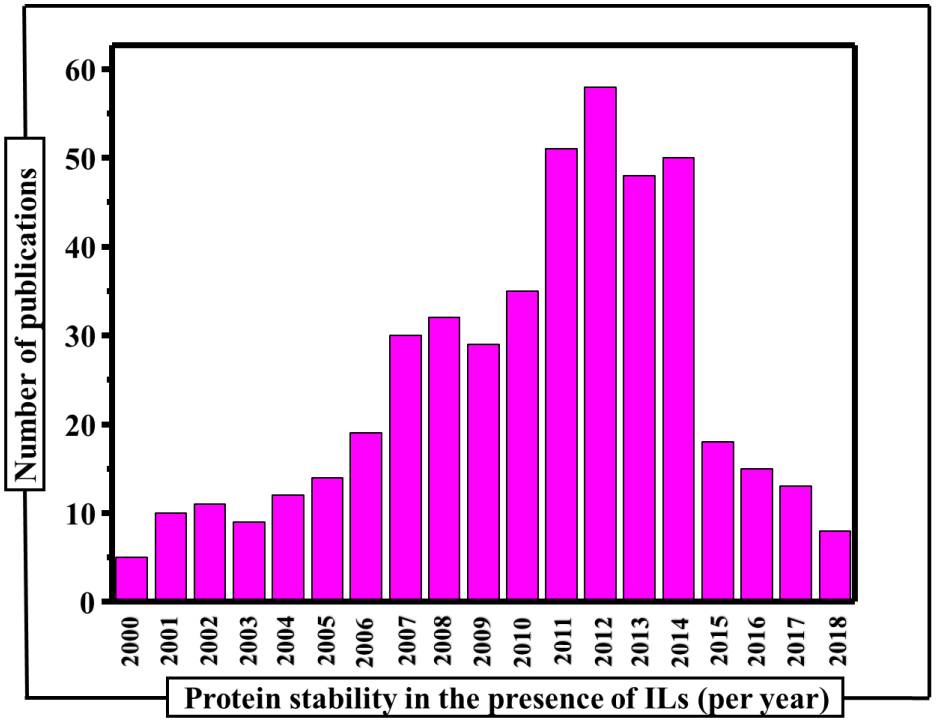

Figure 2.2: A number of publications regarding protein stability in ILs as a function of the year based on our own literature survey up to June 2018.

The protein stability using novel reaction media is definitely and consistently evolving. Biocompatible ILs has been exposed to be suitable media for proteins stabilities and their synthetic reactions. In recent times, these ILs are being recognized as the good solvent media

for the comprehensive study of protein folding/unfolding. ILs have developed as a novel class of solvents that have significantly improved protein stability in surrounding environments [146–149]. Protein folding is usually carried out in dilute aqueous solutions in order to prevent protein aggregation and improvement of a renaturation additive avoiding aggregation. In specific, the influence of ILs on protein structure has only recently become a focus of study and fascinated considerable attention. In the beginning, the first significant statement on the stability of protein in the presence of ILs was explored by Flowers and Summers [150] in 2000. Subsequently, a lot of researchers have been reported plenty of works on the stability of several proteins in different ILs. In this context, Sankaranarayanan et. al., [151] investigated the key role of ILs in folding/unfolding reversible studies of globular protein and also proposed after a specific concentration of ILs change from helical to β-sheet structure conformation takes place which finally resulted in the pre-fibrillar state [152]. Moreover, the stability, activity, and specificity of enzyme/protein are often connected to the solvent properties of ILs such as hydrophobicity, viscosity, polarity, hydrogen-bond basicity, ion kosmotropicity and nucleophilicity of anions.

2.1.1 The influence of imidazolium-based ionic liquids on the stability and activity of various proteins

The stability of proteins is among the most fascinating and essential developing scientific research fields whereas ILs are beginning to play a role in protein science. The major interest of biological applications including proteins and ILs, additional studies has been devoted to many aspects of structure and stability of proteins and enzymes in ILs. Several attention-grabbing studies related to the various ILs interactions with proteins have been carried out focussing on the role of ILs on protein folding/unfolding studies. In this respect, it can be concise that ILs are promising as potential solvents in various scientific applications. Subsequently, dissolving ILs in an aqueous solution as co-solvents have been a more advantageous approach in this area and

will be the focus of this literature survey. The uses of proteins in imidazolium-based ILs have improved because of their outstanding electrochemical properties, for example an extensive potential window, high conductivity, as well as selective tunable extraction properties [153,154]. In recent years, Kumar et al. [155] and Egorova et al. [156] concluded that the imidazolium-based ILs were helped to understand the proposed mechanism behind the identified effects on protein stability, and improve better ILs.

Table 2.1 The influence of various ILs on the stability and activity of proteins.

Author and Reference	Protein	ILs	Stabilized Destabilized	Activity of the biomolecule
Takekiyo et al. [157]	Cyt C and Lyz	(EAN) ([Bmim][SCN])	Stabilized	
Lu et al. (158)	Cyt C	([Emim][Br]), ([Bmim][Br]) and ([HMIM][Br])		
Fujita et al.(159)	Cyt C	([Bmim][DHP]), Bmim][CH_3COO]), ([Bmim][$MeSO_4$]), ([Bmim][Cl]) and ([Bmim][lac])		
Diego et al. (146)	CT	([Emim][NTf2])	Stabilized	
Lozano et al. (160)		([Emim][BF_4]), ([Emim] [NTf_2]), ([Bmim][PF_6])- ([Bmim][BF_4]), ([Bmim][PF_6])and ([MTOA][NTf_2])	Stabilized	
Noritomi et al. (161)		Noritomi ([Emim][FSI]) and ([Emim][PF_6])	Destabilized	
Bisth	BM	([Bmim][Br]) and ([Bmim][Gly])	Stabilized	

et al. (162)				
Jha et al. (163)	BM	([Amim][Cl])	Stabilized	
Lange et al. (164)	Lyz	([Bmim][Cl]), ([OH-Pmim][Cl]) and ([OH-Emim][Cl])	Destabilized	
Wang et al. (165)	Lysozyme	([Bmim][Br]), ([Bmim][BF4]), ([Mmim][I]) and([Bmim][Cl])	Stabilized	
Mandal et al. [166]	Lysozyme	([Bmim][OS])	Destabilized	
Kumari et al. [167]	Lysozyme	([Omim][Cl])		activity increased
Yamaguchi et al. [168]	Lysozyme	([Bmim][Cl])	Destabilized	
Shu et al. [169]	Bovine serum albumin	([DBmim][Cl]), ([Bmim][Cl]) and ([Bmim][NO_3])	Destabilized	
Satish et al. [170]	Bovine serum albumin	([Bmim][Cl])		
Huang et al. [171]	Bovine serum albumin	[Bmim] [Cl], [Hmim] [Cl] and [Omim] [Cl]		
Zang et al. [172]	myoglobin	[Bmim][BF_4^-],[Bmim][NO_3^-], [Bmim][Cl^-], and[Bmim][Br^-]	Destabilized	
Safavi et al. [173]	myoglobin	([Bmim][Cl])		
Jha et al. [174]	haemoglobin	([Bmim][Cl]), ([Emim][Cl]), ([Dmim][Cl]) and ([Hmim][Cl])	Destabilized	
Pei and Li [175]	haemoglobin	([C_6mim][Br]), ([C_8mim][Br]), ([C_4mim][Br]), ([C_6mim][Cl]) and ([C_4mim][Cl]		
Lin et al.	haemoglobin	([Omim][Br])		

[176]				
Akdogan et al. [177]	Human serum albumin	([Emim][NO_3]), ([Emim][DMP]), ([Emim][BF_4]), ([Emim][SCN]), ([Emim][$EtSO_4$]), and ([Emim][DCA])	Destabilized	
Silva et al. [178]	Human serum albumin	([C_2mim][Cl]), ([C_2mim]- [dca]), ([C_4mim][Cl]), ([C_4mim][dca]), ([C_2OHmim][Cl]), ([C_2OHmim][dca]), ([C_4dmim][Cl]) and ([C_3Omim][Cl])	Destabilized	
Bisht et al. [183]	α-chymotrypsin	[Ch][Ac], [Ch][Cl], [Ch][Dhp] and [Ch][OH]	Stabilized	
Weaver et al. [184]		([Ch][DHP])		activity Decreased
Fujita et al. [159]	Cytochrome-C	([Ch][Dhp])		Maintained activity
Fujita et al. [185]	Cytochrome-C	([Ch][Dhp])	Stabilized	Maintained activity
Rodrigues et al. [186]	Lysozyme	([Ch][DHP]), ([Ch][TMA]), ([Ch][Prop]), ([Ch][Hex]), ([Ch][DMP]), ([Ch][TFMS]), ([Ch][TF_2N]), ([Ch][Lac]) and ([Ch][Cl])	Stabilized	
Bisht et al. [187]	Cytochrome-C	([Ch][Glu]) and ([Ch][DHP])	Stabilized	Maintained and increased activity
Vijayaraghavan et al. [188]	DNA	([Ch] [DHP])	Stabilized	
Matias et al. [189]	Cytochrome-C	([Ch][DHP])	Stabilized	
Curto et al. [190]	lactate oxidase	([Ch][DHP]) and ([Ch][Cl])	Stabilized	
Kowacz et al. [191]	Lysozyme	([Ch][Cl]), ([Ch][Ac]), ([Ch][Lac]) and ([Ch][C_1SO_3])	Stabilized	
Constantinescu et al.	RNA	as ([Ch][DHP]), ([Ch][Cl])	Destabilized	

[192]				
Attri et al. [199]	α-chymotrypsin	(TEAP), (TEAA), ([TBP][Br]), ([BZmim][BF_4]) and ([BZmim][Cl]),	Destabilized	
Kennedy et al. [200]	Lysozyme	(EAF), (EOAN), (EAP), (EAN), (EAMs), (EAA), (EAP), (TEOAN), and (EATfA)		
Hekmat et al. [201]	Lysozyme	(EAF), (EAN), (DMEG) and ([MeOEAAc])		activity Decreased
Mann et al. [202]	Lysozyme	(EAF), (PAF) and (MOEAF)	stabilized	
Ebrahimi et al. [203]	Photinus pyralislucifer ase	([TMG][Pro]) and ([TMG][Lac])	stabilized	Maintained activity
Jha et al. [204]	hemoglobin and myoglobin	[TEAH], [TMAH], [TBAH] and [TPAH]	Destabilized	
Kumari et al. [205]	Human serum albumin	([BMOP][Br])		
Cunha et al. [206]	α-chymotrypsin	([BMPYR][Cl]) and ([BMPYR][Cl]).		increased activity
Tarannum et al. [207]	collagen	(PEP) and (PMS)	Destabilized	
Sankaranarayanan et al. [151]	Myoglobin	([Emim][OH])		
Patel et al. [151] [208]	Bovine serum albumin	([DMP][I])	Destabilized	

Takekiyo et al. [157] reported that (EAN) and ([Bmim][SCN]) can be utilized as cryoprotectant of cytochrome C (cyt C) and lysozyme (Lyz). However, these both ILs remarkably reduced the activity and induced unfolding of secondary structure of cyt C and lysozyme. After the exclusion of these two ILs by dialysis after cryo-preservation and consequent heating, the activities of both cyt C and lysozyme regained to > 90% and the

conformation structural changes were recuperated (i.e. refolded) at IL concentrations > 10%. This work revealed that the unfolding effect of imidazolium-based ILs is mostly reversible.

Lu et al. [158] completed the extraction study of Cyt C in the presence of imidazolium-based ILs with variable alkyl chain lengths such as ([Emim][Br]), ([Bmim][Br]) and ([HMIM][Br]). The outcomes revealed that 94% of the Cyt C can be extracted into the rich phase of ILs during the extraction method. From the results, they concluded that this aqueous two-phase system has the potential to be applied to extraction and concentration of Cyt C.

Consequently, Fujita et al.[159] studied the structure and stability of Cyt C in ([Bmim][DHP]), ([Bmim][CH_3COO]), ([Bmim][$MeSO_4$]), ([Bmim][Cl]) and ([Bmim][lac]). From the experimental results, the authors identified that ILs having anions such as tetra fluoroborate and chloride are not noble solvents for Cyt C even after the adding of 20 wt % water, despite the insignificant basicity as well as hydrogen bonding potential.

In other works, Diego and co-workers [146] explored the formation of stabilization capability of ([Emim][NTf2]) on CT and the stability of CT in this IL was compared with 3 M sorbitol, 1-propanol and water. Among all the co-solvents, IL was found to be a good stabilizing agent for CT structure, as compared with different solvent media. Due to their excellent properties, ILs appeared as a good alternative to organic solvents for emerging hygienic biotechnological processes.

Later, Lozano et al. [160] found that the CT stability has improved during esterification process in the presence of ILs such as ([Emim][BF_4]), ([Emim] [NTf_2]), ([Bmim][BF_4]), ([Bmim][PF_6]) and ([MTOA][NTf_2]). Among all the ILs, ([Bmim][PF_6]) was acted as the best stabilizing IL for CT structure. They explicitly anticipated at the first time that ILs were best suitable solvent media for protein stability.

Noritomi et al. [161] revealed that CT exhibited activity in the presence of two different ILs such as ([Emim][FSI]) and ([Emim][PF_6]) at 80 ^{0}C, whereas increasing the temperature of ILs the activity of CT was decreased. Moreover, the activity of CT is strongly affected by various anions of the ILs.

In 2016, Bisth et al. [162] investigated the Interactions of bromelain (BM) with ([Bmim][Br]) and ([Bmim][Gly]) by using different techniques. They were found that the anion moieties of the imidazolium-based ILs play a vital role towards to the structure of the protein. However, the ([Bmim][Br]) not only acted as best stabilizers for the bromelain native state but also defend the BM against thermal unfolding of BM structure. In their results, they observed that as ([Bmim][Br]) is more biocompatible as compared ([Bmim][Gly]) for stabilizing the BM structure. In conclusion, the spectroscopic and enzyme activity results shown that tertiary structure of BM is completely maintained at high concentration (0.05-0.1 M) of both imidazolium family ILs.

Jha et al. [163] observed the conformational stability, enzyme activity and thermal stability of BM in the presence of ([Amim][Cl]) using various spectroscopic methods. Excitingly, CD and fluorescence results indicated that the low concentrations (0.01−0.10 M) of ([Amim][Cl]) are ostensible only altering the structural arrangement of the BM without having strong significances on their enzyme activity and stability. The thermal stability of BM in the presence of IL was continuous decrease with increasing concentration of ILs (except 0.01 M).

Lange et al. [164] Investigated the effect of ([Bmim][Cl]), ([OH-Pmim][Cl]) and ([OH-Emim][Cl]) on the stability of lysozyme. The authors are found that the transition temperature (Tm) of lysozyme (Lyz) decreased remarkably with increasing cation alkyl chain length of the ILs. After testing the effect of all imidazolium family ILs, again they confirmed that increasing the hydrophobicity and the alkyl chain length of cation moiety abnormally

decreases the conformational stability of Lyz. Though, insoluble aggregates were prevented in the higher concentration of 2 M of each IL after denaturation of selected protein and dilution into each IL, and at 0.5 M lower concentrations, ([Hmim][Cl]) was the maximum effective suppressor of insoluble aggregates, whereas less hydrophobic cations were not as active.

Moreover, Wang et al. [165] reported the Tm values of Lyz crystals produced in different imidazolium-based ILs as an additive and thermaly increased from 65.6 to 71.4 °C ([Bmim][Cl]), 81.2 °C ([Bmim][BF_4]), 78.2 °C ([Mmim][I]), and 81.9 °C ([Bmim][Br]). Therefore, the enhanced thermal stability attained with the ILs followed the trend as: ([Bmim][Br]) > ([Bmim][BF4]) > ([Mmim][I]) > ([Bmim][Cl]) . The thermal stability of Lyz crystals was ascribed to enhanced crystal contacts, changes in conformational stability, and intermolecular interactions between ILs and lysozyme molecules, which affected Lyz nucleation and crystal development and morphology.

Mandal et al. [166] studied the destabilizing effect of ([Bmim][OS]) on Lyz. It is very necessary to know the effect of ILs on the structure and stability of lysozyme in an aqueous medium, and understanding the molecular level is required to achieve a deeper insight into the interactions between ILs. The variations in the structure of Lyz were monitored using spectroscopic techniques in phosphate buffer medium (pH 6 and 8) at 25 ^{o}C. Tryptophan residues in the presence of lyz made it fluoresce which was quenched by the interaction with the IL. Both static and dynamic quenching was observed in the presence of fluorescence analysis.

Kumari and co-workers [167] investigated the dependency of the enzymatic activity of hen egg white Lyz (HEWL) in the presence of ([Omim][Cl]). The results showed that IL significantly quenches the fluorophore of lysozyme by static quenching mechanism. The

thermodynamic parameters show that the interaction of ([Omim][Cl]) bind to protein functional groups are dominated by hydrophobic interactions. Additionally, based on the UV and CD results, the authors determined that the imidazolium-based IL induce the conformational change in lysozyme protein and increase its enzymatic activity.

Yamaguchi et al. [168] studied denaturation of Lyz in the presence of different hydrophobic imidazolium cations joined with a Cl anion and observed that refolding was best attained with short N-alkyl chain length of the cations, with ([Bmim][Cl]) attaining the maximum refolding yield of 84%. Furthermore, Increasing the alkyl chain length and hydrophobicity of the cation moiety of the ILs decreased the refolding yield.

Furthermore, Shu et al. [169] studied the interaction of imidazolium family ILs such as ([DBmim][Cl]), ([Bmim][Cl]) and ([Bmim][NO_3]) with bovine serum albumin (BSA). By means of spectroscopic results, they were concluded and interpreted the loss of secondary and tertiary structure of BSA influenced by various amounts of ILs and determined that the driving forces contain hydrophobic and electrostatic interactions. In contrast, the influence of these ILs on the conformation stability of BSA decreased according to the following order of ([Bmim][NO_3]) > ([Bmim][Cl]) ≈ ([DBmim][Cl]).

A study by Satish and Millan [170] on BSA exhibited that imidazolium-based ILs of cations play an important role in stabilizing BSA against thermal denaturation. The thermodynamic investigation revealed that very weak interactions occur in between BSA and ILs. Authors revealed from their study, hydrophobicity played a vital role in the destabilization of BSA as well as destabilization increased promptly as a function of concentration in the presence of more hydrophobic ([Bmim][Cl]). Therefore, it was found that the thermal stability of BSA in the presence of ILs follow the order as ([Emim][ESO_4]) > ([Emim][Cl]) > ([Bmim][Cl]).

Huang et al. [171] explored the interaction of BSA in the presence of fixed imidazolium chloride [Cl^-] anion from three different cations such as [Bmim], [Hmim] and [Omim], by using UV, fluorescence. The obtained results indicated that imidazolium-based ILs interacted with tyrosine (Tyr) and tryptophan (Trp) residues, changing the native structure as well as the internal hydrophobic form of BSA. The UV results exhibited that the after addition of the ILs will cause redshift of BSA absorption peak and decrease the adsorption intensity.

Zang et al. [172] investigated the effect of the same cation 1-butyl-3-methylimidazolium (Bmim) with different combinations of anions such as BF_4^-, NO_3^-, Cl^-, and Br^- in phosphate buffer solution on the stability of myoglobin (Mb). Conforming denaturation intermediates of Mb were nearly related to those obtained results in the absence of sodium salts in phosphate buffer solution. These observed results indicate that [Bmim] cation can promote the unfolding of Mb. Finally, the results revealed that the denaturation ability of imidazolium family ILs increases with increasing alkyl chain length of the cation of ILs as well as that hydroxyl-substituted imidazolium cation could also encourage the unfolding of Mb.

Safavi and research group [173] significantly reported the Mb in IL interaction by using UV-vis spectroscopy and displayed that Mb maintains its native structure in the presence of ([Bmim][Cl]) as a function of temperature. By means of the gradual increasing of ([Bmim][Cl]) up to 0.2 M, there are no significant changes in the UV spectrum was observed. Furthermore, they revealed that the bioactivity of the protein was retained in presence of 0.2 M concentration of IL. This indicates that the Mb is almost stable below these conditions. The conformational variations in the properties of the Mb with the addition of IL might be because of the changes in the environment in Mb.

In 2015, Jha et al. [174] extensively explored the different cationic effect of ([Bmim][Cl]), ([Emim][Cl]), ([Dmim][Cl]) and ([Hmim][Cl]), on the conformational stability of haemoglobin (Hb) protein at various concentrations of ILs in buffer solution, and they concluded that the

destabilization trend of ILs toward Hb increases with increasing the cation chain length of ILs. Moreover, the imidazolium cations of ILs complied with the Hofmeister arrangement when arranged in the sequence of providing stability to protein structure.

Pei and Li [175] reported that 76-100% of the Hb can be extracted into the IL rich phase in only singular point separation in the presence of imidazolium family ILs. It is indicating that partitioning of the proteins is dominated by the hydrophobic interactions between the Hb and cations. In contrast, The ability of the alkyl chain length of the cations of the ILs for phase separation process follows the trend: ([C_6mim][Br]) > ([C_8mim][Br]) > ([C_4mim][Br]) > ([C_6mim][Cl]) > ([C_4mim][Cl]).

Lin et al. [176] identified that 1-octyl-3-methylimidazolium bromide ([Omim][Br]) was the best suitable ionic liquid for extraction and separation of Hb. Absolutely, while the extraction process was ascertained by hydrophobic interaction, electrostatic interaction also played a vital role in the intrinsic factors that were associated with the extraction efficiency of protein.

Akdogan et al. [177] observed the stability of Human serum albumin (HSA) in imidazolium-based ILs for example, ([Emim][NO_3]), ([Emim][DMP]), ([Emim][BF_4]), ([Emim][SCN]), ([Emim][$EtSO_4$]), and ([Emim][DCA]). From the experimental results, they determined that the denaturation of HSA after adding of ILs was concentration dependent also the denaturation of the ILs over HSA follows the trend ([Emim][DMP]) < ([Emim][NO_3]) < ([Emim][BF_4]) < ([Emim][$EtSO_4$]) < ([Emim][SCN]) < ([Emim][DCA]).

Silva et al. [178] observed that longer alkyl side chain lengths of imidazolium cations are more hydrophobic and are related to a greater destabilizing effect on HSA than short alkyl groups. An increase in the alkyl chain length of cations of ILs leads to destabilization of native protein hydrophobic interactions along with a greater aggregate of binding. This conformational limitation affected by ion-interaction makes some difficulty in the three-dimensional structure and although a more squeezed structure.

2.1.2 The conformation structure and stability of various proteins in the presence of choline-based ionic liquids

The different families of ILs, particularly choline-based ILs and their derivatives, have gained great attention in the recent decades for their distinct outcome on protein stability and specious biocompatibility. Hence, the investigation of protein and choline-based IL interaction is necessary to observe the result of a particular effect on the conformational and structural stability of the protein. Moreover, choline family ILs have established as one of the best suitable applicants for stabilization of biopharmaceuticals and biotechnological because of their biocompatibility and distinct effect on protein structure and stability [179,180]. From the previous studies, it was found that cholinium-based ILs are highly biocompatible, metabolism, transport of lipids, less toxic to an acceptable range, biodegradable, cytotoxicity as well as they are able to degrade completely under aerobic conditions [181,182]. According to,

Bisht and Venkatesu [183] comprehensively revealed the effect of choline family ILs on the conformational structure, stability and activity of CT. The conformational and thermal stability of CT in the presence of different choline family ILs followed the trend [Ac] > [Cl] > [DHP] >> [Cit] >> [OH] with ([Ch][Ac]) having the best overall stabilizing effect on CT, increasing Tm values from ~ 49 to 63 ℃ as a function of concentration. Moreover, the activity of CT in the presence of choline-based ILs similarly followed a related order, excluding ([Ch][Cit]) decreased the proteolytic activity of CT more than ([Ch][OH]), and a slight increase in activity was observed with ([Ch][Ac]); such that the according to the follow order: [Ac] > [Cl] > [DHP] >> [OH] >> [Cit]. These results were clearly indicated that the anions of ILs play an important role in affecting the structural stability and the enzymatic activity of CT.

Weaver and Vrikkis [184] investigated the effect of [Ch][DHP] on the thermal and structural stability of Lyz and recombinant human interleukin-2 (RHIL-2) at different concentrations. Increased IL concentrations from (20 to 40% w/v) resulted in increased α-to-β change in the secondary structure of lyz at various pH (pH 4 and 7.2). On the other hand, again increasing the concentrations of IL (0.5 to 12% w/v) enhanced the secondary order of rHIL-2 by reducing the amount of unordered content. The Tm of rHIL-2 was found, particularly at the higher concentration (12% w/v or 680 mM), increasing from 61.7 to 74.2 °C. Lyz Tm values were also increased with increasing concentrations of IL; (40% w/v) ([Ch][DHP]) at pH 7.2 shifted the Tm from 73.7 to 88.8 °C. The experimental results demonstrate that ([Ch][DHP]) prevents denaturation of Lyz and RHIL-2 by interactions on the protein surface but changes the secondary structural features in a way dependent on the Lyz. Furthermore, thermal denaturation of Lyz, as well as RHIL-2, formulated with IL lead to in the development of irreversible aggregates.

Fujita et al. [159] studied that Cyt C displays no important structural change and maintains its activity when dissolved in the [Ch][Dhp]. Additionally, the protein was active even after 18 months of storing at room temperature. Other studies also show related results, [Ch][Dhp] is best biocompatible IL for several biomolecules.

In this same direction, Fujita et al. [185] investigated the stability and utility efficiency of Cyt C in [Ch][Dhp]. From their results, they concluded that IL provides a stabilizing solvent for Cyt C and the structural stability and activity of the protein was maintained even after 180 days of storage at room temperature. However, the thermal stability behavior of protein was slightly changed after 4 months storage in the [Ch][Dhp].

Rodrigues et al. [186] enhanced the structure and stability of Lyz in the presence of a choline-based ILs such as ([Ch][DHP]), ([Ch][TMA]), ([Ch][Prop]), ([Ch][Hex]), ([Ch][DMP]), ([Ch][TFMS]), ([Ch][TF_2N]), ([Ch][Lac]) and ([Ch][Cl]). Authors shown that ([Ch][DHP]) is

best stabilizer, whereas ([Ch][TF_2N]) is weak destabilizer among all studied choline family ILs for Lyz. The stability order for the anions of choline family ILs was observed to be following the order: [DHP] > [DMP] > [Lac] > [Cl] >> || [Prop] > [TFMS] ~ [TMA] > [Hex] > [TF_2N]. The effect of choline family ILs was also found to be totally concentration dependant; for example, ([Ch][DHP]) had a destabilizing effect above 0.5 M and a stabilizing effect above this concentration.

Very recently, Bisht et al. [187] observed various choline ILs coupled to (di-carboxylate) anions -based and DHP as best potential media for long-term stability of cyt C. Among the various choline family ILs investigated, >50- fold catalytic activity of protein was observed in the aqueous solution of choline glutarate [Ch][Glu] at 50% w/v of the IL, compared to phosphate buffer solution (PBS), and >25-fold compared to ([Ch][DHP]) ~ 33% w/v. Moreover, the catalytic activity of the protein in ILs was maintained against various external stimuli, denaturants (H_2O_2 and GuHCl) as well as temperatures about 120 °C, along with long-term storage of up to 21 weeks at room temperature. It is interesting to note that the activity of the enzyme is increased with the partial unfolding of the tertiary structure. Additionally, they discovered that the choline family ILs have more capability to enhance both the stability and activity of Cyt c.

Vijayaraghavan et al. [188] reported that DNA reveal excellent long-term stability in hydrated choline-based ILs and observed that ([Ch] [DHP]) supportive as a best chemical DNA stabilizing agent and a nuclease inhibitor. Interestingly, Uv-CD results indicated that the characteristic positive band at 275 nm and a negative band at 245 nm resulting from the confirmation of DNA in IL. Moreover, these specific CD bands are still present even after 6 months of long-term storage at room temperature.

Later, Matias et al. [189] The obtained results indicate that no significant changes in the redox behavior of Cyt c in ([Ch][DHP]) versus the corresponding buffer PBS were found that

may be attributed to the presence of the IL in the aqueous solutions. These results recommend that by the usage of the cholinium-based IL, protein stabilization and biocompatibility aspects can be judiciously designed and conserved.

Curto and co-workers [190] studied the ions effect of various choline based ILs on the structure, stability and biocatalytic activity of an important enzyme lactate oxidase (Lox). The CD results reveal that the secondary structure of the enzyme exhibited changes in the α-helix and *β*-sheet unperturbed in ([Ch][DHP]) with a noticeable decrease of α-helices and a concomitant increase of β-sheets. Additionally, long-term structural stability results showed a significant ions effect on the Lox, particularly for ([Ch][Cl]), for which dropping to ca. 80% of the original (day 0) activity is retained after storage 140 days at high temperature (51°C). Furthermore, Lox in the presence of DHP and Cl anions thermally denatured at 90°C indicates that irreversible aggregation of the enzyme has occurred. In conclusion, ([Ch][DHP]) performance was well in terms of protein stabilization.

Kowacz et al. [191] observed that the concentration effect of choline family ILs such as ([Ch][Cl]), ([Ch][Ac]), ([Ch][Lac]) and ([Ch][C_1SO_3]) on the crystal structure development of the Lyz. The experimental results reveal that biocompatibility and protein stabilization of cholinium-based ILs can be rationally designed and preserved. Finally, experimental results reveal that Lyz stabilization and biocompatibility physical characteristics can be preserved and designed rationally in the form of the cholinium-based ILs.

The study by Constantinescu et al. [192] reported the Tm values at various concentrations of the choline-based ILs such as ([Ch][DHP]), ([Ch][Cl]) and other ILs for the thermal stability of ribonuclease A (RNA). The results indicated that except for ([Ch][DHP]), among all other ILs show destabilization tendency toward the RNA. In the case of ([Ch][DHP]), while the hydrophobic choline cation is identified to levy destabilization, in the presence of a good

stabilizing anion like dihydrogen phosphate can override the influence of choline to provide stabilization against destabilization, hence the resultant increase in thermal stability.

2.1.3 The conformation structure and stability of proteins in the presence of some other ILs

Apart from above studies, there are still several research activities on stabilization/ destabilization of some other protein in the presence of different ILs [193–198].

Attri et al. [199] identified that the CT structure of the native state is not changed in the presence of ILs. The experimental results clearly differentiate the variation of Tm values, which relate to the transition temperature of CT to the unfolded state, as a function of the concentration of IL. As can be seen that ILs promptly increase Tm values of CT (varying from 42.0 C in the absence of ILs) to 65.0, 62.0, 52.0, 50.0 and 49.0 ^{0}C in the presence of ILs such as (TEAP), (TEAA), ([TBP][Br]), ([BZmim][BF_4]) and ([BZmim][Cl]), respectively.

Kennedy et al. [200] investigated the effect of (EAF), (EOAN), (EAP), (EAN), (EAMs), (EAA), (EAP), (TEOAN), and (EATfA) on the crystallization process of Lyz. Their experimental results reveal that these 10 ILs surrounded by the concentrations of 100–200 mM can be utilized as an effective and suitable solvent for the crystallization process of the Lyz. Afterward, they specified that the impact of the ILs as additives on the crystallization of protein was different for each studied ILs, as well as they, determined that the influence of the ammonium family ILs on Lyz is absolutely IL specific.

Hekmat et al. [201] also examined the activity mechanism of the crystallization process of Lyz in ammonium-based ILs such as (EAF), (EAN), (DMEG) and ([MeOEAAc]). Moreover, the biocompatibility of the protein was also concluded by during long- period measurement of the complete relative protein activities. These authors finally detected that the protein activities were decreased only to 10–15% in ammonium based ILs.

Mann and co-workers [202] found that the (EAF), (PAF) and (MOEAF) were behaved as good stabilizers for Lyz structure as well as threatened the protein against thermal denaturation. From Uv-CD results, authors revealed that the thermal stability of the lysozyme in ILs was depended on the total amount of water in the IL compound. Obviously, the unfolded protein was perceived to be absolutely refolded by all ammonium-based IL in the presence of 25% of water content present in the aqueous solution.

In contrast, Ebrahimi et al. [203] studied the stability and activity of photinus pyralisluciferase in tetramethylguanidine-based ILs such as ([TMG][Pro]) and ([TMG][Lac]). The authors observed that the enzyme activity increased up to 0.25 M concentration of ([TMG][Lac]) similarly the activity reduced in the presence of same concentrations of ([TMG][Pro]). Additional, spectroscopic study of thermal stability exhibit good stability of enzyme only in the presence of ([TMG][Lac]). Finally, they concluded that in the presence of two ILs lactate anion has enhanced thermal stability and activity as compared to propionate anion.

Jha et al. [204] enhanced the extent of stability of heme proteins such as hemoglobin (Hb) and myoglobin (Mb) in different ammonium-based ILs such as [TEAH], [TMAH], [TBAH] and [TPAH]. For both the heme proteins the stabilizing effects of these ammonium based ILs follow the trend TMAH < TEAH < TPAH < TBAH. Consequently, their experimental results exhibit that the after addition of ILs to the both heme proteins diminishes thermal stability and permitting both proteins to be in an unfolded state. Finally, they concluded that less viscous ILs carrying short alkyl chain of TMAH is strongest destabilizers of the heme proteins as compared to the long alkyl chain which is high viscous ILs, such as TBAH.

Kumari and research group [205] observed that the interaction of HSA in the presence of pyrrolidinium-based IL and ([BMOP][Br]) by using spectroscopic methods. The experimental results revealed that the utilization of pyrrolidinium-based IL, BMOP for stabilizing human serum albumin (HAS) native structure is a non-productive endeavor as the BMOP binds with

protein at hydrophobic pocket domain IIA of the protein with hydrophobic, van der Waals and hydrogen bonding whereas hydrophobic interactions were main dominating.

Cunha et al. [206] explored the catalytic activity efficiency of CT that can be increased from 2.74 (in buffer) to 5.36 as well as 6.47 in the presence of pyrrolidinium-based ILs such as ([BMPYR][Cl]) and ([BMPYR][Cl]).

Tarannum et al. [207] observed the effect of phosphonium family ILs such as (PEP) and (PMS) on the stability of collagen. The spectroscopic results illustrated that, the interaction of the ions in the ILs with the protein showing destabilization effect at higher concentration levels. Their spectroscopic results concluded that the anion plays an important role on the higher level of molecular interaction with collagen towards the stabilization or destabilization of protein in the presence of phosphonium based ILs.

Further, Sankaranarayanan et al. [151] were studied the effect of phenylalanine-based IL (Phe-IL) on the structural stability of myoglobin (Mb) in aqueous solution as well as the structural changes in the Mb were experimentally observed using fluorescence and circular dichroism (CD) spectroscopy. The spectroscopic results showed that the stability of the Mb is completely depended on the concentration of the IL. This is probably because of the exposure of the Trp to a more polar environment in Phe-IL.

Patel and group [208] investigated the effect of [DMP][I] on the structural stability of BSA. Fluorescence spectroscopic results confirmed that pyrrolidinium family IL strongly quenches the intrinsic fluorophore of protein. Interestingly, the stability of BSA in pyrrolidinium IL was decreased rapidly with increase in temperature. FTIR results indicated that the conformational stability of BSA in the presence of IL shifted from native folded form towards to unfolded form of protein, respectively. Furthermore, the interaction between BSA and [DMP][I] were mainly dominated by the van der and hydrogen bond interaction forces.

2.1.4 The protein stability in Hofmeister series of ionic liquids

The phenomenon of Hofmeister series includes the particular effects of ions in aqueous solution and was primarily connected to the solubility of biomolecules [209,210]. The Hofmeister series of ions influence the specific interaction of cations and anions of different families of ILs with proteins/enzymes [211,212]. The effect of Hofmeister ions are having a huge impact on a series of biological existences though, it is still very far from thoroughly understood in the research field of protein folding/unfolding studies [213,214].

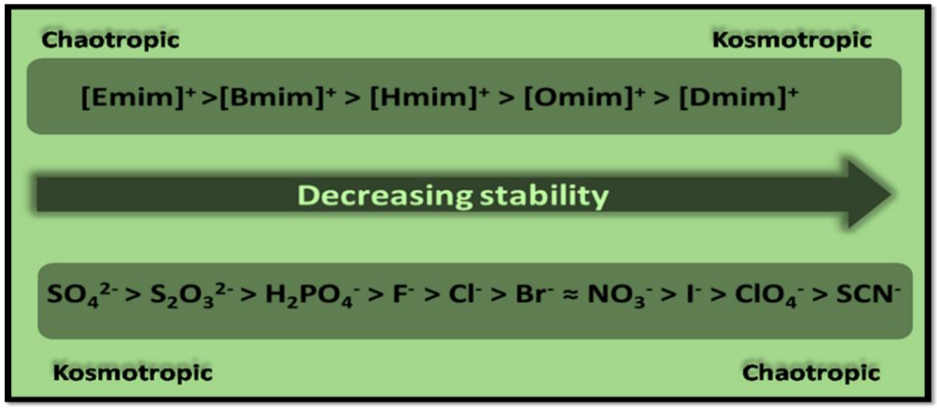

Figure 2.3: The stability order of anions of Hofmeister series.

These biomolecular interactions depend on the basis of ion properties and there are classified as Kosmotropes are known as 'structure-makers' and chaotropes are known as 'structure breakers'. The strong interaction of kosmotropes is mainly considered as 'structure-makers' because they increase the protein/enzyme stability in an aqueous medium. In contrast, weak interaction of chaotropes are the 'structure breakers' and they decrease the stability of proteins in aqueous solution [215,216]. Moreover, a combination of kosmotropic anions and chaotropic cations is the best medium to study the stability/destability of proteins in the presence of ILs [217]. Figure 2.3 shows the stability order of anions of Hofmeister series [330]. In the past few years, series of ion effects involving on protein aggregation was carried out by, Geng et al. [218] studied the interaction of BSA with imidazolium-based IL, [C_{14}mim][Br]. This experimental results showed the structural stability of a secondary structure of the BSA

was completely depends on the concentration of the IL which is used in this study. Interestingly, the hydrophobic interactions were destabilized the protein structure, which is predominant in the case of [C_{14}mim][Br] with a higher number of C-atoms in the chaotropic cation chain length. From all of the above results, authors demonstrated that though the kosmotropic anions of IL play an important role in protein stabilization, although the donating effect of the cation chain cannot be ignored.

Debeljuh et al. [219] studied a reversed Hofmeister series when protic ammonium-based ILs were listed in order of fibrilization rate and structure association of Aβ16-22 peptides sequence. These authors found that PILs having kosmotropic anions such as phosphate (PO_4^{3-}) and sulfate (SO_4^{2-}) encourage fibrilization with developed fibrils making inside whereas PILs consisting the mesylate (Ms) anion totally quashes amyloid fibrillization. The addition of highly ordered anions might cause the disorderliness of the protein.

Heitz et al. [220] investigated the effect of imidazolium family ILs such as ([Bmim][Cl]), ([Hmim][Cl]), ([Emim][NO_3]), ([Emim] [$MeSO_3$]), ([Emim] [TFMS]), ([Emim] [Tf_2N]) and ([Bmim][$MeSO_3$]) on the enzyme activity of mushroom Tyrosinase enzyme. Concurrently, the increased hydrophobic interaction prompt stronger ion-ion interaction, therefore, the pattern was consistent with Hofmeister series. The results revealed that the enzyme activity was repressed by the ions of ILs with consistent of Hofmeister series. Moreover, Hofmeister series of more kosmotropic cations and chaotropic anions were the highest inhibition effect.

Yamamoto et al. [221] studied refolding effect of Lyz in the presence of pyridinium family series of ILs such as ([MPy][Cl]), ([AlPy][Cl]), ([BPy][Cl]), ([OPy][Cl]) and ([HexPy][Cl]). Though, all pyridinium-based ILs are unsuccessful to retain the native structure of the protein against the thermal denaturation of Lyz. On the other hand, the thermal stability of protein decreased with the increase in the alkyl chain length of the cation in the presence of IL.

Akdogan and Hinderberger [177] enhanced the protein stability of human serum albumin (HAS) in imidazolium-family ILs for example, ([Emim][NO_3]), ([Emim][DMP]), ([Emim][BF_4]), ([Emim][DCA]), ([Emim][$EtSO_4$]), and ([Emim][SCN]). The experimental results determined that the destabilization of protein after addition of ILs was concentration dependent manner (Protein was stable up to 35% of all ILs) and the denaturation action of the ILs over HSA follows the trend [DMP] < [[NO_3] > [BF_4] < [$EtSO_4$] < [SCN] < [DCA], respectively.

Shi and research group [222] explored the effect of ([Bmim][Cl]), ([Bmim][Br]), ([Bmim][PF_6]), ([Bmim][BF_4]), ([Bmim][OTf]) and ([Emim][Cl]) ILs on the catalytic features of alcohol dehydrogenase(ADH). Apparently, ADH exhibited higher activity and good stability in the presence of ([Emim][Cl]), ([Bmim][Br]), ([Bmim][Cl]), and ([BMIM][PF_6]) than especially displayed significant less activity and stability in the presence of ([Bmim][OTf]) or ([Bmim][BF_4]). Furthermore, the results revealed that Cl^- anion protects the ADH from thermo-inactivation more effectively than PF_6 anion. In addition, the authors concluded that the decrease in the stability of the ADH in the anions such as PF_6^- or OTF^- ILs is because of the maximum exposure of the Tyr AA residues of the ADH in the presence of selected ILs.

Recent years they are receiving a very good response from the industrial point because of their high surface activity, less aqueous toxicity as well as resistance to oxidation and reduction processes. Finally, similarly to imidazolium-based ILs, cholinium family ILs have also found intersting in protein stability studies. However, unexpectedly choline based ILs are found more biocompatible and less toxic than imidazolium-based ILs for BM structure.

To the best of our knowledge, there is no report in literature for BM + selected imidazolium or cholinium based ILs.

2.2 A review of the thermophysical properties of binary mixtures

An extensive literature review reveals that significant data have been accumulated on the thermodynamic/thermophysical studies of ionic liquids (ILs) and their binary mixtures. In many of the investigations, thermophysical properties that have been measured such as density (ρ), viscosity (η), speed of sound (u) and refractive index (n_D) as well as their excess/apparent parameters. Moreover, the extensive studies of composition dependency of the thermodynamic/thermophysical properties are used to understand the nature and macroscopic effects of the different types of molecular interactions which are present in liquids and their mixtures [223–225]. The understanding of the thermophysical properties of ILs with various solvents is one of the great significance for chemists as well as chemical engineers. In recent decades, huge numbers of various solvents have been utilized for several processes in academia by many scientific researchers from all disciplines associated to both academic and in industrial processes [2,226,227]. The thermodynamic/thermophysical properties of some of the investigated binary mixtures are listed below.

2.2.1 Excess molar properties

Table 2.2 Summary of the binary systems from literature is given below.

Author and Reference	Systems	V^E/ V_φ	$\Delta\kappa_s/ K_\varphi$	$\Delta\eta$	Δn_D
Xu et al.(228)	(N_4NO_3 + ethanol, methanol, 1-propanol, 1-butanol)	negative		negative	
Xu et al.(229)	(N_4AC+ methanol, ethanol, n-butanol, n-propanol)	positive		positive	negative
Bettencourt	([N_4Ac], [N_4Pro], [N_4Hex],	negative	negative	negative	

et al. (230)	and [N_4Dec] + ethanol)				
Olivieri et al. (231)	(NBAO + 1-butanol, 1-pentanol, 1-propanol, and 1-hexanol)				
Alvarez et al. (232)	(2-HEAA+ water, ethanol and methanol)	negative	negative		
Kurnia et al. (233)	(BHEAA + 1- propanol, methanol and ethanol)	negative			
Kurnia et al. (233)	(BHEMF+ methanol, ethanol, and 1-propanol)	negative		negative	
Massel et al. (234)	([N_{1114}]-[Tf_2N] +ethanol, 1-propanol) and (N,N-dimethylformamide (DMF))	Positive negative			
MohdTaib et.al(234)	([BHEAA]+ water) And ([BHEAA]+ [MEA])	Negative positive			
Pinto et al. (236)	([HEAP], [HEAB], [HDEAH], [HEAH] + water)	negative			
Umapathi et al.(237)	([DEAS], [DEAA], [TMAS], [TEAS], [TEAA and [TMAA] with water)	negative	negative	positive	positive
Hou et al. (238)	(N2Ac) and (N3Ac) with water	negative			positive

Attri et al. (239)	([TMAS], [TMAA] and [TMAP] + [DMF])	negative	negative	
Attri et al. (240)	([TEAH], [TMAH], [TPAH] [TPAH]+DMF)	negative	negative	
Kavitha et al.(241)	([DEAA], [DEAS], [TEAA], [TEAS]+ [NMP])			
Chhotaray et al. (242)	([PAF], [3-HPAA][3-PAF], [PAA], [3-HPATFA] +water and[NMP])			
Kavitha et al.(243)	([TPAH], [TMAH], [TBAH] ,[TEAH]+ (NMP))			
Usula et al. (244)	([XAN] with (NMP))	negative		
Govinda. et al (245)	([TEAH], [TBAH], TMAH], [TPAH]([Emim][$MeSO_4$]) + ([Emim][Cl]), [Bmim][Cl]), ([Bmim][BF_4]), [DMSO])			
Fan et al. (246)	([Emim][BF_4])+[DMF], and [DMA])	negative		negative
Wuet al. (247)	([C4mim][BF_4]) + (DMA), (DMF), (NMP), methanol, Acetonitrile)	negative		negative
Zarei et	([Emim][BF_4]), [DMA] and	negative	negative	

al.(248)	[DMF]		
Bahadur et al. [249]	([BMPYR][Br]) + water and methanol	positive	
Panda et al. [250]	([NMP][HSO_4]) and ([PY][HSO_4]) + water and [DMSO]	positive	positive and negative
Sumana et al. [251]	([PMPY][I]) and ([EMPY][I]) with acetonitrile	positive	negative
Alvarez et al. [252]	[2-HEAA] + water, ethanol and methanol	positive	positive
Kumar et al. [253]	([BHEA][CH_3COO]) and ([BHEA][For]) + water and ethanol	positive	positive
Dasthaiah et al. [254]	[BDMAH], [BDMAP] and [BDMAA] + water and ethanol	positive	positive and negative
Cai et al. [255]	([DMSCA][Tos]) + water and methanol	positive	
Kulhavy et al. [256]	(2-HDEAL) + water, methanol and ethanol	positive	positive and negative
Bahadur et al. [257]	([MOA][Tf_2N]) with ethanol and ethyl acetate	positive	positive
Bahadur et al. {Formatting Citation}	[MOA][Tf_2N] + methyl acetate and methanol	positive	positive and negative
Muscle et al. [259]	[DEAA], [DEAF], [DEAB] and [DEAP] + water	positive	positive
Pinto et al. [236]	[HEAP], [HEAB], [HDEAH], and [HEAH] + water	positive	
Gyanendra et al. [260]	[DEEAP] + water	positive	positive
Zafarani-Moattar et al. [261]	([TBA][PF_6]) and ([Bmim][PF_6]) and +methanol, [DMA], tetrahydrofuran, acetonitrile, and [DMSO]		

Zafarani-Moattar et al. [262]	([Bmim][Br]) + ethanol, methanol and water	positive
Shekaari et al. [223]	[Hmim][Br] + water	
Abdulagatov et al. [263]	([Bmim][BF_4]) + ethanol	negative
Gonzalez et al. [264]	([Hmim][TfO]) + 1-propanol, 1-pentanol 2-propanol, 2-butanol and 1-butanol	positive

Xu et al. [228] reported the ρ and η of (N_4NO_3) and its binary mixtures with alcohols such as ethanol, methanol, 1-propanol, and 1-butanol at various temperatures from (298.15 to 313.15K) and found the negative values for both excess molar volumes (V^E) and deviations viscosities ($\Delta\eta$) for all binary mixtures. The V^E values of all investigated binary mixtures increased with increasing the chain length of alcohols as well as decreased as a function of temperature. On the other hand, $\Delta\eta$ in the studied all binary systems increase rapidly as the temperature increases. Therefore, obtained negative results indicated that the V^E and $\Delta\eta$ values of four binary mixtures can be attracted to strong interactions as well as van der Waals interactions between IL and organic solvents due to an effective packing of the components in the mixture.

Xu and co-workers [229] performed the η, ρ and n_D for IL (N_4AC) with methanol, ethanol, n-butanol and n-propanol and their binary mixture under atmospheric pressure and temperature range (293.15 to 313.15) K. In other words they reported the n_D of above mentioned systems temperature range only at 298.15 K. The values of V^E, Δ_{nD} and $\Delta\eta$ were attained from the experimental values and fitted with the Redlich−Kister type equation. Positive values were obtained for V^E and $\Delta\eta$, while negative values were obtained for Δ_{nD} over the whole range of composition. The obtained results were discussed in terms of interactions and structural aspects of IL + alcohols mixtures.

Later, Bettencourt et al. [230] investigated the thermophysical properties such as ρ, η and u for binary mixtures of ammonium family IL such as [N_4Ac], [N_4Pro], [N_4Hex], and [N_4Dec] with ethanol at (293.15–313.15) K. In the case, all binary mixture, the V^E, and $\Delta\kappa_s$ values are more negative except for viscosity deviations $\Delta\eta$ (less negative) over the complete composition range at all studied temperatures. The obtained thermodynamic results were deliberated in terms of structural effects and efficient intermolecular interactions between ILs and solvent molecules.

Olivieri and research group [231] evaluated ρ and u for [NBAO] and its binary mixtures with 1-butanol, 1-pentanol 1-propanol, and 1-hexanol over the complete range of composition at temperatures from (288.15–308.15) K and under atmospheric pressure. The calculated results were interpreted in terms of dispersion-type interactions and structural effects between IL and Alcohol mixtures.

Further, Alvarez et al. observed the experimental ρ and u data of binary mixtures of an IL containing [2-HEAA] with water, ethanol and methanol throughout the complete composition range and the temperature at T = (288.15 to 323.15) K under atmospheric pressure. The V^E and $\Delta\kappa_s$ were calculated from the measured data. The obtained V^E and $\Delta\kappa_s$ values were negative throughout the entire composition range studied. Isentropic compressibility results in combination with NMR measurements shown that the formation of complex because of ion-pair interactions beyond a higher concentration of the IL in the binary mixtures.

Kurnia et al. [232] examined the thermophysical properties such as ρ for the binary mixtures of [BHEAA] with 1- propanol, methanol and ethanol over the whole composition range from (293.15 to 323.15) K, respectively. The ρ values are positive and decreased with an increase in both mole fraction and temperatures of all binary systems. The authors found that the calculated values obtained for excess molar volumes are negative for all systems. For the

investigated binary systems, these V^E values are more negative when temperature increases and indicating that the strong interaction between IL and alcohols.

Kurnia et al. [233] further studied the ρ and η for the binary mixtures of [BHEMF] with methanol, ethanol, and 1-propanol at temperatures from (293.15 to 323.15) K under atmospheric pressure. The derived properties of V^E and $\Delta\eta$ were calculated from experimental ρ and η, respectively. The negative values were obtained for V^E and these results attributed to ion-dipole interactions between the molecules of IL and alcohols. The $\Delta\eta$ values are also negative over the entire composition range, and their $\Delta\eta$ values become less negative as the temperature increases.

Massel et al. [234] investigated the thermodynamic properties of ρ for binary mixtures of $[N_{1114}]$-$[Tf_2N]$ with ethanol, 1-propanol and N,N-dimethylformamide (DMF) over the whole compositions range at (308.15 to 323.15) K under atmospheric pressure. The V^E values for all the studied binary systems were calculated from the experimental data. The V^E values were positive for the mixture with DMF and negative for the mixtures with alcohols.

Mohd Taib and Murugesan [235] reported the ρ and V^E for the binary mixtures containing ILs of [BHEAA] with monoethanolamine [MEA] and water over the entire composition range and temperatures at T= 303.15 to 353.15) K. The derived properties of V^E were calculated from experimental data. Authors concluded that the measured densities of both binary mixtures decreased with increasing temperature, whereas the V^E values were completely negative for IL + water mixtures while positive for the IL + MEA binary system except at higher temperatures, demonstrating the nature of the molecular interactions between IL and used solvents.

Pinto et al. [236] measured the ρ and n_D values for the binary mixtures of PILS such as [HEAP], [HEAB], [HDEAH], and [HEAH] with water $[H_2O]$ temperature range at T = (298.15 and 323.15 K). The derived thermophysical properties for V^E were explored from the

measurement data.The obtained V^E values were negative and exhibited a smooth difference with increasing ILs chain length. Negative values recommended that the packing efficiency capability or attractive interactions take place in between the ILs + water mixtures.

Umapathi et al. [237] reported ρ, η, u and n_D for the binary mixtures of ammonium family ILs such as [DEAS], [DEAA], [TMAS], [TEAS], [TEAA] and [TMAA] with water over the full composition range at 298.15 K under atmospheric pressure. The V^E and $\Delta\kappa_s$ values for the all above systems are negative while the values for $\Delta\eta$ and Δn_D were positive at the same experimental conditions.

Hou and coworkers [238] investigated the ρ and n_D of two ammonium based ILs such as (N_2Ac) and (N_3Ac) with water at 298.15 K. Using the experimental experiments data, V^E and Δn_D values were calculated. The V^E values of the above-mentioned both systems are negative, whereas the Δn_D values are positive. The results were discussed in terms of intermolecular interactions and structural effects between the ILs and water of binary systems.

Attri et al. [239] studied the thermodynamic properties of ρ and u of a series of common cation and different anions containing ammonium family ILs such as [TMAS], [TMAA] and [TMAP] with *N*,*N*-dimethylformamide [DMF] binary mixtures over the whole composition range and at temperature from T = (298.15 to 323.15 K) atmospheric pressure. The derived properties of V^E and $\Delta\kappa s$ were obtained from experimental results. The results of V^E value are negative at all composition ranges, except TMAS or TMAP with DMF at 298.15 K. The negative V^E values indicated that strong attractive interaction, and effective packing upon mixing of the IL and DMF. Furthermore, negative V^E decreased with an increase in IL concentration that can be attributed to the weakening of hydrogen bonding interaction. On the other hand, they were found negative $\Delta_{\kappa s}$ values for all studied systems and temperatures, except TMAA + DMF binary system.

Moreover, Attri et al. [240] investigated the influence of molecular interactions between highly polar solvent of DMF and ammonium-based ILs include [TEAH], [TMAH] and [TPAH]. The V^E and ΔKs were calculated from the experimental data at a temperature range from (298.15 to 323.15) K atmospheric pressure. The V^E is negative and exhibited variation from negative to positive with an increase in the concentration of ILs. These negative results revealed that the strong interactions as well as more efficient packing upon mixing the ILs. On the other hand, the ΔKs were negative for all studied binary systems and also credited the more attractive interactions owing to the solvation of the ions in these mixtures, respectively.

Later, Kavitha et al. [241] studied , ρ, η and u of a series of ammonium family ILs such as [DEAA], [DEAS], [TEAA] and [TEAS], with *N*-methyl-2-pyrrolidone [NMP] over the whole range of composition and at the temperature range starting from (298.15- 313.15) K. From the derived properties, authors concluded that the fascinating results were obtained for effective structural based as well as temperature dependent on properties ILs with an organic solvent.

Chhotaray et al. [242] reported experimental ρ and u of ammonium based ILs namely, propylammonium formate [PAF], [3-HPAF], [PAA], [3-HPATFA] and [3-HPAA] with water and N-methyl-2-pyrrolidone at temperatures from (293.15 to 333.15) K. The experimental ρ and u data have been used to calculate thermal expansion of coefficient, isentropic compressibility V^E and κ_s of investigated binary mixtures. The obtained results were discussed in terms of hydrogen bonding, ion–dipole interaction and interstitial packing between ILs and molecular solvents.

Kavitha et al. [243] investigated the thermodynamic properties of ρ, u and η for binary mixtures of (TPAH), (TMAH), (TBAH) and (TEAH) with (NMP) over the whole compositions range at (298.15 to 313.15) K and at atmospheric pressure. The obtained results

were discussed in terms of the ion-pair interactions, ion-dipole, and hydrogen bonding interaction between ammonium based ILs and solvent molecules.

Usula et al. [244] measured the ρ for a binary mixture of IL: (XAN) with (NMP) at 298.15 K over the complete composition range and at under atmospheric pressure. The measured ρ values were used to calculate V^E. Negative V^E values were observed for IL+NMP for studied system at 298.15 K temperature. It indicated that strong attractive interactions between the IL and organic solvents.

Govinda et al. [245] explored the ions effect of two different families of ILs include [TEAH], [TBAH], [TMAH] and [TPAH] from ammonium family and ([Emim][$MeSO_4$]), ([Emim][Cl]), ([Bmim][Cl]) and ([Bmim][BF_4]) from imidazolium family of ILs with dimethyl sulfoxide [DMSO] over the entire range of concentrations of ILs at temperatures range from (298.15 to 323.15) K. The derived properties of V^E, $\Delta\eta$ and $\Delta\kappa_s$ were calculated from density, viscosity and speed of sound, respectively. Obviously, their fascinating results revealed that the IL cation size was accountable for the modification of the thermophysical properties such as V^E, $\Delta\kappa_s$, and $\Delta\eta$ of all binary mixtures. Finally, their studies were illustrated that these derived properties completely depend on the cations alkyl chain length of ammonium-family ILs along with the anions of imidazolium ring containing ILs.

Subsequently, Fan et al. [246] investigated the thermophysical properties of binary systems containing IL ([Emim][BF_4]) besides organic solvents such as [DMF], dimethylacetamide [DMA] under atmospheric pressure, at temperatures range between (303.15 to 333.15) K over the whole composition range. The derived V^E and $\Delta\eta$ properties were calculated from the experimental ρ and η data. Obviously, the both V^E and $\Delta\eta$ exhibited negative values due to the weak interactions ions of ([Emim][BF_4]) with organic solvents in the all binary mixtures.

Moving further, Wu researcher's group [247] evaluated the measurements of ρ and η of binary mixtures containing IL: ([C4mim][BF_4]) with (DMA), (DMF), (NMP), methanol and acetonitrile solvents were made at under atmospheric pressure in the temperature range from (303.15 to 333.15) K. The V^E and $\Delta\eta$ values were calculated from experimental ρ and η of mixtures, respectively. The obtained V^E and $\Delta\eta$ both values were negative for all studied binary systems over the whole range of composition at all studied temperatures.

Zarei and Keley [248] have reported the thermophysical properties of ρ and u for pure ([Emim][BF_4]), [DMA] and [DMF] and their binary mixture systems over the complete range of compositions and temperature at (293.15 to 343.1)5 K. The obtained V^E values of both binary systems were negative in mole fraction from 0.1 to 0.8 M, after that they were positive in ≥ 0.8 M, as well as they became more negative with increase in the temperatures. On the other hand, the $\Delta\kappa_s$ values were negative and become more negative values with an increase in the temperature for both binary systems.

Therefore, there is no research work in literature on has explored for DMF + selected ammonium based ILs.

2.2.2 Apparent molar properties

Bahadur and his research group [249] studied the experimental ρ and V_φ for a binary mixture of [BMPYR][Br] with water and methanol at various temperatures from 293.15 to 343.15 K and over the entire composition range. In the case of both systems, the V_φ values were decreased with an increase in the concentration of IL and also demonstrated that the resulting of ion−ion interactions are decreased, when the IL concentration was increased. Moreover, the limiting apparent molar volumes, V_φ^0 values were increased as temperature increases for both binary mixtures as well as V_φ^0 values indicated that the intermolecular interactions for IL + water are stronger than for IL + methanol.

Panda et al. [250] reported the experimental ρ and u of pyrrolidinium-based ILs such as ([NMP][HSO_4]) and ([PY][HSO_4]) with water and [DMSO] as a function of concentration of ILs at different temperatures from (293.15–333.15) K and under atmospheric pressure. The derived properties, namely apparent molar volumes (V_φ) as well as adiabatic compressibilities (K_φ) were calculated and correlated using to the Redlich–Mayer type equation. From this obtained data, they have concluded that the limiting apparent molar volumes for the aqueous system are higher than the conforming values for the solvent system at various temperatures. The results exhibited that ion-solvent interactions are stronger for IL + water system than those of (IL + DMSO) binary mixture containing systems.

Sumana and Ramesh [251] have been explored the solute-solvent and solute-solute interactions between the pyrrolidinium-based ILs with organic solvent. In their work, they have investigated the thermophysical properties of ρ and u for binary mixtures of ([PMPY][I]) and ([EMPY][I]) with acetonitrile over the complete range of concentration and different temperatures from (293.15 to 328.15) K. Additionally, the Redlich-Mayer polynomial equation was used for correlating these obtained derived properties, namely V_φ and K_φ in order to estimate the type of interactions arising between the ILs and molecular solvent.

Alvarez et al. [252] measured the thermophysical properties of ρ and u for [2-HEAA] with water, ethanol and methanol over the complete concentration range at different temperature from (288.15 to 323.15) K. Derived properties such as the V_φ and K_φ were evaluated from the experimental data. These V_φ and K_φ values were positive, the values of three binary mixtures increased promptly at the range of lower concentration, whereas at high concentrations levels of three systems values were almost constant. Finally, the obtained limiting apparent molar volumes (V_φ^0), indicated that high temperature for the aqueous mixture is stronger than the alcoholic containing mixtures.

Kumar et al. [253] determined experimental ρ and u of ammonium family ILs include ([BHEA][CH_3COO]) and ([BHEA][For]) with water and ethanol at several temperatures ranging from (293.15 to 318.15) K as a function of molality under atmospheric pressure. The obtained derived properties namely V_φ, K_φ, V_φ^0 and k_φ^0 were calculated from experimental data. The results obtained indicated that V_φ and K_φ values for both systems were decreased with an increase in the concentration of ILs and increased with temperature increases. Moreover, the corresponding V_φ^0 and k_φ^0 values revealed that ILs+ ethanol interactions become stronger than the ILs–water systems.

Dasthaiah et al. [254] evaluated the ρ and u of binary mixtures containing ammonium family IL namely [BDMAH], [BDMAP] and [BDMAA] in water and ethanol at various temperatures from (293.15 to 318.15) K. The Redlich–Mayer equation was used to analyze the V_φ and K_φ as well as the corresponding parameters. The V_φ and K_φ values of calculated (ILs + water or ethanol) binary systems increased with increasing in ILs concentration and temperature, except in the case of (BDMAA + water) at 293.15 K, whereas V_φ values decreased with a concentration of BDMAA have been observed. Further, the V_φ^0 values increase by increasing size of studied anions as well as temperature. On the other hand, the obtained limiting apparent molar adiabatic compressibility (k_φ^0) values were positive and negative for studied all binary mixtures.

Cai and coworkers [255] studied ρ of ([DMSCA][Tos]) with water and methanol at various temperatures from (303.15 to 328.15) K. The experimental results indicated that both properties of binary systems were decreased with increasing the temperature. The V_φ values were positive for the IL in the water system and increased with temperature, whereas they decreased with temperature increases in methanol. In addition, The V_φ^0 values of the IL in water system are higher than those in the other system (IL + methanol), which suggested that

the ion-solvent interactions for (IL + water) binary system are stronger than those for IL + methanol system.

Kulhavy et al. [256] investigated the experimental ρ and u of PIL (2-HDEAL) with water, methanol and ethanol at temperatures ranging from (288.15 to 323.15) K. the experimental data were used to obtain the derived properties such as V_φ, K_φ and isobaric thermal expansion coefficients for all studied binary systems. The obtained results reveal that IL interactions in alcoholic mixtures are stronger than in the studied IL in water mixture.

Bahadur and Deenadayalu [257] have measured the ρ and u of the mixtures containing the IL, ([MOA][Tf_2N]) with ethanol and ethyl acetate at (298.15-313.15) K. The values for apparent molar volume and apparent molar adiabatic compressibilities were positive and increased as temperature increased for all binary system. From the derived results authors concluded that the values of limiting apparent molar volumes for (IL + ethanol) was greater than for (IL + ethyl acetate) system at all temperatures. On the other hand, positive limiting apparent molar isentropic compressibilities values of both systems were interpreted in terms of increased in the isentropic compressibilities of the solution as compared to the pure (ethanol and ethyl acetate) solvents.

In the same direction, Bahadur and Deenadayalu [258] reported the ρ and u of the binary mixtures containing IL [MOA][Tf_2N] with methyl acetate and methanol at various temperatures from (298.15 to 313.15) K. For the binary systems explored, the apparent molar volumes and molar isentropic compressibilities have been evaluated and fitted to the Redlich–Mayer equation from which the consistent apparent limiting values were acquired. The limiting apparent molar volume and limiting apparent molar isentropic compressibilities values demonstrated that intermolecular interactions for ([MOA][Tf_2N] + methyl acetate) system are stronger than for ([MOA][Tf_2N] + methanol) system at all temperatures excluding at 298.15 K.

Muscle et al. [259] evaluated ρ and u for binary mixtures of [DEAA], [DEAF], [DEAB] and [DEAP] with water. These thermophysical properties were measured over the complete compositions range at (293.15 to 313.15) K as well as the u at 298.15 K. The values of V_φ decreased with an increase in the concentration, whereas these values increased as the temperature increases. Moreover, K_φ values increased with increasing in the concentrations at 298.15 K. The obtained results have been interpreted in terms of temperature as well as concentration-dependent, hydrophobic ion interaction and water structural variations.

Pinto et al. [236] investigated the ρ for binary mixtures of ammonium family ILs such as [HEAP], [HEAB], [HDEAH], and [HEAH] with water at different temperatures from (298.15 to 323.15) K. The obtained V_φ revealed that the maximum considerable changes occurred in the solvent rich region. The V_φ values are positive and also suggested that the strong ion-solvent interactions between the ILs and water molecules, as well as these interactions, become stronger when the temperature increased.

Gyanendra et al. [260] determined the ρ and u of [DEEAP] and its binary mixture with water. The thermophysical measurements were measured at an under atmospheric pressure at various temperatures from (298.15 to 328.15) K. Furthermore, Redlich-Mayer equation was fitted to analyze V_φ, K_φ, and its corresponding adjustable parameters. Positive values of V_φ and K_φ derived properties were found for all binary systems.

Zafarani-Moattar and Shekaari [261] reported experimental ρ and u of two different families of same anion different cations of ILs such as ([TBA][PF_6]) and ([Bmim][PF_6]) and their binary mixtures with methanol, [DMA], tetrahydrofuran, acetonitrile, and [DMSO]. Authors were concluded that the nature and strength of particular interaction between the ionic liquid ([TBA][PF_6]) or ([Bmim][PF_6]) with the organic solvents studied have followed the trend DMSO > DMA > MeCN > MeOH > THF. The obtained derived values for $V_\varphi^0$and k_φ^0 have

been used to attain some extensive information about ion-solvent interactions in the studied binary systems.

Zafarani-Moattar and Shekaari [262] determined ρ and u for three binary mixtures comprising of IL ([Bmim][Br]) and different solvents, namely ethanol, methanol and water under atmospheric pressure and various temperature from (303.15 to 333.15) K over the entire composition range. The derived properties such as V_φ and K_φ values were calculated from the measured data and correlated using the Redlich Mayer polynomial equation from which the V_φ^0 and k_φ^0 of the binary solutions have also been evaluated at all studied temperatures. The results revealed that (IL + water) interactions are very stronger than the ethanol and methanol solutions.

Shekaari et al. [223] measured the ρ and u of IL, [Hmim][Br] and their binary mixture with water under atmospheric pressure and different temperatures from (283.15 to 308.15) K over the whole composition range. Using experimental data, the V_φ and K_φ have been calculated at all temperatures. These corresponding values indicated that the molecular interactions between IL and water decreased with an increase in the temperature. Moreover, the derived limiting apparent molar expansibility results also support this conclusion.

Abdulagatov and research group [263] examined the experimental ρ for the binary mixtures of ([Bmim][BF_4]) and ethanol over the full scope of composition and different temperatures from T = (298.15 to 398.15) K and at atmospheric pressures up to 40 MPa. The experimental ρ have been performed to obtain the V_φ values. The V_φ values increased promptly at low concentrations, whereas the values are almost constant at higher concentrations. Authors have revealed that the V_φ values increased with temperature at concentrations levels above 0.3147 M, whereas at low concentrations below 0.3147 M, the V_φ values decreased marginally up to a temperature of 373.15 K and then decreased significantly at higher temperatures.

Gonzalez et al. [264] reported measurement of ρ for five binary mixtures containing IL ([Hmim][TfO]) and alcohols such as 1-propanol, 1-pentanol 2-propanol, 2-butanol and 1-butanol over the complete range of composition and at 323.15 K. From this experimental ρ, the corresponding values of V_φ were calculated as well as correlated using the Redlich–Mayer polynomial type equation. The obtained V_φ results for all binary mixtures increased with molality and increased by the increasing the chain length of the cation of IL, whereas values are constant at higher concentrations of ([Hmim][TfO]). The investigated binary systems comprising a primary alcohol present V_φ values were greater than the mixtures with a secondary alcohol binary system. Finally, they concluded that the molecular interactions between the secondary alcohols and the ([Hmim][TfO]) systems are stronger than the primary alcohols and the ([Hmim][TfO]) systems attributed to weaker interactions with the ions of IL.

Therefore, there is no research reported in literature on 1-methyl-1-propyl pyrrolidinium tetrafluoroborate [MPpyr] [BF_4] + water, alcohols (methanol and ethanol).

CHAPTER 3

EXPERIMENTAL METHODS & THEORETICAL FRAMEWORK

3.1 Materials and Sample preparation

3.1.1. Materials

All of the chemicals used are of high purity and obtained from several sources and are given in Table 3.1. Here, we have given the summary of all chemicals and protiens, which have been used all over the work. Figure 3.1 represent the chemical structure of the ILs and other solvents used in the present work.

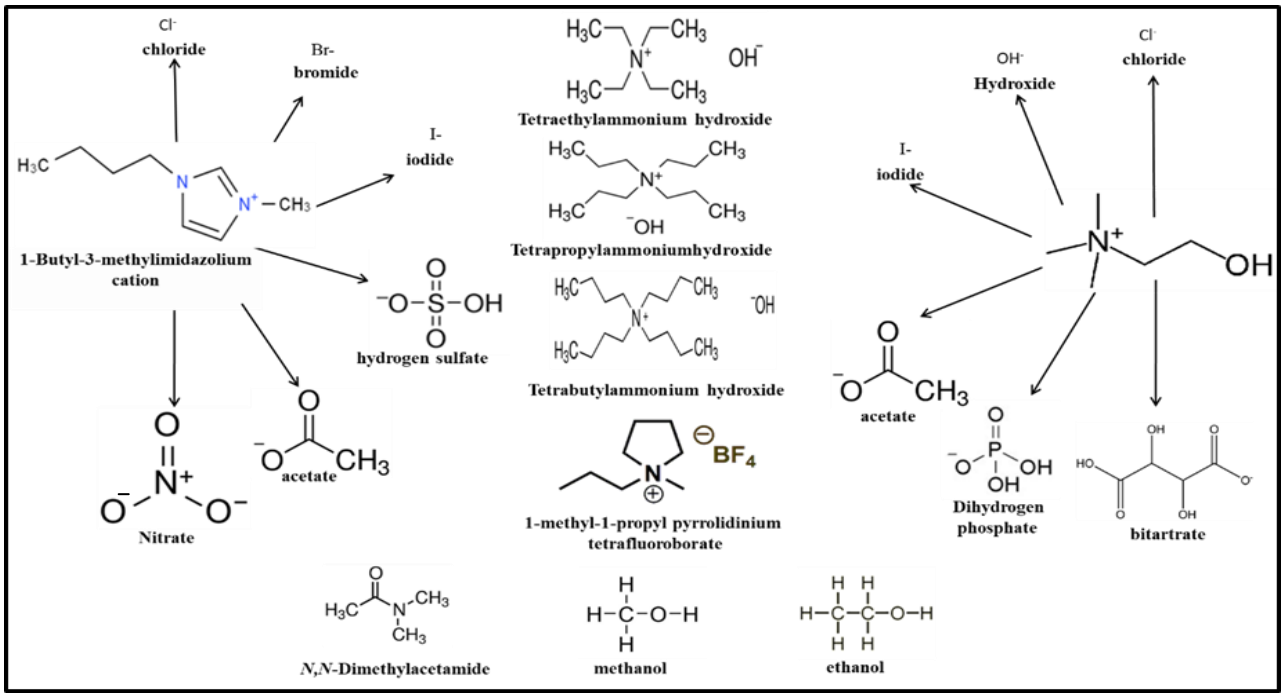

Figure 3.1: Chemical structure of the different families of ILs and other solvents used in the present work.

Table 3.1: A division into groups of chemical compounds: Ionic liquids, proteins, solvents

Chemicals	Supplier	Mass fraction Purity (%)	Molar mass (g/mol)	CAS No.
Bromelain	Sigma-Aldrich	≥99.0%	23kDa	37189347
[Bmim][Cl]	Sigma-Aldrich	≥99.0%	174.67	79917901
[Bmim][Br]	Sigma-Aldrich	>97.0%	219.12	85100772
[Bmim][I]	Sigma-Aldrich	>99.0%	266.12	65039056
[Bmim][HSO_4]	Sigma-Aldrich	≥94.5%	236.29	262297132
[Bmim][CH_3COO]	Sigma-Aldrich	≥95.0%	198.26	284049758
[Bmim][NO_3]	Sigma-Aldrich	≥95.0%	201.22	179075888
[Ch][Ac]	Sigma-Aldrich	≥98.0%	163.21	14586357
[Ch][Bit]	Sigma-Aldrich	99%	253.25	87672
[Ch][OH]	Sigma-Aldrich	46 wt% in H_2O	121.18	123411
DMA	Sigma-Aldrich	>99	87.12	127195
[Ch][Cl]	Alfa aesar	≥99%	139.62	67481
[Ch][I]	Alfa aesar	98%	231.08	17773103
[Ch][Dhp]	Iolitech	>98%	201.16	83846928
[MPpyr][BF_4]	Iolitech	>98 %	215.04	327022593
casein	Sisco	>95%	23.6 kDa	9000719
Methanol	Fluka	>99.9%	32.04	67561
Ethanol	Fluka	>99.9%	46.07	64175
trichloroacetic acid	SRL	>99	163.38	76039
sodium phosphate monobasic	SRL	>99%	119.98	7558807
sodium phosphate dibasic dehydrate	SRL	>99.5%	177.99	10028247

Ammonium-based ILs such as tetraethylammoniumhydroxide (TEAH), tetrapropylammonium hydroxide (TPAH) and tetrabutylammonium hydroxide (TBAH) are synthesized in our laboratory [243].

3.1.2 Structure of stem bromelain (BM) used in the present work

Stem bromelain (SBM) is well-known proteolytic enzymes and belongs to cysteine proteinase family, a glycoprotein isolated from the stem of pineapple (Ananas cosmosus), which is having an asparagine-linked particular hetero oligosaccharide chain unit per molecule [265–268]. The polypeptide chain of BM consists of 212 amino acid residues with highly identical to that of papain. It also contains three disulfide bonds and a single free cysteine (Cys) residue. BM protein belongs to the α+ß class of protein with helix, sheet and turns structure and has a molecular weight of 23,800 Da. BM finds extensive applications in several areas such as food, pharmaceutical and industrial fields [267,269–271]. Furthermore, BM has been used for the treatment of arthritis, anti-inflammatory, immunomodulator, antiedematous, fibrinolytic, anti-metastatic, anticancer, antibiotic, anticoagulative and antithrombotic functions [162,271,272]. BM possess a wide range of numerous therapeutic benefits such as malignant cell growth, thrombus formation, inhibition of platelet aggregation, dermatological properties, skin debridement properties, pyelonephritis, surgical traumas, enhanced wound healing, modulation of cytokines and immunity, reversible inhibition of platelet aggregation, enhanced absorption of other drugs, angina pectoris, mucolytic properties, bronchitis, sinusitis, digestive assistance and cardiovascular and circulatory improvement [273–277]. In addition, the structure of BM has aromatic amino acids such as tryptophan (Trp), phenylalanine (Phe) and tyrosine (Tyr) have 5, 6 and 14, respectively [269,278]. The chemical structure of BM has displayed in Figure 3.2.

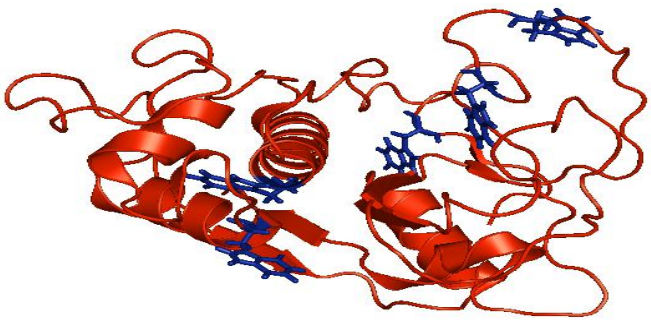

Figure 3.2: Schematic diagram of the structure of BM.

3.2. Sample preparation

All samples were prepared gravimetrically by using a Mettler Toledo analytical balance (Japan) with a precision of ± 0.0001 g. In order to check the concentration-dependent effect of different ILs on the protein structure and stability, a set of ILs concentrations have been taken. The set consists of aqueous (i.e. in the PBS buffer) IL solutions range between (0.01-1.5) M. The concentration of protein ~0.5 mg/ml was used for UV-absorption, steady-state fluorescence, thermal fluorescence, and circular dichroism (CD) measurements. On the other hand, ~2 mg/ml of protein was used for dynamic light scattering (DLS) measurements. All protein samples were also filtered with 0.45 µm disposal filter (Millipore, Millex-GS) through syringe prior measurement and were incubated for 30 min at 25 ^{o}C in order to obtain complete equilibrium before performing experiments.

All mixtures with composition spanning the whole mole fraction and molality range prepared for thermophysical properties. The binary mixtures prepared by transferring with a disposable syringe, the pure liquids into stoppered bottles (to prevent evaporation). The ILs were first added into an air-tight stoppered 5 cm^3 plastic vial and weighed. By using a Mettler Toledo balance for the determination of mass of each component with a precision of ±0.0001 g. The approximate uncertainty on the mole fraction and molality compositions are found to be less than 0.0005 and ± 0.0001 $mol \cdot kg^{-1}$, respectively. The binary mixtures are shaken in order to make sure complete homogeneity of the two compounds. To avoid the formation of bubbles inside the vibrating U-shape tube of the densimeter, injections are done slowly. All the chemicals were kept in tightly closed vials with screw caps to ensure a secure seal and to prevent evaporation.

3.3 Experimental methods

3.3.1 Spectroscopic techniques

3.3.1.1 UV-visible spectroscopy

UV- visible absorption spectroscopy is a simple and effective method that processes the interaction of different molecules with electromagnetic radiation. Light in the near-ultraviolet/ visible (UV-vis) range of the electromagnetic range has a force of about 150–400 kJ mol^{-1} [15]. As shown in Figure 3.3 [15], the force of the light is used to push the electrons from the ground state to an excited state. Molecules with electrons in delocalized aromatic structures frequently absorb the energy of light in the near-UV (150–400 nm) or the visible (400–800 nm) region and their particular band is achieved when the absorption spectra of light are calculated as a function of wavelength or frequency. The absorbance of a protein in a solvent depends linearly on its concentration and then absorption spectroscopy is perfectly suitable for quantitative measurements for the proteins studies. Proteins represent the broad peak in between 250–300 nm range of the ultraviolet spectrum composed of several overlapping bands from the aromatic residues mainly in terms of $\pi \rightarrow \pi^*$ transitions involving the electrons of their aromatic rings [15,17].

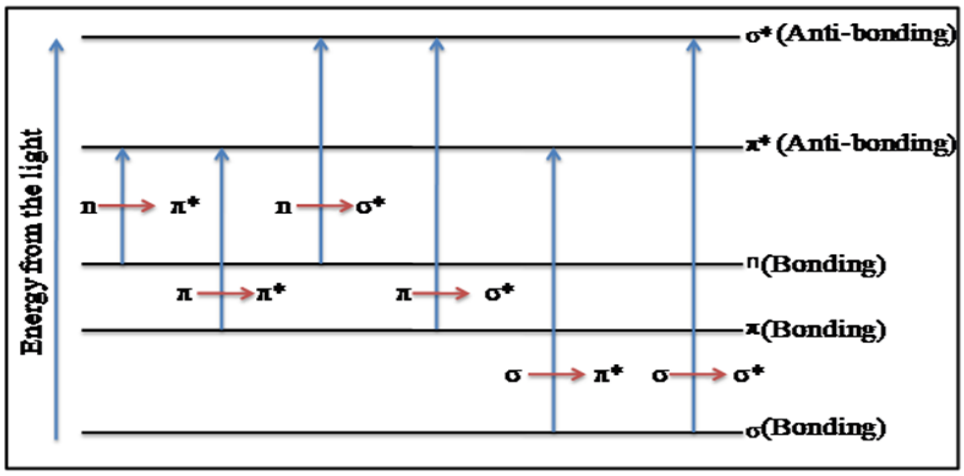

Figure 3.3: The possible electronic transitions in UV-vis spectroscopy.

As illustrated, the absorption bands in between 275 and 280 nm region are affected by the absorbance of the two aromatic AA_s, Trp, and Tyr to a small extent, by the absorbance of Cys [17]. Furthermore, the absorption bands of Trp and Tyr depend strongly on their microenvironment, and they are observed to be slightly red-shifted or either quenched when transferred from a polar to a non-polar environment, for example in the interior of a globular protein or vice versa. Apparently, changes in the secondary, tertiary, and quaternary structures of protein, all affect absorbance, thus factors such as pH, ionic strength and co-solvents can easily vary the characteristic absorbance bands of the protein [18].

Figure 3.4: UV-visible spectrophotometer (UV-1800, from Shimadzu Co.).

The UV-vis spectrophotometer which has been used in this work is shown in Figure 4. UV-Vis absorption spectra of the protein aqueous buffer solution were recorded between 190 to 600 nm through a double beam UV-visible spectrophotometer (UV-1800, from Shimadzu Co., Japan) at room temperature. An aliquot of sample solution (2.5 ml) was transported into the quartz cell of 1.0 cm path length. The spectrophotometer has quartz cells, with a spectral bandwidth of 1.0 nm with a wavelength accuracy of ± 0.3 nm along with an automatic wavelength adjustment.

3.3.1.2 Enzymatic activity of bromelain protein

Enzymatic activity of BM was measured by using casein as the substrate with the help of UV–vis spectrophotometer (UV-1800 Shimadzu, Japan). A denatured casein solution (0.5 mL of 0.2%), pH 7.0 is incubated for 10 min at 37 ^{0}C with BM in buffer (0.5 mg/mL) pre-treated with the different concentrations of the ILs. The undigested casein is separated by the centrifugation the precipitates which are formed owing to the addition of 1 mL of 110 mM trichloroacetic acid (TCA) to prevent the reaction after 10 min [279]. Reaction outcome is associated with the absorbance spectra values which are spectrophotometrically determined at 275 nm against a substance blank. From the standard spectrum of absorbance of well-known quantities of the Tyr, the activity of BM samples can be measured in terms of units per mL which is the measure of the micromoles of Tyr equivalents out from the casein per minute. The BM enzyme activity (units/mL) was calculated using the following equation.

$$Activity = \frac{(\mu\, mole\ tyrosine\ equivalents\ released)\ (V)}{((times\ of\ assay\ in\ minutes)(v_1)(v_2))} \qquad (3.1)$$

Where V is total volume of assay in mL, v_2 is volume of enzyme used in mL, v_2 is the volume of sample in mL used for UV measurements.

3.3.1.3 Fluorescence spectroscopy

Fluorescence is a method of photon emission of light by a compound which occurs during molecular relaxation from the lowest level of singlet electronic excited states and is usually depicted by well-known Jablonski diagram [280] which is presented in Figure 3.5. In biophysical chemistry, the use of fluorescence is very important. The fluorescence spectrum is very much sensitive to the biochemical atmosphere of the fluorophore [281]. Therefore, in specific, the measurements of the fluorescence spectrum, is a great method of studying the stability of proteins in a biological system. Emission spectra alter extensively and are depends

upon the chemical shape of the fluorophore and the co-solvent in which it is dissolved. Fluorescence spectral values are usually displayed as emission spectra [204]. A significant feature of the fluorescence is high sensitive detector for the polarity of the fluorophore microenvironment [204].

The intrinsic fluorescence spectrums for the AAs are highly sensitive for studying the conformational changes of proteins containing fluorophore aromatic residues such as Trp, Tyr and Phe. Because of their distinct absorption wavelengths, they fluctuate in their emission spectral wavelengths [281]. Quantum yield of Trp fluorescent is higher than Tyr or Phe. This is owing to Trp's much higher quantum yield; the resonance energy transfer is higher and is overpowering the emission spectra of Tyr and Phe. Consequently, the fluorescence spectrum of a protein including the three AA_s (Trp, Tyr and Phe) generally resembles that of Trp [282]. The measurement of fluorescence spectra reported in this thesis is Trp fluorescence of bromelain protein in the presence of ILs. Trp and Tyr both AAs will be exited at the excitation wavelength of 280 nm. But selectively Trp excite only wavelength of 295 nm must be used [283].

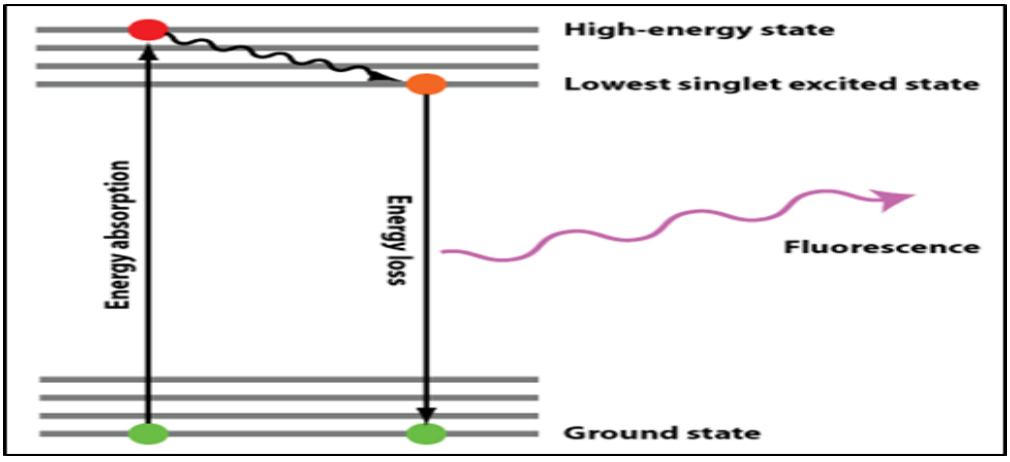

Figure 3.5: Schematic representation of a Jablonski diagram (energy diagram) representing fluorescence mechanism.

The most significant evidence is that the fluorescent quantum yield of Trp is mostly depending on the solvent. Following universal phenomena, as the polarity of the solvent decreases the

spectrum changes to slighter wavelengths and increases in fluorescence intensity. Due to this reason, Trp residues buried in hydrophobic domains of the folded state of proteins expose a spectral shift of ~ 10 to 20 nm. This phenomenon has been utilized to study protein stability in the presence of co-solvents and solutes [280].

As shown in figure 3.6, a Cary Eclipse spectrofluorimeter (Varian Optical Spectroscopy instruments, Mulgrave, Victoria, Australia) was used to display the fluorescence emission bands of protein sample that was prepared with thermostated cell holders and temperature was set aside constant through a rotating water bath handling a peltier device (accuracy of $\pm$ 0.01 ^{0}C) connected to the sample holder of the fluorimeter.

Figure 3.6: Varian Cary eclipse fluorescence spectrophotometer.

The steady-state fluorescence measurement was conducted at a fixed temperature (25.00 ^{0}C). The excitation wavelength was fixed at 295 nm in order to determine the contribution of the Trp and Tyr residues to the complete fluorescence emission of protein BM all over the experiments. The experiments were conducted using a 1.0 cm closed cell and both emission and excitation slit width was fixed at 5 nm and adjusted for background signal. The fluorescence intensity at the emission wavelength maximum for the native all proteins (~332 nm for Trp and ~303 for Tyr) were continuously recorded with increasing temperature was

starting from 25 to 85 ^{0}C at an approximate rate of 2.0 ^{0}C/min with an accuracy of the temperature changes were ± 0.01 ^{0}C. This allowed complete temperature equilibration time for the spectrum analysis of the small structural alteration in the proteins/enzymes. Apparently, the variations in the fluorescence intensity and the maximum shift in wavelength were reported and analyzed the protein structure.

3.3.1.3.1 Thermodynamics analysis of protein unfolding using fluorescence spectroscopy

Fluorescence properties such as fluorescence intensities (I_{max}) and the emission wavelength (λ_{max}) of Trp in a protein changes upon unfolding. Thus, the thermal fluorescence unfolding of the proteins in the presence of co-solvents (ILs) was monitored by using fluorescence spectroscopy [284,285]. Figure 3.7 display the fraction of the unfolded protein (aqueous medium) in ILs versus function of temperature. This is a reversible two-step folding mechanism observed in which the transition from folded state to unfolded state is without any intermediate states. Using Figure 3.7, the overall process of calculating the thermodynamic parameters such as transition temperature (T_m), free energy change (ΔG), enthalpy changes (ΔH) and heat capacity (ΔC_p) changes were calculated which is discussed below [286–288].

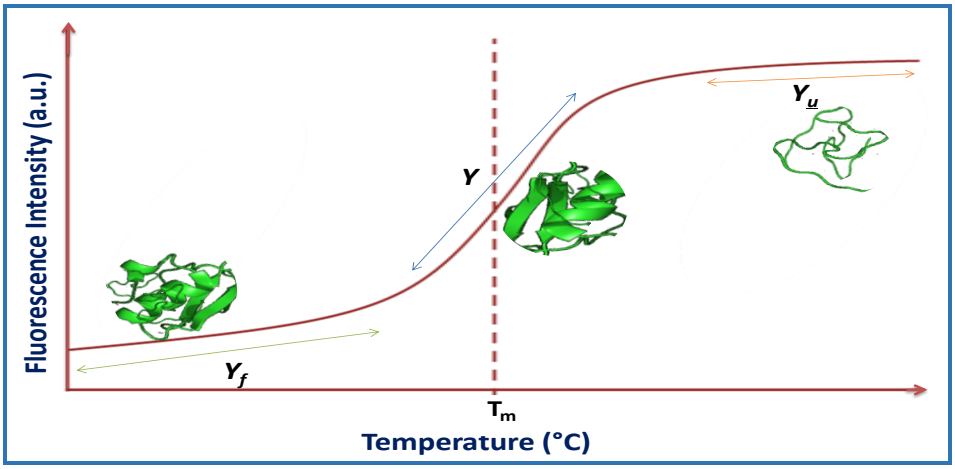

Figure 3.7: Schematic representation of two-state unfolding transitions in a protein as a function of temperature.

As presented in Figure 3.7, the sigmoidal fluorescence transition curve of a globular protein can be divided into three regions on the origin of the vary in fluorescence properties [289]. These three regions include,

(a) The pre-transition region in which the fluorescence emission (Y_F) of the protein changes slowly with the temperature

(b) The transition region (*Y*) represents the major structural changes as the unfolding proceeds with temperature

(c) The post-transition region (Y_U) represents which indicates slow changes in the fluorescence emission of the completely unfolded protein

For each thermal transition curve, the value of the fraction of unfolded (f_U) protein can be calculated using the following equations,

For each thermal curve, the value of the fraction of unfolded (f_U) protein can be calculated using the following equations [284,285],

$$f_u = \frac{Y_F - Y}{Y_F - Y_U} \tag{3.2}$$

In an equation, f_u is the fraction of unfolded protein, *Y* is the measured intensity at a given temperature, Y_f is the measured fluorescence intensity of the folded state, and Y_u is the intensity of the totally unfolded state. The T_m of the protein is the temperature at the fraction of unfolded protein is equal to 0.5.

The equilibrium constant (*K*) between the native/folded and the denatured states at a particular temperature was obtained using the following equation

$$K = \frac{f_F}{1 - f_U} = \frac{Y_F - Y}{Y - Y_U} \tag{3.3}$$

The difference in free energy between the denatured and the native conformations (ΔG) can be calculated using the equation as given below,

$$\Delta G = -RT \ln K_{eq} \quad (3.4)$$

Where R is the gas constant (1.987 Cal mol^{-1}) and T is the absolute temperature.

The difference in free energy between the denatured and the native conformations (ΔG) can then be calculated using the equation as below,

$$\Delta G = -RT \ln K \quad (3.5)$$

Where R is the gas constant (R= 1.987 Cal mol^{-1}) and T is the absolute temperature.

At equilibrium,

$$\Delta G = 0 \quad (3.6)$$

Using K, free energy change of unfolding (ΔG_u) at a temperature T (K) can be obtained according to the relation presented in equation 4. The value of T_m can be calculated by analysis of the plot of ΔG_u vs T (K) where ΔG is 0. Furthermore, a detailed understanding about the stability of proteins in the presence of ILs can be understood by additional thermodynamic parameters, for example, the enthalpy change of unfolding (ΔH_u) and entropy change of unfolding (ΔS_u) and heat capacity change (ΔC_p) associated protein unfolding, using Gibbs-Helmholtz equation expressed below [286–288].

$$\Delta G_u(T) = \Delta H\left[1 - \left(\frac{T}{T_m}\right)\right] - \Delta C_P\left[(T_m - T) + T\ln\left(\frac{T}{T_m}\right)\right] \quad (3.7)$$

ΔC_p is the key parameter required to extrapolate the thermal unfolding result at any temperature. ΔH_u and ΔS_u at each temperature can be originated by use of the following equation. Consequently, all these thermodynamic parameters expected during unfolding studies are helpful in providing detailed information about the molecule interactions which are playing the main role in stabilizing enzyme/protein providing structural arrangements.

3.3.1.4 Circular dichroism (CD) spectroscopy

CD spectroscopy is one of the most commonly used technique to determine the conformational changes in the protein structure [290]. CD spectroscopy provides differences in the absorption of right-handed polarized light as opposed to left-handed polarized light which arises because of structural asymmetry in a molecule. CD spectroscopy is an excellent instrument for examining the interactions, structure and stability of proteins in solvents. The absence of expected structure results in zero CD absorption signals, whereas a controlled structure consequence in a spectrum which may have equally negative and positive signals. CD uses a basis of circularly polarized light, in which the vectors oscillates rotationally to the left and right, form a helix around the axis of circulation [291,292].

The chromophores existent in proteins are polypeptide bond (absorption in between 190-240 nm), aromatic AA residues such as Tyr, Trp, Phe and His (absorption in the range 260-320 nm) and disulfide bonds (weak absorption bands centered nearby 260 nm). Absorption spectra range between 190 to 240 nm is known as far-UV CD region and absorption spectra in the range of 260 to 320 nm is known as near-UV CD region. The signal strength in the far-UV CD region is much strong than that of the near-UV CD region [293]. Therefore, for near-UV CD measurement require more concentrated sample than near-UV CD measurement. Far-UV CD spectroscopy provides detailed information about the secondary structure as well as near-UV CD spectroscopy may give complete information about conformation changes in the tertiary structure of proteins. The advantages of using the CD spectroscopy is that it is very sensitive to the changes in the conformation despite the spectral regions of the protein, secondly, the CD is applicable to a particularly broad range of solvent environment is available to study with relatively small amounts of material. In the present thesis, the secondary and tertiary structures of protein were monitored by using far-UV (190-240) spectra, (0.1 cm path length cuvette) and

near-UV (250-300 nm), (1.0 cm path length cuvette), respectively. These both CD structural results for the proteins are commonly used as the mean residue and molar ellipticity [θ].

$$[\theta] = \frac{\theta \times 100 \times M}{C \times l \times n} \tag{3.8}$$

Where, [θ] is molar ellipticity in deg.cm^2.dmol^{-1}.

θ is the ellipticity in degrees,

l is the optical path length in cm,

M is the molecular weight,

n is the number of residues in the protein,

C is the concentration in (mg/ml).

3.3.1.4.1 Analysis of the secondary structure of a protein using CD

CD spectroscopy examines the secondary structure of proteins due to the peptide bond is asymmetric in nature and molecules without a plane of symmetry. The amide chromophore of the peptide bond dominates the CD spectrum of proteins/enzymes at less than 250 nm. The characteristics of far-UV CD spectra provides the information about the percentage contents of all α-helix, β-sheet and random coil in the arrangement of protein structure. Absorption in this region is below 240 nm and is mainly because of the peptide bond; there is a weak broad n → π* transition centered approximately ~ 220 nm and a more strong π → π* transition approximately ~190 nm [293].

These both transitions states dominate the interest of far-UV region in CD spectroscopy (< 240 nm). The transition n → π* is electrically prohibited, but, it is magnetically acceptable, accountable for the negative bands of similar magnitude at 222 and 216-218 nm, which are the characteristics of α-helix and the β-sheet spectrum, respectively, which is shown in Figure 3.8.

The transition π → π * is mainly answerable for the positive band at ~ 190 nm and the negative band at 208 nm, distinctive of the α-helix spectrum, and for the positive band at ~ 198 nm, distinctive of the β-sheet spectrum [293,294].

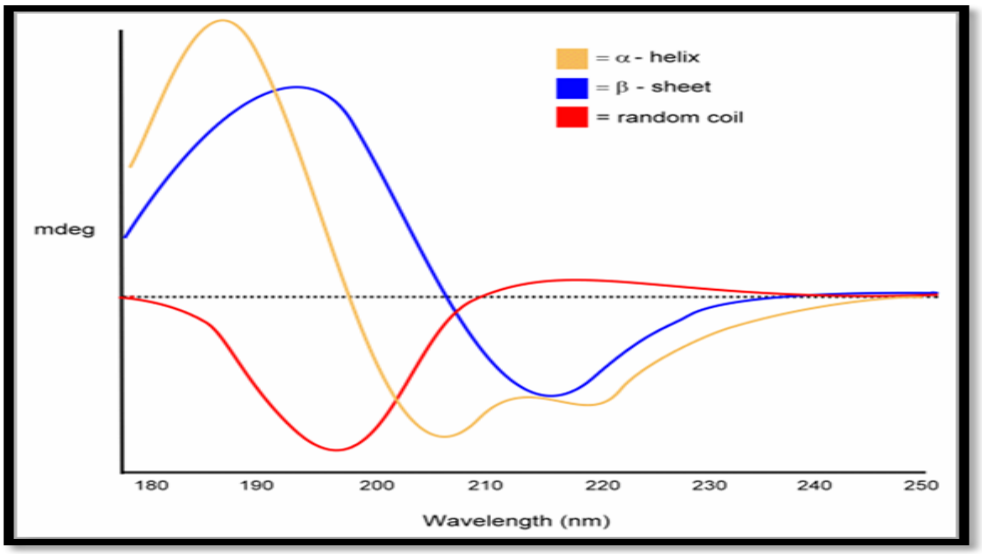

Figure 3.8: The analysis of α-helix, β-sheet and random coil using CD spectroscopy.

3.3.1.4.2 Analysis of the tertiary structure of proteins using CD

The near-UV CD spectra in the wavelength range between 260 to 320 nm reflect the bio-environment of the aromatic AAs side chains and it gives information about the tertiary structure of the protein [295]. Aromatic residues such as Trp, Try and Phe exhibit CD spectra with π → π* absorption at between 250 and 300 nm. Trp residue shows a fine structure peak between 270 and 305 nm as well as Tyr a band between 275 and 282 nm, with a shoulder at higher wavelengths frequently obscured by bands because of Trp and Phe show generally weaker however sharper bands with well structure peak between 255 and 270 nm. On the other hand, disulfide bonds also give rise to weak broad signals around 260 nm. The magnitude and shape of the near-UV CD spectra of a protein will depend on the number of each kind of aromatic AA existing, their flexibility, the nature of their environment (H-bonding and

polarizability) and their three-dimensional disposition in the protein. Disulfide bonds also have CD related to a transition n → σ* at around 290 nm [293,295,296].

All CD spectroscopic studies were performed using a Pistar-180 spectrophotometer (Applied Photophysics, UK) equipped with a Peltier system for temperature control. The diagram of CD instrument is presented in Figure 3.9. CD calibrations were performed using (1S)-(+)-10-camphorsulphonic acid (Aldrich, Milwaukee, WI), which shows a 34.5 M/cm molar extermination coefficient and 2.36 M/cm molar ellipticity (θ) at 285, 295 nm wavelengths, respectively. The sample was pre-equilibrated at the required temperature for 15 min and the scan speed was fixed (error $\pm$ 0.01) with a reaction time of 1 sec and 1nm bandwidth. Each and every spectrum was collected by averaging six spectra. All sample spectrums were attained by deducting suitable blank media having no protein from the experimental original spectrum [146].

Figure 3.9: CD instrument (PiStar-180 spectrophotometer, Applied Photophysics, UK).

3.3.1.5 Dynamic light scattering (DLS)

Dynamic light scattering (DLS) is a technique for measuring the intensity of light that is scattered from dissolved macromolecules or suspended particles within a liquid. DLS measures the scattering owing to Brownian motion and relates this to the analysis of the particle size of the proteins in solution [294,297]. By means of classification, the Brownian motion is the random group of particles due to the attack by the solvent molecules that surround them. In contrast, a small particle would be "kicked" by the solvent molecules and their motion would be more rapidly. A precisely well-known temperature is required for DLS because the understanding of the viscosity is compulsory (because the viscosity of a liquid is correlated to its temperature).

The hydrodynamic radius size of particles and molecules can be calculated from the translational diffusion coefficients by using the Stokes-Einstein equation

$$d(H) = \frac{kT}{3\pi\eta D} \tag{3.9}$$

Where,

d(H) = hydrodynamic diameter

D = translational diffusion coefficient

k = Boltzmann's constant

T = absolute temperature

η = viscosity of the solution mixture

To investigate more information about the phenomenal changes of IL on protein structure and stability, we have performed the DLS experiments for different protein samples through Malvern Zetasizer Nano instrument, U. K., which is displayed in Figure 3.10. The instrument

was equipped with 4mW He-Ne laser (633 nm); fixed with an automatic laser attenuator with the transmission of 100% to 0.0003%. The time-dependent fluctuations in the intensity were measured at a fixed scattering angle of 90^0. All protein samples of the DLS experiments were measured at a fixed temperature of 25 °C. Moreover, progressive avalanche photodiode, Q.E. > 50% at 633 nm was utilised as a detector. The measurements for each of the constant temperature was accomplished and recorded frequently for 50 times to develop the signal-to-noise ratio of the experimentation. All data obtained that can be analyzed by using Malvern Zetasizer Software, version 7.01. The DLS instrument is having an inbuilt automatic correlator for the exposure of the scattered intensity and the significant autocorrelation function calculations were conducted by the instrument using advanced method utilities and different analysis algorithms.

Figure 3.10: Malvern zetasizer nano dynamic light scattering (DLS) instrument.

3.3.2 Measurement of excess molar volumes and apparent molar volumes

3.3.2.1 The vibrating tube densitomer (Anton paar DMA 4500 M)

The densities have been measured using an Anton Paar DMA 4500M vibrating U-tube densimeter. The densimeter contains an in-built device controller capable of maintaining the temperature range of (0–90) ^{o}C. Typically, density precisions are ±0.00005 g.cm^{-3}. Prior to each experimental run, the cell is first flushed with acetone or ethanol. After flushing compressed dry air is blown through the cell. The ultra-pure water supplied by syringe calibration (used as the calibration standard) is then introduced into the cell through a glass syringe. The injection process carried out slowly, allowing the liquid to totally wet the tube walls, and also to lighten the risk of trapping air bubbles in the U-tube. A diagram of the density measuring apparatus used in this work is presented in Figure 3.15. The density of air and water is set for the calibration. The compounds were introduced into the sample cell in accurately the same method as for the ultra-pure water. Density values of water and pure solvents are determined between each solution injection, to permit a continuous check on both sample purity and densitometer operation.

Figure 3.11: Anton-paar densitometer 4500M

3.3.2.2 Ultrasonic interferometer

In the present thesis ultrasonic sound velocities (u) in pure liquids and binary mixtures were measured at various temperatures (2 MHz frequency) using a variable path single crystal ultrasonic interferometer (model F-05) from Mittal Enterprises, New Delhi, India. The cell temperature is maintained from (25 to 40 ^{o}C) by circulating water bath (LAUDA alpha 6, Japan) from a thermostat which is controlled to within ±0.02 K. It is a simple and direct technique to determine the ultrasonic velocity in liquids with a high degree of accuracy. A diagram displaying the ultrasonic interferometer F-05 and interferometer is shown in Figures 3.12 and 3.13. The interferometer cell of capacity 12 cm^3 is made up of a stainless steel tube of internal diameter 1.6 cm. A gold plated quartz crystal of diameter 0.9 cm is covered to the bottom of the cell. The waves move from this crystal till they are reflected back through the movable fused quartz rod reflector. A heavy base provides the measuring cell the require it being from a thermostatically controlled bath into a jacket around it measuring space to continue the experimental sample at a constant temperature during the experiment. Moreover, two controls to regulate sensitivity and to adjust the initial current of the meter are also provided. This distance between the quartz transducer and the reflector plate is moved by the screw downwards. To improve the accuracy of the measurement, several maxima are passed and their number n counted. The anode current is finally adjusted to the maximum and the reading of the micrometer was again recorded. The frequency of the quartz crystal f being accurate known (2 MHz), the sound velocity, u, is calculated using the relation,

$$u = \lambda \times f \tag{3.11}$$

where u is the sound velocity, λ is wavelength, (λ) and (f) frequency, respectively.

Figure 3.12: Mittal-ultrasonic interferometer model F-05

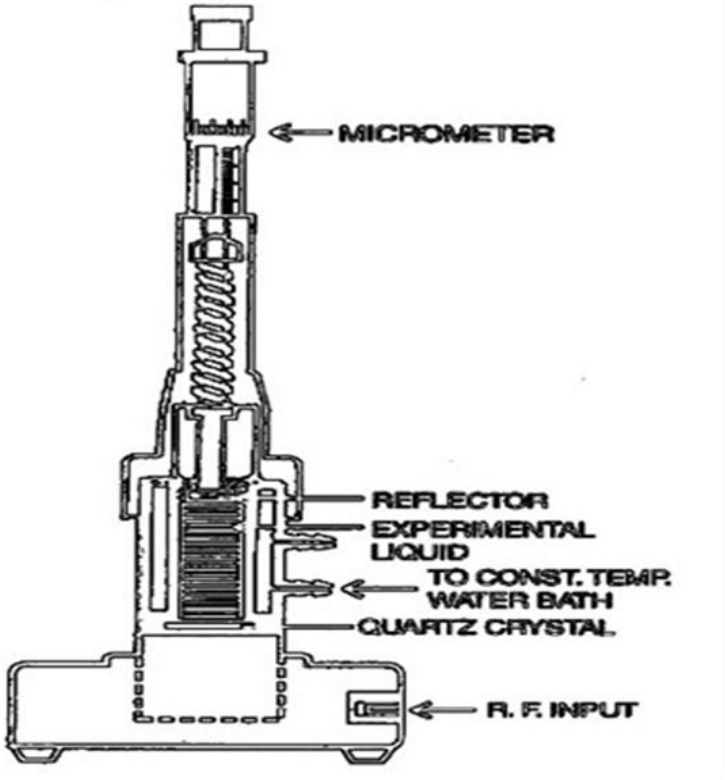

Figure 3.13: Diagram of interferometer cell

3.3.2.3 Viscosity measurements (Sine-wave Vibro viscometer)

In the present work viscosities of pure liquids and binary mixtures were measured using sine-wave vibro viscometer (Model: SV-10 A&D Company Limited, Japan). It is a simple and direct device to determine the viscosity in liquids with a high degree of accuracy. The viscometer has been shown in Figure 3.18. The instrument has been equipped with two sensor plates of gold covering. These two plates vibrate with electromagnetic force at the same frequency as well as immersed into the sample cell which was mounted on the adjustable base. The calculated viscosity values were read from a digital display unit, which is attached to *SV*-viscometer. The experimental samples were taken at sufficient heating rate for getting the thermodynamic equilibrium. Usually, the uncertainty of the viscosity measurement is to be 1%. The experiment was performed at temperatures ranging from (25 to 40) ^{o}C by using a circulating water bath (LAUDA alpha 6, Japan) to control the cell temperature to an accuracy of ± 0.02 K.

Figure 3.14: Sine-wave vibro viscometer (Model: SV-10 A&D Company Limited).

3.3.2.4 Refractive Index Measurements

Refractive index values of the pure ILs and their compounds were determined using Abbe Digital refractometer from Mittal Enterprises, New Delhi, India. It has been shown in Figure 3.19. The refractometer connected integrated peltier with thermostatically controlled circulating water to measure the refractive index measurements of these systems at various temperatures. Refractometer was calibrated by measuring the n_D values of the high-purity water and an accuracy of n_D is ±0.0002. All results such as present temperature, measurement values, measurement temperature, etc., are electronically displayed.

Figure 3.15: Illustration of Abbe digital refractometer from Mittal enterprises

3.4 Theoretical study of thermophysical properties

3.4.1 Density (ρ)

The density (ρ) is a measure of a substance of the ratio of its mass and its unit volume. The volume and mass both are extensive quantities. Density of liquid compounds and associated volumetric properties are essential for several applicative aspects as well as for theoretical investigations. The ρ of liquids is a fundamental element for research and industrial field. Furthermore, using this ρ data to calculate the excess molar volume (V^E) and apparent

molar volume (V_φ) at infinite dilution which is one of the vital thermodynamic properties of liquid compounds and signifies the first derivative of Gibb's function with respect to pressure. Especially, ρ is used to resolve the several types of problems such as quality control and quality assurance in the production of industrial fluids or concentration determination in the beverages and food processing industries, as in determining sugar and alcohols concentration. Thermodynamic studies of the apparent molar volumes or partial molar volumes and excess molar volume of solutions are used to explore the ion-ion, solvent-solvent and ion-solvent interactions.

Density (ρ) is a function of temperature for pure liquids. It can be defined as:

$$\rho = kT + m' \tag{3.12}$$

k and m' are constants and T is temperature.

3.4.2 Excess and apparent molar volume (V^E and V_φ)

The correction terms which relevant to the properties of real mixtures to those of ideal mixtures are called as an excess function [298, 299]. An excess thermodynamic volume of mixing, V^E is defined as the alteration between the amount of mixing of a real compound and the value corresponding of the ideal mixture at the same environments of composition, temperature and pressure which is provided by the equation [300–304] of the excess volume below,

$$V^E = V^M_{real} - V^M_{ideal} \tag{3.13}$$

The volume change on mixing arises due to the arrangement of the following factors:

- Variations in size and shape of the component molecule,
- Development of novel chemical species,

- The variance in the molecular interaction energy between similar and dissimilar molecules,
- Structural variations such as in the correlation of molecular interactions, and
- Hydrogen bonding.

Excess and apparent volumes data are also useful in the conversion of thermodynamic functions determined at a fixed pressure to the conditions of mixing at a fixed volume, in determining composition from ρ measurements of compounds, in obtaining the other virial coefficient. Therefore, the complexity connected with the origin of excess volume coupled with the simplify with which is the later can be achieved experimentally with better precision makes it a penetrating tool in challenging the theories of liquid solutions. By definition [305–309] the excess molar volume, and apparent molar volumes are given by:

$$V_m^E = \left[\frac{x_1 M_1 + x_2 M_2}{\rho} - \left(\frac{x_1 M_1}{\rho_1} + \frac{x_2 M_2}{\rho_2} \right) \right] \tag{3.14}$$

where V^E the excess molar volume, x_1 and x_2 are the mole fractions, M_1 and M_2 are molar masses ρ_1 and ρ_2 are the densities where *1* and *2* refers to the component *1* and *2*, respectively.

$$V_\varphi = \frac{M}{\rho} - \frac{(\rho - \rho_0)}{m\rho\rho_0} \tag{3.15}$$

where M is the molar mass of the solute, m is the molality and ρ, ρ_0 is the densities of the solution and pure solvent, respectively [310].

3.4.3 Sound velocity (*u*)

Ultrasonic sound velocity (u) in liquid mixtures is mainly determined by its adiabatic properties. The u data provide direct and detailed information about the adiabatic properties of the fluids. The measurement of u in liquid gives a way to acquiring some equilibrium

thermodynamic information which is not promptly possible by other experimental techniques. The equation state of *u* is closely related to the derivatives. The research on *u* measurements has been asserted to be an essential device in the classification of intermolecular forces present in solutions and liquid compounds. This might be accomplished through the assessment of some determined properties like isentropic compressibilities and excess isentropic compressibilities. These derived properties are calculated by using the Newton-Laplace equation:

$$\mathrm{K}_S = \frac{1}{\rho u^2} \tag{3.16}$$

where ρ the density and u is the sound velocity of the binary mixtures.

3.4.4 Deviation in isentropic compressibilities ($\Delta\kappa_s$)

The isentropic Compressibilities deviation is therefore written as:

$$\Delta\kappa_S = \kappa_S - \left(X_1\kappa_{S1} + X_2\kappa_{S2}\right) \tag{3.17}$$

where x_1 and x_2 are the mole fractions, κ_{S1} and κ_{S2} are the isentropic compressibility for component 1 and 2, respectively.

3.4.5 Viscosity (η)

Viscosity (η) is a measure of the internal friction of a fluid, which has a tendency to compete with any dynamic change in the fluid motion. The dynamic viscosity "η" is well-defined as force per unit essential to maintain a unit velocity gradient in between two similar layers which are at a unit distance separately. η is transport property of liquids, is a leading tool to define different physical characteristics of the liquid and liquid mixtures. In the case of liquid mixtures, the greatness of the recessive dragging forces differs because of variation in surface area and velocity gradient due to the presence of interactions between the component molecules

of the binary mixture. The knowledge of η embraces the idea of the internal friction between the particles of the liquid for, whenever any portion of a liquid is caused to move, neighboring parts have a tendency to be carried along too. This resistance to the improvement of velocity changes inside a fluid is the important feature of viscosity and its methods the basis of the quantitative assessment of η.

Viscosity measurement has additionally turned out to be a valuable tool for the physical scientific chemist since the viscosity coefficient is significantly affected by the size, shape and arrangement of the molecules. For laminar flow of a Newtonian liquid, the dynamic viscosity, η can be characterized just as the force per unit region required to sustain unit variance in velocity between two parallel layers of the liquid which are unit expanse apart by Stokes and Mills. It might be composed as:

$$\eta = \frac{\tau}{\left(\partial u / \partial y\right)} \tag{3.18}$$

where η is the viscosity, τ is the force per unit area and $\left(\partial u / \partial y\right)$ is the velocity gradient standard to the planes of flow. Because η seems as a proportionality aspect between the shear stress and velocity gradient, it is generally called as the coefficient of viscosity. The kinematic viscosity is a measure of the resistive flow of a liquid below the effect of gravity. It is expressed as the ratio of absolute viscosity to density and can be given by the following expression:

$$\nu = \frac{\eta}{\rho} \tag{3.19}$$

The viscosity, is defined as force per unit area essential to sustain a unit velocity gradient between two parallel layers which are at a unit distance separated. Numerous researchers proposed experimental and semi-experimental relations, which signify the necessity of

viscosity of binary mixtures on composition and viscosities of pure liquids components. Therefore we have measured the deviation in viscosities of binary mixtures.

3.4.6 Deviation in viscosity ($\Delta\eta$)

The deviation in viscosities, of binary liquid mixtures, can be expressed by the relation:

$$\Delta\eta = \eta - \left(X_1\eta_1 + X_2\eta_2\right) \tag{3.20}$$

Where η is the viscosity of the mixture η_1, η_2 viscosities and x_1, x_2 are the mole fraction of the pure components 1 and 2, respectively.

3.4.7 Refractive index (n_D)

By definition, the refractive index, n_D, is given by:

$$n = \frac{Speed\ of\ light\ in\ material\ 1}{Speed\ of\ light\ in\ material\ 2} = \frac{sin\ \theta 1}{sin\ \theta 2} \tag{3.21}$$

This is written as the refractive index in material 2 relative to material 1. The incident light is in material 1 and the refracted light is in material 2.

If the instance light is in a vacuum this value is known as the absolute refractive index of material 2. By definition, the refractive index in a vacuum is 1. Actually, air makes a slight change to the refraction of light with a complete refractive index of 1.0008, so the value of the absolute n_D can be used assuming the incident light is in the air. The n_D is also defined as the ratio of the speed of a wave either light or sound in a reference medium to a second medium. Frequently it is used in the environment of the speed of the wave moment of light with a vacuum as a reference medium, although historically other reference media (e.g. air at a standardized pressure and temperature) have been used. In the case of light, the n_D is written by:

$$n_d = \sqrt{\varepsilon_r \mu_r} \tag{3.22}$$

where n_D is a fractive index, μ_r is its relative permeability and ε_r is relative permittivity [311].

3.4.8 Refractive index deviation (Δn_D)

Finally, the deviation refractive index (Δn_D) of binary liquid mixtures can be expressed by the relation:

$$\Delta n_D = n_D - \left(x_1 n_{D1} + x_2 n_{D2} \right) \tag{3.23}$$

where n_D is the refractive index of the mixture n_{D1} and n_{D2} refractive index 1 and 2, respectively.

CHAPTER 4
RESULTS & DISCUSSION

4.1 Investigation of structure and stability of bromelain (BM) in the presence of [Bmim][Cl], [Bmim][Br] and [Bmim][I] using spectroscopic studies

The present study is an attempt has been made to understand the structure and conformational stability of BM in the presence of imidazolium based ILs Such as [Bmim][Cl], [Bmim][Br] and [Bmim][I] by using different biophysical techniques such as UV-vis, fluorescence spectroscopy, circular dichroism (CD) and dynamic light clattering (DLS). Results from spectroscopic analysis are shown in figures 4.1A-4.6A (Appendix II). Obtained transition temperature (T_m) and hydrodynamic diameter (d_H) values for BM in the presence of ILs are presented in Table 4.1A-4.2A (Appendix II). The observed results were discussed in terms of BM stability/destability, which has been published [312].

4.2 Influence of imidazolium-based ionic liquids on the structure and stability of stem bromelain (BM)

4.2.1 Absorption spectroscopy of BM in Imidazolium-Based ILs

UV- absorption spectroscopy is a easy and effective technique to inspect the conformational changes in the structure of protein when present along with co-solvent media [313,314]. In the case of proteins, the UV absorption maxima between 275-280 are due to aromatic residues such as tryptophan (Trp), tyrosine (Tyr) and phenylalanine (Phe) [314]. In many cases, the absorbance differences of a protein are especially useful for observing the conformational changes of a protein [315]. The protein folding and unfolding can be assessed from the absorbance of aromatic AAs [195,316,317]. For BM in aqueous buffer, the intensity of absorption maximum occurs approximately at 280 nm. UV–visible spectra of BM with imidazolium-based ILs such as [Bmim][HSO_4], [Bmim][CH_3COO] and [Bmim][NO_3] at different concentrations of ILs (0.01 to 1.5 M) have been represented in Figure 4.7. The low

concentration of ILs (0.01–0.05 M), absorbance at 280 nm was observed to be almost same as that in the case of BM in buffer as can be seen in Figure 4.7.

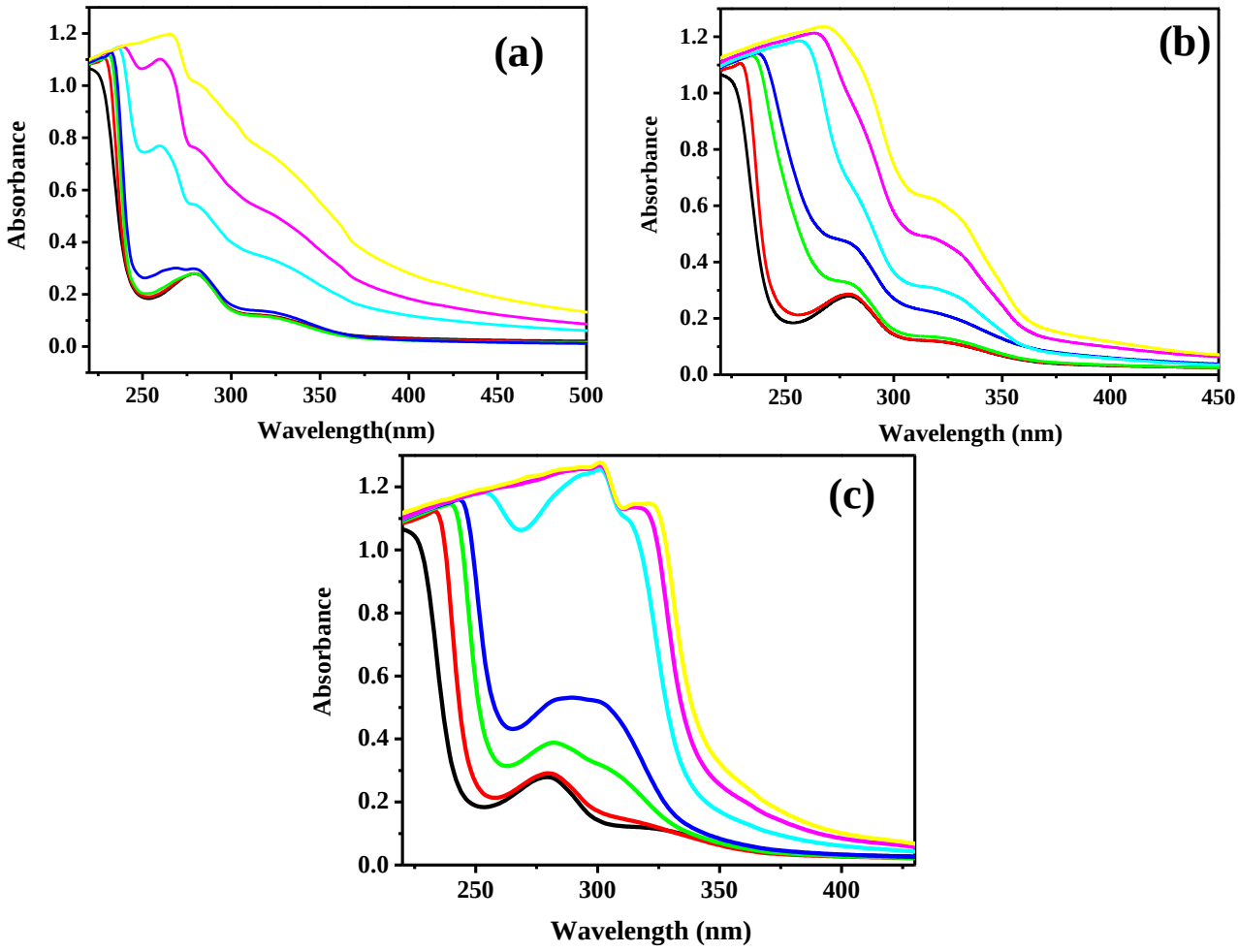

Figure 4.7: UV-vis spectra analysis of BM in buffer (black) and in (a) [Bmim][HSO_4] with 0.01 M (red), 0.05 M (green), 0.10 M (blue), 0.50 M (cyan), 1.0 M (magenta), 1.5 M (yellow) at 25 ^{0}C (b) [Bmim][CH_3COO] with 0.01 M (red), 0.05 M (green), 0.10 M (blue), 0.50 M (cyan), 1.0 M (magenta), 1.5 M (yellow) at 25 ^{0}C and (c) [Bmim][NO_3] with 0.01 M (red), 0.05 M (green), 0.10 M (blue), 0.50 M (cyan), 1.0 M (magenta), 1.5 M (yellow) at 25 ^{0}C.

The absorption intensities are observed to be continuously increased with increasing concentration of [Bmim][HSO_4], [Bmim][CH_3COO] and [Bmim][NO_3] as shown with simultaneous loss of band at 28 nm. This indicates more exposure of the aromatic residues to the solvent resulting in more absorbance intensity of BM at higher concentration of ILs (0.10-

1.5 M). Here, less compact conformation of BM can be assumed as compared to that in aqueous buffer. This may be attribute to some kind of unstability in the hydrophobic pocket of the proteins which result in exhibition of more aromatic amino acid residue to the solvent environment ultimately results in more absorbance. It can be predicted that the ILs have decreased the stability of BM in the presence of ILs with increasing concentration of [0.10-1.5 M] ILs.

4.2.2. Analysis of BM structure and stability with the aid of fluorescence spectroscopy

Steady-state fluorescence spectroscopy is an easy and rapid method for evaluating structures and conformation stability of protein in solvent media . Intrinsic fluorescence of proteins containing aromatic residues such as Trp, Tyr, and Phe are very responsive to study the interactions between protein and ILs and concurrently to explore the quenching mechanism, binding constants, conformational transition, denaturation, and so on [318,319]. The investigation of microenvironment around the Trp of BM can give detailed insight into the conformational stability of in the presence of varying concentrations (0.01, 0.05, 0.10, 0.50, 1.0 and 1.5 M) of different imidazolium-based ILs the spectra has displayed in Figure 4.8. The alteration in the maximum intensity (I_{max}) as well as the maximum emission wavelength (λ_{max}) in the fluorescence spectroscopy are very responsive to the polarity of the microenvironment around Trp. Figure 4.8, represents the interaction of the fluorophore present in BM in the buffer and also in the presence of different concentrations such as [0.01-1.5 M] of ILs. BM contains total 5 Trp residues in which three are unfolded in the hydrophobic core and two are revealed to solvent. The Trp fluorescence of BM displayed a λ_{max} band located at around 348 nm, with the excitation wavelength of 295 nm. We observed with increasing concentration of the ILs such as [[Bmim][HSO_4], [Bmim][CH_3COO] and [Bmim] [NO_3], the fluorescence intensity continuously decreased with increasing the concentration of ILs. As can be visualized from Figure 4.8 a and b that the fluorescence

spectra of BM in [Bmim][HSO_4] and [Bmim][CH_3COO] decreased with redshift at higher concentrations (0.5 to 1.5 M) of ILs.

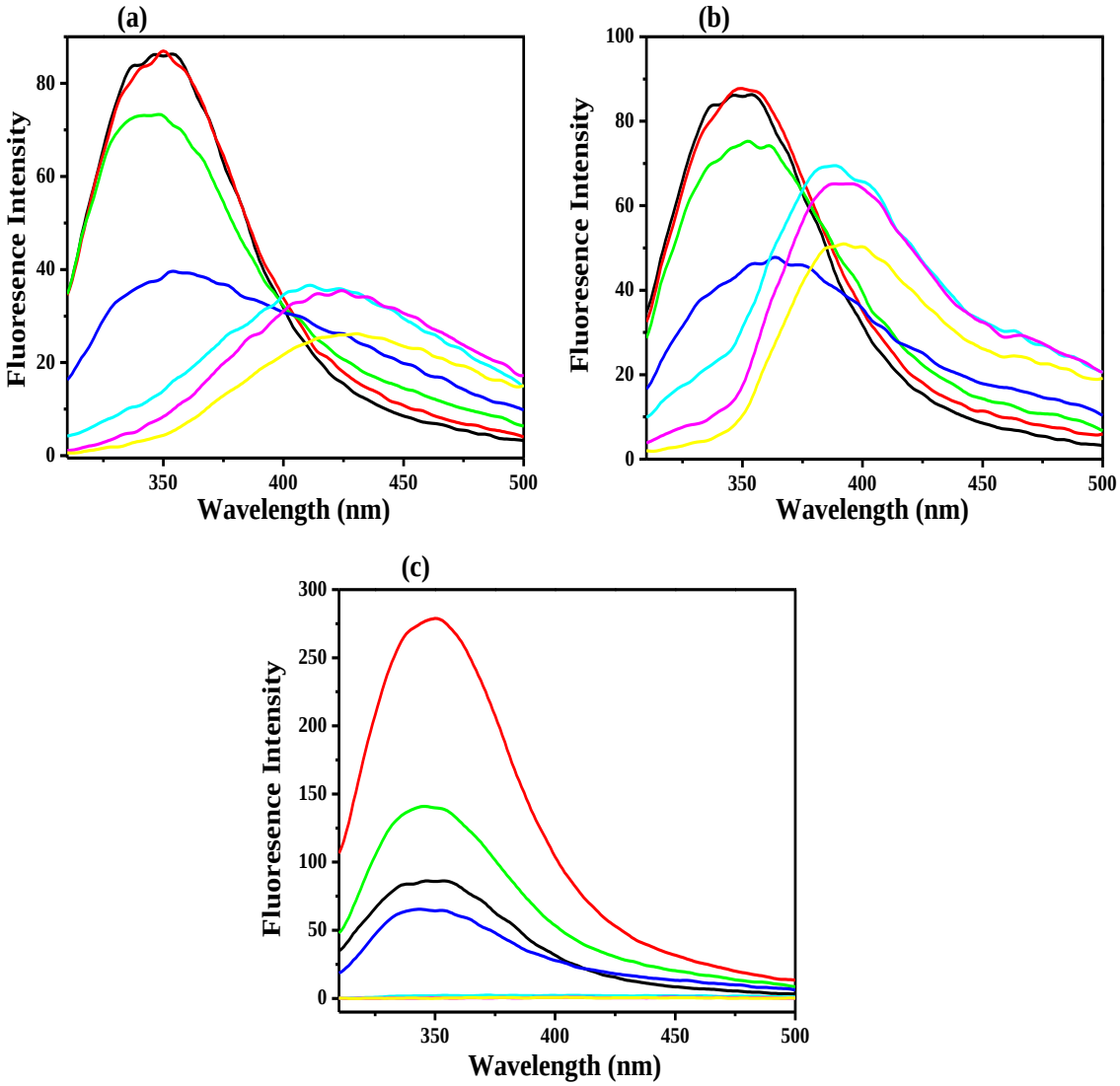

Figure 4.8: Fluorescence spectra analysis of BM in buffer (black) and in (a) [Bmim][HSO_4] with red 0.01 M (red), 0.05 M (green), 0.10 M (blue), 0.50 M (cyan), 1.0 M (magenta), 1.5 M (yellow) at 25 0C (b) [Bmim][CH_3COO] with 0.01 M (red), 0.05 M (green), 0.10 M (blue), 0.50 M (cyan), 1.0 M (magenta), 1.5 M (yellow) at 25 0C and (c) [Bmim][NO_3] with red 0.01 M (red), 0.05 M (green), 0.10 M (blue), 0.50 M (cyan), 1.0 M (magenta), 1.5 M (yellow) at 25 ^{0}C.

The results indicate that the addition of [Bmim][HSO_4] to the BM shifted λ_{max} from 348 to 430 nm as there is increase in the concentration of IL from 0.01 to 1.5 M. In the case of [Bmim][CH_3COO] when compared to [Bmim][HSO_4] fluorescence intensity decreased from 86 to 50 a.u and λ_{max} shifted from 348 to 395 nm at the same concentrations of IL. Asan be

seen from Figure 4.8 a and b, in the presence of 0.01M there were no considerable changes in the fluorescence spectra of BM when it is compared to the spectra of BM in buffer. Until 0.1 M, there was decreased fluorescence intensity without any shift observed in the spectra of BM in [Bmim][HSO_4] and [Bmim][CH_3COO]. Moreover, while enhancing the higher concentrations of ILs from 0.5 M to 1.5 M there was quenching of the fluorescence emission of the Tyr residue and redshift was observed [Bmim][HSO_4]. Both bathochromic shift and hypochromic shift in the spectra of BM in the presence of [Bmim][HSO_4] and [Bmim][CH_3COO] might indicate of the exposure of Trp towards the more polar environment. As compared to [Bmim][HSO_4] and [Bmim][CH_3COO] in case of [Bmim][NO_3] at higher concentration (0.5-1.5 M) has been observed almost negligible fluorescence intensity. However, a marked increase in intensity was observed upon the addition of 0.01 and 0.05 M [Bmim][NO_3]. While increasing the higher concentration such 0.50, 1.0 and 1.5 M the fluorescence intensity was completely decreased. Here, more quenching is observed in the Trp fluorescence in the presence of NO_3^- containing IL. This decreased fluorescence intensity was suggested the unfolding of BM at such a high concentration of IL. Evidently the stability of BM with the increasing concentration of ILs at pH 7.0 the quenching was found to be in the order of $NO_3^- > CH_3COO^- > HSO_4^-$.

4.2.3. Thermal stability of BM in ILs

The transition temperature (T_m) results are required us to find out the thermal stability of BM in the presence of imidazolium-based ILs and results have been shown in Figure 4.9 and corresponding values have been collected in Table 4.3. The T_m of BM in buffer was found to be 67.61 °C. The thermal stability of the BM in low concentrations of ILs was observed to be much higher with respect to the T_m of BM in buffer. As compared to BM in the buffer,the T_m values in the presence of each ILs, there was an increase in T_m value with increase in the

concentrations of ILs (up to 0.50 M) clearly exhibits a significant stabilizing effect by the ILs.

Table 4.3 Transition temperatures (T_m) of the BM in the presence of different concentrations of ILs.

Concentration	[Bmim][HSo_4] (T_m)/ (^{0}C)	[Bmim][CH_3COO] (T_m)/ (^{0}C)	[Bmim][NO_3] (T_m)/ (^{0}C)
Buffer	67.61	67.61	67.61
0.01 M	70.77	69.93	69.22
0.05 M	69.44	69.21	68.64
0.10 M	------*	68.90	------*
0.50 M	------*	68.35	------*
1.00 M	------*	------*	------*
1.50 M	------*	------*	------*

*The error value for T_m is ± 0.2 ^{0}C.

Table 4.3 shows that T_m values of 67.61, 70.77, and 69.44 **^{0}C** for 0.0, 0.01 and 0.05 M of [Bmim][HSO_4], respectively. On the other hand, we obtained the T_m values 67.61, 69.93, 69.21, 68.90, and 68.35 for 0.0, 0.01, 0.05, 0.10 and 0.50 M of [Bmim][CH_3COO] and 67.61, 69.22 and 68.64 for 0.0, 0.01 and 0.05 M of [Bmim][NO_3], respectively. Obviously, we have observed that the T_m values in all the concentrations of ILs were still quite higher than pure. Except [Bmim][CH_3COO], in the case of [Bmim][HSO_4] and [Bmim][NO_3]dramatically follows the same panache with respect to increasing temperature. We were unable to find the T_m value for higher concentrations such as 1.0 and 1.5 M of all the ILs, since we did not observe any thermal fluorescence transition as a function of temperature. Finally, the results show that the addition of lower concentrations (0.01, 0.05, 0.10 and 0.50 M) of all ILs to the BM increases its thermal stability and the keeps enzyme to be in the folded state. Therefore,

from the above results dictates that the increasing order of thermal stability of BM in the presence of studied ILs.

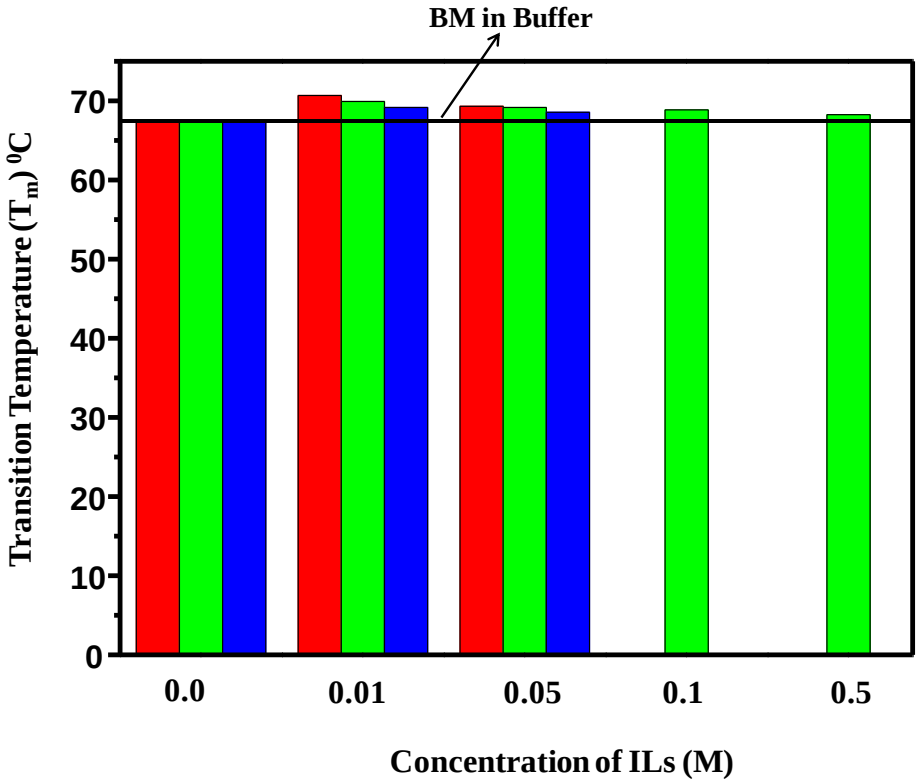

Figure 4.9: The variation in Tm values of BM in buffer (black) with red ([Bmim][HSO_4]), green ([Bmim][CH_3COO]) and blue ([Bmim][NO_3]) which is obtained from fluorescence analysis.

4.2.4. Changes in the secondary structure of BM in the presence of imidazolium-based ILs

We have performed far-UV CD spectroscopy to monitor the changes in the secondary structure of BM in imidazolium-based ILs. Figure 4.10 shows the secondary structure of BM in the presence as well as in the absence of ILs. The far-UV CD spectra of BM in buffer consist of two negative bands one band at 208 nm and second band at 222 nm where the band at 208 is more extreme than at 222 nm (can be seen a black in Figure 4.10) suggesting that the BM lies into the category of α + β class of enzyme. The band at 208 nm parallels to Π to Π* transitions of the α-helix, while the shallow band at 222 nm corresponds to Π to Π*

transition for both α-helix and random coil are observed. As shown in Figure. 4.10a and b, there is decreased negative ellipticities of these band with increasing concentration of the [Bmim][HSO_4] and [Bmim][CH_3COO].On the other hand, the secondary structure of the BM was still maintained in the presence of lower concentrations (0.01 and0.05 M) of the [Bmim][HSO_4] and [Bmim] [CH_3COO]. Figures 4.10a and b represent secondary structure destabilization at higher concentration of [Bmim] [CH_3COO] and [Bmim][HSO_4] except at lower concentrations such as 0.01 and 0.05 M. Exceptionally, in the case of [Bmim] [NO_3] we didn't found any noticeable secondary structures. Therefore, it directs to the overall loss of secondary structure of BM in the presence of [Bmim] [NO_3].

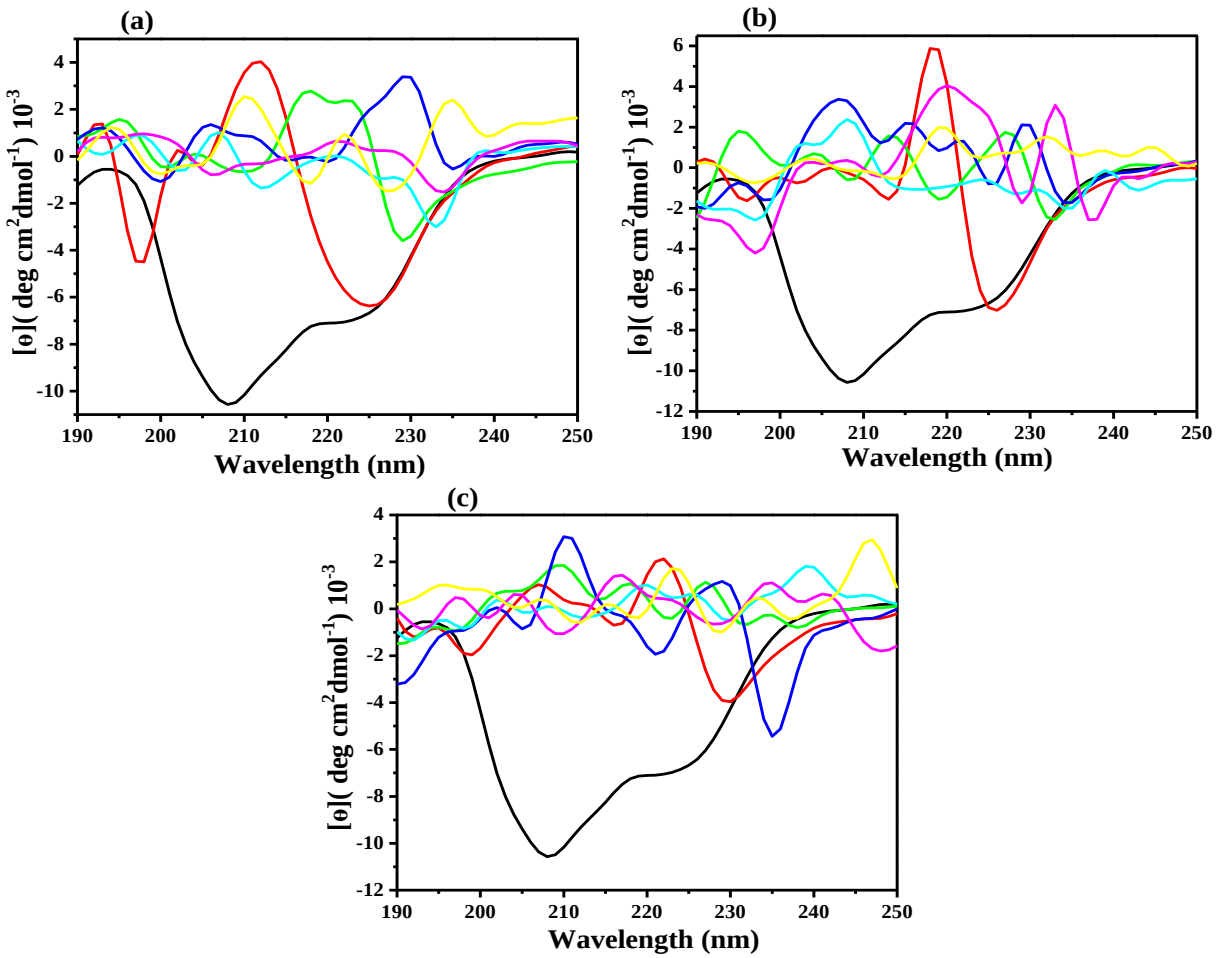

Figure 4.10: Influence of (a) [Bmim][HSO_4], (b) [Bmim][CH_3COO] and (c) [Bmim][NO_3] on the structure of BM in buffer (black), from far-UV CD analysis with 0.01 M (red), 0.05 M (green), 0.10 M (blue), 0.50 M (cyan), 1.0 M (magenta), 1.5 M (yellow) at 25 ^{0}C.

4.2.5 Changes in the tertiary structure of BM in the presence of imidazolium-based ILs

We further performed Near-UV CD to observe the changes in the tertiary structure of BM in the presence of various concentrations of [Bmim][HSO_4], [Bmim] [CH_3COO] and [Bmim] [NO_3] which has been displayed in Figure 4.11. The tertiary structure of BM in the buffer is characterized by negative and positive bands between 270−300 nm that mostly originate from the environments of Phe, Tyr and Trp, respectively. As can be seen in Figure 4.11 that negative ellipticity is decreased with increasing the concentrations of [Bmim][HSO_4], which reflects loss compact structure of the enzyme at a higher concentration such as 0.50, 1.0 and 1.5 M. However, Figure 4.11a indicates that the tertiary structure of BM completely lost in the presence of [Bmim][HSO_4] at their higher concentrations. The near-UV spectrum of BM shows positive at 270−282 nm and negative 300 nm. In the Trp spectra shows a peak close to 300 nm, Tyr shows a peak around 282 nm. However, the tertiary structure changes in BM interpreted by these bands. In the rest of the higher concentrations, we couldn't find the tertiary structure of BM in the presence of [Bmim][CH_3COO] and [Bmim][NO_3]. Therefore, our near UV CD results represent the tertiary structure of BM was completely interrupted at higher concentrations of [Bmim][CH_3COO] and [Bmim][NO_3] (Figures. 4.11b and c), respectively.

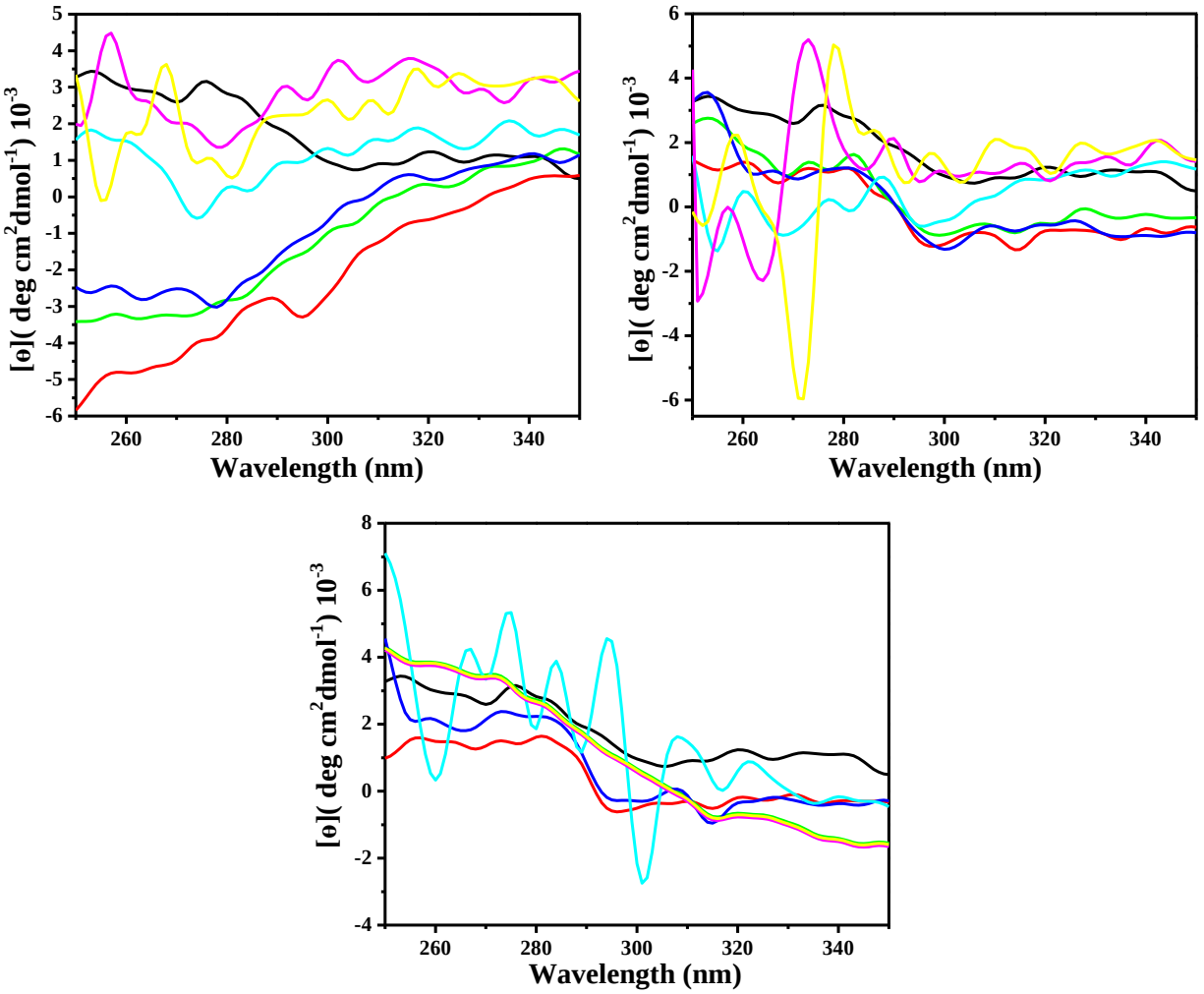

Figure 4.11: Influence of (a) [Bmim][HSO_4], (b) [Bmim][CH_3COO] and (c) [Bmim][NO_3] on the structure of BM in buffer (black), from near-UV CD analysis with 0.01 M (red), 0.05 M (green), 0.10 M (blue), 0.50 M (cyan), 1.0 M (magenta), 1.5 M (yellow) at 25 ^{0}C.

4.2.6 Exploration of hydrodynamic diameter of BM in the presence of imidazolium-based ILs

Dynamic light scattering (DLS) is one of the well accepted methods used to determine the size and shape of the biomolecule [318–321]. To further establish experimental results, we have performed DLS measurements to observe the variation in the size of the particles in terms of the hydrodynamic diameter (d_H) of BM in the absence and presence of the different concentrations of [Bmim][HSO_4], [Bmim][CH_3COO] and [Bmim][NO_3]. Figure 4.12

elucidates intensity distribution graph of BM in water and in varying concentration of different ILs.

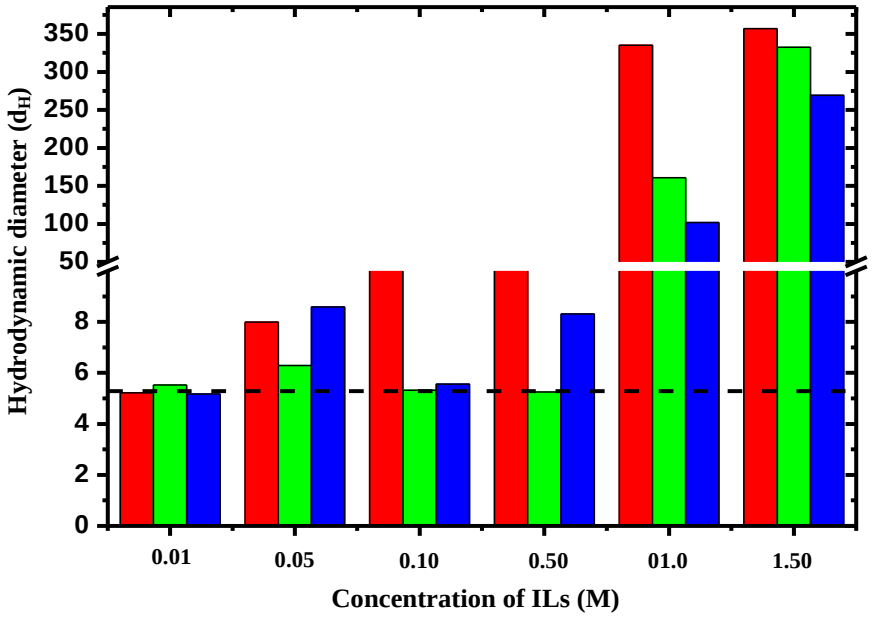

Figure 4.12: Hydrodynamic diameter (d_H) obtained from the intensity distribution graph for BM in buffer with red ([Bmim][HSO_4]), green ([Bmim][CH_3COO]) and blue ([Bmim][NO_3]) at different concentrations.

The deionized water has been used in the preparation of the protein samples in order to avoid any intrusion caused by the ions present in the buffer and the pH is maintained approximately equal to ~7. As depicted in Figure 4.12 that the characterization of size distribution graph of BM in water in the presence of varying concentration of [Bmim][HSO_4], [Bmim][CH_3COO] and [Bmim][NO_3] at constant temperature of 25 °C. The d_H values of BM in the presence of different concentrations (0.01 to 1.5 M) of all three ILs are presented in Table 4.4. The d_H values in Table 4.4 clearly show that the concentration of 0.01 M, the d_H value is almost similar in the case of all the studied ILs. As can be seen from Figure 4.12 as well as Table 4.4 in water the d_H of BM was pivoted around 6.22 nm and it was 5.22 and 7.99 in 0.01 and 0.05 M of [Bmim][HSO_4], respectively. We observe minimal enhancement in the size of the BM in the presence of [Bmim][HSO_4], however, at 0.10 and 0.50 M of [Bmim][HSO_4], there is

the existence of the loose conformation of the protein as a result of slow denaturation of protein at these concentrations. When there is a further increase of the concentration of this IL, there is a substantial increase in the size of BM being 335.2 and 356.8 nm in 1.0 and 1.5 M [Bmim][HSO_4], respectively. In the presence of rest of the ILs such as [Bmim][CH_3COO] and [Bmim][NO_3] up to the concentration of 0.50 M, we find that there is a minimal increase in the d_H values as compared to BM in water. In the case of all the ILs at higher concentrations 1.0 and 1.5 M respectively, there exists an aggregated form of the protein due to complete denaturation of both the ILs. It can be clearly seen from Figures 4.12b and c that the d_H values of BM first decreases at low concentration and then increases at high concentration of ILs. These indicate the fact that the protein acted as a destabilizer in the presence of high concentrations of ILs. Consequently, the obtained results confirming the complete denaturation of BM protein at high concentration of [Bmim][HSO_4], [Bmim][CH_3COO] and [Bmim][NO_3].

Table 4.4 Hydrodynamic diameter (d_H) of BM in different concentrations of ILs.

Concentration of ILs	[Bmim][HSO_4]/(nm)	[Bmim][CH_3COO]/(nm)	[Bmim][NO_3]/(nm)
0.0	6.22	6.22	6.22
0.01	5.22	5.52	5.17
0.05	7.99	6.29	8.58
0.10	16.48	5.32	5.56
0.50	23.44	5.25	8.31
1.0	335.2	160.9	101.8
1.5	356.8	332.3	269.1

Our spectroscopic and DLS results represent the interaction between BM in the presence of imidazolium-based ILs and it was found to be concentration dependent. In this study, we considered all results to explain the mechanism of stabilization/destabilization of BM in the presence of different concentrations of ILs. We found a considerable absorbance of Tyr residue in UV in the presence of [Bmim][HSO_4], [Bmim][CH_3COO] and [Bmim][NO_3] ILs at their lower concentrations up to 0.05 M. On further increase in the concentration of IL the absorption intensity bands are very broad in the presence of rest of all concentration (0.10 to 1.5 M) of ILs. An increase in the absorption intensities indicates the BM in the ILs can be accredited to the alternations in the solvent system in the case of all ILs, the increase UV-vis absorption intensity suggests that the polarity around the hydrophobic chromophore is decreased due to the interaction between BM and ILs. The fluorescence intensity was decreased with red shift of the spectra, which means there was a quenching of the fluorophore with simultaneously decreased hydrophobicity around Trp residue to the polar environment on addition of different concentration of HSO_4 and CH_3COO. On the other hand, in the case of [Bmim][NO_3] intensity continuously decreases with increasing the concentration of IL up to 0.10 M. On further increasing the concentration of IL, the fluorescence intensity was completely decreased. The large decrease in intensity suggested that unfolding has taken place, which indicates that the BM protein completely denatured in the presence of such a higher concentration. The order of the fluorescence quenching and destabilization of BM protein in the presence of imidazolium-based ILs is found to be NO_3^-> CH_3COO^- >HSO_4^-.

Moreover, in this study, we performed thermal fluorescence as a function of temperature to characterize the effect on the thermal behavior of BM. With the addition of low concentrations of all ILs shifted the T_m values of BM towards a higher value. However, our thermal results demonstrate that the thermal stability of BM was enhanced in the presence of all ILs at lower concentrations. On further increasing the concentration of ILs we did not

observe any thermal fluorescence transition as a function of temperature. This thermal T_m value indicates that the BM protein destabilized at higher concentrations of all ILs order of destabilization $NO_3^- < CH_3COO^- < HSO_4^-$. Also, the thermal values are accordance with UV and fluorescence analysis with each other, which estimate that in a low concentration of ILs the BM, are stabilized. Accordingly, far- UV CD spectroscopy analysis results show the BM Secondary structure slightly perturbed after the addition of ILs at high concentration (From 0.10 to 1.5 M). From the results,it is quite clear that BM has maintained overall Secondary structure in the presence of low concentration up to 0.05 M of all ILs, which is consistent with our UV and Fluorescence results. On the other hand, Near-UV CD results also accordance with far- UV CD results. There were no appreciable changes in the tertiary structure of all ILs at higher concentrations. Furthermore, to expand the experimental results we have performed DLS as well. In DLS, the particle size of BM stabilized at the lower concentration up to 0.05 M of [Bmim][HSO_4]. In the case of [Bmim] [CH_3COO] and [Bmim] [NO_3], there is the maintenance of the hydrodynamic size of BM up to 0.50 M as compared to BM in the buffer. Further increasing the concentration of all ILs, we observed huge aggregates with a particle size in the range of 150−400 nm. Consequently, the obtained results have been reported that the structure and conformational stability of BM in imidazolium-based ILs at pH 7.0 is in the order of $HSO_4^- > CH_3COO^- > NO_3^-$. Moreover, it seems that these anions are following the Hofmeister stability order. Therefore, this anionic of series may be suitable for explaining the protein folding/unfolding studies.

Finally, we observed from these results in the case of ILs, the structure of BM acted as a stabilizer at lower concentration and acted as a destabilizer at higher concentration. However, at a lower concentration of ILs such as 0.01 and 0.05 M were found to be stabilizing the BM structure completely. As can be seen the opposite effect at high concentration. In other words, the HSO_4 anion of IL considered as most kosmotropic anion as well as almost stabilizer while

NO_3 anion of IL considered chemotropic anion as well as least destabilizer for the structure of BM. In the presence of particular ions can be best understood the mechanism relating to unfolding/folding of proteins of the varying hydration levels by addressing which take place surface of the protein. As a consequence of all the above results reveal that this type of interaction for stabilization/destabilization of a protein depends not only on the hydrophilicity of the anion of ILs but also hydrophobicity of amino acid side chains. Still, using these results cannot be finalized only by imidazolium-based ionic liquids, so already we started working on wide range of amino-acid containing ionic liquids to find out the new strategies in the field of protein stabilization/destabilization by using the AAILs.

The Hofmeister series has been observed to have large impact on the wide range of biological phenomenon including protein folding/unfolding. However, most aspect is that the effect of Hofmeister series is still vague and unexplained. Some of the available reports suggest that this series is only observable at high salt concentration while in some other cases the series is observed to be partially & fully reversed whenever there is alternation in the concentration of ion [322].

From the above results as well as from the previous results [312] it can be clearly observed that the BM is able to sustain its folded conformation only at low concentration of the ILs (i.e, 0.01 and 0.05 M). Therefore, it would be suitable to predict whether the series of anions from the present work as well as from previous work would fallow the Hofmeister series at 0.05 M concentration of IL. The above results dictate the order of ions to be HSO_4^- > CH_3COO^- > NO_3^- in the stabilization of BM structure while the previous results [312] dictate the order to be Cl^- > Br^- > I^-. From both of these results it is quite clear that CH_3COO^- is stabilizer for the BM structure while I^- is observed to be destabilizer for the BM structure. By looking at the T_m values of BM at 0.05 M concentration of ILs, it is observed that the series of ILs are not exactly being followed by these ions. However, the CH_3COO^- ion being

stabilizer and I^- being destabilizer is consistent with the Hofmeister series. Our series of Hofmeister ions are found to be in the order of $HSO_4^- > CH_3COO^- > NO_3^- > Cl^- > Br^- > I^-$. By looking closely at the series only the placement of NO_3^- seems to be described. I^- is a large univalent ion of low charge density which can behave similar to hydrophobic solutes and easily participate in H^- bonding. This type of ion can be supposed to be associated with their counter ion in the solution [323]. In contrast anion such as CH_3COO^- is supposed to be found in less association with their counter ions (in this case imidazolium) and this ultimately may result in the stabilization on the hydration of the charged portion of a protein.

In some of the reports it has been seen that there is reversal of the Hofmeister series at low salt concentration while a direct Hofmeister series is exhibited at high salt concentration [324]. The reason accounted for this was that the adsorption of more polarizable ion is enhanced at low salt concentration by ion surface dispersion interactions. While at high salt concentration adsorption of more polarizable anions ultimately results in effective revert in surface charge which leads to an increase in cation adsorption results increase in surface force. However, in the presence of ions of ILs, such reversal of the series is not observed even at high concentration. In this contrast only, stability of the protein in the presence of ILs was reviewed by Shu et. al [169] proposed that the exit a complicated combination of mechanism in the presence of ion of ILs. This complicate mechanism can be due to combined effect of hydrophobicity, nucleophilicity and H- bond basicity of ILs.

4.3 Influence of choline-based ionic liquids on the structure, stability and activity of stem bromelain (BM)

To ascertain the role of anions of the ILs on the stability and activity of BM, we have conducted experiments with ILs sharing a common choline cation combined with the various anions forming ILs such as: [Ch][Cl], [Ch][Ac], [Ch][Dhp], [Ch][Bit], [Ch][I] and [Ch][OH].

These results analyzed conformational stability, thermal stability and activity of the BM in the presence of different concentrations of choline based ILs by many biophysical techniques.

4.3.1 Absorption spectroscopy analysis for BM in choline-based ILs

UV-visible absorption measurement is a simple and efficacious method to explore conformational changes of protein in the solvent media [313]. In the spectrum of proteins, absorption in the 210-220 nm range is because of the peptide bond. The absorption bands between 275 and 280 nm are affected by the absorbance of tyrosine (Tyr) and tryptophan (Trp) in addition to a small amount, by the absorbance of cysteine (Cys) residue [313,162,278] . Figure 4.13 signifies the spectral variations in UV absorbance of BM in different concentrations of ILs. As shown in Figure 4.13, there is a strong absorption band at around 280 nm for BM which is mainly due to the n-π^* transition of aromatic amino acids (AAs) [313]. As can be seen in Figure 4.13, the absorbance of BM progressively decreases with increasing the concentration of [Ch][Cl], [Ch][Ac] and [Ch][Dhp], while in case of [Ch][Bit] absorbance decreases upto 0.1 M of [Ch][Bit] and then it starts to increase with red shift at higher concentration (1.5 M). Due to high absorbance of pure [Ch][I] in the range of 250-280 nm the interpretation of spectra is difficult. In the case of [Ch][OH] shows a sharp increase in the absorbance even at lowest concentration 0.01 M, and after increasing the concentration of [Ch][OH] leads to hiking in absorbance escorted with insignificant red shift (0.05 M). Moreover, at higher concentrations after 0.05 M of [Ch][OH], the analysis of UV-spectra for BM is quite hard due to intrinsic absorbance of pure [Ch][OH]. As one can see from Figure 4.13 (a-c), the absorption decreases with increasing the concentrations of [Ch][Cl], [Ch][Ac] and [Ch][Dhp], respectively, which indicates that the aromatic residues of BM may be not as much of exposure to the solvent allowing less absorbance, in order, BM can be expected in the more compact structure as compared to that in PBS buffer. On the

other hand, [Ch][OH] exhibits a distinctive behavior in difference to the other ILs. An increased absorbance of BM with increasing concentration of [Ch][OH] may be ascribed to exposure of many aromatic residues to the polar solvent media, therefore, high absorbance.

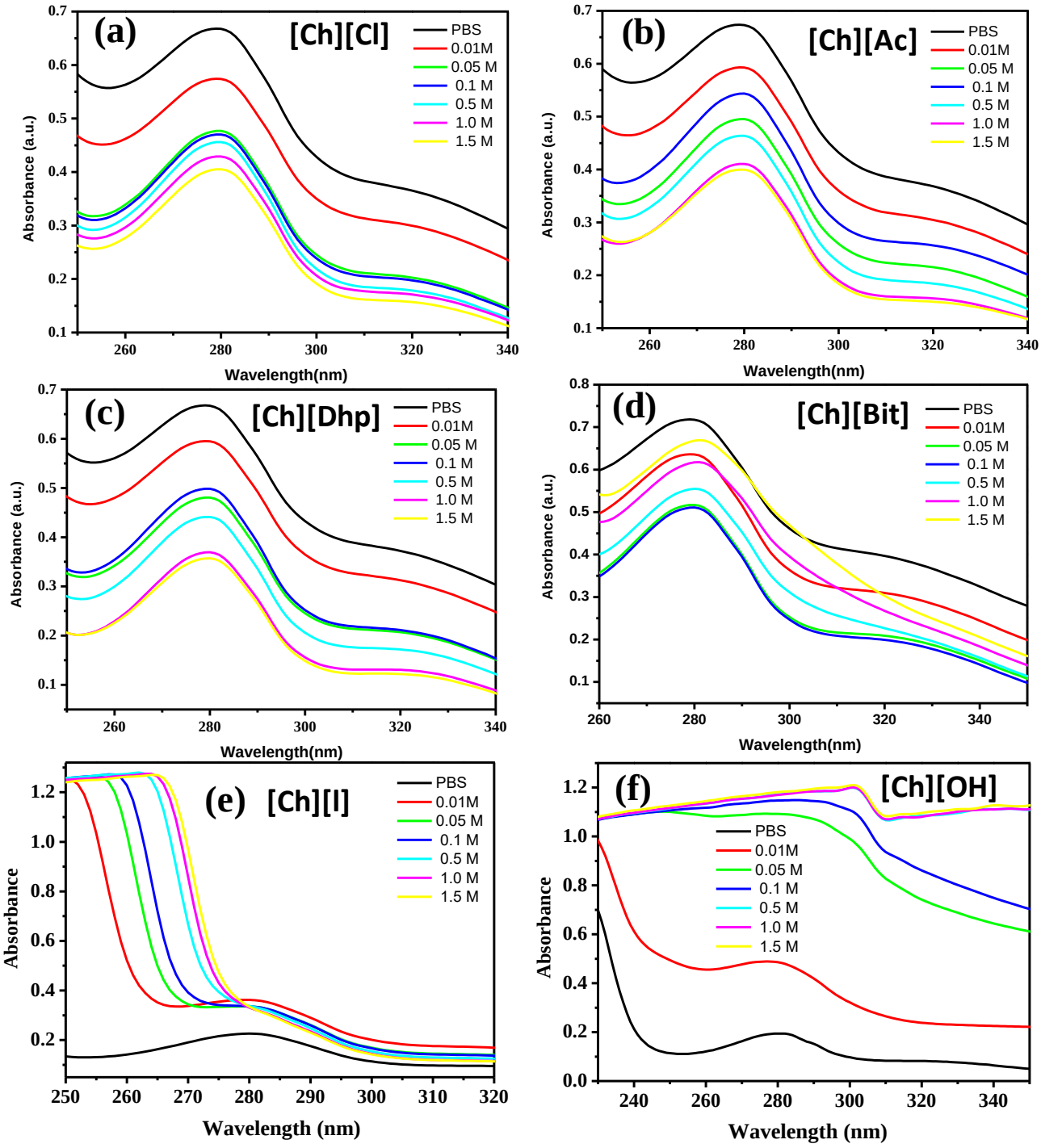

Figure 4.13: UV-visible absorption spectra of BM in PBS and varying concentrations of ILs at 25 °C.

4.3.2 Analysis of steady-state fluorescence of BM in choline-based ILs

Fluorescence spectroscopy detection is highly sensitive for studying the conformational changes of proteins containing fluorophore residues such as Trp, Tyr and Phe. The fluorescence spectral parameters such as maximum emission wavelength (λ_{max}) and maximum intensity (I_{max}) are highly susceptible to the polarity change around the microenvironment of fluorophore. The fluorescence emission from Trp residues is more sensitive as compare to Tyr and Phe [317]. As mentioned earlier, BM has 5 Trp residues among all three are buried in the hydrophobic environment and two are exposed in the protein surface[282]. Figure 4.14 represents Trp fluorescence of BM in PBS as well as in the presence of different concentrations of various choline-based ILs. The λ_{max} of native BM in PBS at pH 7.0 is at 347 nm (black spectra) after excitation at 295 nm. It is quite clear from the Figure 4.14 that all ILs are perturbing the microenvironment around the Trp of BM. As can be clearly observed in Figure 4.14 the fluorescence intensity (I_{max}) of BM in [Ch][Cl] and [Ch][Ac] is gradually increase with increase in the concentrations of both ILs, while varying concentrations of ILs do not cause any shift in λ_{max}. On the other hand, a chronic decrease in the I_{max} with blue shift is observed in case of increasing concentration of [Ch][Dhp] as compared to that of control. I_{max} for BM is also found to decrease with blue shift as a function of concentration for [Ch][Bit]. We observed a slight increase of the emission spectra of fluorescence on the addition of [Ch][I] upto 0.1 M however, after this concentration there is a considerable decrease in the I_{max} with blue shift for BM on increasing the concentration of [Ch][I]. In case of of [Ch][OH] a rapid decrease in the I_{max} is observed even at lowest concentration (0.01M) which is a indication of entirely denatured conformation of protein. From fluorescence results, it is clear that [Ch][Cl] and [Ch][Ac] are behaving in similar way at all concentration which is well consistent with UV results. By these results we can also

predict that Trp of BM is getting more exposed to the hydrophilic environment due to unfolding of the protein in presence of [Ch][OH] as compare to other ILs.

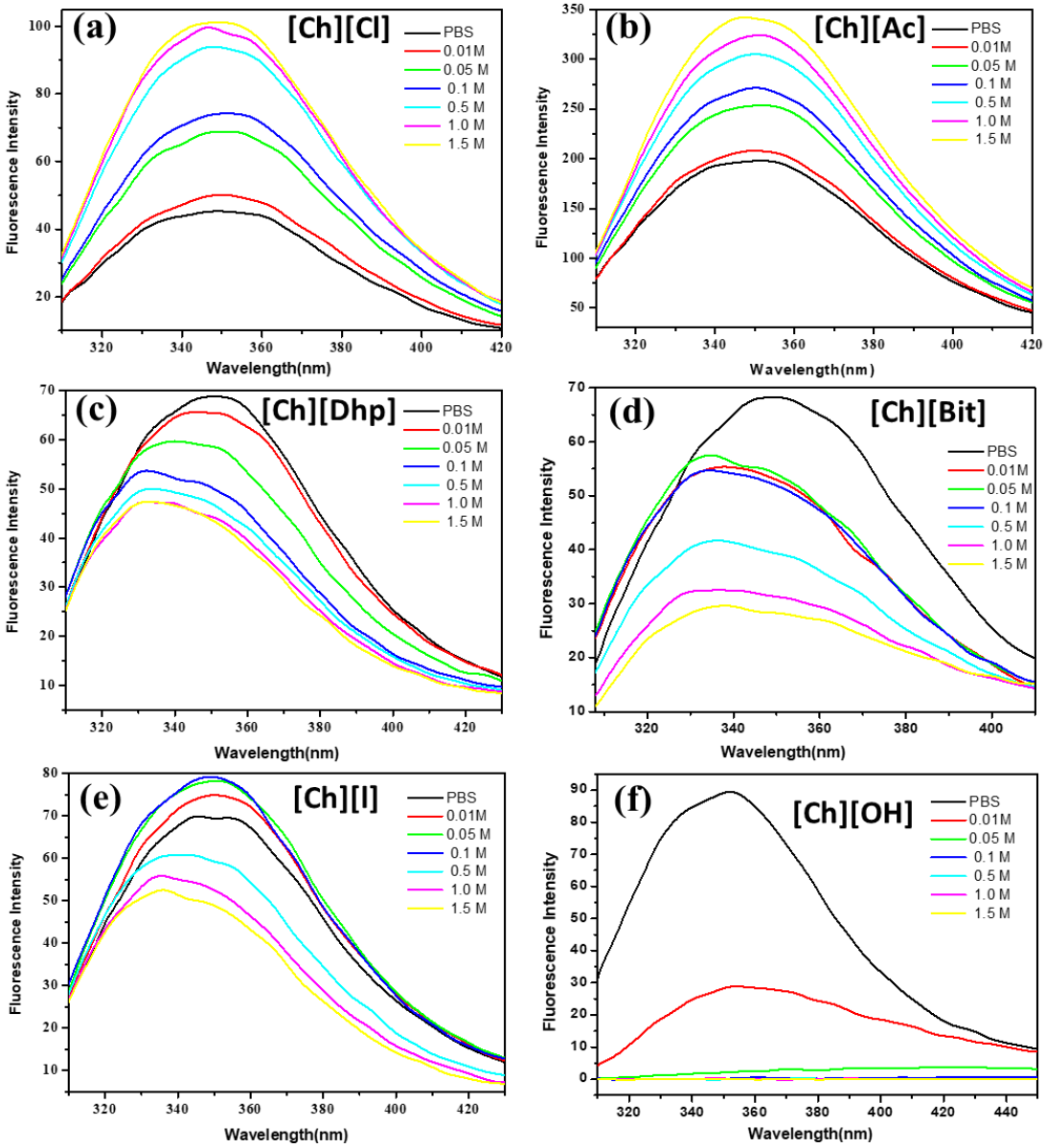

Figure 4.14: Trp fluorescence spectra of BM at 25 ^{o}C in the presence of PBS and varying concentrations of ILs.

4.3.3 Thermal stabilization of BM in presence of choline-based ILs

The thermal stability of BM was examined with the help of transition temperature (T_m), it is an important thermodynamic parameter for calibrating the thermal stability of a protein in

solvent media [204]. The T_m values of BM in the buffer and in different ILs with varying concentration are displayed in Table 4.5 and Figure 4.15. The T_m of BM in buffer is 66.0 ^{0}C. As can be seen from Figure 4.15, that the T_m values of BM increase in presence of [Ch][Cl] as a function of concentration, T_m values increase from 66 ^{0}C (PBS) to 71 ^{0}C (at 1.5 M IL). Whereas in case of [Ch][Ac], the T_m values increase upto 1.0 M concentration and then start to decrease. In presence of [Ch][Dhp] initially there is slight increase in the T_m values of the BM at lower concentrations up to the 0.1 M of IL, later T_m values start to decrease at higher concentrations (after > 0.1 M). However, T_m of BM is largely affected in the presence of [Ch][Bit] and [Ch][I], there is remarkably decreased in the T_m values with increasing concentration of ILs. While in case of [Ch][OH] due to exceptionally quenching of flourophore groups transition curves is not obtained except at the lowest concentration. By comparison it can be conclude that thermal stability of BM is lowest in case of [Ch][OH] as compare to all ILs. The thermal stability results are well consistent with steady state fluorescence results. Thermal stability of BM in different ILs follow the order as : [Ch][Cl] > [Ch][Ac] > [Ch][Dhp] > [Ch][I] > [Ch][Bit] > [Ch][OH] according to T_m values provided in the Table 4.5 and Figure 4.15.

Table 4.5: T_m values of BM in the presence of PBS at various concentrations of ILs.

	T_m (^{0}C)					
Concentration of ILs	Ch [Cl]	Ch [Ac]	Ch [Dhp]	Ch [Bit]	Ch [I]	Ch [OH]
0.0 M	66.0	66.0	66.0	66.0	66.0	66.0
0.01 M	66.5	65	66.8	64	64.5	58.2
0.05 M	67.0	67.8	67.1	59.0	63.2	–
0.1 M	67.8	67.5	66.8	57.5	62.5	–
0.5 M	69.5	67.5	64.7	56.5	62.0	–

1.0 M	70.0	68.8	63.6	54.2	61.6	–
1.5 M	71.0	67.5	62.5	53.2	60.1	–

*The error value for T_m is ± 0.2 ^{0}C.

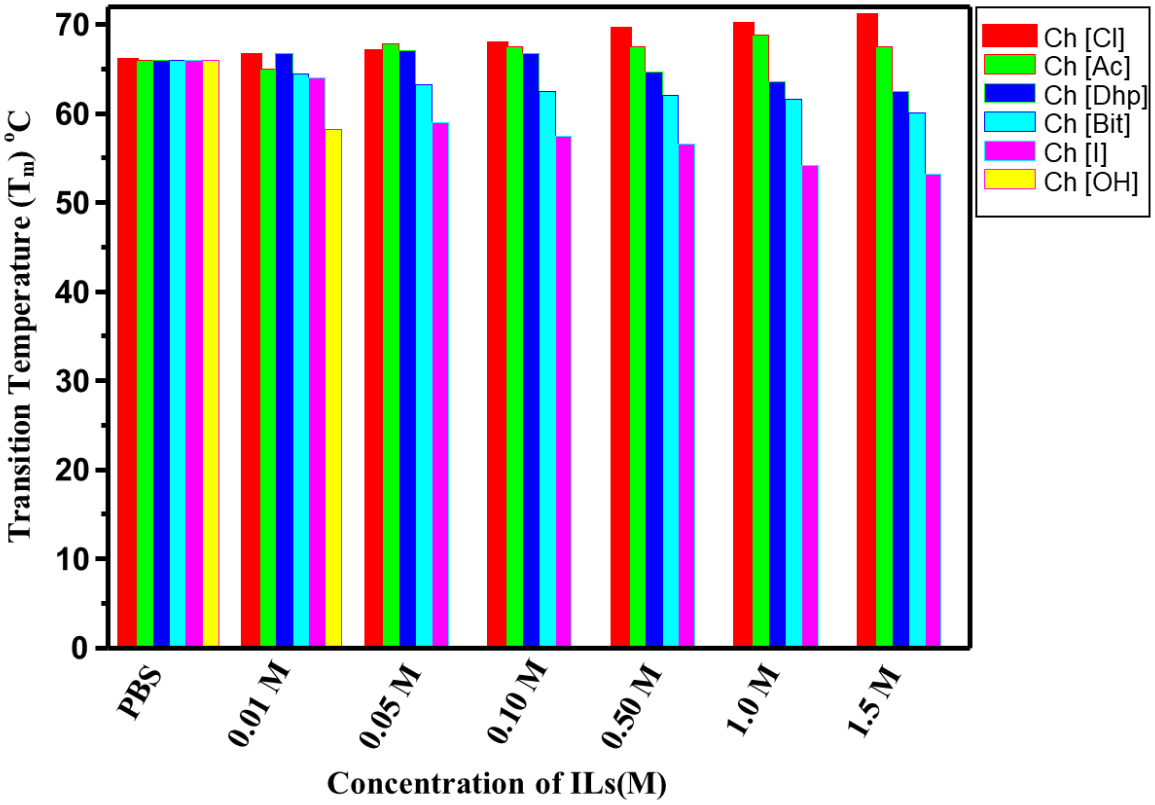

Figure 4.15: The variation in T_m values of BM in the presence of PBS and varying concentrations of ILs.

4.3.4 CD spectral analysis for BM in presence of choline-based ILs

Circular dichroism (CD) spectroscopy is considered as a most suitable tool to determine any conformational transitions of BM in presence of any co-solvents [293]. We used CD spectroscopy to examine further secondary and tertiary structural changes of BM conformation in the absence and presence of ILs. The near-UV CD band in the wavelength range from 260 to 320 nm give information about the environments of the aromatic AAs side

chains. Trp shows a band near to 290 nm with unique structure of peak between 290 and 305 nm, Tyr give a band between 275 and 282 nm, with a shoulder at longer wavelengths [293]. The spectrum of BM shows positive bands around 270, 280 nm and a negative band at 299 nm [282]. Unfortunately, due to interference of the ILs, the interpretation of the spectra is difficult in near UV region, only far region of the CD spectrum (190–250 nm) of BM could be investigated, which can provide further insights for secondary structure changes.

Figure 4.16 signifies the secondary structure of BM conformational changes in presence of different concentrations of various ILs. Far-UV CD spectra of BM shows two negative bands at ~208 nm and ~222 nm (shown black in Figure 4.16) which suggests that BM is the typical α + β class of enzyme [325]. In Figure 4.16, in presence of [Ch][Cl], there is minimal decrease in ellipticities for negative band at 208 and 222 nm with almost no shifting of 208 nm band. These results show maintaince of α-structures or secondary structure of BM at all concentration of [Ch][Cl]. In case of [Ch][Ac] there is considerable increase in α- helical structures at lower concentration upto 0.1 M, after this concentration, there is comprehensive shifting of 208 nm band towards higher wavenumber nearby 213 nm. At higher concentration (1.5 M) it is found that negative band shifted to 224 nm and a positive band shifted at 213 nm with complete disappearance of α + β structures [326]. As is clear from the Figure 4.16 for [Ch][Dhp] that negative ellipticity is increasing upto 0.5 M concentration of IL, after this negative ellipticity start to decrease but still more than the PBS which reflects more compact structure of BM at all concentration of [Ch][Dhp].

From Figure 4.16 (d), it is clear that in presence of [Ch][Bit] secondary structure of BM is disturbed even at low concentration. In Figure 4.16 (f) it can be observed that with increase in concentration of [Ch][OH], there is decrease in α- structure with red shift of 208 nm band trend towards the specific wavenumber of the β-sheet. Further increase in concentrations (at 1.0 and 1.5 M), there is complete disruption of secondary structure which is apparent from

the replacement of whole negative bands. Again CD result of [Ch][OH] is well consistent with UV, steady state fluorescence and thermal fluorescence results which shows that [Ch][OH] is behave as a destabilizer.

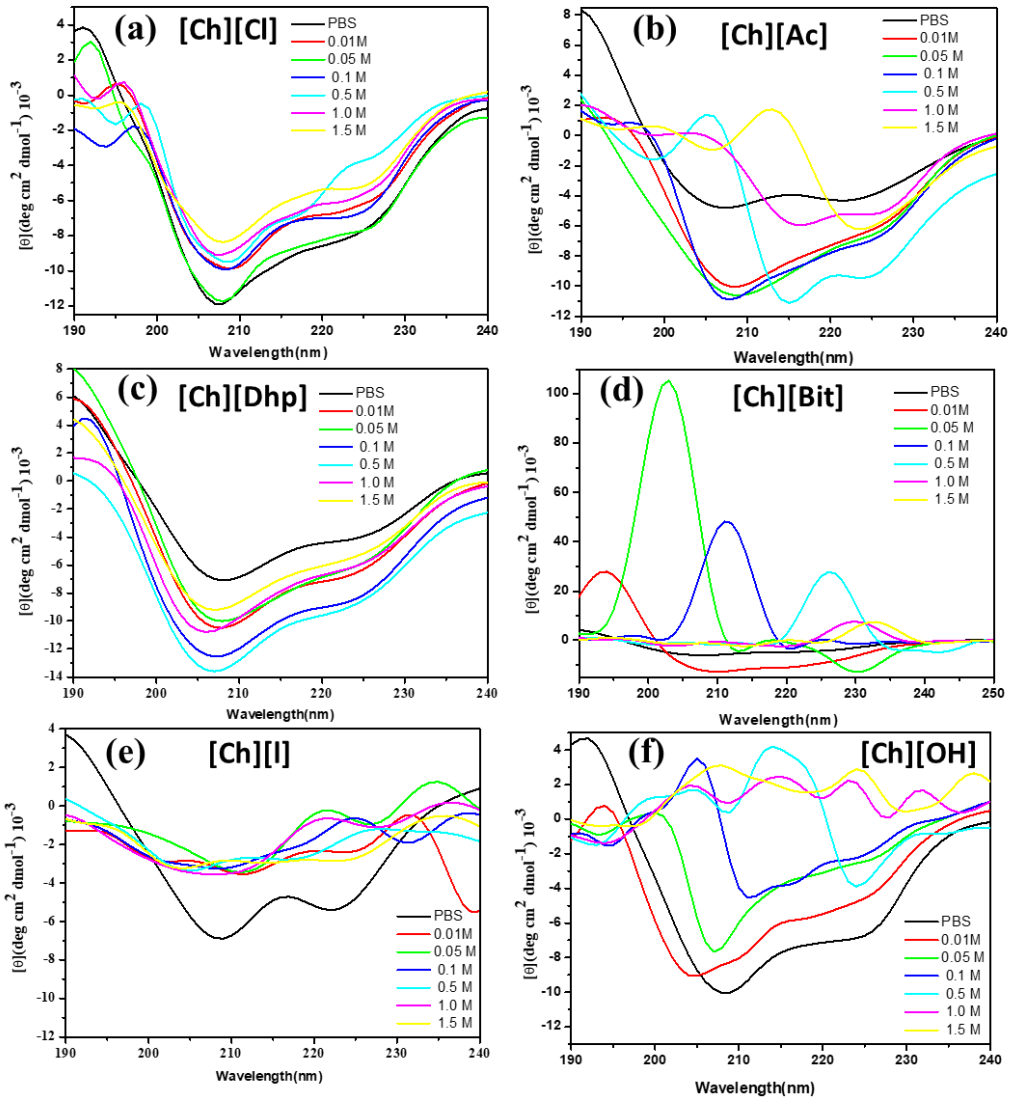

Figure 4.16: Far- UV CD spectra of BM at 25 ^{o}C in the presence of PBS and varying concentrations of ILs**.**

Unexpectedly, because of high absorbance of the [Ch][I] exact interpret the secondary structure changes of BM is difficult but it can be seen from the results that the secondary structure is not disturbed much as compare to the [Ch][Bit] and [Ch][OH].

4.3.5 Influence of choline-based ILs on the hydrodynamic diameter (d_H) of BM by dynamic light scattering (DLS) measurements

To further confirm these results, we have performed DLS measurements. DLS is very popular biophysical technique to determine the particles size in any solvent system [297]. Table 4.6 demonstrates hydrodynamic diameter (d_H) of BM in PBS and various concentration of ILs. Figure 4.17 displays the volume distribution curve of BM in PBS and in the presence of different concentration of ILs. As can be seen in the Figure 4.17, BM shows d_H value around 4.53 nm. From Figure 4.17 (a) and (b) it can clear that there no substantial change in size of BM in presence of [Ch][Cl] and [Ch][Ac] and the size is less change in presence of [Ch][Cl] as compare to [Ch][Ac]. The DLS results also showed that there is no only slight shifting of d_H towards the higher values as a function of increasing concentrations, however, change in size is more at 1.5 M. However, in case of [Ch][Bit], [Ch][I] and [Ch][OH] the d_H values drastically changes from ~4.5 nm (control) to >100 nm at higher concentrations (>0.5 M) of ILs which represent highly denatured state or aggregate state of BM at these concentration.

Table 4.6: Hydrodynamic diameter (d_H) of BM in buffer and various concentrations of choline based ILs.

Concentration	Hydrodynamic diameter (d_H)/nm					
of ILs	Ch [Cl]	Ch [Ac]	Ch [Dhp]	Ch [Bit]	Ch [I]	Ch [OH]
0.0	4.53	4.53	4.53	4.53	4.53	4.53
0.01 M	5.65	5.40	5.63	5.11	5.34	6.25
0.05 M	5.55	6.00	5.82	4.40	5.93	6.42
0.1 M	5.77	6.01	5.56	6.04	6.16	50.74
0.5 M	5.86	6.20	6.54	6.04	108.2	125.4
1.0 M	6.02	6.36	6.77	--	178.3	165.5

1.5 M	6.98	6.94	7.85	--	296.5	--

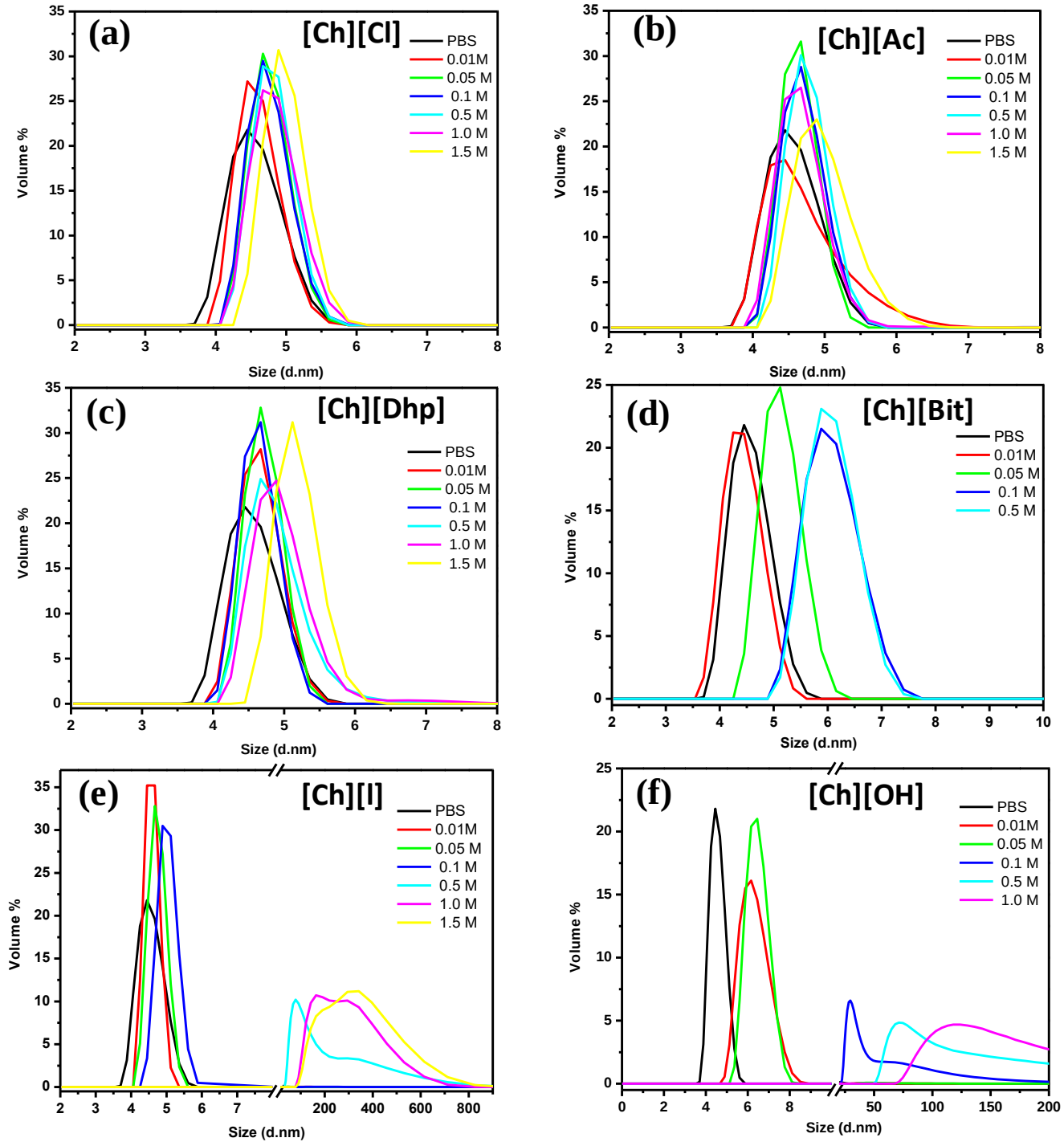

Figure 4.17: Hydrodynamic diameter (d_H) of BM in the presence of PBS and various concentration of ILs.

4.3.6 Evaluation of activity of BM in the presence of choline-based ILs

After confirming the structural variations of BM in the presence of ILs by UV, fluorescence, CD and DLS spectroscopic techniques, later the enzyme activity of BM was also confirmed by enzyme assay. The enzymatic activity of the BM was measured using casein as substrate [162] in presence of ILs at different concentration using ILs. Figure 4.18 displays the relative activity pattern of BM in presence of different ILs. It can be observed from Figure 4.18 that the caseinolytic activity of BM increase in case of [Ch][Ac] and [Ch][Cl] up to 0.5 M, the activity starts to decrease upon further increase in the concentration of these ILs. Here it is important to note that the activity increase more in case of [Ch][Ac] than that of [Ch][Cl] upto 0.5 M, while enzyme activity is decreases in presence of [Ch][Dhp]. In case of [Ch][Bit], the activity decreased sharply even with lower concentration (Figure 4.18), and this decrease is continuous with increase in concentration of ILs. On the other hand, as can be seen from the Figure 4.18 the enzyme deactivation is not much sharp in case of [Ch][I], the enzyme activity is decreasing slowly with increase in concentration of IL. In case of [Ch][OH], there is a remarkable decrease in activity of enzymes with concentration of IL. The overall activity order of BM in presence of different choline based ILs are as: [Ch][Ac] > [Ch][Cl] > [Ch][I] > [Ch][Dhp] >[Ch][Bit] > [Ch][OH]. Therefore, present results revealed that enzyme activity in ILs is anion as well as concentration of IL dependent. The ILs vary in the anions connected to the choline cation, hence, probably varying in their ability and hydrophobicity to combine with the enzyme [183].

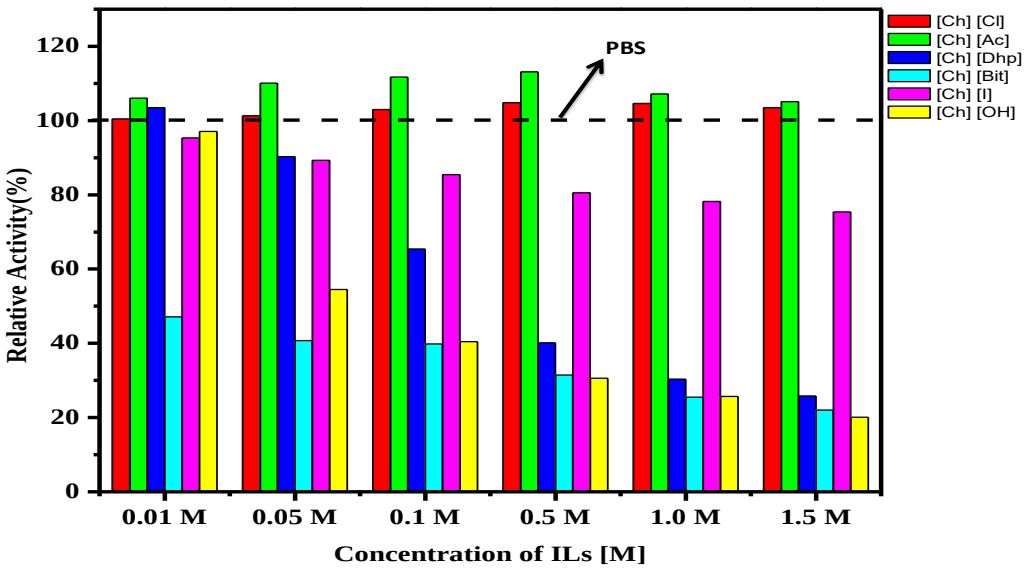

Figure 4.18: Relative proteolytic activity measurements of BM in PBS and in presence of ILs at 25 °C

All the above results clearly illustrate that the stabilization/destabilization of BM in presence of choline as a cation depends on anions and concentrations of ILs. All ILs have different effect on the structure stability and activity of BM which shows that anions of ILs are playing an important role on the stability of BM. It was found that interaction of ions of ILs with protein is dependent on the interaction between ions and the AAs present in the enzyme/protein [217,327,328]. Therefore, anions present in the choline-based ILs plays a crucial role in the ascertaining the class of interaction between ILs and enzyme. After comprehensive analysis of all above obtained results, we can understand that BM can form more stable and active structure in presence of [Ch][Cl], [Ch][Ac] and [Ch][Dhp] as compared to same concentrations of [Ch][I], [Ch][Bit] and [Ch][OH]. Overall stability order of BM in presence of various choline-based ILs follow the order as [Ch][Cl] > [Ch][Ac] > [Ch][Dhp] > [Ch][I] >[Ch][Bit]> [Ch][OH].

As is clear from the literature survey, that the stability and activity of protein is much influenced by the chaotropicity/kosmotropicity characteristics of the ions of ILs [329,330]. Xue et al. [331] have revealed that [Ch][Ac] can improved the catalytic activity of Candida

rogusa lipase in AOT inverse micelles. Kumar et al. [332] found that the anions such as CH_3COO^- and Cl^- of imidazolium-based IL with a common cation such as 1-butyl-3-methylimidazolium, ($[Bmim]^+$) can enhanced the stability of CT. Very recently, Bisht et al [183] have revealed that structural stability and enzymatic activity of CT was maintained in presence of [Ch][Ac], [Ch][Cl] and [Ch][Dhp] whereas choline dihydrogen citrate ([Ch][Dhp]) and [Ch][OH] were found destabilizer for CT structure. These results shows that only kosmotropcity of ions does not determine the stability of enzyme, other factors such as polarity, H-bonding, anion nucleophilicity, hydrogen-bond basicity and interaction between ILs and protein are also important factor for consideration [297,333,334]. The type of interaction between protein and ILs can influence the protein performance either by direct interaction with the protein functional groups or by changing the microenvironment in and around the protein because of their several physicochemical properties [297,334]. In present study ILs with the AC^- and Cl^- anions are more kosmotropic so they have more hydrogen-bond basicity, which replicates their high affinity or polarity for water hence the promote water structure of the protein and showed a more stabilizing feature as compared to other ILs [183,335].

The destabilization of BM in presence of [Ch][Bit] and [Ch][OH] may be due to the direct interaction these ions with enzymes, which can form strong H-bonds with the polypeptide backbone of enzyme which stripping off the essential water associated with the enzyme that maintain the structural integrity of protein. In this regards Jha et al. [204] demonstrated that the addition of hydroxide-based ILs to the hemoglobin (Hb) and myoglobin (Mb) decreases the protein's stability. Further studies also recommend that polar ILs shred water molecules from biomolecules, attributed to their extraordinarily high hydrogen bond basicity leading to protein unfolding [336,337]. While anions such as Cl^-, CH_3COO^- and Dhp^- may not forming direct bond with BM protein but reorganize the water structure only around the protein and

hence stabilize the BM structure. The overall conclusion thorough analysis of all results is that the stabilizing ability of the proteins in ILs is dependent on cation as well anion of ILs, concentration and other physiological conditions. Therefore, it can be concluded that the stability of one protein cannot be extrapolated from the studies of other proteins. Present work might help us to resolve main issues such as protein folding/unfolding, activity, stability and function by correct selection of ILs. The ILs behaves quite differently in dilute and concentrated conditions. For example in present study [Ch][I] behaved as stabilizers at lower concentrations and destabilizer at their higher concentrations for BM.

4.4 Studies on thermophysical properties of binary mixtures of ammonium based ionic liquids containing different anions with N, N-dimethylacetamide (DMA)

The studies were carried out to elucidate the thermophysical properties, such as ρ, u, η and n_D of various alkyl chain lengths of ammonium-based ILs and their binary mixtures with DMA at atmospheric pressure and in the temperature range of 25-40°C. Thermodynamic properties such as excess molar volumes (V^E), deviation in isentropic compressibilities ($\Delta\kappa_s$), deviation in viscosities ($\Delta\eta$) and deviation in refractive indices (Δn_D) were calculated with the help of experimental data and the results are listed in Table 4.7A (Appendix III) and graphically represented in Figures. 4.19A-4.22A (Appendix III) at all studied temperatures as a function of ILs concentration. We have displayed the data of ρ, u, η and n_D for DMA with all studied ILs at 25 °C in Figures. 4.23A. The values of V^E, $\Delta\kappa_s$, $\Delta\eta$ and Δn_D for the binary mixtures at several temperatures as a function of ILs concentrations are mentioned in Table 4.7A (Appendix III). Figures 4.24A-4.27A (Appendix III) demonstrates the values of V^E, $\Delta\kappa_s$, $\Delta\eta$ and Δn_D along with the fitted curves, correspondingly, at different temperatures. Furthermore, the values of V^E, $\Delta\kappa_s$, $\Delta\eta$ and Δn_D for ILs with DMA over the complete composition range at

25 °C are graphically presented in Figure 4.28A (Appendix III). Values of the fitted parameters are reported in Table 4.8A along with the values of standard deviations. The obtained results have been described in published literature [338].

4.5 Studies on apparent molar properties of binary mixtures of 1-methyl-1-propyl pyrrolidinium tetrafluoroborate ([MPpyr][BF_4]) with water and alcohols

4.5.1. Density values for binary mixtures

The density (ρ) data for the binary systems ([MPpyr][BF_4] + water or methanol or ethanol) have been measured at 25 °C, 30 °C, 35 °C and 40 °C and are the data presented in Table 4.9 and are also graphically shown in Figure 4.29. It has been observed that the ρ values increase with increasing the IL concentration and decrease as temperature increases for all binary systems.

Table 4.10: Molality (m), densities (ρ) and apparent molar volumes (V_φ) for ([MPpyr][BF_4] + water or methanol or ethanol) at 25 °C, 30 °C, 35 °C and 40 °C.

m (mol .kg^{-1})	ρ (kg .m^{-3})	$10^3 \times V_\varphi$ (m^3 .mol^{-1})
	([MPpyr][BF_4] + water)	
T = 25 °C		
0.0517	997.20	0.2123
0.1033	998.80	0.1981
0.1550	1000.3	0.1938
0.2067	1001.7	0.1921
0.2583	1003.0	0.1913
0.3100	1004.3	0.1907
0.4134	1006.9	0.1898
0.5167	1009.6	0.1888
T = 30 °C		
0.0517	995.70	0.2146
0.1033	997.20	0.2003
0.1550	998.70	0.1954

0.2067	1000.1	0.1933
0.2583	1001.4	0.1923
0.3100	1002.7	0.1916
0.4134	1005.3	0.1905
0.5167	1007.9	0.1897
T = 35 °C		
0.0517	994.00	0.2169
0.1033	995.50	0.2016
0.1550	996.90	0.1970
0.2067	998.20	0.1951
0.2583	999.60	0.1934
0.3100	1000.9	0.1926
0.4134	1003.4	0.1916
0.5167	1005.8	0.1910
T= 40 °C		
0.0517	991.90	0.2217
0.1033	993.60	0.2022
0.1550	994.90	0.1982
0.2067	996.20	0.1960
0.2583	997.60	0.1942
0.3100	998.90	0.1933
0.4134	1001.3	0.1925
0.5167	1003.6	0.1920
	([MPpyr][BF_4] + methanol)	
T = 25 °C		
0.0530	790.36	0.2154
0.1055	793.58	0.1939
0.1558	797.40	0.1787
0.2078	800.85	0.1743
0.2595	804.28	0.1714
0.3104	807.29	0.1712
0.4147	813.74	0.1694
0.5183	819.91	0.1685
T = 30 °C		
0.0530	785.78	0.2123
0.1055	789.20	0.1894
0.1558	793.21	0.1737
0.2078	796.81	0.1695
0.2595	800.25	0.1675
0.3104	803.37	0.1675
0.4147	809.95	0.1661
0.5183	816.44	0.1649
T = 35 °C		
0.0530	781.26	0.2067
0.1055	784.74	0.1858
0.1558	788.85	0.1702
0.2078	792.62	0.1656
0.2595	795.98	0.1649
0.3104	799.31	0.1642

0.4147	806.01	0.1633
0.5183	812.83	0.1616
T = 40 °C		
0.0530	776.69	0.2015
0.1055	780.36	0.1803
0.1558	784.58	0.1654
0.2078	788.43	0.1613
0.2595	792.18	0.1590
0.3104	795.73	0.1581
0.4147	802.79	0.1573
0.5183	809.39	0.1576
	([MPpyr][BF_4] + ethanol)	
T = 25 °C		
0.0534	789.90	0.2392
0.1048	792.56	0.2139
0.1565	795.54	0.2017
0.2088	798.47	0.1958
0.2605	801.48	0.1913
0.3113	804.00	0.1905
0.4147	808.60	0.1911
0.5183	813.87	0.1889
T = 30 °C		
0.0534	784.62	0.2369
0.1048	787.29	0.2129
0.1565	790.38	0.2001
0.2088	793.40	0.1940
0.2605	796.54	0.1891
0.3113	799.24	0.1878
0.4147	804.42	0.1869
0.5183	809.67	0.1857
T = 35 °C		
0.0534	780.29	0.2359
0.1048	782.97	0.2125
0.1565	786.06	0.1999
0.2088	789.11	0.1937
0.2605	792.25	0.1890
0.3113	794.96	0.1877
0.4147	800.15	0.1869
0.5183	805.42	0.1857
T = 40 °C		
0.0534	775.82	0.2329
0.1048	778.61	0.2095
0.1565	781.72	0.1978
0.2088	784.78	0.1922
0.2605	787.91	0.1879
0.3113	790.63	0.1868
0.4147	795.85	0.1863
0.5183	801.14	0.1853

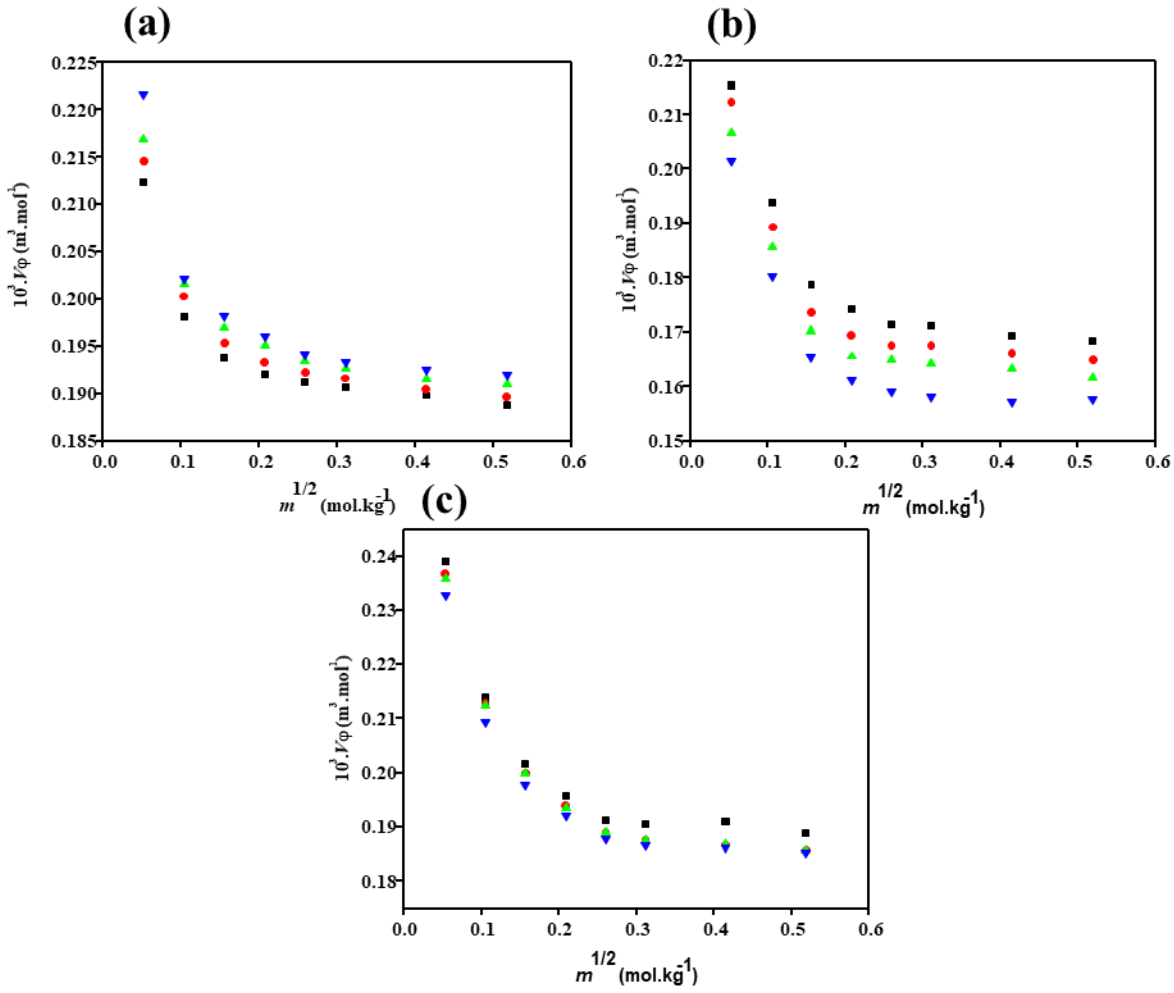

Figure 4.29: Density (ρ), for the mixtures of (a) ([MPpyr][BF_4] + water), (b) ([MPpyr][BF_4] + methanol) and (c) ([MPpyr][BF_4] + ethanol) at 25 °C (■), 30 °C (♦), 35 °C (▲) and 40 °C (▼).

4.5.2 Apparent molar volumes

The apparent molar volumes, V_φ, for the binary systems ([MPpyr][BF_4] + water or methanol or ethanol) at several temperatures (25, 30, 35 and 40 °C) are collected in Tables 4.9 and as displayed in Figure 4.30 (a–c). Figure 4.30 (a–c) represents that the V_φ values decrease with increasing the temperature for all binary systems except ([MPpyr][BF_4] + water) whereas increases. The V_φ values are positive for all systems and decrease with an increase in concentration of solute for all binary systems at all studied temperatures. At low molalities of

IL the ions are nearby solvent molecules, suggesting strong IL-solvent interaction, and an increase in the solute molality decreases the ion–ion interactions resulting in smaller V_φ values. In the system ([MPpyr][BF_4] + water) the values of V_φ increases with increasing the temperature, is consisting with the literatures [262, 339]. The results indicate that the ion-solvent packing of molecular interactions play the main role in the binary solutions.

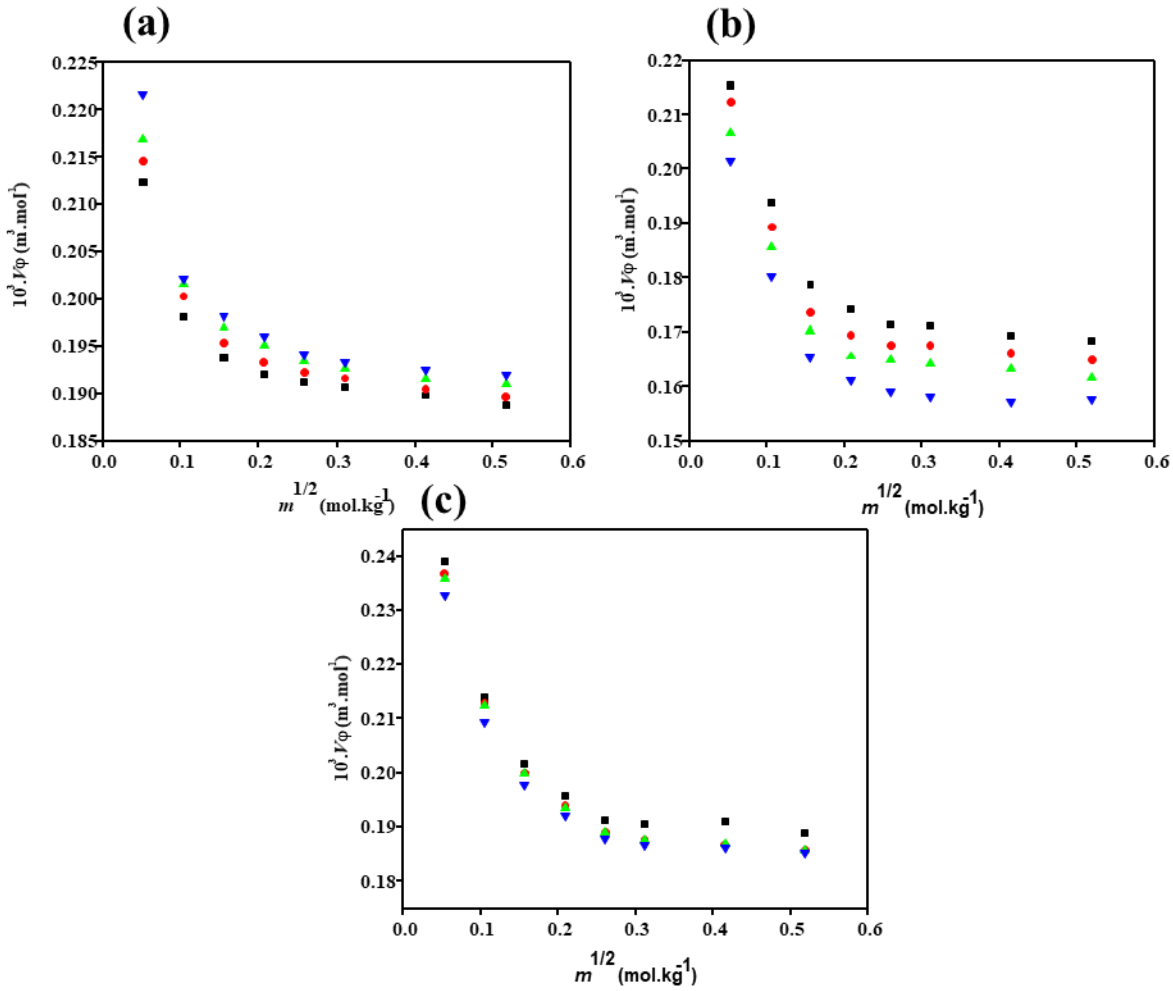

Figure 4.30: Apparent molar volume (V_φ) for the mixtures of (a) ([MPpyr][BF_4] + water), (b) [MPpyr][BF_4] + methanol) and (c) ([MPpyr][BF_4] + ethanol) at 25 °C (■), 30 °C (♦), 35 °C (▲) and 40 °C (▼).

The parameters of a Redlich–Mayer type equation [340], given below, were fitted to the apparent molar volume data:

$$V_{\varphi} = V_{\varphi}^{0} + S_V m^{1/2} + B_V m \qquad (4.2)$$

where V_{φ}^{0} is refers the limiting apparent molar volume of solute ([MPpyr][BF_4]) at each temperature, B_V and S_V are experimental parameters. The values of V_{φ}^{0} at each temperature of all binary systems were gained from Eq. 27 together with B_V and S_V are presented in Table 4.10. The data in Table 4.10 represent that V_{φ}^{0} values are positive for all the systems. The V_{φ}^{0} values increase with an increase in temperatures for binary system ([MPpyr][BF_4] + water) whereas decreases for the systems ([MPpyr][BF_4] + methanol or ethanol). Interestingly, the observed conclusion is consisting with the literature i e. in N, N-dimethyl-N-(3-sulfopropyl) cyclohexylammonium tosylate + water (30 to 55 °C) [255]. For the ([MPpyr][BF_4] + ethanol) system V_{φ}^{0} values is greater than for the ([MPpyr][BF_4] + methanol) at all temperatures indicating that the (ion + solvent) interactions of ([MPpyr][BF_4] + ethanol) are stronger than of ([MPpyr][BF_4] + methanol). This may be due to the effect of addition alkyl chain of ethanol. For the binary system ([MPpyr][BF_4] + water) V_{φ}^{0} is smaller indicating that the (ion + solvent) interactions of ([MPpyr][BF_4] + water) are weaker.

Table 4.11: Limiting apparent molar volumes (V_{φ}^{0}), and fitting parameters (S_V and B_V) and standard deviation (σ) of IL (solute) in water or Methanol or Ethanol (solvents) at 25 °C, 30 °C, 35 °C and 40 °C.

T (°C)	$10^6 \times V_{\varphi}^{0}$ (m^3. mol^{-1})	$10^6 \times S_V$ (m3. $mol^{-3/2}$.$kg^{1/2}$)	$10^6 \times B_V$ (m^3. mol^{-2}.kg)	$10^6 \times \sigma$
		([MPpyr][BF_4] + water)		
25	0.244	-0.181	0.148	0.002
30	0.248	-0.191	0.156	0.002
35	0.252	-0.199	0.162	0.002
40	0.263	-0.237	0.197	0.003
		([MPpyr][BF_4] + methanol)		
25	0.287	-0.389	0.336	0.003
30	0.286	-0.385	0.320	0.003
35	0.277	-0.383	0.315	0.003
40	0.273	-0.379	0.310	0.002
		([MPpyr][BF_4] + ethanol)		
25	0.315	-0.416	0.339	0.003
30	0.312	-0.407	0.325	0.002
35	0.310	-0.400	0.320	0.002
40	0.304	-0.389	0.315	0.002

The values of S_v are negative for all binary mixtures and increase with temperature for the ([MPpyr][BF_4] + methanol or ethanol) systems whereas decreases for ([MPpyr][BF_4] + water) system. The IL ion–ion interaction is stronger for the ([MPpyr][BF_4] + water) than for the ([MPpyr][BF_4] + methanol) than for the ([MPpyr][BF_4] + ethanol) systems at all temperatures. The ion–ion interactions decrease with an increase in temperature for the (([MPpyr][BF_4] + water) system and increase for the (([MPpyr][BF_4] + methanol or ethanol) systems.

The B_v values are positive for all the systems at different temperature, indicating the hydrogen bonding interactions between the [MPpyr][BF_4] with water, methanol and ethanol. For the ([MPpyr][BF_4] + ethanol) system B_v values is greater than for the ([MPpyr][BF_4] + methanol) at all temperatures indicating that the hydrogen bonding interactions between the [MPpyr][BF_4] with ethanol are stronger than of ([MPpyr][BF_4] with methanol. This may be due to the effect of addition alkyl chain of ethanol. For the system ([MPpyr][BF_4] + water) B_v is smaller indicating that the weak hydrogen bonding interactions between ([MPpyr][BF_4] with water. The B_v value of increases with an increase in the temperature for system ([MPpyr][BF_4] + water) whearas deceases for the systems ([MPpyr] [BF_4] + methanol or ethanol).

The temperature dependence of V_φ^0 can be displayed as follows:

$$V_\varphi^0 = A + BT + C_T^2 \tag{4.3}$$

where A, B, and C are refers to experimental parameters and T is the absolute temperature. The infinite dilution apparent molar expansibility E_φ^0 can be obtained by using Eq. (29) with respect to temperature.

$$E_\varphi^0 = \left(\frac{\partial V_\varphi^0}{\partial T}\right)_P = B + 2CT \tag{4.4}$$

The E_φ^0 values for all three binary systems are showed in Table 4.11 and provide detailed information about the (solute–solvent) interactions [341]. As can be seen in Table 4.11, the values of E_φ^0 are positive for the systems ([MPpyr][BF_4] + water or methanol). The obtained E_φ^0 values are positive and increases with increasing the temperature of binary systems

([MPpyr][BF_4] + water or methanol) due to thermal agitation increases with temperature, resultant in water or methanol molecules being released from [MPpyr][BF_4], thereby increasing the solution volume to a greater extent than for the pure solvent. The positive values of E_φ^0 indicated the distinctive of electrostriction and solvation (the reduction of the solvent surrounding ions) of electrolytes in mixtures. In contrast, ethanol in IL E_φ^0 values are negative and decreases with temperature indicating that the pure ethanol increasing more rapidly than the solution having the [MPpyr][BF_4] ions. The negative values of E_φ^0 indicated that the weak interactions between the solute– solvent in the binary system.

Table 4.12: The limiting apparent molar expansibility (E_φ^0) and isobaric thermal expansion coefficients (α_P).

Solute	Solvent	$10^6 \times E_\varphi^0$ (m^3. mol^{-1}.K^{-1})			
		T = 25 °C	T = 30 °C	T = 35 °C	T = 40 °C
[MPpyr][BF_4]	water	0.0002	0.0009	0.0015	0.0022
[MPpyr][BF_4]	methanol	0.0324	0.0326	0.0329	0.0332
[MPpyr][BF_4]	ethanol	-0.0003	-0.0006	-0.0008	-0.0010
		$10^6 \times \alpha_P$ (K^{-1})			
[MPpyr][BF_4]	water	0.0008	0.0036	0.0059	0.0084
[MPpyr][BF_4]	methanol	0.1128	0.1138	0.1188	0.1214
[MPpyr][BF_4]	ethanol	-0.0010	-0.0019	-0.0026	-0.0033

Using the apparent molar volume and expansibility the thermal expansion coefficient were calculated as well as presented in Table 4.11.

$$\alpha_P = \frac{1}{V_\varphi^0}\left(\frac{\partial V_\varphi^0}{\partial T}\right)_P = \frac{V_\varphi^0}{E_\varphi^0} \tag{4.5}$$

It can be observed from the Table 4.11 that the values of α_P are positive for ([MPpyr][BF_4] + water or methanol) whereas negative for ([MPpyr][BF_4] + ethanol) at all temperatures.

CHAPTER 5
CONCLUSION

The first part of this thesis deals with the studies of protein folding/unfolding and their functional consequences, which are essential in understanding the basis of the cellular life cycle. The studies of biomolecules and ILs remain a subject of the active area of scientific research. Therefore, it is necessary to find out the suitable co-solvent systems that are more biocompatible and can stabilize the protein structure with different physiological environment including temperature, pressure, pH, ionic strength, cold, high salinity as well as concentrations. In this regard, ILs are the found to be one of the best suitable biocompatible co-solvents for stabilizing some of the proteins. Therefore, two different families of ILs namely imidazolium and cholinium-based ILs were selected and the stability of bromelain (BM) has been studied in the presence of these ILs.

The stability/destability of BM in the presence of imidazolium-based ILs such as ([Bmim][Cl]), ([Bmim][Br]), ([Bmim][I]), ([Bmim][HSO_4]), ([Bmim][CH_3COO]) and ([Bmim][NO_3]) were observed. The conformational stability and structural changes of the protein were investigated using spectroscopic techniques and DLS measurements. Finally, from the two techniques, we have observed the quenching of fluorescence spectra with simultaneous loss of secondary as well as tertiary structures by varying concentrations of ILs. It can be also seen that the concentration of the ILs played an important role towards structure and stability of BM. In addition, it was also concluded that the stability of BM was harshly affected at higher concentrations (0.50-1.5 M) of ILs. From both of these results, it is quite clear that HSO_4^- is a stabilizer for the BM structure while I^- is observed to be destabilizer for the BM structure. Fascinatingly, this imidazolium family ILs followed the Hofmeister series. Clearly, series of Hofmeister ions are found to be in the trend of $HSO_4^- > CH_3COO^- > NO_3^- > Cl^- > Br^- > I^-$.

On the other hand, we successfully explored the role of concentration and anion of ILs as well as related it to well-known Hofmeister series on the structure, stability and activity of BM. For this purpose, choline-based ILs such as choline chloride [Ch][Cl], choline acetate [Ch][Ac], choline dihydrogen phosphate [Ch][Dhp], choline bitartrate [Ch][Bit], choline iodide [Ch][I] and choline hydroxide [Ch][OH] were used and found that the lower concentrations of all ILs show a different behavior in comparison to a higher concentration of ILs. From the experimental results we conclude that the overall stability order of BM follow the trend as: [Ch][Cl] > [Ch][Ac] > [Ch][Dhp] > [Ch][I] >[Ch][Bit]> [Ch][OH]. The concentration of ILs is very essential in deciding its role either as stabilizer or destabilizer for the structure of BM. The overall summary of the protiens work is that the stabilizing ability of the proteins in ILs is dependent on the cation and anion of the ILs as well as concentration of IL. Also, it is not essential that an IL which is a destabilizer will still act as a destabilizing agent for a different protein. We believe that the experimental result formed here on the folding and unfolding of different families of ILs will be helpful in future for advance biotechnology and biomedical applications.

The overall conclusion is that the stabilizing ability of the ILs on BM is different and is depending on the cation and anion of the ILs as well as concentration of IL. A mutual effect of the hydrophobic, as well as the electrostatic interactions between the ILs and protein, played important role in elucidating protein folding and unfolding. We believe that the experimental outcome produced hither on the protein folding/unfolding of various families of ILs which is helpful in future for further biomedical and biotechnology applications.

The second part of this thesis deals with the studies on thermophysical properties such as density (ρ), excess molar volume (V^E), sound velocity (u), deviations in isentropic compressibility ($\Delta\kappa_s$), viscosity (η), deviations in viscosity ($\Delta\eta$), refractive index (n_D) and deviations in refractive index (Δn_D) of the binary mixtures (TEAH or TPAH or TBAH +

DMA) at different temperatures from 25 to 40 ^{o}C in steps of 5 ^{o}C under atmospheric pressure. The interesting results are obtained for structure-based and temperature dependent properties of ILs with DMA.

The negative V^E values observed for the lower alkyl chain length of TEAH whereas the large alkyl chain length of ILs such as TPAH and TBAH displayed negative to positive V^E values. The calculated values of ΔKs are negative complete ranges of composition, indicating that attention of stronger attractive ion-dipole interactions between ions of ILs and DMA. The positive values of $\Delta\eta$ for the investigated binary systems suggest that the attractive forces and/or highest effective packing occur between the ions of ILs and DMA. The positive Δn_D values of (TEAH + DMA) system is attributed to the hydrogen bond association between the ions of ILs and DMA at low concentration and negative Δn_D values of binary systems (TPAH or TBAH + DMA) suggested that self-ion-pair interactions formed between the ions of ILs and DMA at higher concentration.

In addition to above, the apparent molar volume (V_φ), limiting apparent molar volumes (V_φ^0), the limiting apparent molar expansibility (E_φ^0), and thermal expansion coefficients (α_P) were evaluated from experimental ρ data of binary mixtures containing 1-methyl-1-propyl pyrrolidinium tetrafluoroborate ([MPpyr][BF_4]) with water, methanol and ethanol at various temperatures from (25 to 40 ^{o}C) under atmospheric pressure were aslo investigated. The V_φ values are positive for all systems and decrease with an increase in concentration of solute for all binary systems at all studied temperatures. For the ([MPpyr][BF_4] + ethanol) system V_φ^0 values is greater than for the ([MPpyr][BF_4] + methanol) at all temperatures indicating that the (ion + solvent) interactions of ([MPpyr][BF_4] + ethanol) are stronger than of ([MPpyr][BF_4] + methanol). This may be due to the effect of addition alkyl chain of ethanol.

For the binary system ([MPpyr][BF_4] + water) V_φ^0 is smaller indicating that the (ion + solvent) interactions of ([MPpyr][BF_4] + water) are weaker.

The positive values of E_φ^0 for the systems ([MPpyr][BF_4] + water or methanol) indicated the characteristic of solvation and electrostriction of electrolytes in solutions. In contrast, ethanol in IL E_φ^0 values are negative and decreases with temperature indicating that the pure ethanol expanding more rapidly than the solution containing the [MPpyr][BF_4] ions. The negative values of E_φ^0 for system ([MPpyr][BF_4] + ethanol) indicated that the weak interactions between the solute– solvent in the binary system. Furthermore, the influence of anion on thermophysical properties of ionic liquids with organic solvent is also explained. We believed that certainly this work will enrich the knowledge of understanding the thermophysical and thermodynamic properties of binary mixtures of ionic liquids and organic solvents.

REFERENCES

[1] R.D. Rogers, K.R. Seddon, Ionic Liquids - Solvents of the Future, Science (80). 302 (2003) 792–793.

[2] T.L. Greaves, C.J. Drummond, Protic ionic liquids: Properties and applications, Chem. Rev. 108 (2008) 206–237.

[3] A. Kumar, P. Venkatesu, Overview of the stability of α-chymotrypsin in different solvent media, Chem. Rev. 112 (2012) 4283–4307.

[4] H. Olivier-Bourbigou, L. Magna, D. Morvan, Ionic liquids and catalysis: Recent progress from knowledge to applications, Appl. Catal. A Gen. 373 (2010) 1–56.

[5] S. Singh, Thermo-physical properties and activity coefficients at infinite dilution for ionic liquid systems at several temperatures, Ph D Thesis, Durban University of Technology, Durban, South Africa, 2017.

[6] M.D. Bermdez, A.E. Jimenez, J. Sanes, F.J. Carrion, Ionic liquids as advanced lubricant fluids, Molecules. 14 (2009) 2888–2908.

[7] A.P. Carneiro, O. Rodríguez, E.A. MacEdo, Solubility of xylitol and sorbitol in ionic liquids - Experimental data and modeling, J. Chem. Thermodyn. 55 (2012) 184–192.

[8] T.W. P. Wasserscheid, Fontmatter, in: Ion. Liq. Synth. Second Ed., Wiley-VCH, 2008: pp. V–XXVI. doi:10.1002/9783527619559.

[9] T. Welton, Room-Temperature Ionic Liquids. Solvents for Synthesis and Catalysis, Chem. Rev. 99 (1999) 2071–2084.

[10] M. Moniruzzaman, K. Nakashima, N. Kamiya, M. Goto, Recent advances of enzymatic reactions in ionic liquids, Biochem. Eng. J. 48 (2010) 295–314.

[11] L. Satish, S. Millan, H. Sahoo, Spectroscopic insight into the interaction of bovine

serum albumin with imidazolium-based ionic liquids in aqueous solution, Luminescence. 32 (2017) 695–705.

[12] K.R. Seddon, Ionic liquids for clean technology, in: J. Chem. Technol. Biotechnol., Wiley-Blackwell, 1997: pp. 351–356.

[13] P. Walden, Molecular weights and electrical conductivity of several fused salts, Bull. Acad. Imper. Sci.(St. Petersburg). 8 (1914) 405–422.

[14] F.H. Hurley, T.P. WIer, The Electrodeposition of Aluminum from Nonaqueous Solutions at Room Temperature, J. Electrochem. Soc. 98 (1951) 207.

[15] J.A. Boon, J.A. Levisky, J.L. Pflug, J.S. Wilkes, Friedel-Crafts Reactions in Ambient-Temperature Molten Salts, J. Org. Chem. 51 (1986) 480–483.

[16] S.E. Fry, N.J. Pienta, Effects of Molten Salts on Reactions. Nucleophilic Aromatic Substitution by Halide Ions in Molten Dodecyltributylphosphonium Salts1, J. Am. Chem. Soc. 107 (1985) 6399–6400.

[17] J.S. Wilkes, J.A. Levisky, R.A. Wilson, C.L. Hussey, Dialkylimidazolium Chloroaluminate Melts: A New Classof Room-Temperature Ionic Liquids for Electrochemistry,Spectroscopy, and Synthesis, Inorg. Chem. 21 (1982) 1263–1264.

[18] J.S. Wilkes, A short history of ionic liquids—from molten salts to neoteric solvents, Green Chem. 4 (2002) 73–80.

[19] J.F. Brennecke, E.J. Maginn, Ionic liquids: Innovative fluids for chemical processing, AIChE J. 47 (2001) 2384–2389.

[20] B. Nuthakki, T.L. Greaves, I. Krodkiewska, A. Weerawardena, M.I. Burgar, R.J. Mulder, C.J. Drummond, Protic ionic liquids and ionicity, Aust. J. Chem. 60 (2007) 21–28.

[21] L. Crowhurst, N.L. Lancaster, J.M. Pérez Arlandis, T. Welton, Manipulating solute nucleophilicity with room temperature ionic liquids, J. Am. Chem. Soc. 126 (2004) 11549–11555.

[22] K. Dong, S. Zhang, Hydrogen bonds: A structural insight into ionic liquids, Chem. - A Eur. J. 18 (2012) 2748–2761.

[23] C.A. Angell, N. Byrne, J.P. Belieres, Parallel developments in aprotic and protic ionic liquids: Physical chemistry and applications, Acc. Chem. Res. 40 (2007) 1228–1236.

[24] J.M.S.S. Esperanca, J.N.C. Lopes, M. Tariq, L.M.N.B.F. Santos, J.W. Magee, L.P.N. Rebelo, Volatility of aprotic ionic liquids- A review, J. Chem. Eng. Data. 55 (2010) 3–12.

[25] J.P. Hallett, T. Welton, Room-temperature ionic liquids: Solvents for synthesis and catalysis. 2, Chem. Rev. 111 (2011) 3508–3576.

[26] P. Attri, P. Venkatesu, A. Kumar, N. Byrne, A protic ionic liquid attenuates the deleterious actions of urea on α-chymotrypsin, Phys. Chem. Chem. Phys. 13 (2011) 17023.

[27] K. Fujita, D.R. MacFarlane, M. Forsyth, Protein solubilising and stabilising ionic liquids, Chem. Commun. (2005) 4804–4806.

[28] I. Jha, P. Venkatesu, Endeavour to simplify the frustrated concept of protein-ammonium family ionic liquid interactions., Phys. Chem. Chem. Phys. 17 (2015) 20466–20484.

[29] T. Welton, Ionic liquids in Green Chemistry, Green Chem. 13 (2011) 225–225.

[30] M. Freemantle, Designer Solvents, Chem. Eng. News. 76 (1998) 32–37.

[31] N. Byrne, C.A. Angell, The solubility of hen lysozyme in ethylammonium nitrate/H2O mixtures and a novel approach to protein crystallization, Molecules. 15 (2010) 793–803.

[32] P. Heimer, A.A. Tietze, M. Böhm, R. Giernoth, A. Kuchenbuch, A. Stark, E. Leipold, S.H. Heinemann, C. Kandt, D. Imhof, Application of room-temperature aprotic and protic ionic liquids for oxidative folding of cysteine-rich peptides, ChemBioChem. 15 (2014) 2754–2765.

[33] K. Rawat, H.B. Bohidar, Heparin-like native protein aggregate dissociation by 1-alkyl-3-methyl imidazolium chloride ionic liquids, Int. J. Biol. Macromol. 73 (2015) 23–30.

[34] D.K. Magnuson, J.W. Bodley, D.F. Evans, The activity and stability of alkaline phosphatase in solutions of water and the fused salt ethylammonium nitrate, J. Solution Chem. 13 (1984) 583–587.

[35] J. Chen, Y. Wang, Q. Zeng, X. Ding, Y. Huang, Partition of proteins with extraction in aqueous two-phase system by hydroxyl ammonium-based ionic liquid, Anal. Methods. 6 (2014) 4067–4076.

[36] M. Galiński, A. Lewandowski, I. Stepniak, Ionic liquids as electrolytes, Electrochim. Acta. 51 (2006) 5567–5580.

[37] T. Sato, G. Masuda, K. Takagi, Electrochemical properties of novel ionic liquids for electric double layer capacitor applications, Electrochim. Acta. 49 (2004) 3603–3611.

[38] P. Kuberský, J. Altšmíd, A. Hamáček, S. Nešpůrek, O. Zmeškal, An electrochemical NO2 sensor based on ionic liquid: Influence of the morphology of the polymer electrolyte on sensor sensitivity, Sensors. 15 (2015) 28421–28434.

[39] C. Ye, W. Liu, Y. Chen, L. Yu, Room-temperature ionic liquids: a novel versatile

lubricant., Chem. Commun. 0 (2001) 2244–2245.

[40] S. Keskin, D. Kayrak-Talay, U. Akman, Ö. Hortaçsu, A review of ionic liquids towards supercritical fluid applications, J. Supercrit. Fluids. 43 (2007) 150–180.

[41] S. Seki, Y. Ohno, Y. Kobayashi, H. Miyashiro, A. Usami, Y. Mita, H. Tokuda, M. Watanabe, K. Hayamizu, S. Tsuzuki, M. Hattori, N. Terada, Imidazolium-Based Room-Temperature Ionic Liquid for Lithium Secondary Batteries, J. Electrochem. Soc. 154 (2007) A173–A177.

[42] H. Zhao, S. Xia, P. Ma, Use of ionic liquids as "green" solvents for extractions, J. Chem. Technol. Biotechnol. 80 (2005) 1089–1096.

[43] I. Kilpeläinen, H. Xie, A. King, M. Granstrom, S. Heikkinen, D.S. Argyropoulos, Dissolution of wood in ionic liquids, J. Agric. Food Chem. 55 (2007) 9142–9148.

[44] P. Du, S. Liu, P. Wu, C. Cai, Preparation and characterization of room temperature ionic liquid/single-walled carbon nanotube nanocomposites and their application to the direct electrochemistry of heme-containing proteins/enzymes, Electrochim. Acta. 52 (2007) 6534–6547.

[45] K.S. Egorova, V.P. Ananikov, Toxicity of ionic liquids: Eco(cyto)activity as complicated, but unavoidable parameter for task-specific optimization, ChemSusChem. 7 (2014) 336–360.

[46] S. Singh, I. Bahadur, P. Naidoo, G. Redhi, D. Ramjugernath, Application of 1-butyl-3-methylimidazolium bis(trifluoromethylsulfonyl) imide ionic liquid for the different types of separations problem: Activity coefficients at infinite dilution measurements using gas-liquid chromatography technique, J. Mol. Liq. 220 (2016) 33–40.

[47] B. Peng, J. Chen, Functional materials with high-efficiency energy storage and

conversion for batteries and fuel cells, Coord. Chem. Rev. 253 (2009) 2805–2813.

[48] M. Larhed, C. Moberg, A. Hallberg, Microwave-accelerated homogeneous catalysis in organic chemistry, Acc. Chem. Res. 35 (2002) 717–727.

[49] Z. Lei, B. Chen, Y.M. Koo, D.R. Macfarlane, Introduction: Ionic Liquids, Chem. Rev. 117 (2017) 6633–6635.

[50] R. Buchfink, A. Tischer, G. Patil, R. Rudolph, C. Lange, Ionic liquids as refolding additives: Variation of the anion, J. Biotechnol. 150 (2010) 64–72.

[51] E. V Kuzmenkina, C.D. Heyes, G.U. Nienhaus, Single-molecule Förster resonance energy transfer study of protein dynamics under denaturing conditions, Proc. Natl. Acad. Sci. 102 (2005) 15471–15476.

[52] M.P. Stevens, Polymer chemistry: An introduction, Third Edition, J. Chem. Educ. 77 (2000) 35–35.

[53] S. Ohnishi, K. Takano, Amyloid fibrils from the viewpoint of protein folding, Cell. Mol. Life Sci. 61 (2004) 511–524.

[54] A.M. Lesk, Introduction to protein science : architecture, function, and genomics, Acta Cryst. 72 (2016) 1308–1309.

[55] J. Krochta, Proteins as Raw Materials for Films and Coatings, Protein-Based Film. Coatings, (2002) 1–41.

[56] A. Gutteridge, J.M. Thornton, Understanding nature's catalytic toolkit, Trends Biochem. Sci. 30 (2005) 622–629.

[57] J. Hey, A. Posch, A. Cohen, N. Liu, A. Harbers, Fractionation of complex protein mixtures by liquid-phase isoelectric focusing., Methods Mol. Biol. 424 (2008) 225–39.

[58] A. Lehninger, D.L. Nelson, M.M. Cox, Glycolysis, Gluconeogenesis, and the Pentose Phosphate Pathway, Lehninger Princ. Biochem. Fourth Ed. (2008) 556–557.

[59] T.E. Creighton, Disulphide bonds and protein stability, Bio. Essays. 8 (1988) 57–63.

[60] S. Doonan, Peptides and Proteins, Royal.Soci. Chem. (2002) 1–186.

[61] T E Creighton, Protein Folding W. H. Freeman and Company, New York, 1992.

[62] T.E. Creighton, Proteins : structures and molecular properties, W.H. Freeman, 1993.

[63] C.I. Branden, J. Tooze, Introduction to Protein Structure, Garland Pub, 1999.

[64] J.M. Thornton, C.A. Orengo, A.E. Todd, F.M.. Pearl, Protein folds, functions and evolution, J. Mol. Biol. 293 (1999) 333–342.

[65] A.M. Lesk, Introduction to protein science : architecture, function, and genomics, 2nd edition. (2010) 1–455.

[66] N.R. Seddon, Biochemistry (third edition), Biochem. Educ. 16 (1988) 181–182.

[67] G. Hartmann, The Structure and Action of Proteins. Von R. E. Dickerson und I. Geis. Harper and Row, Publishers, New York-Evanston-London 1969. 1. Aufl., VIII, 120 S., zahlr. Abb., Paperback DM 20.50, Angew. Chemie. 82 (1970) 780.

[68] A. Uzman, Molecular Cell Biology (4th edition) Harvey Lodish, Arnold Berk, S. Lawrence Zipursky, Paul Matsudaira, David Baltimore and James Darnell; Freeman &amp, Biochem. Mol. Biol. Educ. 29 (2001) 126–128.

[69] K. Thomas, ProteinFoldingKinetics, Springer, Protein Stability and Folding. 40 (2003) 313-341.

[70] C.M. Dobson, Principles of protein folding, misfolding and aggregation, in: Semin. Cell Dev. Biol., 2004: pp. 3–16.

[71] D. Häussinger, T. Pfohl, Biophysical chemistry., Chimia (Aarau). 64 (2010) 874–876.

[72] E. Buxbaum Portsmouth, Fundamentals of Protein Structure and Function, Springer. (2007) 13–37.

[73] D. Herries, Enzyme Structure and Mechanism (Second Edition), Biochem. Educ. 13 (1985) 146–146.

[74] C.M. Dobson, A. Šali, M. Karplus, Protein folding: A perspective from theory and experiment, Angew. Chemie - Int. Ed. 37 (1998) 868–893.

[75] H. Neurath, J.P. Greenstein, F.W. Putnam, J.O. Erickson, The chemistry of protein denaturation, Chem. Rev. 34 (1944) 157–265.

[76] W. Kauzmann, Some Factors in the Interpretation of Protein Denaturation, Adv. Protein Chem. 14 (1959) 1–63.

[77] A. M. Hermansson, Physico-Chemical Aspects of Soy Proteins Structure Formation, J. Tex. Stud. 9 (1965) 33–58.

[78] D.R. Canchi, A.E. García, Cosolvent Effects on Protein Stability, Annu. Rev. Phys. Chem. 64 (2013) 273–293.

[79] J. Roche, J.A. Caro, D.R. Norberto, P. Barthe, C. Roumestand, J.L. Schlessman, A.E. Garcia, B. Garcia-Moreno E.C.A. Royer, Cavities determine the pressure unfolding of proteins, Proc. Natl. Acad. Sci. 109 (2012) 6945–6950.

[80] A. Sadana, Biocatalysis: fundamentals of enzyme deactivation kinetics, Prentice Hall, 1991.

[81] R. Srinivas, T. Panda, Enhancing the feasibility of many biotechnological processes through enzyme deactivation studies, Bioprocess Eng. 21 (1999) 363–369.

[82] D. Porter, F. Vollrath, The role of kinetics of water and amide bonding in protein stability, Soft Matter. 4 (2008) 328–336.

[83] R.J. Ellis, T.J.T. Pinheiro, Danger - Misfolding proteins, Nature. 416 (2002) 483–484.

[84] G.R. Grimsley, B.M.P. Huyghues-Despointes, C.N. Pace, J.M. Scholtz, Measuring the Conformational Stability of a Protein by NMR, Cold Spring Harb. Protoc. 1 (2006) 527–533.

[85] L.O. Narhi, J.S. Philo, B. Sun, B.S. Chang, T. Arakawa, Reversibility of heat-induced denaturation of the recombinant human megakaryocyte growth and development factor, Pharm. Res. 16 (1999) 799–807.

[86] E. Shakhnovich, Protein folding thermodynamics and dynamics: Where physics, chemistry, and biology meet, Chem. Rev. 106 (2006) 1559–1588.

[87] P. Venkatesu, M.J. Lee, H.M. Lin, Thermodynamic characterization of the osmolyte effect on protein stability and the effect of GdnHCl on the protein denatured state, J. Phys. Chem. B. 111 (2007) 9045–9056.

[88] P. Venkatesu, M.J. Lee, H. mu Lin, Trimethylamine N-oxide counteracts the denaturing effects of urea or GdnHCl on protein denatured state, Arch. Biochem. Biophys. 466 (2007) 106–115.

[89] C.N. Pace, S. Trevino, E. Prabhakaran, J.M. Scholtz, Protein structure, stability and solubility in water and other solvents, Philos. Trans. R. Soc. London Ser. B-Biological Sci. 359 (2004) 1225–1234.

[90] R.A. Blevins, A. Tulinsky, Comparison of the independent solvent structures of dimeric α-chymotrypsin with themselves and with γ-chymotrypsin, J. Biol. Chem. 260 (1985) 8865–8872.

[91] S.N. Timasheff, The Control of Protein Stability and Association by Weak Interactions with Water: How Do Solvents Affect These Processes?, Annu. Rev. Biophys. Biomol. Struct. 22 (1993) 67–97.

[92] S.N. Timasheff, Water as ligand: Preferential binding and exclusion of denaturedants in protein unfolding, Biochemistry. 31 (1992) 9857–9864.

[93] A. Pertsemlidis, A.M.M. Saxena, A.K.K. Soper, T. Head-Gordon, R.M.M. Glaeser, Direct evidence for modified solvent structure within the hydration shell of a hydrophobic amino acid., Proc. Natl. Acad. Sci. U. S. A. 93 (1996) 10769–10774.

[94] M.L.M. Serralheiro, J.M.S. Cabral, Thermal stability of α-chymotrypsin, native and chemically modified, inside reverse micelles during peptide synthesis, Biocatal. Biotransformation. 17 (1999) 3–19.

[95] F.C.L. Almeida, A.P. Valante, H. Chaimovich, Stability and activity modulation of chymotrypsins in AOT reversed micelles by protein-interface interaction, Biotechnol. Bioeng. 59 (1998) 360–363.

[96] K. Fujita, D.R. MacFarlane, M. Forsyth, Protein solubilising and stabilising ionic liquids, Chem. Commun. (2005) 4804–4806.

[97] A. Balk, U. Holzgrabe, L. Meinel, Pro et contra' ionic liquid drugs - Challenges and opportunities for pharmaceutical translation, Eur. J. Pharm. Biopharm. 94 (2015) 291–304.

[98] H.D. Williams, Y. Sahbaz, L. Ford, T.-H. Nguyen, P.J. Scammells, C.J.H. Porter, Ionic liquids provide unique opportunities for oral drug delivery: structure optimization and in vivo evidence of utility, Chem. Commun. 50 (2014) 1688–1690.

[99] D.D.L. Chung, Composite materials: Science and Application, Springer (2010) 1–371.

[100] D. Rooney, J. Jacquemin, R. Gardas, Thermophysical properties of ionic liquids, Top. Curr. Chem. 290 (2009) 185–212.

[101] Y.A.& Y.M. Koichiro Nakanishi, Proceedings of the Ninth International Conference on Properties and Phase Equilibria for Product and Process Design (PPEPPD) ScienceDirect.com, Fluid Phase Equilibria. (2002) 194–197.

[102] R. Ge, C. Hardacre, J. Jacquemin, D.W. Rooney, Thermophysical properties of ionic liquids, in: ACS Symp. Ser. (2009) 43–60.

[103] G. Douhéret, M.I. Davis, Measurement, analysis, and utility of excess molar volumes, Chem. Soc. Rev. 22 (1993) 43–50.

[104] P. Venkatesu, Thermophysical contribution of N,N-dimethylformamide in the molecular interactions with other solvents, Fluid Phase Equilib. 298 (2010) 173–191.

[105] M.J. Blandamer, M.I. Davis, G. Douhéret, J.C.R. Reis, Apparent molar isentropic compressions and expansions of solutions, Chem. Soc. Rev. 30 (2001) 8–15.

[106] R.T. Jones, Thermodynamics and its applications – an overview, Thermo.pdf (1997) 1–28.

[107] V. Govinda, P. Attri, P. Venkatesu, P. Venkateswarlu, Temperature effect on the molecular interactions between two ammonium ionic liquids and dimethylsulfoxide, J. Mol. Liq. 164 (2011) 218–225.

[108] A. Bejan, Thermodynamics Fundamentals, Mech. Eng. Handb. Ener. Power, Third Edition. 4 (2006) 94–116.

[109] L.A. Blanchard, Z. Gu, J.F. Brennecke, High-Pressure Phase Behavior of Ionic Liquid/CO 2 Systems, J. Phys. Chem. B. 105 (2001) 2437–2444.

[110] H. Tokuda, K. Hayamizu, K. Ishii, M.A.B.H. Susan, M. Watanabe, Physicochemical properties and structures of room temperature ionic liquids. 2. variation of alkyl chain length in imidazolium cation, J. Phys. Chem. B. 109 (2005) 6103–6110.

[111] H. Wang, W. Liu, J. Huang, Densities and volumetric properties of a (xylene + dimethyl sulfoxide) at temperature from (293.15 to 353.15) K, J. Chem. Thermodyn. 36 (2004) 743–752.

[112] M.B. Ewing, B.J. Levien, K.N. Marsh, R.H. Stokes, Excess enthalpies, excess volumes, and excess gibbs free energies for mixtures of cyclo-octane+cyclopentane at 288.15, 298.15, and 308.15 K, J. Chem. Thermodyn. 2 (1970) 689–695.

[113] M. Sattari, F. Gharagheizi, Development of a group contribution method for the estimation of heat capacities of ionic liquids, J Therm Anal Calorim. 115 (2014) 1863–1882.

[114] S. Porcedda, B. Marongiu, M. Schirru, D. Falconieri, A. Piras, Excess enthalpy and excess volume for binary systems of two ionic liquids + water, in: J. Therm. Anal. Calorim., Springer Netherlands, 2011: pp. 29–33.

[115] P. Venkatesu, M.J. Lee, H.M. Lin, Volumetric properties of (N,N-dimethylformamide + aliphatic diethers) at temperatures ranging from (298.15 to 358.15) K, J. Chem. Thermodyn. 37 (2005) 996–1002.

[116] P. Gnanakumari, P. Venkatesu, K.R. Mohan, M.V.V.P. Rao, D.H.L. Prasad, Excess volumes and excess enthalpies of N-methyl-2-pyrrolidone with branched alcohols, Fluid Phase Equilib. 252 (2007) 137–142.

[117] F.I. El-Dossoki, Refractive index and density measurements for selected binary protic-protic, aprotic-aprotic, and aprotic-protic systems at temperatures from 298.15 K to

308.15 K, J. Chinese Chem. Soc. 54 (2007) 1129–1137.

[118] P.J. Flory, Discussions of the Faraday Society, (1970) 1–287.

[119] K. Raju, B. Rajamannan, C. Rakkappan, Ultrasonic study of molecular interactions in binary mixtures of aprotic and inert solvents, J. Mol. Liq. 100 (2002) 113–118.

[120] T. Kavitha, P. Attri, P. Venkatesu, R.S. Rama Devi, T. Hofman, Influence of temperature on thermophysical properties of ammonium ionic liquids with N-methyl-2-pyrrolidone, Thermochim. Acta. 545 (2012) 131–140.

[121] M. Radhamma, P. Venkatesu, M.V.V.P. Rao, M.J. Lee, H. mu Lin, Excess molar volumes and ultrasonic studies of dimethylsulphoxide with ketones at T = 303.15 K, J. Chem. Thermodyn. 40 (2008) 492–497.

[122] A.B. Pereiro, M.J. Pastoriza-Gallego, K. Shimizu, I.M. Marrucho, J.N.C. Lopes, M.M. Piñeiro, L.P.N. Rebelo, On the formation of a third, nanostructured domain in ionic liquids, J. Phys. Chem. B. 117 (2013) 10826–10833.

[123] U. Domańska, Thermophysical properties and thermodynamic phase behavior of ionic liquids, Thermochim. Acta. 448 (2006) 19–30.

[124] H. Tokuda, K. Hayamizu, K. Ishii, M.A.B.H. Susan, M. Watanabe, Physicochemical properties and structures of room temperature ionic liquids. 1. Variation of anionic species, J. Phys. Chem. B. 108 (2004) 16593–16600.

[125] H. Tokuda, K. Ishii, M.A.B.H. Susan, S. Tsuzuki, K. Hayamizu, M. Watanabe, Physicochemical properties and structures of room-temperature ionic liquids. 3. Variation of cationic structures, J. Phys. Chem. B. 110 (2006) 2833–2839.

[126] R. Gomes De Azevedo, J.M.S.S. Esperança, J. Szydlowski, Z.P. Visak, P.F. Pires, H.J.R. Guedes, L.P.N. Rebelo, Thermophysical and thermodynamic properties of ionic

liquids over an extended pressure range: [Bmim][NTf_2] and [Hmim][NTf_2], J. Chem. Thermodyn. 37 (2005) 888–899.

[127] U. Domańska, Solubilities and thermophysical properties of ionic liquids, Pure Appl. Chem. 77 (2005) 543–557.

[128] A.B. Pereiro, P. Verdía, E. Tojo, A. Rodríguez, Physical properties of 1-butyl-3-methylimidazolium methyl sulfate as a function of temperature, J. Chem. Eng. Data. 52 (2007) 377–380.

[129] H. Mizuuchi, V. Jaitely, S. Murdan, A.T. Florence, Room temperature ionic liquids and their mixtures: Potential pharmaceutical solvents, Eur. J. Pharm. Sci. 33 (2008) 326–331.

[130] M.A. Korany, H. Mahgoub, R.S. Haggag, M.A.A. Ragab, O.A. Elmallah, Green chemistry: Analytical and chromatography, J. Liq. Chromatogr. Relat. Technol. 40 (2017) 839–852.

[131] J. Dupont, R.F. De Souza, P.A.Z. Suarez, Ionic liquid (molten salt) phase organometallic catalysis, Chem. Rev. 102 (2002) 3667–3692.

[132] S. Karlapudi, R.L. Gardas, P. Venkateswarlu, K. Siva Kumar, Excess thermodynamic properties and FT-IR spectroscopic study of binary liquid mixtures of dichloro and trichlorobenzenes with 1-nonanol at T=(298.15, 303.15 and 308.15) K, J. Mol. Liq. 194 (2014) 227–233.

[133] M. Behroozi, H. Zarei, Volumetric properties of binary mixtures of tributylamine with benzene derivatives and comparison with ERAS model results at temperatures from (293.15 to 333.15) K, J. Chem. Thermodyn. 47 (2012) 276–287.

[134] M.S. AlTuwaim, K. Alkhaldi, A.S. Al-Jimaz, A.A. Mohammad, Comparative study of

physico-chemical properties of binary mixtures of N,N-dimethylformamide with 1-alkanols at different temperatures, J. Chem. Thermodyn. 48 (2012) 39–47.

[135] R. Gomes de Azevedo, J. Szydlowski, P.F. Pires, J.M.S.S. Esperança, H.J.R. Guedes, L.P.N. Rebelo, A novel non-intrusive microcell for sound-speed measurements in liquids. Speed of sound and thermodynamic properties of 2-propanone at pressures up to 160 MPa, J. Chem. Thermodyn. 36 (2004) 211–222.

[136] M. Janardhanaiah, S. Gangadhar, V. Govinda, K. Sreenivasulu, P. Venkateswarlu, Effect of alkanol chain length on excess thermodynamic properties of p-cresol with 1-alkanol at 298.15, 303.15, 308.15 and 313.15 K, J. Mol. Liq. 211 (2015) 169–177.

[137] T.M. Letcher, A. Marciniak, M. Marciniak, U. Domańska, Determination of activity coefficients at infinite dilution of solutes in the ionic liquid 1-butyl-3-methylimidazolium octyl sulfate using gas-liquid chromatography at a temperature of 298.15 K, 313.15 K, or 328.15 K, J. Chem. Eng. Data. 50 (2005) 1294–1298.

[138] D. Zhao, M. Wu, Y. Kou, E. Min, Ionic liquids: Applications in catalysis, Catal. Today. 74 (2002) 157–189.

[139] K.R. Seddon, A. Stark, M.-J. Torres, Influence of chloride, water, and organic solvents on the physical properties of ionic liquids, Pure Appl. Chem. 72 (2000) 2275–2287.

[140] R.C. Radziejewska, G. Lesnierowski, J. Kijowski, Properties and application of egg white lysozyme and its modified preparations - a review, Polish J. Food Nutr. Sci. 58 (2008) 5–10.

[141] S. Mangialardo, L. Gontrani, F. Leonelli, R. Caminiti, P. Postorino, Role of ionic liquids in protein refolding: Native/fibrillar versus treated lysozyme, RSC Adv. 2 (2012) 12329–12336.

[142] Y.H. Moon, S.M. Lee, S.H. Ha, Y.-M. Koo, Enzyme-catalyzed reactions in ionic liquids, Korean J. Chem. Eng. 23 (2006) 247–263.

[143] F. Van Rantwijk, R.M. Lau, R.A. Sheldon, Biocatalytic transformations in ionic liquids, Trends Biotechnol. 21 (2003) 131–138.

[144] A.A. Tietze, F. Bordusa, R. Giernoth, D. Imhof, T. Lenzer, A. Maaß, C. Mrestani-Klaus, I. Neundorf, K. Oum, D. Reith, A. Stark, On the nature of interactions between ionic liquids and small amino-acid-based biomolecules, ChemPhysChem. 14 (2013) 4044–4064.

[145] H. Noritomi, K. Minamisawa, R. Kamiya, S. Kato, Thermal stability of proteins in the presence of aprotic ionic liquids, J. Biomed. Sci. Eng. 04 (2011) 94–99.

[146] T. De Diego, P. Lozano, S. Gmouh, M. Vaultier, J.L. Iborra, Fluorescence and CD spectroscopic analysis of the α-chymotrypsin stabilization by the ionic liquid, 1-ethyl-3-methylimidazolium bis[(trifluoromethyl)sulfonyl]amide, Biotechnol. Bioeng. 88 (2004) 916–924.

[147] X. Han, D.W. Armstrong, Ionic liquids in separations, Acc. Chem. Res. 40 (2007) 1079–1086.

[148] J. Lin Huang, M.E. Noss, K.M. Schmidt, L. Murray, M.R. Bunagan, The effect of neat ionic liquid on the folding of short peptides, Chem. Commun. 47 (2011) 8007–8009.

[149] L.P.N. Rebelo, V. Najdanovic-Visak, Z.P. Visak, M. Nunes da Ponte, J. Szydlowski, C.A. Cerdeiriña, J. Troncoso, L. Romaní, J.M.S.S. Esperanza, H.J.R. Guedes, H.C. de Sousa, A detailed thermodynamic analysis of [C4mim][BF4] + water as a case study to model ionic liquid aqueous solutions, Green Chem. 6 (2004) 369–381.

[150] C.A. Summers, R.A. Flowers, Protein renaturation by the liquid organic salt

ethylammonium nitrate, Protein Sci. 9 (2000) 2001–2008.

[151] K. Sankaranarayanan, G. Sathyaraj, B.U. Nair, A. Dhathathreyan, Reversible and irreversible conformational transitions in myoglobin: Role of hydrated amino acid ionic liquid, J. Phys. Chem. B. 116 (2012) 4175–4180.

[152] P. Wasserscheid and T. Welton, Ionic Liquids in Synthesis, Org. Process Res. Dev. 7 (2003) 223–224.

[153] Y. Shu, L. Han, X. Wang, X. Chen, J. Wang, Fluorescence enhancement of imidazolium ionic liquid by its confinement on pvc for in situ selective quantification of hemoglobin, ACS Appl. Mater. Interfaces. 5 (2013) 12156–12162.

[154] W. Sun, X.Q. Li, K. Jiao, Direct electron transfer of hemoglobin on a carbon ionic liquid electrode with TiO_2 nanopatricle as enhancer, J. Chinese Chem. Soc. 55 (2008) 1074–1079.

[155] A. Kumar, M. Bisht, P. Venkatesu, Biocompatibility of ionic liquids towards protein stability: A comprehensive overview on the current understanding and their implications, Int. J. Biol. Macromol. 96 (2017) 611–651.

[156] K.S. Egorova, E.G. Gordeev, V.P. Ananikov, Biological Activity of Ionic Liquids and Their Application in Pharmaceutics and Medicine, Chem. Rev. 117 (2017) 7132–7189.

[157] T. Takekiyo, Y. Ishikawa, Y. Yoshimura, Cryopreservation of Proteins Using Ionic Liquids: A Case Study of Cytochrome c, J. Phys. Chem. B. 121 (2017) 7614–7620.

[158] Y. Lu, W. Lu, W. Wang, Q. Guo, Y. Yang, Thermodynamic studies of partitioning behavior of cytochrome c in ionic liquid-based aqueous two-phase system, Talanta. 85 (2011) 1621–1626.

[159] K. Fujita, D.R. MacFarlene, M. Forsyth, M. Yoshizawa-Fujita, K. Murata, N.

Nakamura, H. Ohno, Solubility and stability of cytochrome c in hydrated ionic liquids: Effect of oxo acid residues and kosmotropicity, Biomacromolecules. 8 (2007) 2080–2086.

[160] P. Lozano, T. De Diego, J.P. Guegan, M. Vaultier, J.L. Iborra, Stabilization of α-chymotrypsin by ionic liquids in transesterification reactions, Biotechnol. Bioeng. 75 (2001) 563–569.

[161] H. Noritomi, K. Suzuki, M. Kikuta, S. Kato, Catalytic activity of α-chymotrypsin in enzymatic peptide synthesis in ionic liquids, Biochem. Eng. J. 47 (2009) 27–30.

[162] M. Bisht, I. Jha, P. Venkatesu, Comprehensive Evaluation of Biomolecular Interactions between Protein and Amino Acid Based-Ionic Liquids: A Comparable Study between [Bmim][Br] and [Bmim][Gly] Ionic Liquids, ChemistrySelect. 1 (2016) 3510–3519.

[163] I. Jha, M. Bisht, P. Venkatesu, Does 1-Allyl-3-methylimidazolium chloride Act as a Biocompatible Solvent for Stem Bromelain?, J. Phys. Chem. B. 120 (2016) 5625–5633.

[164] C. Lange, G. Patil, R. Rudolph, Ionic liquids as refolding additives: N′-alkyl and N′-(ω-hydroxyalkyl) N-methylimidazolium chlorides, Protein Sci. 14 (2005) 2693–2701.

[165] Z. Wang, L. Dang, Y. Han, P. Jiang, H. Wei, Crystallization control of thermal stability and morphology of hen egg white lysozyme crystals by ionic liquids, J. Agric. Food Chem. 58 (2010) 5444–5448.

[166] B. Mandal, S. Mondal, A. Pan, S.P. Moulik, S. Ghosh, Physicochemical study of the interaction of lysozyme with surface active ionic liquid 1-butyl-3-methylimidazolium octylsulfate [Bmim][OS] in aqueous and buffer media, Colloids Surfaces A

Physicochem. Eng. Asp. 484 (2015) 345–353.

[167] M. Kumari, N. Dohare, N. Maurya, R. Dohare, R. Patel, Effect of 1-methyl-3-octyleimmidazolium chloride on the stability and activity of lysozyme: a spectroscopic and molecular dynamics studies, J. Biomol. Struct. Dyn. 35 (2017) 2016–2030.

[168] S. Yamaguchi, E. Yamamoto, S. Tsukiji, T. Nagamune, Successful control of aggregation and folding rates during refolding of denatured lysozyme by adding N-methylimidazolium cations with various N-substituents, Biotechnol. Prog. 24 (2008) 402–408.

[169] Y. Shu, M. Liu, S. Chen, X. Chen, J. Wang, New insight into molecular interactions of imidazolium ionic liquids with bovine serum albumin, J. Phys. Chem. B. 115 (2011) 12306–12314.

[170] L. Satish, S. Rana, M. Arakha, L. Rout, B. Ekka, S. Jha, P. Dash, H. Sahoo, Impact of imidazolium-based ionic liquids on the structure and stability of lysozyme, Spectrosc. Lett. 49 (2016) 383–390.

[171] R. Huang, S. Zhang, L. Pan, J. Li, F. Liu, H. Liu, Spectroscopic studies on the interactions between imidazolium chloride ionic liquids and bovine serum albumin, Spectrochim. Acta - Part A Mol. Biomol. Spectrosc. 104 (2013) 377–382.

[172] C. Zhang, A. Yu, R. Lu, Cationic effect of imidazolium-based ionic liquid on the stability of myoglobin, Process Biochem. 58 (2017) 181–185.

[173] A. Safavi, F. Farjami, Hydrogen peroxide biosensor based on a myoglobin/hydrophilic room temperature ionic liquid film, Anal. Biochem. 402 (2010) 20–25.

[174] I. Jha, A. Kumar, P. Venkatesu, The Overriding Roles of Concentration and Hydrophobic Effect on Structure and Stability of Heme Protein Induced by

Imidazolium-Based Ionic Liquids, J. Phys. Chem. B. 119 (2015) 8357–8368.

[175] Y. Pei, L. Li, Z. Li, C. Wu, J. Wang, Partitioning Behavior of Wastewater Proteins in Some Ionic Liquids-Based Aqueous Two-Phase Systems, Sep. Sci. Technol. 47 (2012) 277–283.

[176] X. Lin, Y. Wang, Q. Zeng, X. Ding, J. Chen, Extraction and separation of proteins by ionic liquid aqueous two-phase system, Analyst. 138 (2013) 6445–6453.

[177] Y. Akdogan, D. Hinderberger, Solvent-induced protein refolding at low temperatures, J. Phys. Chem. B. 115 (2011) 15422–15429.

[178] M. Silva, A.M. Figueiredo, E.J. Cabrita, Epitope mapping of imidazolium cations in ionic liquid-protein interactions unveils the balance between hydrophobicity and electrostatics towards protein destabilisation, Phys. Chem. Chem. Phys. 16 (2014) 23394–23403.

[179] D. Mondal, M. Sharma, M. V. Quental, A.P.M. Tavares, K. Prasad, M.G. Freire, Suitability of bio-based ionic liquids for the extraction and purification of IgG antibodies, Green Chem. 18 (2016) 6071–6081.

[180] A. Mehta, J. Raghava Rao, N.N. Fathima, Electrostatic Forces Mediated by Choline Dihydrogen Phosphate Stabilize Collagen, J. Phys. Chem. B. 119 (2015) 12816–12827.

[181] X.D. Hou, Q.P. Liu, T.J. Smith, N. Li, M.H. Zong, Evaluation of Toxicity and Biodegradability of Cholinium Amino Acids Ionic Liquids, Plos. One. 8 (2013) 1–7.

[182] J.I. Santos, A.M.M. Gonçalves, J.L. Pereira, B.F.H.T. Figueiredo, F.A.E. Silva, J.A.P. Coutinho, S.P.M. Ventura, F. Gonçalves, Environmental safety of cholinium-based ionic liquids: assessing structure-ecotoxicity relationships, Green Chem. 17 (2015)

4657–4668.

[183] M. Bisht, P. Venkatesu, Influence of cholinium-based ionic liquids on the structural stability and activity of α-chymotrypsin, New J. Chem. 41 (2017) 13902–13911.

[184] K.D. Weaver, R.M. Vrikkis, M.P. Van Vorst, J. Trullinger, R. Vijayaraghavan, D.M. Foureau, I.H. McKillop, D.R. MacFarlane, J.K. Krueger, G.D. Elliott, Structure and function of proteins in hydrated choline dihydrogen phosphate ionic liquid, Phys. Chem. Chem. Phys. 14 (2012) 790–801.

[185] K. Fujita, M. Forsyth, D.R. MacFarlane, R.W. Reid, G.D. Elliott, Unexpected improvement in stability and utility of cytochrome c by solution in biocompatible ionic liquids, Biotechnol. Bioeng. 94 (2006) 1209–1213.

[186] J. V. Rodrigues, V. Prosinecki, I. Marrucho, L.P.N. Rebelo, C.M. Gomes, Protein stability in an ionic liquid milieu: On the use of differential scanning fluorimetry, Phys. Chem. Chem. Phys. 13 (2011) 13614–13616.

[187] M. Bisht, D. Mondal, M.M. Pereira, M.G. Freire, P. Venkatesu, J.A.P. Coutinho, Long-term protein packaging in cholinium-based ionic liquids: Improved catalytic activity and enhanced stability of cytochrome c against multiple stresses, Green Chem. 19 (2017) 4900–4911.

[188] R. Vijayaraghavan, A. Izgorodin, V. Ganesh, M. Surianarayanan, D.R. MacFarlane, Long-term structural and chemical stability of DNA in hydrated ionic liquids, Angew. Chemie - Int. Ed. 49 (2010) 1631–1633.

[189] S.C. Matias, N.M.T. Lourenço, L.J.P. Fonseca, C.M. Cordas, Comparative Electrochemical Behavior of Cytochrome c on Aqueous Solutions Containing Choline-Based Room Temperature Ionic Liquids, ChemistrySelect. 2 (2017) 8701–8705.

[190] V.F. Curto, S. Scheuermann, R.M. Owens, V. Ranganathan, D.R. Macfarlane, F. Benito-Lopez, D. Diamond, Probing the specific ion effects of biocompatible hydrated choline ionic liquids on lactate oxidase biofunctionality in sensor applications, Phys. Chem. Chem. Phys. 16 (2014) 1841–1849.

[191] M. Kowacz, A. Mukhopadhyay, A.L. Carvalho, J.M.S.S. Esperança, M.J. Romão, L.P.N. Rebelo, Hofmeister effects of ionic liquids in protein crystallization: Direct and water-mediated interactions, CrystEngComm. 14 (2012) 4912–4921.

[192] D. Constatinescu, C. Herrmann, H. Weingärtner, Patterns of protein unfolding and protein aggregation in ionic liquids, Phys. Chem. Chem. Phys. 12 (2010) 1756–1763.

[193] A.M. Figueiredo, J. Sardinha, G.R. Moore, E.J. Cabrita, Protein destabilisation in ionic liquids: The role of preferential interactions in denaturation, Phys. Chem. Chem. Phys. 15 (2013) 19632–19643.

[194] Y.C. Fan, S.L. Zhang, Q. Wang, J.H. Li, H.T. Fan, D.K. Shan, Investigation of the Interaction of Pepsin with Ionic Liquids by Using Fluorescence Spectroscopy, Appl. Spectrosc. 67 (2013) 648–655.

[195] M. Bekhouche, L.J. Blum, B. Doum??che, Contribution of dynamic and static quenchers for the study of protein conformation in ionic liquids by steady-state fluorescence spectroscopy, J. Phys. Chem. B. 116 (2012) 413–423.

[196] D. Ajloo, M. Sangian, M. Ghadamgahi, M. Evini, A.A. Saboury, Effect of two imidazolium derivatives of ionic liquids on the structure and activity of adenosine deaminase, Int. J. Biol. Macromol. 55 (2013) 47–61.

[197] B. Dabirmanesh, S. Daneshjou, A.A. Sepahi, B. Ranjbar, R.A. Khavari-Nejad, P. Gill, A. Heydari, K. Khajeh, Effect of ionic liquids on the structure, stability and activity of

two related α-amylases, Int. J. Biol. Macromol. 48 (2011) 93–97.

[198] V.W. Jaeger, J. Pfaendtner, Structure, dynamics, and activity of xylanase solvated in binary mixtures of ionic liquid and water, ACS Chem. Biol. 8 (2013) 1179–1186.

[199] P. Attri, P. Venkatesu, A. Kumar, Activity and stability of α-chymotrypsin in biocompatible ionic liquids: Enzyme refolding by triethyl ammonium acetate, Phys. Chem. Chem. Phys. 13 (2011) 2788–2796.

[200] D.F. Kennedy, C.J. Drummond, T.S. Peat, J. Newman, Evaluating protic ionic liquids as protein crystallization additives, Cryst. Growth Des. 11 (2011) 1777–1785.

[201] D. Hekmat, D. Hebel, S. Joswig, M. Schmidt, D. Weuster-Botz, Advanced protein crystallization using water-soluble ionic liquids as crystallization additives, Biotechnol. Lett. 29 (2007) 1703–1711.

[202] J.P. Mann, A. McLuskey, R. Atkin, Activity and thermal stability of lysozyme in alkylammonium formate ionic liquids - Influence of cation modification, Green Chem. 11 (2009) 785–792.

[203] M. Ebrahimi, S. Hosseinkhani, A. Heydari, R.A. Khavari-Nejad, J. Akbari, Controversial effect of two methylguanidine-based ionic liquids on firefly luciferase, Photochem. Photobiol. Sci. 11 (2012) 828–834.

[204] I. Jha, P. Attri, P. Venkatesu, Unexpected effects of the alteration of structure and stability of myoglobin and hemoglobin in ammonium-based ionic liquids, Phys. Chem. Chem. Phys. 16 (2014) 5514–5526.

[205] M. Kumari, J.K. Maurya, M. Tasleem, P. Singh, R. Patel, Probing HSA-ionic liquid interactions by spectroscopic and molecular docking methods, J. Photochem. Photobiol. B Biol. 138 (2014) 27–35.

[206] E. Cunha, M.L.C. Passos, P.C.A.G. Pinto, M.L.M.F.S. Saraiva, Improved activity of α-chymotrypsin in mixed micelles of cetyltrimethylammonium bromide (CTAB) and ionic liquids: A kinetic study resorting to sequential injection analysis, Colloids Surfaces B Biointerfaces. 118 (2014) 172–178.

[207] A. Tarannum, C. Muvva, A. Mehta, J.R. Rao, N.N. Fathima, Phosphonium based ionic liquids-stabilizing or destabilizing agents for collagen?, RSC Adv. 6 (2016) 4022–4033.

[208] R. Patel, M. Kumari, Interaction between Pyrrolidinium Based Ionic Liquid and Bovine Serum Albumin: A Spectroscopic and Molecular Docking Insight, Biochem. Anal. Biochem. 5 (2016).

[209] Y. Zhang, P.S. Cremer, Interactions between macromolecules and ions: the Hofmeister series, Curr. Opin. Chem. Biol. 10 (2006) 658–663.

[210] W. Kunz, Specific ion effects in colloidal and biological systems, Curr. Opin. Colloid Interface Sci. 15 (2010) 34–39.

[211] Z. Yang, Y.J. Yue, W.C. Huang, X.M. Zhuang, Z.T. Chen, M. Xing, Importance of the ionic nature of ionic liquids in affecting enzyme performance, J. Biochem. 145 (2009) 355–364.

[212] H.D.B. Jenkins, Y. Marcus, Viscosity B-Coefficients of Ions in Solution, Chem. Rev. 95 (1995) 2695–2724.

[213] L.M. Pegram, T. Wendorff, R. Erdmann, I. Shkel, D. Bellissimo, D.J. Felitsky, M.T. Record, Why Hofmeister effects of many salts favor protein folding but not DNA helix formation, Proc. Natl. Acad. Sci. 107 (2010) 7716–7721.

[214] W. Kunz, P. Lo Nostro, B.W. Ninham, The present state of affairs with Hofmeister

effects, Curr. Opin. Colloid Interface Sci. 9 (2004) 1–18.

[215] D.K. Eggers, J.S. Valentine, Crowding and hydration effects on protein conformation: A study with sol-gel encapsulated proteins, J. Mol. Biol. 314 (2001) 911–922.

[216] K.D. Collins, Charge density-dependent strength of hydration and biological structure, Biophys. J. 72 (1997) 65–76.

[217] Z. Yang, Hofmeister effects: an explanation for the impact of ionic liquids on biocatalysis, J. Biotechnol. 144 (2009) 12–22.

[218] F. Geng, L. Zheng, L. Yu, G. Li, C. Tung, Interaction of bovine serum albumin and long-chain imidazolium ionic liquid measured by fluorescence spectra and surface tension, Process Biochem. 45 (2010) 306–311.

[219] N. Debeljuh, C.J. Barrow, N. Byrne, The impact of ionic liquids on amyloid fibrilization of Aβ16-22: Tuning the rate of fibrilization using a reverse Hofmeister strategy, Phys. Chem. Chem. Phys. 13 (2011) 16534–16536.

[220] M.P. Heitz, J.W. Rupp, K.W. Horn, Biocatalytic Activity of Mushroom Tyrosinase in Ionic Liquids: Specific Ion Effects and the Hofmeister Series, Insigh. Enzym. Res. 2 (2018) 1–9.

[221] E. Yamamoto, S. Yamaguchi, T. Nagamune, Protein refolding by N-alkylpyridinium and n-alkyl-n-methylpyrrolidinium ionic liquids, Appl. Biochem. Biotechnol. 164 (2011) 957–967.

[222] X.A. Shi, M.-H. Zong, W.-Y. Lou, Effect of Ionic Liquids on Catalytic Characteristics of Horse Liver Alcohol Dehydrogenase, Chinese J. Chem. 24 (2006) 1643–1647.

[223] H. Shekaari, Y. Mansoori, R. Sadeghi, Density, speed of sound, and electrical conductance of ionic liquid 1-hexyl-3-methyl-imidazolium bromide in water at

different temperatures, J. Chem. Thermodyn. 40 (2008) 852–859.

[224] M. Teodorescu, Isothermal (vapour + liquid) equilibrium and thermophysical properties for (1-butyl-3-methylimidazolium iodide + 1-butanol) binary system, J. Chem. Thermodyn. 87 (2015) 58–64.

[225] M. Srinivasa Reddy, I. Khan, K.T.S.S. Raju, P. Suresh, B. Hari Babu, The study of molecular interactions in 1-ethyl-3-methylimidazolium trifluoromethanesulfonate + 1-pentanol from density, speed of sound and refractive index measurements, J. Chem. Thermodyn. 98 (2016) 298–308.

[226] N.S.M. Vieira, A. Luís, P.M. Reis, P.J. Carvalho, J.A. Lopes-Da-Silva, J.M.S.S. Esperança, J.M.M. Araújo, L.P.N. Rebelo, M.G. Freire, A.B. Pereiro, Fluorination effects on the thermodynamic, thermophysical and surface properties of ionic liquids, J. Chem. Thermodyn. 97 (2016) 354–361.

[227] I. Bahadur, M. Kgomotso, E.E. Ebenso, G. Redhi, Influence of temperature on molecular interactions of imidazolium-based ionic liquids with acetophenone: thermodynamic properties and quantum chemical studies, RSC Adv. 6 (2016) 104708–104723.

[228] Y. Xu, B. Chen, W. Qian, H. Li, Properties of pure n-butylammonium nitrate ionic liquid and its binary mixtures of with alcohols at T=(293.15 to 313.15)K, J. Chem. Thermodyn. 58 (2013) 449–459.

[229] Y. Xu, J. Yao, C. Wang, H. Li, Density, viscosity, and refractive index properties for the binary mixtures of n -butylammonium acetate ionic liquid + alkanols at sveral temperatures, J. Chem. Eng. Data. 57 (2012) 298–308.

[230] S.S. Bittencourt, H.E. Hoga, R.B. Torres, J.V.H. D'Angelo, Thermodynamic

properties of binary mixtures of n-butylammonium-based ionic liquids with ethanol at T = (293.15–313.15) K, J. Therm. Anal. Calorim. (2018). doi:10.1007/s10973-018-7399-0.

[231] G. Vieira Olivieri, C. Sarem, D. Cunha, B**.** Lilian, S. Martins, P. Ainis, M. Paegle, B. Satya, D. Nuncio, R.B. Torres, Thermodynamic and spectroscopic study of binary mixtures of n-butylammonium oleate ionic liquid + alcohol at T = 288.15–308.15 K, J. Therm. Anal. Calorim. 131 (2018) 2925–2942.

[232] K.A. Kurnia, B. Ariwahjoedi, M.I.A. Mutalib, T. Murugesan, Density and excess molar volume of the protic ionic liquid bis(2-hydroxyethyl)ammonium acetate with alcohols, J. Solution Chem. 40 (2011) 470–480.

[233] K.A. Kurnia, M.I.A. Mutalib, T. Murugesan, B. Ariwahjoedi, Physicochemical Properties of Binary Mixtures of the Protic Ionic Liquid Bis(2-hydroxyethyl)methylammonium Formate with Methanol, Ethanol, and 1-Propanol, J. Solution Chem. 40 (2011) 818–831.

[234] M. Massel, A.L. Revelli, E. Paharik, M. Rauh, L.O. Mark, J.F. Brennecke, Phase equilibrium, excess enthalpies, and densities of binary mixtures of trimethylbutylammonium bis(trifluoromethylsulfonyl)imide with ethanol, 1-propanol, and dimethylformamide, J. Chem. Eng. Data. 60 (2015) 65–73.

[235] M.M. Taib, T. Murugesan, Densities and excess molar volumes of binary mixtures of bis(2-hydroxyethyl)ammonium acetate + water and monoethanolamine + Bis(2-hydroxyethyl)ammonium acetate at temperatures from (303.15 to 353.15) K, J. Chem. Eng. Data. 55 (2010) 5910–5913.

[236] R.R. Pinto, D. Santos, S. Mattedi, M. Aznar, Density, refractive index, apparent volumes and excess molar volumes of four protic ionic liquids + water at T=298.15

and 323.15 K, in: Brazilian J. Chem. Eng., Associação Brasileira de Engenharia Química, 2015: pp. 671–682.

[237] R. Umapathi, P. Attri, P. Venkatesu, Thermophysical Properties of Aqueous Solution of Ammonium-Based Ionic Liquids, J. Phys. Chem. B. 118 (2014) 5971–5982.

[238] M. Hou, Y. Xu, Y. Han, B. Chen, W. Zhang, Q. Ye, J. Sun, Thermodynamic properties of aqueous solutions of two ammonium-based protic ionic liquids at 298.15 K, J. Mol. Liq. 178 (2013) 149–155.

[239] P. Attri, P. Venkatesu, T. Hofman, Temperature dependence measurements and structural characterization of trimethyl ammonium ionic liquids with a highly polar solvent, J. Phys. Chem. B. 115 (2011) 10086–10097.

[240] P. Attri, P. Venkatesu, A. Kumar, Temperature effect on the molecular interactions between ammonium ionic liquids and N, N-dimethylformamide, J. Phys. Chem. B. 114 (2010) 13415–13425.

[241] T. Kavitha, P. Attri, P. Venkatesu, R.S. Rama Devi, T. Hofman, Temperature dependence measurements and molecular interactions for ammonium ionic liquid with N-methyl-2-pyrrolidone, J. Chem. Thermodyn. 54 (2012) 223–237.

[242] P.K. Chhotaray, S. Jella, R.L. Gardas, Structural and compositional effect on the acoustic and volumetric properties of ammonium based ionic liquids with water and N-methyl-2-pyrrolidone, J. Mol. Liq. 219 (2016) 829–844.

[243] T. Kavitha, P. Attri, P. Venkatesu, R.S.R. Devi, T. Hofman, Influence of alkyl chain length and temperature on thermophysical properties of ammonium-based ionic liquids with molecular solvent, J. Phys. Chem. B. 116 (2012) 4561–4574.

[244] M. Usula, E. Matteoli, F. Leonelli, F. Mocci, F.C. Marincola, L. Gontrani, S.

Porcedda, Thermo-physical properties of ammonium-based ionic liquid + N-methyl-2-pyrrolidone mixtures at 298.15K, Fluid Phase Equilib. 383 (2014) 49–54.

[245] V. Govinda, P. Attri, P. Venkatesu, P. Venkateswarlu, Evaluation of thermophysical properties of ionic liquids with polar solvent: A comparable study of two families of ionic liquids with various ions, J. Phys. Chem. B. 117 (2013) 12535–12548.

[246] X.H. Fan, Y.P. Chen, C.S. Su, Density and Viscosity Measurements for Binary Mixtures of 1-Ethyl-3-methylimidazolium Tetrafluoroborate ([Emim][BF4]) with Dimethylacetamide, Dimethylformamide, and Dimethyl Sulfoxide, J. Chem. Eng. Data. 61 (2016) 920–927.

[247] J.Y. Wu, Y.P. Chen, C.S. Su, Density and viscosity of ionic liquid binary mixtures of 1-n-butyl-3-methylimidazolium tetrafluoroborate with acetonitrile, N,N-dimethylacetamide, methanol, and N-methyl-2-pyrrolidone, J. Solution Chem. 44 (2015) 395–412.

[248] H. Zarei, V. Keley, Density and Speed of Sound of Binary Mixtures of Ionic Liquid 1-Ethyl-3-methylimidazolium Tetrafluoroborate, N,N-Dimethylformamide, and N,N-Dimethylacetamide at Temperature Range of 293.15-343.15 K: Measurement and PC-SAFT Modeling, J. Chem. Eng. Data. 62 (2017) 913–923.

[249] I. Bahadur, E. Sapei, S. Singh, E.E. Ebenso, G.G. Redhi, Physicochemical Properties of N -Butyl- N -methyl-2-oxopyrrolidonium Bromide and Its Binary Mixtures with Water or Methanol, ACS Sustain. Chem. Eng. 4 (2016) 601–608.

[250] S. Panda, S. Ray, V. Losetty, R.L. Gardas, Synthesis and thermophysical properties of pyrrolidonium based ionic liquids and their binary mixtures with water and DMSO at T=(293.15 to 333.15) K, J. Mol. Liq. 224 (2016) 882–892.

[251] S. Brahma, R.L. Gardas, Understanding the solvation behavior of pyrrolidinium based ionic liquids in acetonitrile through thermophysical properties at 293.15 to 328.15 K, J. Mol. Liq. 256 (2018) 22–28.

[252] V.H. Alvarez, S. Mattedi, M. Martin-Pastor, M. Aznar, M. Iglesias, Thermophysical properties of binary mixtures of {ionic liquid 2-hydroxy ethylammonium acetate + (water, methanol, or ethanol)}, J. Chem. Thermodyn. 43 (2011) 997–1010.

[253] B.K. Chennuri, V. Losetty, R.L. Gardas, Apparent molar properties of hydroxyethyl ammonium based ionic liquids with water and ethanol at various temperatures, J. Mol. Liq. 212 (2015) 444–450.

[254] D. Keshapolla, V. Singh, A. Gupta, R.L. Gardas, Apparent molar properties of benzyldimethylammonium based protic ionic liquids in water and ethanol at different temperatures, Fluid Phase Equilib. 385 (2015) 92–104.

[255] D. Cai, J. Yang, H. Da, L. Li, H. Wang, T. Qiu, Densities and viscosities of binary mixtures N,N-dimethyl-N-(3-sulfopropyl)cyclohexylammonium tosylate with water and methanol at T = (303.15 to 328.15) K, J. Mol. Liq. 229 (2017) 389–395.

[256] J. Kulhavy, R. Andrade, S. Barros, J. Serra, M. Iglesias, Influence of temperature on thermodynamics of protic ionic liquid 2-hydroxy diethylammonium lactate (2-HDEAL) + short hydroxylic solvents, J. Mol. Liq. 213 (2016) 92–106.

[257] I. Bahadur, N. Deenadayalu, Thermochimica Acta Apparent molar volume and apparent molar isentropic compressibility for the binary systems { methyltrioctylammoniumbis (trifluoromethylsulfonyl) imide + ethyl acetate or ethanol } at different temperatures under atmospheric pressure, Thermochim. Acta. 566 (2013) 77–83.

[258] I. Bahadur, N. Deenadayalu, Apparent molar volume and isentropic compressibility for the binary systems {methyltrioctylammonium bis(trifluoromethylsulfonyl)imide + methyl acetate or methanol} and (methanol + methyl acetate) at T=298.15, 303.15, 308.15 and 313.15 K and atmospheric pr, J. Solution Chem. 40 (2011) 1528–1543.

[259] S.P. Musale, K.R. Patil, R.J. Gavhane, D.H. Dagade, Density and Speed-of-Sound Measurements for Dilute Binary Mixtures of Diethylammonium-Based Protic Ionic Liquids with Water, J. Chem. Eng. Data. 63 (2018) 1859–1876.

[260] G. Sharma, V. Singh, R.L. Gardas, Apparent molar properties of aqueous protic ionic liquid solutions at T = (293.15 to 328.15) K, Ionics (Kiel). 21 (2015) 1959–1965.

[261] M.T. Zafarani-Moattar, H. Shekaari, Volumetric and compressibility behaviour of ionic liquid, 1-n-butyl-3-methylimidazolium hexafluorophosphate and tetrabutylammonium hexafluorophosphate in organic solvents at T = 298.15 K, J. Chem. Thermodyn. 38 (2006) 624–633.

[262] M.T. Zafarani-Moattar, H. Shekaari, Apparent molar volume and isentropic compressibility of ionic liquid 1-butyl-3-methylimidazolium bromide in water, methanol, and ethanol at T = (298.15 to 318.15) K, J. Chem. Thermodyn. 37 (2005) 1029–1035.

[263] I.M. Abdulagatov, A. Tekin, J. Safarov, A. Shahverdiyev, E. Hassel, Densities and excess, apparent, and partial molar volumes of binary mixtures of [Bmim][BF_4]+ ethanol as a function of temperature, pressure, and concentration, Int. J. Thermophys. 29 (2008) 505–533.

[264] E.J. González, N. Calvar, E.A. Macedo, Osmotic coefficients and apparent molar volumes of 1-hexyl-3- methylimidazolium trifluoromethanesulfonate ionic liquid in alcohols, J. Chem. Thermodyn. 69 (2014) 93–100.

[265] P.J. Artymiuk, C.C.F. Blake, Refinement of human lysozyme at 1.5 Å resolution analysis of non-bonded and hydrogen-bond interactions, J. Mol. Biol. 152 (1981) 737–762.

[266] A.J. Marengo-Rowe, Structure-function relations of human hemoglobins, Proc. Bayl. Univ. Med. Cent. 19 (2006) 239–45.

[267] A. Ritonja, A.D. Rowan, D.J. Buttle, N.D. Rawlings, V. Turk, A.J. Barrett, Stem bromelain: Amino acid sequence and implications for weak binding of cystatin, FEBS Lett. 247 (1989) 419–424.

[268] I.G. Kamphuis, J. Drenth, E.N. Baker, Thiol proteases. Comparative studies based on the high-resolution structures of papain and actinidin, and on amino acid sequence information for cathepsins B and H, and stem bromelain, J. Mol. Biol. 182 (1985) 317–329.

[269] A. Rani, P. Venkatesu, Insights into the interactions between enzyme and co-solvents: Stability and activity of stem bromelain, Int. J. Biol. Macromol. 73 (2015) 189–201.

[270] B.K. Bhattacharyya, Bromelain: An overview, Indian J. Nat. Prod. Resour. 7 (2008) 359–363.

[271] H.R. Maurer, Bromelain: biochemistry, pharmacology and medical use, Cell. Mol. Life Sci. 58 (2001) 1234–1245.

[272] R.R. White, F.E. Crawley, M. Vellini, L.A. Rovati, Bioavailability of 125I bromelain after oral administration to rats., Biopharm. Drug Dispos. 9 (1988) 397–403.

[273] D. MacKay, A.L. Miller, Nutritional support for wound healing., Altern. Med. Rev. 8 (2003) 359–77.

[274] M.E. Errasti, A. Prospitti, C.A. Viana, M.M. Gonzalez, M. V. Ramos, A.E. Rotelli,

N.O. Caffini, Effects on fibrinogen, fibrin, and blood coagulation of proteolytic extracts from fruits of Pseudananas macrodontes, Bromelia balansae, and B. hieronymi (Bromeliaceae) in comparison with bromelain, Blood Coagul. Fibrinolysis. 27 (2016) 441–449.

[275] K. Pillai, J. Akhter, T.C. Chua, D.L. Morris, Anticancer property of bromelain with therapeutic potential in malignant peritoneal mesothelioma, Cancer Invest. 31 (2013) 241–250.

[276] R.A. Orsini, Bromelain, Plast. Reconstr. Surg. 118 (2006) 1640–1644.

[277] W. Hu, A.M. Wang, S.Y. Wu, B. Zhang, S. Liu, Y. Bin Gou, J.M. Wang, Debriding effect of bromelain on firearm wounds in pigs, J. Trauma - Inj. Infect. Crit. Care. 71 (2011) 966–972.

[278] L.W. Cohen, V.M. Coghlan, L.C. Dihel, Cloning and sequencing of papain-encoding cDNA, Gene. 48 (1986) 219–227.

[279] A. Rani, A. Jayaraj, B. Jayaram, V. Pannuru, Trimethylamine-N-oxide switches from stabilizing nature: A mechanistic outlook through experimental techniques and molecular dynamics simulation, Sci. Rep. 6 (2016) 1–14.

[280] J.R. Lakowicz, Principles of fluorescence spectroscopy, Springer US, (2006) 1-954.

[281] L. Brand, M.L. Johnson, Fluorescence spectroscopy, Academic Press, 278 (1997) 1-628.

[282] S. Habib, M.A. Khan, H. Younus, Thermal destabilization of stem bromelain by trehalose, Protein J. 26 (2007) 117–124.

[283] J.C. Lindon, G.E. Tranter, J.L. (John L. Holmes, Encyclopedia of spectroscopy and spectrometry, Academic Press, 2000.

[284] C.N. Pace, D. V. Laurents, A New Method for Determining the Heat Capacity Change for Protein Folding, Biochemistry. 28 (1989) 2520–2525.

[285] J.-L. Mergny, L. Lacroix, Analysis of Thermal Melting Curves, Oligonucleotides. 13 (2003) 515–537.

[286] C.N. Pace, Evaluating contribution of hydrogen bonding and hydrophobic bonding to protein folding, Methods Enzymol. 259 (1995) 538–554.

[287] A. Waheed, M.A. Qasim, A. Salahuddin, Characterization of Stable Conformational States in Urea-Induced Transition in Ovomucoid, Eur. J. Biochem. 76 (1977) 383–390.

[288] T. Azuma, K. Hamaguchi, S. Migita, Denaturation of Bence Jones Proteins by Guanidine Hydrochloride, J. Biochem. 72 (1972) 1457–1467.

[289] E.M. Nicholson, J.M. Scholtz, Conformational stability of the Escherichia coli HPr protein: Test of the linear extrapolation method and a thermodynamic characterization of cold denaturation, Biochemistry. 35 (1996) 11369–11378.

[290] D. Correcirc, C. Ramos, The use of circular dichroism spectroscopy to study protein folding, form and function, African J. Biochem. 3 (2009) 164–173.

[291] N. Berova, K. Nakanishi, R. Woody, Circular dichroism : principles and applications, J. Med. Chem. 44 (2000) 1122–1122.

[292] G.D. Fasman, Circular Dichroism and the Conformational Analysis of Biomolecules, Springers. (1996) 1–697.

[293] S.M. Kelly, T.J. Jess, N.C. Price, How to study proteins by circular dichroism, Biochim. Biophys. Acta - Proteins Proteomics. 1751 (2005) 119–139.

[294] B. Lorber, F. Fischer, M. Bailly, H. Roy, D. Kern, Protein analysis by dynamic light

scattering: Methods and techniques for students, Biochem. Mol. Biol. Educ. 40 (2012) 372–382.

[295] N.J. Greenfield, Determination of the folding of proteins as a function of denaturants, osmolytes or ligands using circular dichroism, Nat. Protoc. 1 (2007) 2733–2741.

[296] D.T. Clarke, Circular Dichroism and Its Use in Protein-Folding Studies, in: Methods Mol. Biol., 2011: pp. 59–72.

[297] I. Jha, P. Venkatesu, Unprecedented Improvement in the Stability of Hemoglobin in the Presence of Promising Green Solvent 1-Allyl-3-methylimidazolium Chloride, ACS Sustain. Chem. Eng. 4 (2016) 413–421.

[298] Y.P. Handa, G.C. Benson, Volume changes on mixing two liquids: A review of the experimental techniques and the literature data, Fluid Phase Equilib. 3 (1979) 185–249.

[299] W.E. William, E. Acree, Thermodynamic Properties of Nonelectrolyte Solutions - William Acree - Google Books, (1984) 308.

[300] D.B. Keyes, J.H. Hildebrand, A study of the system aniline-hexane, J. Am. Chem. Soc. 39 (1917) 2126–2137.

[301] M.K. Kumaran, M.L. McGlashan, An improved dilution dilatometer for measurements of excess volumes, J. Chem. Thermodyn. 9 (1977) 259–267.

[302] G.G. Redhi, Thermodynamics of liquid mixtures containing carboxylic acids, Tesis PhD. (2003) 6–16.

[303] S.E. Wood, J.P. Brusie, The Volume of Mixing and the Thermodynamic Functions of Benzene—Carbon Tetrachloride Mixture, J. Am. Chem. Soc. 65 (1943) 1891–1895.

[304] I. Brown and J.E. Lane, Recommended Reference Materials for Realization of Physicochemical Properties, Pure Appl. Chem. 45 (1976) 1–9.

[305] F. Franks, H.. Smith, Apparent molal volumes and expansibilities of electrolytes in dilute aqueous solution, Trans. Faraday Soc. 63 (1967) 2586–2598.

[306] S.M. Walas, Phase Equilibria in Chemical Engineering, Elsevier. (1985) 1–671.

[307] T.M. Letcher, The excess volumes of some mixtures of saturated and unsaturated C6hydrocarbons, J. Chem. Thermodyn. 7 (1975) 205–209.

[308] S. Zhang, N. Sun, X. He, X. Lu, X. Zhang, Physical properties of ionic liquids: Database and evaluation, J. Phys. Chem. Ref. Data. 35 (2006) 1475–1517.

[309] T.L. Greaves, A. Weerawardena, C. Fong, I. Krodkiewska, C.J. Drummond, Protic ionic liquids: Solvents with tunable phase behavior and physicochemical properties, J. Phys. Chem. B. 110 (2006) 22479–22487.

[310] K.N. Marsh, J.A. Boxall, R. Lichtenthaler, Room temperature ionic liquids and their mixtures - A review, in: Fluid. Phase. Equilib. 219 (2004) 93–98.

[311] M.A. Iglesias-Otero, J. Troncoso, E. Carballo, L. Romaní, Density and refractive index in mixtures of ionic liquids and organic solvents: Correlations and predictions, J. Chem. Thermodyn. 40 (2008) 949–956.

[312] P.K. Kumar, I. Jha, P. Venkatesu, I. Bahadur, E.E. Ebenso, A comparative study of the stability of stem bromelain based on the variation of anions of imidazolium-based ionic liquids, J. Mol. Liq. 246 (2017) 178–186.

[313] E. Pinho Melo, M.R. Aires-Barros, S.M.B. Costa, J.M.S. Cabral, Thermal unfolding of proteins at high pH range studied by UV absorbance, J. Biochem. Biophys. Methods. 34 (1997) 45–59.

[314] S.M.T. Shaikh, J. Seetharamappa, S. Ashoka, P.B. Kandagal, A study of the interaction between bromopyrogallol red and bovine serum albumin by spectroscopic methods, Dye. Pigment. 73 (2007) 211–216.

[315] A.N. Glazer, E.L. Smith, Studies on the ultraviolet difference spectra of proteins and polypeptides., J. Biol. Chem. 236 (1961) 2942–2947.

[316] H. Mach, G. Sanyal, D.B. Volkin, C. Russell Middaugh, Applications of Ultraviolet Absorption Spectroscopy to the Analysis of Biopharmaceuticals, ACS Symp. Ser. 675 (1997) 186–205.

[317] G. Marsche, S. Frank, J.G. Raynes, K.F. Kozarsky, W. Sattler, E. Malle, The lipidation status of acute-phase protein serum amyloid A determines cholesterol mobilization via scavenger receptor class B, type I, Biochem. J. 402 (2007) 117–124.

[318] M. Sauer, J. Hofkens J. Enderlein, Basic Principles of Fluorescence Spectroscopy, in: Handb. Fluoresc. Spectrosc. Imaging, Wiley-VCH Verlag GmbH & Co. KGaA, Weinheim, Germany, 2011: pp. 1–30.

[319] P.G.D. J., Quasielastic Light Scattering, Anal. Chem. 62 (1990) 1049–1057A.

[320] N.C. Santos, M.A.R.B. Castanho, Teaching light scattering spectroscopy: The dimension and shape of tobacco mosaic virus, Biophys. J. 71 (1996) 1641–1650.

[321] D. Lochmann, J. Weyermann, C. Georgens, R. Prassl, A. Zimmer, Albumin-protamine-oligonucleotide nanoparticles as a new antisense delivery system. Part 1: Physicochemical characterization, Eur. J. Pharm. Biopharm. 59 (2005) 419–429.

[322] A. Kumar, P. Venkatesu, A comparative study of myoglobin stability in the presence of Hofmeister anions of ionic liquids and ionic salts, Process Biochem. 49 (2014) 2158–2169.

[323] M. Rousselot, E. Jaenicke, T. Lamkemeyer, J.R. Harris, R. Pirow, Native and subunit molecular mass and quarternary structure of the hemoglobin from the primitive branchiopod crustacean Triops cancriformis, FEBS J. 273 (2006) 4055–4071.

[324] M. Boström, D.F. Parsons, A. Salis, B.W. Ninham, M. Monduzzi, Possible origin of the inverse and direct hofmeister series for lysozyme at low and high salt concentrations, Langmuir. 27 (2011) 9504–9511.

[325] A. Arroyo-Reyna, A. Hernandez-Arana, R. Arreguin-Espinosa, Circular dichroism of stem bromelain: a third spectral class within the family of cysteine proteinases., Biochem. J. 300 (Pt 1 (1994) 107–110.

[326] A. Rani, P. Venkatesu, A Distinct Proof on Interplay between Trehalose and Guanidinium Chloride for the Stability of Stem Bromelain, J. Phys. Chem. B. 120 (2016) 8863–8872.

[327] J. Wu, J.T. Yang, C.S.C. Wu, β-II conformation of all-β proteins can be distinguished from unordered form by circular dichroism, Anal. Biochem. 200 (1992) 359–364.

[328] A. Kumar, P. Venkatesu, Does the stability of proteins in ionic liquids obey the Hofmeister series?, Int. J. Biol. Macromol. 63 (2014) 244–253.

[329] H. Zhao, S. Campbell, J. Solomon, Z.Y. Song, O. Olubajo, Improving the enzyme catalytic efficiency using ionic liquids with kosmotropic anions, Chinese J. Chem. 24 (2006) 580–584.

[330] C. Schröder, Proteins in Ionic Liquids: Current Status of Experiments and Simulations, Top. Curr. Chem. 375 (2017) 1–26.

[331] L. Xue, Y. Zhao, L. Yu, Y. Sun, K. Yan, Y. Li, X. Huang, Y. Qu, Choline acetate enhanced the catalytic performance of Candida rogusa lipase in AOT reverse micelles,

Colloids Surfaces B Biointerfaces. 105 (2013) 81–86.

[332] A. Kumar, A. Rani, P. Venkatesu, A comparative study of the effects of the Hofmeister series anions of the ionic salts and ionic liquids on the stability of α-chymotrypsin, New J. Chem. 39 (2015) 938–952.

[333] E.C. Wijaya, F. Separovic, C.J. Drummond, T.L. Greaves, Stability and activity of lysozyme in stoichiometric and non-stoichiometric protic ionic liquid (PIL)-water systems, J. Chem. Phys. 148 (2018) 193838.

[334] H. Zhao, Effect of ions and other compatible solutes on enzyme activity, and its implication for biocatalysis using ionic liquids, J. Mol. Catal. B Enzym. 37 (2005) 16–25.

[335] A.F.M. Cláudio, L. Swift, J.P. Hallett, T. Welton, J.A.P. Coutinho, M.G. Freire, Extended scale for the hydrogen-bond basicity of ionic liquids, Phys. Chem. Chem. Phys. 16 (2014) 6593–6601.

[336] C. Herrera, G. García, M. Atilhan, S. Aparicio, A molecular dynamics study on aminoacid-based ionic liquids, J. Mol. Liq. 213 (2016) 201–212.

[337] M.B. Turner, S.K. Spear, J.G. Huddleston, J.D. Holbrey, R.D. Rogers, Ionic liquid salt-induced inactivation and unfolding of cellulase from Trichoderma reesei, Green Chem. 5 (2003) 443–447.

[338] P.K. Kumar, V. Govinda, K. Sreenuvasulu, P. Venkatesu, I. Bahadur, E.E. Ebenso, A study of the molecular interactions between ammonium-based ionic liquids and N , N -dimethylacetamide, J. Mol. Liq. 223 (2016) 687–698.

[339] R. Sadeghi, H. Shekaari, R. Hosseini, Effect of alkyl chain length and temperature on the thermodynamic properties of ionic liquids 1-alkyl-3-methylimidazolium bromide

in aqueous and non-aqueous solutions at different temperatures, J. Chem. Thermodyn. 41 (2009) 273–289.

[340] B. González, A. Domínguez, J. Tojo, Dynamic viscosities, densities, and speed of sound and derived properties of the binary systems acetic acid with water, methanol, ethanol, ethyl acetate and methyl acetate at T = (293.15, 298.15, and 303.15) K at atmospheric pressure, J. Chem. Eng. Data. 49 (2004) 1590–1596.

[341] H. Shekaari, S.S. Mousavi, Y. Mansoori, Thermophysical properties of ionic liquid, 1-pentyl-3-methylimidazolium chloride in water at different temperatures, Int. J. Thermophys. 30 (2009) 499–514.

APPENDIX I

List of Publications

[1] **P. Kiran Kumar,** V. Govinda, K.Sreenuvasulu, P. Venkatesu, I. Bahadur, E. E. Ebenso, "A study of the molecular interactions between ammonium-based ionic liquids and N,N-dimethylacetamide" **Journal of Molecular Liquids, 223 (2016) 687–698.**

[2] **P. Kiran Kumar,** A. Rani, L. Olasunkanmi, P. Venkatesu, I. Bahadur, E. E. Ebenso, "Probing Molecular Interactions between Ammonium-Based Ionic Liquids and N,N-Dimethylacetamide: A Combined FTIR, DLS, and DFT Study" **J. Phys. Chem. B, 120 (2016) 12584−12595.**

[3] **P. Kiran Kumar,** I. Jha , P. Venkatesu, I. Bahadur, E. E. Ebenso, "A comparative study of the stability of Stem bromelain based on the variation of anions of imidazolium-based ionic liquids". **Journal of Molecular Liquids, 246 (2017) 178–186.**

[4] **P. Kiran Kumar,** M. Bisth, P. Venkatesu, I. Bahadur, E. E. Ebenso, " Exploring the effect of choline based ionic liquids on the conformation stability and activity of Stem Bromelain" **J. Phys. Chem. B, 122 (2016) 110435−10444.**

[5] **P. Kiran Kumar,** I. Jha , P. Venkatesu, I. Bahadur, E. E. Ebenso, " Investigation of the biomolecular interaction between stem bromelain and imidazolium-based ionic liquids using spectroscopic techniques" **International Journal of Biological Macromolecules (under review).**

[6] **P. Kiran Kumar,** I. Bahadur, E. E. Ebenso, P. Venkatesu, " Influence of temperature on apparent molar volume, and adiabatic compressibility of pyrrolidinium-based ionic

liquid with water or alcohols" **The Journal of Chemical Thermodynamics (under review).**

Conference presentations

Oral Presentation

[1] **P. Kiran Kumar,** I. Bahadur and E. E. Ebenso, The influence of concentration and anion effect of imidazolium-based ionic liquids on the structure and stability of stem bromelain in **6th annual NWU postdoctoral conference,** August 07, 2018, at Sports Village, Potchefstroom, North-West University, South Africa.

Poster presentation

[1] **P. Kiran Kumar,** I. Jha, I. Bahadur, P. Venkatesu and E. E. Ebenso, The role of concentration and anion effect of imidazolium-based Ionic Liquids on the structure and stability of stem bromelain in **6th National Conference On Chemical & Environmental Sciences,** March 18, 2017 at Arya P.G. College, Panipat, Haryana, India.

[2] P. Kiran Kumar. I participated in **the 10th national Conference on Thermodynamics of Pharmaceutical, Chemical and Biological Systems,** November 20 to 21, 2015, at University Institute of Pharmaceutical Sciences & Department of Chemistry, Panjab University, Chandigarh, India.

[3] P. Kiran Kumar. I participated in **the 10th Mid-year chemical research society of india (CRSI) Symposium in chemistry,** July 23 to 25, 2015 at National Institute of Technology, Trichy, Tamil Nadu, India.

APPENDIX II

SUPLEMENTARY FIGURES AND TABLES FOR 4.1

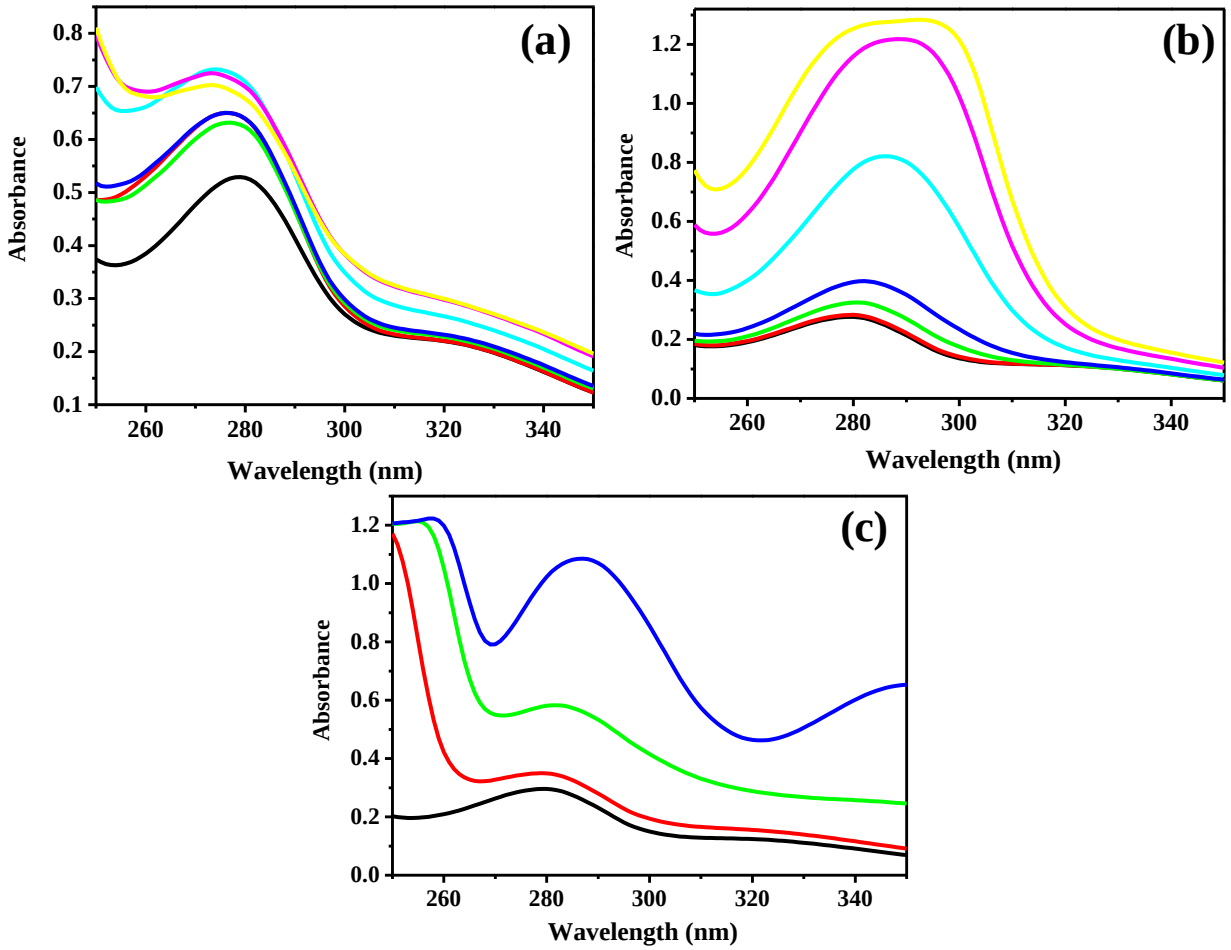

Figure 4.1A: UV–vis spectra analysis of BM in buffer (black) and in (a) [Bmim][Cl] with red (0.01M), green (0.05M), blue (0.10 M), cyan (0.50 M), magenta (1.0M), yellow (1.5 M) at 25 °C (b) [Bmim][Br] with red (0.01 M), green (0.05 M), blue (0.10 M), cyan (0.50 M), magenta (1.0 M), yellow (1.5 M) and (c) [Bmim][I] with red (0.01 M), green (0.05 M), blue (0.10 M), cyan (0.50 M), magenta (1.0 M), yellow (1.5 M) at 25 °C at 25 °C.

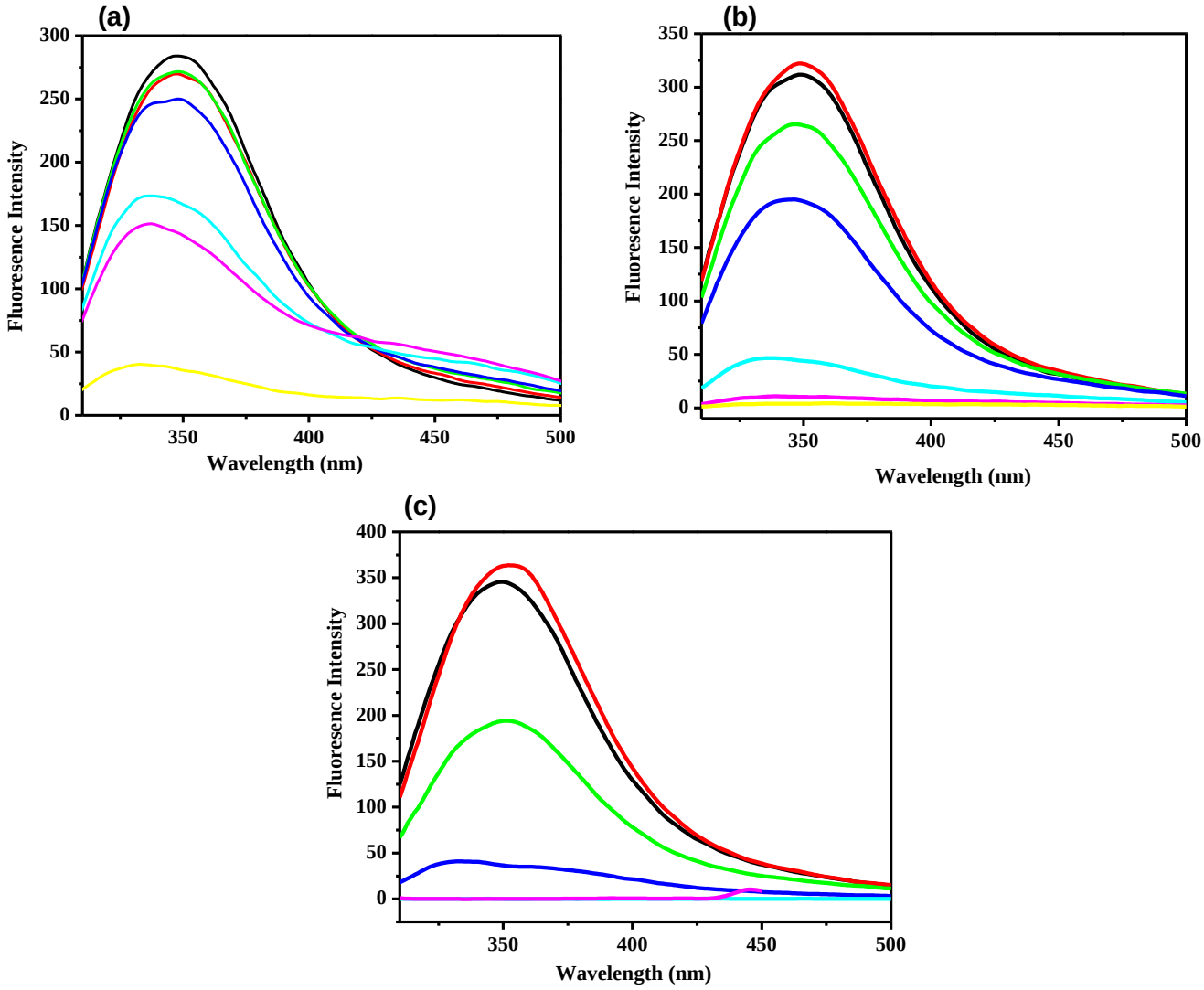

Figure 4.2A: Fluorescence spectra analysis of BM in buffer (black) and in (a) [Bmim][Cl]with red (0.01 M), green (0.05 M), blue (0.10M), cyan (0.50M),magenta (1.0 M), yellow(1.5 M) at 25 °C (b) [Bmim][Br]with red (0.01M), green (0.05M), blue (0.10 M), cyan (0.50 M),magenta (1.0M), yellow(1.5 M) and (c) [Bmim][I] with red (0.01 M), green (0.05 M), blue (0.10M), cyan (0.50 M), magenta (1.0 M), yellow (1.5 M) at 25 °C at 25 °C.

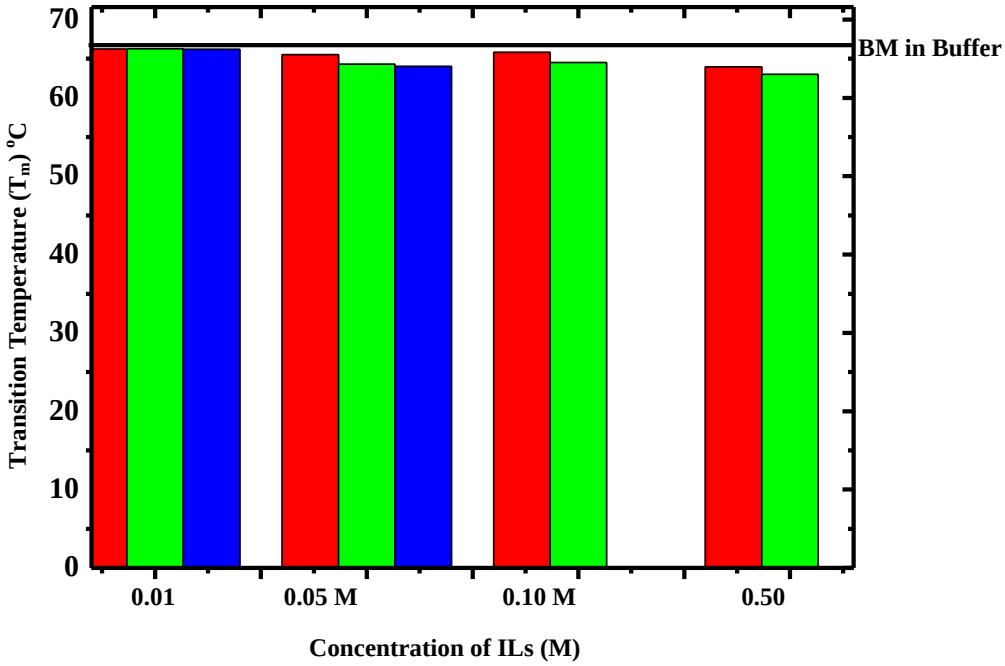

Figure 4.3A: The variation in Tm values of BM in buffer (black) with [Bmim][Cl] (red), [Bmim][Br] (green) and [Bmim][I] (blue) which is obtained from fluorescence analysis.

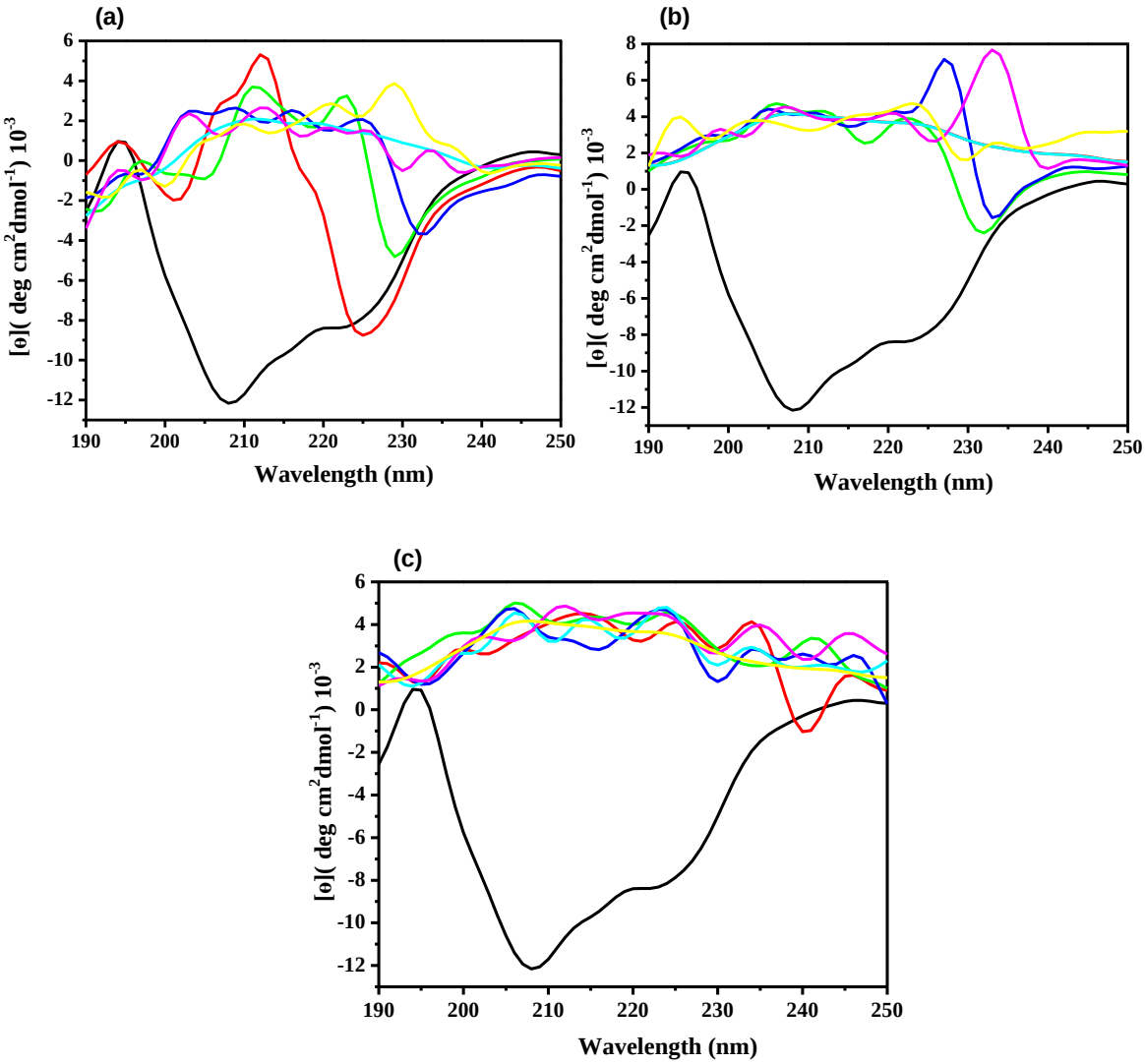

Figure 4.4A: Influence of [Bmim][Cl], [Bmim][Br] and [Bmim][I] on the structure of BM in buffer (black), from far-UV CD analysis with red (0.01 M), green (0.05 M), blue (0.10 M), cyan (0.50 M), magenta (1.0 M), yellow (1.5 M) at 25 °C.

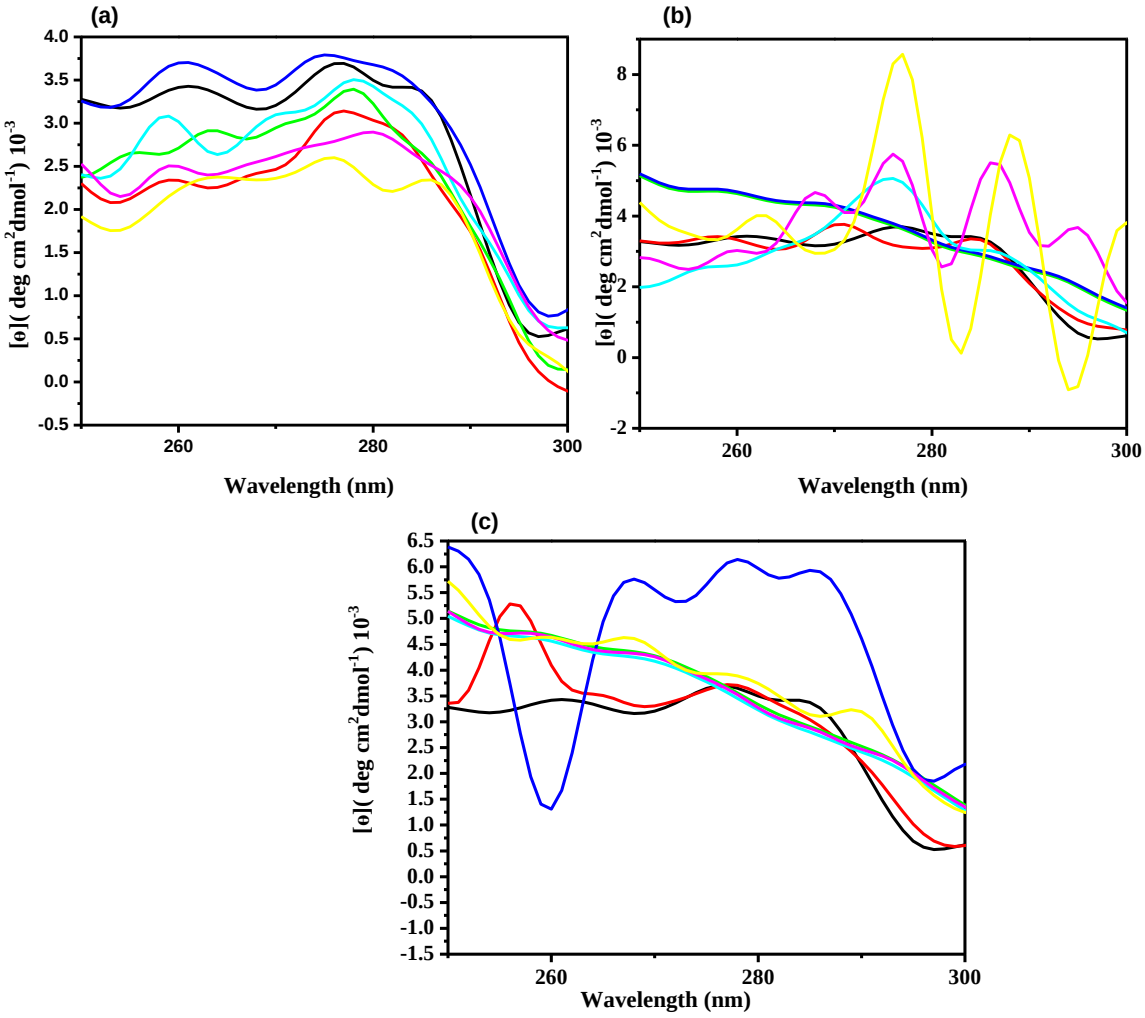

Figure 4.5A: Influence of [Bmim][Cl], [Bmim][Br] and [Bmim][I] on the structure of BM in buffer (black), from near-UV CD analysis with red (0.01M), green (0.05M), blue (0.10M), cyan (0.50M), magenta (1.0 M), yellow (1.5 M) at 25 °C.

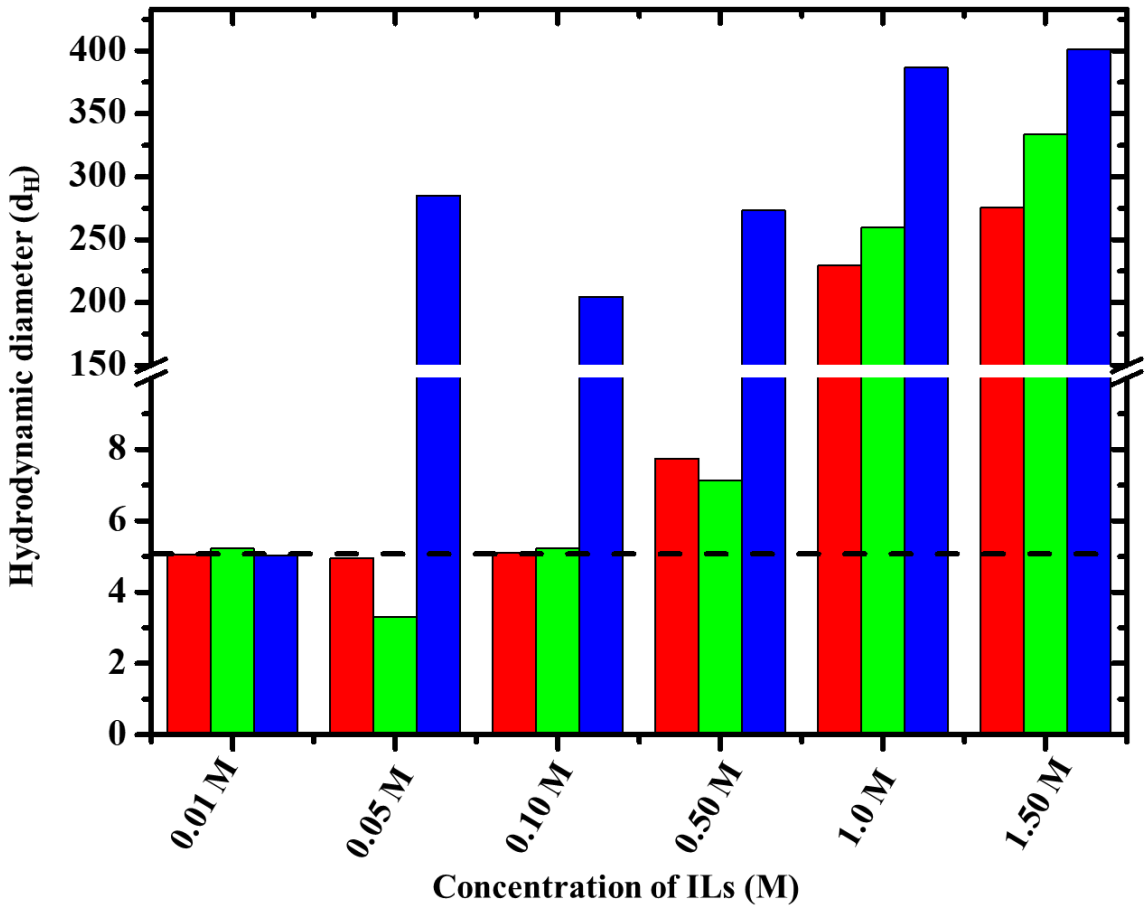

Figure 4.6A: Hydrodynamic diameter (dH) obtained from the intensity distribution graph for BM in buffer with [Bmim][Cl] (red), [Bmim][Br] (green) and [Bmim][I] (blue) at different concentrations.

Table 4.1A: Transition temperature (T_m) of the BM in different concentrations of ILs.

Concentration	[Bmim][Cl] (T_m)/ (^{0}C)	[Bmim][Br] (T_m)/ (^{0}C)	[Bmim][I] (T_m)/ (^{0}C)
Buffer	66.25	66.25	66.25
0.01 M	66.24	66.29	66.21
0.05 M	65.53	64.30	64.00
0.10 M	65.83	64.50	------*
0.50 M	63.97	63.00	------*
1.00 M	------*	------*	------*
1.50	------*	------*	------*

*The error value for T_m is $\pm$ 0.2 ^{0}C.

Table 4.2A: Hydrodynamic diameter (dH) of BM in different concentrations of ILs.

Concentration of ILs	[Bmim][Cl])/(nm)	[Bmim][Br])/(nm)	[Bmim][I])/ (nm)
0.0	5.14	5.14	5.14
0.01	5.05	5.23	5.04
0.05	4.954	3.31	285.08
0.10	5.09	5.23	204.65
0.50	7.75	7.12	273.23
1.0	229.3	259.56	386.46
1.5	275.5	333.53	401.1

APPENDIX III

SUPLEMENTARY FIGURES AND TABLES FOR 4.4

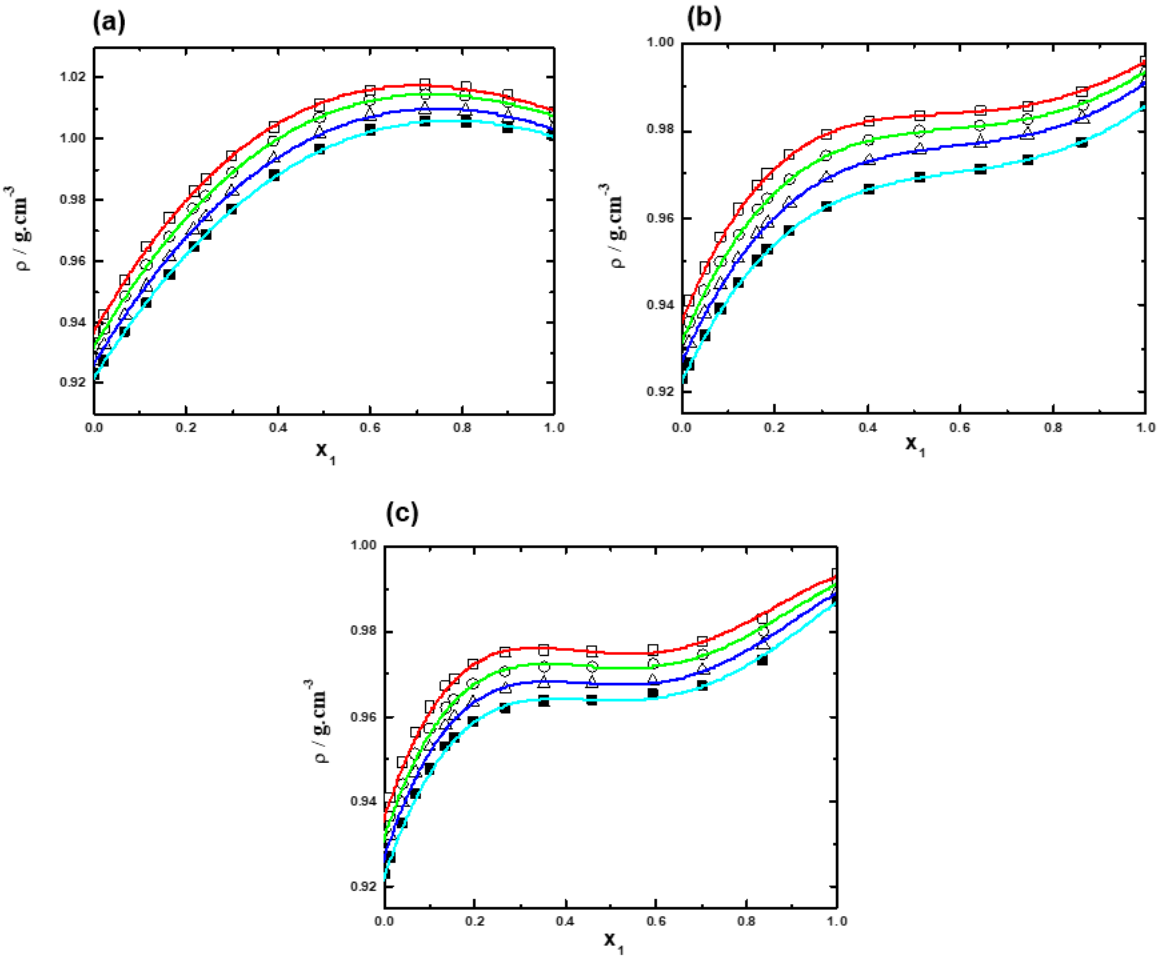

Figure 4.19A: Plots of densities (ρ) for the mixtures of ILs with DMA vs. mole fraction (x_1) of IL for (a) TEAH (b) TPAH or (c) TBAH + DMA (x_2) at different temperatures, 25 °C (□), 30 °C (○), 35 °C (△) and 40 °C (■).The solid lines represent the smoothness of the data.

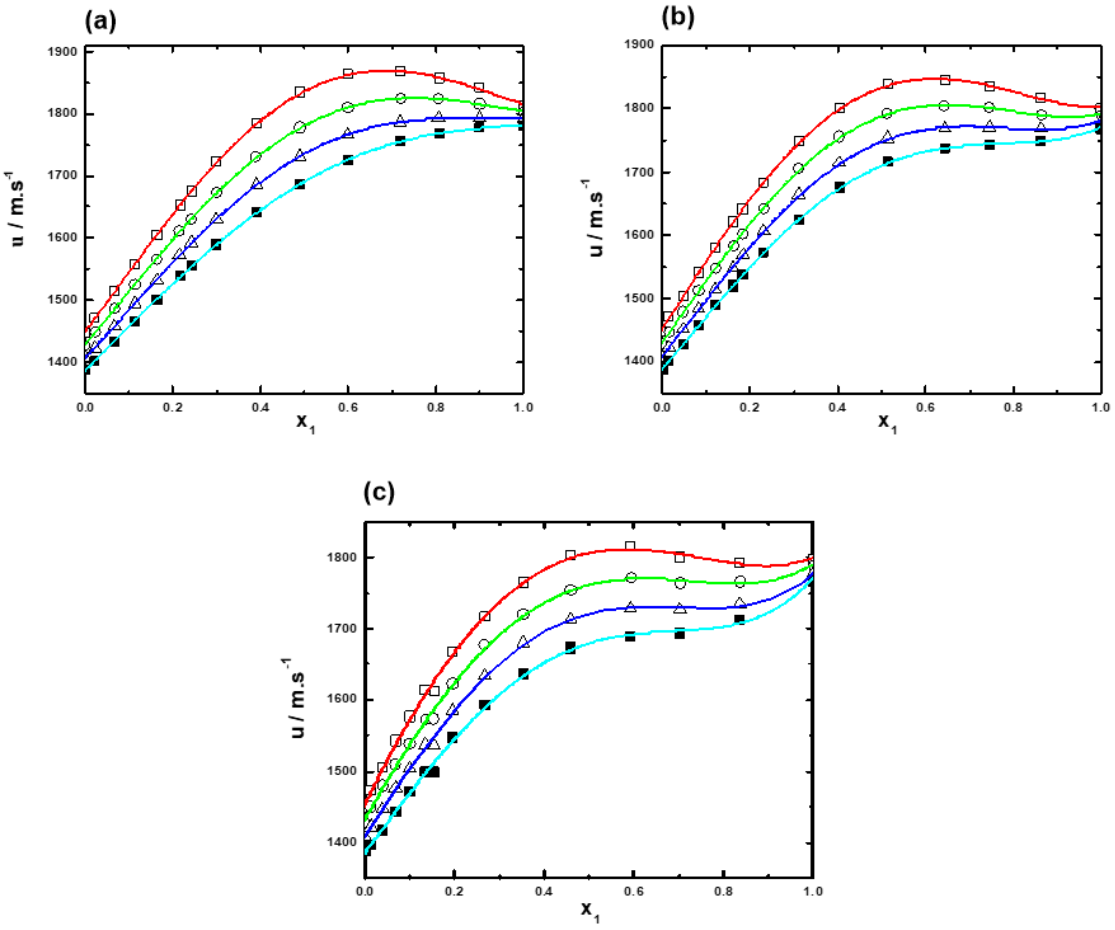

Figure 4.20A: Plots of ultrasonic sound velocities (u) for the mixtures of ILs with DMA vs. mole fraction (x_1) of IL for (a) TEAH (b) TPAH or (c) TBAH + DMA (x_2) at different temperatures, 25 °C (□), 30 °C (○), 35 °C (△) and 40 °C (■).The solid lines represent the smoothness of the data.

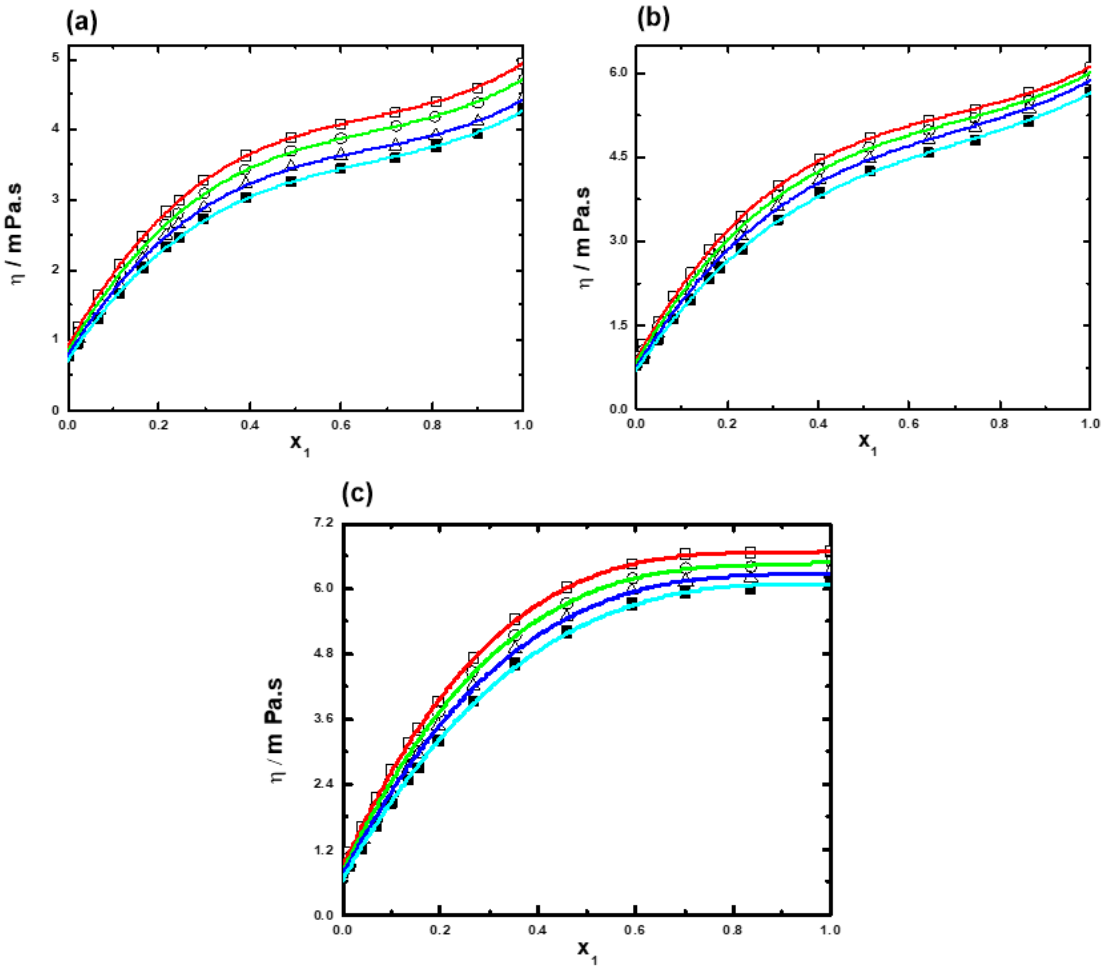

Figure 4.21A: Plots of viscosities (η) for the mixtures of ILs with DMA vs. mole fraction (x_1) of IL for (a) TEAH (b) TPAH or (c) TBAH + DMA (x_2) at different temperatures, 25 °C (□), 30 °C (○), 35 °C (△) and 40 °C (■).The solid lines represent the smoothness of the data.

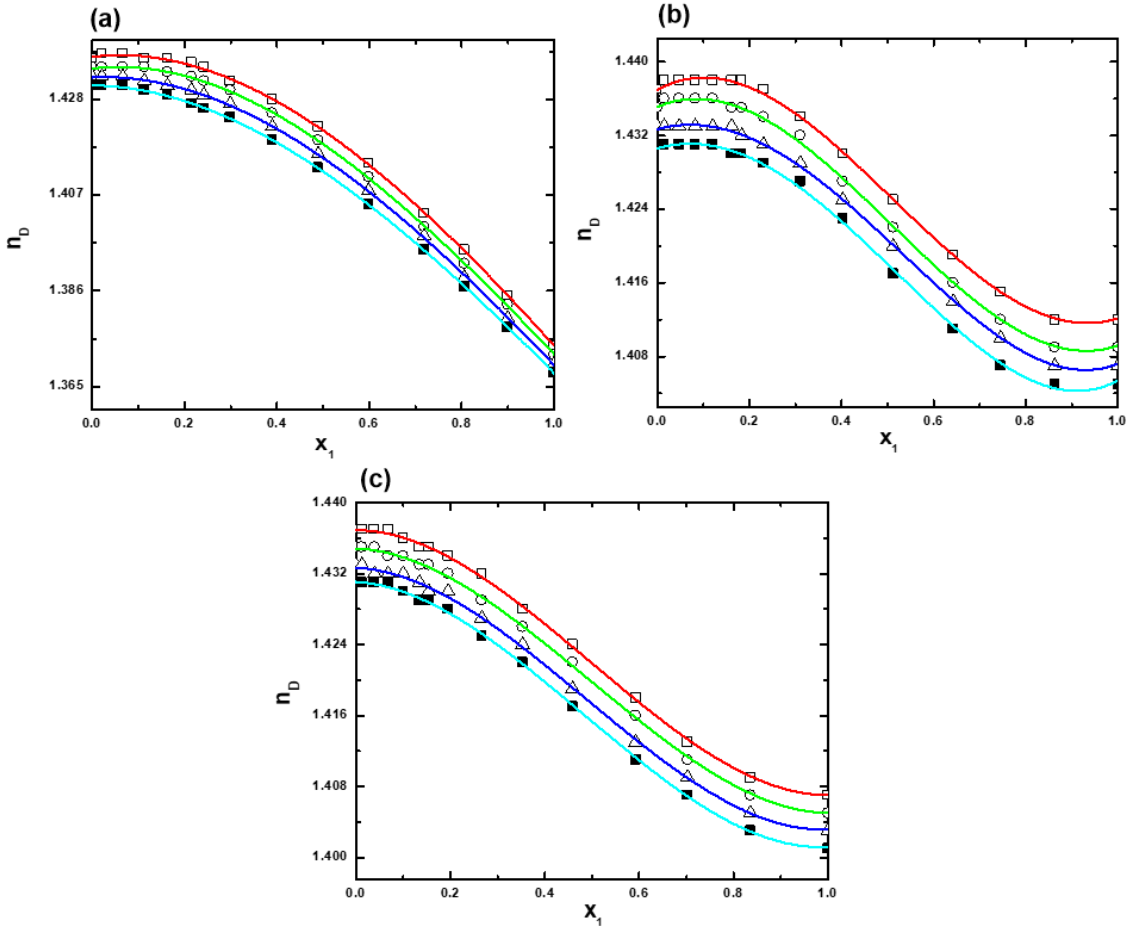

Figure 4.22A: Plots of refractive indices (n_D) for the mixtures of ILs with DMA vs. mole fraction (x_1) of IL for (a) TEAH (b) TPAH or (c) TBAH + DMA (x_2) at different temperatures, 25 °C (□), 30 °C (○), 35 °C (△) and 40 °C (■).The solid lines represent the smoothness of the data.

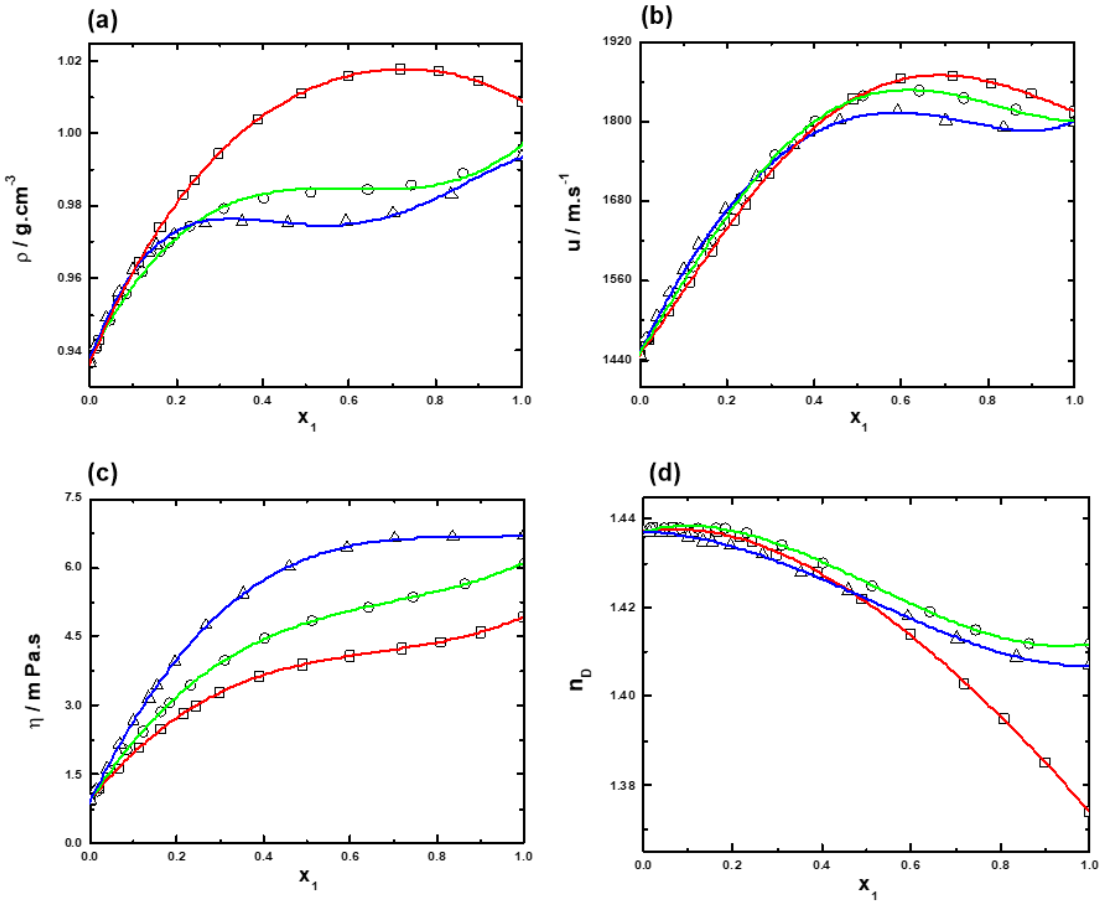

Figure 4.23A: Plots of (a) densities (ρ) (b) ultrasonic sound velocities (u) (c) viscosities (η) (d) refractive indices (n_D) for the mixtures of ILs + DMA as function of the mole fraction (x_1) of IL; (□) TEAH; (○) TPAH and (Δ) TBAH at 25 °C. The solid lines represent the smoothness of the data.

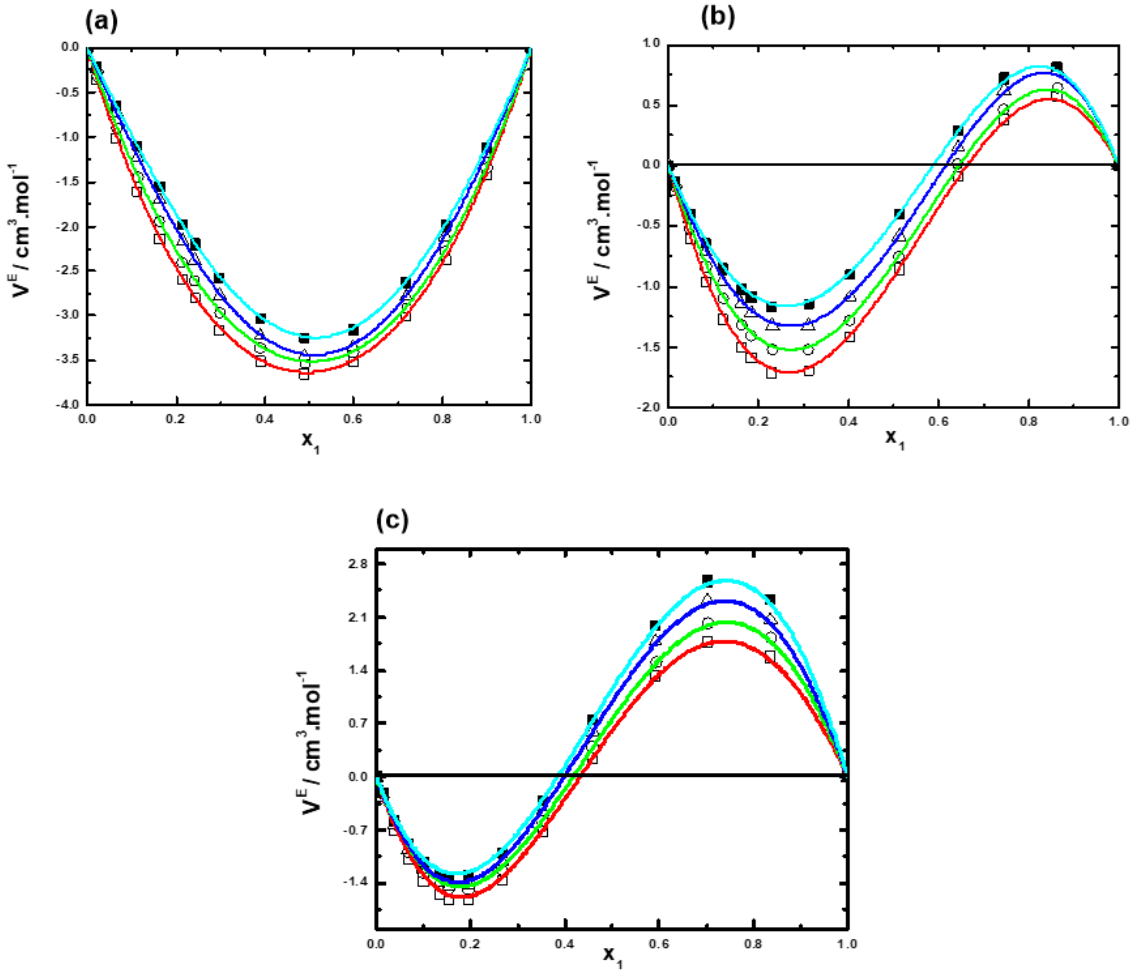

Figure 4.24A: Plots of excess molar volumes (V^E) for the mixtures of ILs with DMA vs. mole fraction (x_1) of IL for (a) TEAH (b) TPAH or (c) TBAH + DMA (x_2) at different temperatures, 25 °C (□), 30 °C (○), 35 °C (△) and 40 °C (■).The solid (–) lines correlated by Redlich–Kister equation.

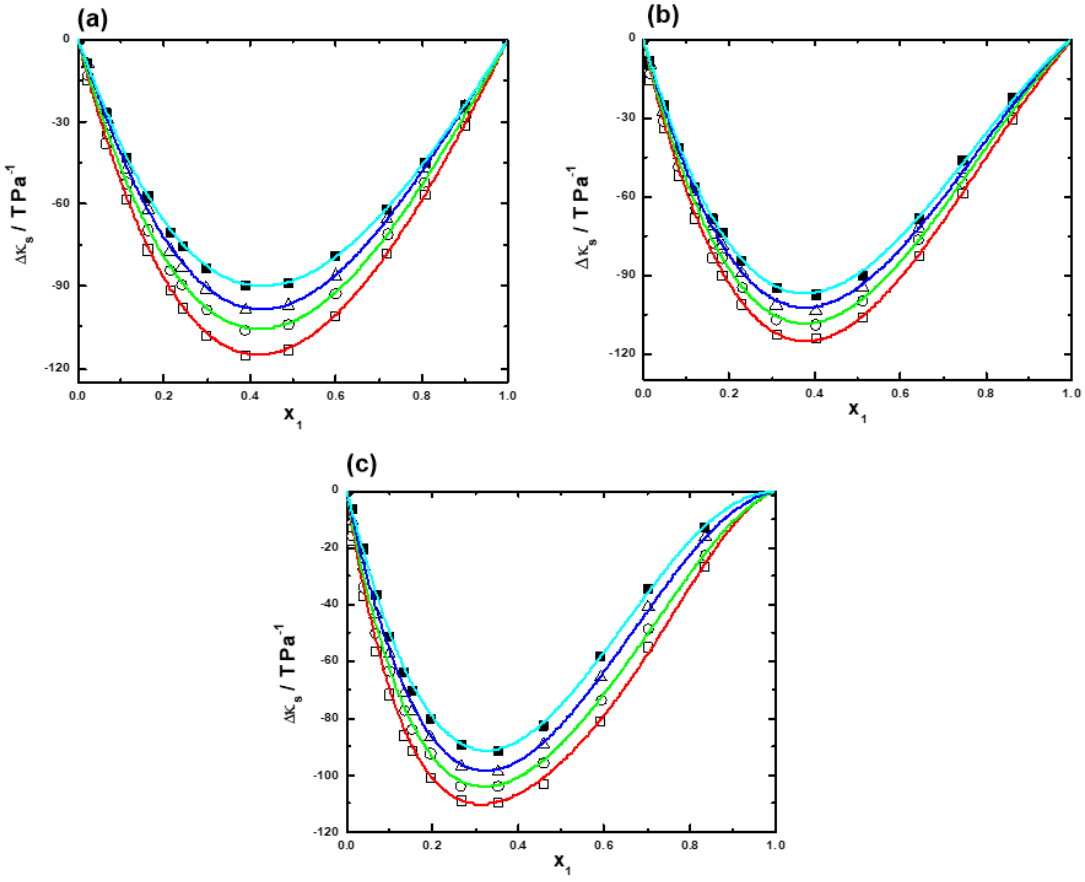

Figure 4.25A: Plots of deviation in isentropic compressibilities ($\Delta\kappa_s$) for the mixtures of ILs with DMA vs. mole fraction (x_1) of IL for (a) TEAH (b) TPAH or (c) TBAH + DMA (x_2) at different temperatures, 25 °C (□), 30 °C (○), 35 °C (△) and 40 °C (■). The solid (–) lines correlated by Redlich-Kister equation.

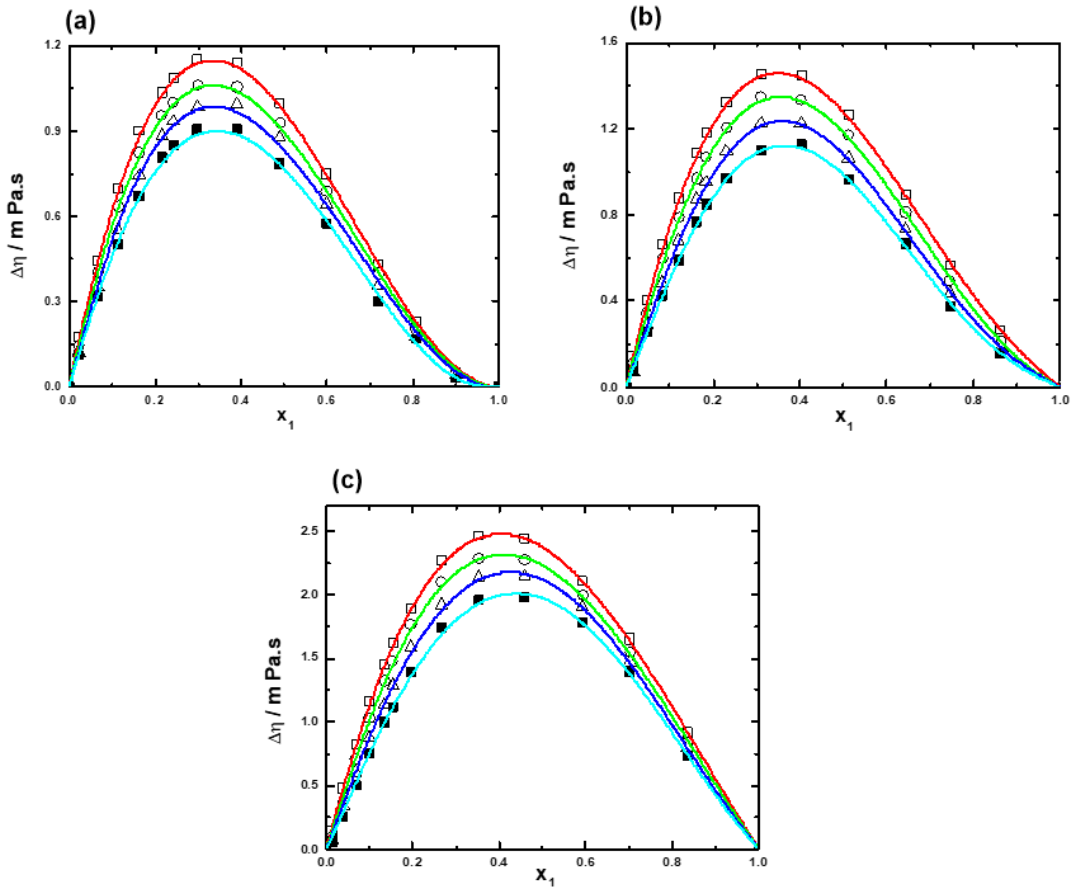

Figure 4.26A: Plots of deviation in viscosities ($\Delta\eta$) for the mixtures of ILs with DMA vs. mole fraction (x_1) of IL for (a) TEAH (b) TPAH or (c) TBAH + DMA (x_2) at different temperatures, 25 °C (□), 30 °C (○), 35 °C (△) and 40 °C (■).The solid (–) lines correlated by Redlich-Kister equation.

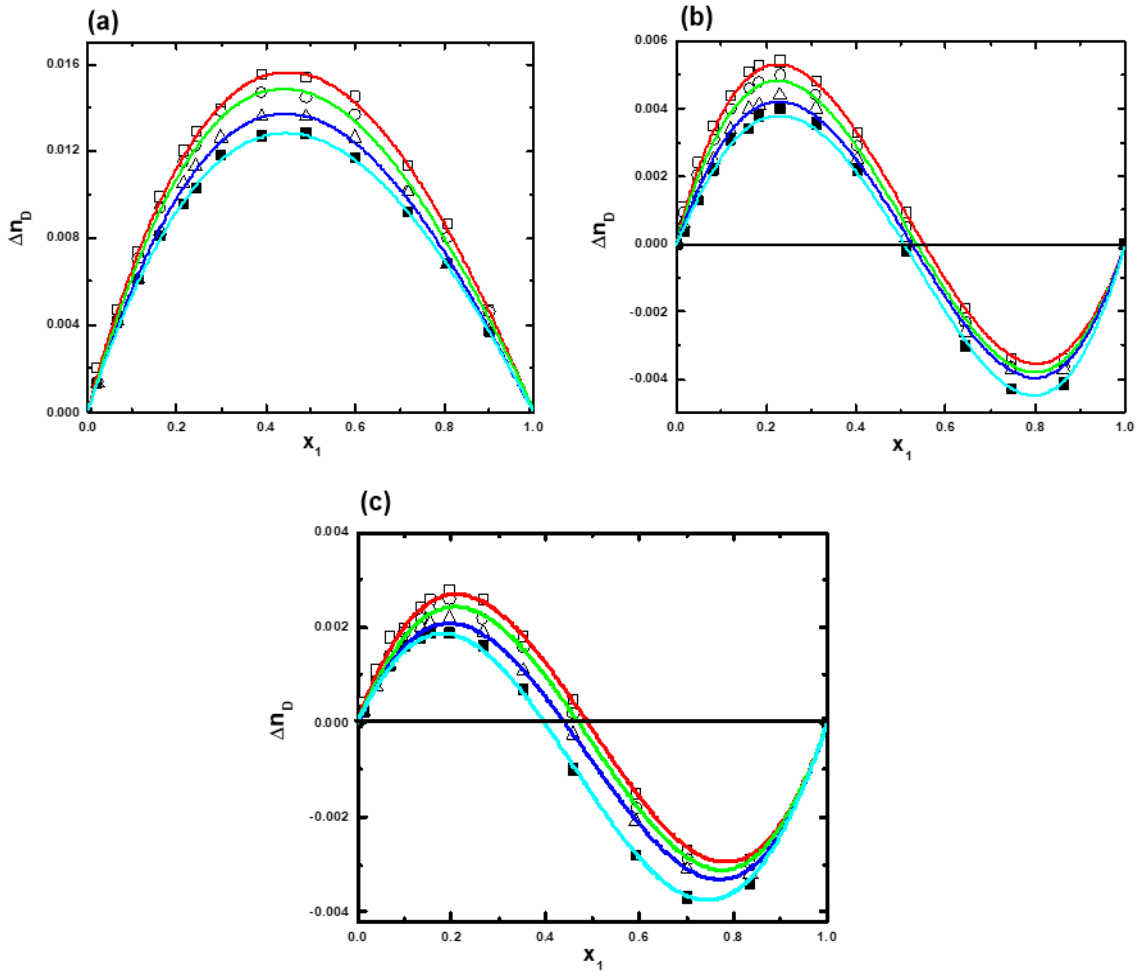

Figure 4.27A: Plots of deviation in refractive indices (Δn_D) for the mixtures of ILs with DMA vs. mole fraction (x_1) of IL for (a) TEAH (b) TPAH or (c) TBAH + DMA (x_2) at different temperatures, 25 °C (□), 30 °C (○), 35 °C (△) and 40 °C (■).The solid (–) lines correlated by Redlich–Kister equation.

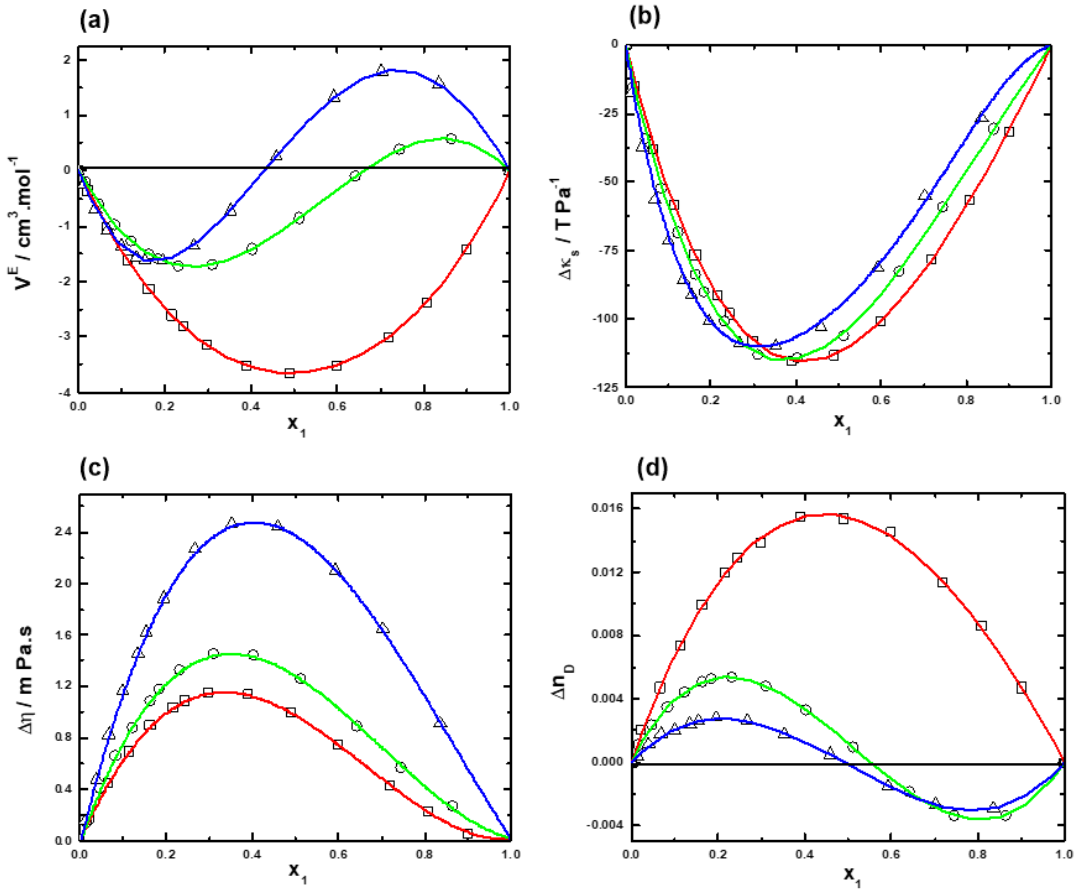

Figure 4.28A: Plots of (a) excess molar volumes (V^E) (b) deviations in isentropic compressibilities ($\Delta\kappa_s$) (c) deviations in viscosities ($\Delta\eta$) (d) deviations in refractive indices (Δn_D) for the mixtures of ILs + DMA as function of the mole fraction (x_1) of IL; (□) TEAH; (○) TPAH and (Δ) TBAH at 25 °C. The solid (–) lines correlated by Redlich-Kister equation.

Table 4.7A
Molecular mass (MW), solvent purity, density (ρ), speed of sound (u), viscosity (η) and refractive index (n_D) for ammonium-based ILs and DMA at T = 30 °C.

		ρ (g·cm^{-3})		u (m·s^{-1})		η (mPa·s)		n_D	
Solvent	MW (g.mol^{-1})	Expt.	Lit.	Expt.	Lit.	Expt.	Lit.	Expt.	Lit.
TEAH	147.26	1.00731	1.00731[a,b]	1803	1803[a,b]	4.72	4.72[a,b]	1.372	1.372[a]
TPAH	203.25	0.99360	0.99360[a,b]	1790	1790[a,b]	6.01	6.01[a,b]	1.409	1.409[a]
TBAH	259.34	0.99170	0.99170[a,b]	1788	1788[a,b]	6.49	6.49[a,b]	1.405	1.405[a]
DMA	87.12	0.93224	0.93240[c]	1428	---	0.88	0.882[d]	1.435	----
			0.93168[d]				0.862[e]		
			0.93169[e]						

[a] Reference [245]
[b] Reference [243]
[c] Reference [247]
[d] Reference [248]
[e] Reference [246]

Table 4.8A: Mole fraction (x_1) of ILs, Density (ρ), Ultrasonic Sound Velocity (u), Viscosity (η), Refractive Index (n_D), Excess Molar Volumes (V^E), Isentropic Compressibility(κ_s), Deviation in Isentropic Compressibility ($\Delta\kappa_s$), Deviation in Viscosity ($\Delta\eta$) and Deviation in Refractive Index (Δn_D) for TEAH, TPAH and TBAH with DMA system at different temperatures.

x_1	ρ (g.cm^{-3})	u (m.s^{1})	η (mPa.s)	n_D	V^E (cm^3.mol^{-1})	κ_s (TPa^{-1})	$\Delta\kappa_s$ (TPa^{-1})	$\Delta\eta$ (*mPa*.s)	Δn_D
				(TEAH + DMA)					
T = 25 °C									
0.0000	0.93683	1448	0.93	1.437	0.000	509	0.0	0.000	0.0000
0.0216	0.94283	1472	1.19	1.438	-0.358	490	-15.1	0.174	0.0020
0.0663	0.95407	1514	1.64	1.438	-1.014	457	-38.1	0.444	0.0047
0.1133	0.96456	1558	2.08	1.437	-1.612	427	-58.4	0.696	0.0074
0.1628	0.97422	1605	2.49	1.437	-2.144	399	-76.8	0.901	0.0099
0.2150	0.98300	1652	2.83	1.436	-2.605	373	-91.6	1.037	0.0120
0.2422	0.98707	1676	2.99	1.435	-2.808	361	-98.1	1.088	0.0129
0.2988	0.99454	1722	3.28	1.432	-3.158	339	-108	1.152	0.0139
0.3899	1.00392	1785	3.63	1.428	-3.514	313	-113	1.141	0.0155

0.4894	1.01112	1834	3.89	1.422	-3.652	294	-113	0.999	0.0154
0.5986	1.01588	1863	4.08	1.414	-3.513	284	-101	0.750	0.0145
0.7188	1.01782	1868	4.24	1.403	-3.009	282	-78.1	0.428	0.0113
0.8060	1.01707	1858	4.39	1.395	-2.379	285	-56.8	0.228	0.0086
0.8995	1.01426	1842	4.59	1.385	-1.419	291	-31.6	0.053	0.0047
1.0000	1.00881	1814	4.94	1.374	0.000	301	0.0	0.000	0.0000

T = 30 °C

0.0000	0.93224	1428	0.88	1.435	0.000	526	0	0	0.0000
0.0216	0.93783	1449	1.11	1.435	-0.311	508	-13.2	0.147	0.0014
0.0663	0.94851	1487	1.54	1.435	-0.896	477	-34.5	0.405	0.0042
0.1133	0.95869	1525	1.95	1.435	-1.446	449	-52.5	0.635	0.0071
0.1628	0.96825	1567	2.33	1.434	-1.950	421	-69.5	0.825	0.0094
0.2150	0.97715	1611	2.66	1.433	-2.401	394	-84.2	0.955	0.0115
0.2422	0.98133	1631	2.81	1.432	-2.605	383	-89.4	1.000	0.0122
0.2988	0.98910	1673	3.09	1.430	-2.963	361	-98.8	1.063	0.0138
0.3899	0.99920	1731	3.43	1.425	-3.358	334	-106	1.055	0.0147
0.4894	1.00707	1778	3.69	1.419	-3.529	314	-104	0.930	0.0146
0.5986	1.01247	1810	3.87	1.411	-3.418	302	-92.6	0.691	0.0137
0.7188	1.01480	1824	4.04	1.400	-2.913	296	-71.2	0.399	0.0102
0.8060	1.01436	1825	4.18	1.392	-2.287	296	-52.1	0.205	0.0080
0.8995	1.01197	1816	4.38	1.383	-1.346	300	-28.0	0.046	0.0046
1.0000	1.00731	1803	4.72	1.372	0.000	305	0.0	0.000	0.0000

T = 35 °C

0.0000	0.92761	1408	0.83	1.433	0.000	544	0.0	0.000	0.0000
0.0216	0.93249	1423	1.03	1.433	-0.239	530	-9.1	0.122	0.0013
0.0663	0.94225	1458	1.42	1.433	-0.728	499	-29.0	0.351	0.0042
0.1133	0.95190	1495	1.79	1.432	-1.221	470	-47.3	0.552	0.0061
0.1628	0.96130	1532	2.16	1.431	-1.702	443	-62.5	0.744	0.0083
0.2150	0.97033	1573	2.49	1.430	-2.161	417	-77.1	0.886	0.0105
0.2422	0.97468	1593	2.64	1.429	-2.379	404	-82.9	0.935	0.0113
0.2988	0.98288	1630	2.89	1.427	-2.775	383	-91.1	0.985	0.0126
0.3899	0.99367	1686	3.23	1.422	-3.232	354	-98.7	0.996	0.0136
0.4894	1.00211	1732	3.47	1.416	-3.452	333	-96.9	0.878	0.0136
0.5986	1.00768	1767	3.63	1.408	-3.343	318	-86.1	0.645	0.0126
0.7188	1.00978	1787	3.77	1.398	-2.785	310	-65.8	0.355	0.0101
0.8060	1.00920	1793	3.91	1.389	-2.119	308	-47.1	0.178	0.0068
0.8995	1.00710	1793	4.11	1.380	-1.192	309	-24.9	0.042	0.0037
1.0000	1.00369	1792	4.43	1.370	0.000	310	0.0	0.000	0.0000

T = 40 °C

0.0000	0.92298	1388	0.77	1.431	0.000	562	0.0	0.000	0.0000
0.0216	0.92764	1402	0.96	1.431	-0.211	548	-8.6	0.114	0.0013
0.0663	0.93701	1434	1.32	1.431	-0.650	519	-27.0	0.318	0.0041
0.1133	0.94638	1467	1.67	1.430	-1.101	491	-43.3	0.503	0.0061
0.1628	0.95563	1501	2.01	1.429	-1.554	464	-57.6	0.670	0.0081
0.2150	0.96458	1538	2.33	1.427	-1.989	438	-70.8	0.807	0.0096
0.2422	0.96893	1555	2.47	1.426	-2.199	427	-75.5	0.852	0.0103
0.2988	0.97716	1590	2.72	1.424	-2.581	405	-83.6	0.904	0.0118
0.3899	0.98812	1641	3.04	1.419	-3.027	376	-90.0	0.905	0.0127
0.4894	0.99647	1687	3.27	1.413	-3.251	353	-88.6	0.787	0.0128
0.5986	1.00292	1725	3.44	1.405	-3.155	335	-79.1	0.574	0.0117
0.7188	1.00561	1756	3.59	1.395	-2.626	323	-61.9	0.304	0.0092
0.8060	1.00554	1769	3.76	1.387	-1.993	318	-45.1	0.169	0.0068
0.8995	1.00401	1777	3.95	1.378	-1.112	315	-24.2	0.032	0.0037
1.0000	1.00138	1781	4.27	1.368	0.000	315	0.0	0.000	0.0000

(TPAH + DMA)

T = 25 °C

0.0000	0.93683	1448	0.93	1.437	0.000	509	0.0	0.000	0.0000
0.0153	0.94089	1472	1.15	1.438	-0.212	491	-15.5	0.141	0.0011
0.0476	0.94855	1505	1.58	1.438	-0.609	465	-34.2	0.404	0.0024
0.0826	0.95564	1541	2.02	1.438	-0.968	441	-52.0	0.662	0.0035
0.1205	0.96197	1580	2.43	1.438	-1.269	416	-68.5	0.877	0.0044
0.1617	0.96754	1621	2.85	1.438	-1.505	393	-83.5	1.084	0.0051
0.1837	0.97003	1642	3.06	1.438	-1.596	382	-90.0	1.180	0.0053
0.2308	0.97437	1684	3.45	1.437	-1.712	362	-101	1.327	0.0054
0.3104	0.97924	1749	3.99	1.434	-1.696	334	-113	1.455	0.0048
0.4030	0.98221	1800	4.46	1.430	-1.415	314	-113	1.446	0.0033
0.5122	0.98368	1839	4.84	1.425	-0.856	301	-106	1.262	0.0009
0.6429	0.98458	1846	5.15	1.419	-0.096	298	-82.7	0.896	-0.0019
0.7453	0.98585	1835	5.35	1.415	0.380	301	-59.0	0.568	-0.0034
0.8630	0.98895	1817	5.66	1.412	0.573	306	-30.6	0.268	-0.0034
1.0000	0.99594	1801	6.10	1.412	0.000	310	0.0	0.000	0.0000

T = 30 °C

0.0000	0.93224	1428	0.88	1.435	0.000	526	0.0	0.000	0.0000
0.0153	0.93601	1448	1.07	1.436	-0.178	510	-13.4	0.112	0.0009

0.0476	0.94327	1479	1.47	1.436	-0.521	485	-31.2	0.346	0.0020
0.0826	0.95008	1513	1.90	1.436	-0.835	460	-48.5	0.596	0.0031
0.1205	0.95627	1549	2.29	1.436	-1.103	436	-64.5	0.791	0.0040
0.1617	0.96187	1584	2.68	1.435	-1.321	414	-77.6	0.970	0.0046
0.1837	0.96440	1603	2.89	1.435	-1.405	404	-83.4	1.068	0.0048
0.2308	0.96892	1643	3.27	1.434	-1.518	382	-94.6	1.207	0.0050
0.3104	0.97427	1706	3.82	1.432	-1.519	353	-107	1.348	0.0044
0.4030	0.97785	1756	4.28	1.427	-1.273	332	-109	1.333	0.0029
0.5122	0.97992	1792	4.68	1.422	-0.754	318	-99.6	1.172	0.0005
0.6429	0.98110	1804	4.99	1.416	0.015	313	-76.5	0.813	-0.0023
0.7453	0.98274	1802	5.20	1.412	0.463	313	-54.7	0.497	-0.0036
0.8630	0.98607	1790	5.52	1.409	0.648	317	-26.5	0.213	-0.0036
1.0000	0.99360	1790	6.01	1.409	0.000	314	0.0	0.000	0.0000

T = 35 °C

0.0000	0.92761	1408	0.83	1.433	0.000	544	0.0	0.000	0.0000
0.0153	0.93117	1423	0.98	1.433	-0.151	530	-10.0	0.073	0.0006
0.0476	0.93804	1452	1.36	1.433	-0.442	506	-27.4	0.289	0.0017
0.0826	0.94460	1484	1.73	1.433	-0.715	481	-44.5	0.482	0.0025
0.1205	0.95068	1515	2.12	1.433	-0.953	458	-58.4	0.680	0.0034
0.1617	0.95619	1549	2.52	1.433	-1.141	436	-71.5	0.873	0.0040
0.1837	0.95875	1569	2.71	1.432	-1.218	424	-78.8	0.952	0.0041
0.2308	0.96341	1606	3.09	1.431	-1.323	402	-89.4	1.094	0.0044
0.3104	0.96909	1664	3.62	1.429	-1.325	373	-101	1.223	0.0040
0.4030	0.97307	1715	4.09	1.425	-1.086	349	-103	1.224	0.0025
0.5122	0.97559	1753	4.48	1.42	-0.581	334	-94.8	1.063	0.0002
0.6429	0.97732	1768	4.81	1.414	0.155	327	-71.8	0.733	-0.0026
0.7453	0.97906	1770	5.03	1.41	0.625	326	-50.0	0.436	-0.0037
0.8630	0.98275	1769	5.37	1.407	0.784	325	-24.5	0.181	-0.0037
1.0000	0.99111	1779	5.88	1.407	0.000	319	0.0	0.000	0.0000

T = 40 °C

0.0000	0.92298	1388	0.77	1.431	0.000	562	0.0	0.000	0.0000
0.0153	0.92635	1401	0.92	1.431	-0.136	550	-8.7	0.075	0.0003
0.0476	0.93290	1428	1.26	1.431	-0.399	526	-25.4	0.257	0.0013
0.0826	0.93914	1458	1.60	1.431	-0.644	501	-41.7	0.426	0.0022
0.1205	0.94494	1490	1.95	1.431	-0.855	477	-56.9	0.591	0.0031
0.1617	0.95022	1520	2.33	1.43	-1.021	456	-68.4	0.769	0.0034
0.1837	0.95267	1537	2.52	1.43	-1.085	444	-74.2	0.851	0.0038
0.2308	0.95712	1572	2.87	1.429	-1.165	423	-84.6	0.971	0.0040
0.3104	0.96261	1625	3.39	1.427	-1.139	393	-95.0	1.102	0.0036

0.4030	0.96662	1675	3.87	1.423	-0.898	369	-97.6	1.129	0.0022
0.5122	0.96927	1716	4.24	1.417	-0.402	350	-90.0	0.965	-0.0002
0.6429	0.97134	1738	4.58	1.411	0.292	341	-68.4	0.666	-0.0030
0.7453	0.97333	1742	4.79	1.407	0.720	339	-46.3	0.375	-0.0043
0.8630	0.97732	1749	5.15	1.405	0.818	334	-22.3	0.159	-0.0041
1.0000	0.98576	1769	5.66	1.405	0.000	324	0.0	0.000	0.0000

(TBAH + DMA)

T = 25 °C

0.0000	0.93683	1448	0.93	1.437	0.000	509	0.0	0.000	0.0000
0.0124	0.94123	1474	1.15	1.437	-0.249	489	-17.7	0.149	0 .0004
0.0388	0.94924	1506	1.63	1.437	-0.695	464	-37.0	0.477	0.0011
0.0678	0.95629	1543	2.15	1.437	-1.074	439	-56.6	0.828	0.0018
0.0996	0.96230	1577	2.67	1.436	-1.370	418	-71.6	1.165	0.0020
0.1348	0.96716	1615	3.16	1.435	-1.562	396	-86.0	1.454	0.0024
0.1538	0.96918	1613	3.44	1.435	-1.615	397	-91.3	1.624	0.0026
0.1951	0.97236	1668	3.94	1.434	-1.623	370	-101	1.886	0.0028
0.2666	0.97511	1717	4.74	1.432	-1.358	348	-109	2.274	0.0026
0.3529	0.97578	1765	5.43	1.428	-0.721	329	-110	2.467	0.0018
0.4589	0.97535	1802	6.02	1.424	0.253	316	-103	2.447	0.0005
0.5925	0.97571	1816	6.45	1.418	1.324	311	-81.1	2.107	-0.0015
0.7026	0.97789	1801	6.63	1.413	1.784	315	-54.9	1.653	-0.0027
0.8358	0.98325	1791	6.66	1.409	1.571	317	-26.7	0.916	-0.0029
1.0000	0.99358	1798	6.69	1.407	0.000	311	0.0	0.000	0.0000

T = 30 °C

0.0000	0.93224	1428	0.88	1.435	0.000	526	0.0	0.000	0.0000
0.0124	0.93648	1450	1.05	1.435	-0.226	508	-15.9	0.101	0.0003
0.0388	0.94427	1480	1.47	1.435	-0.634	484	-34.0	0.372	0.0008
0.0678	0.95124	1510	1.97	1.434	-0.985	461	-50.0	0.710	0.0014
0.0996	0.95720	1539	2.47	1.434	-1.255	442	-63.5	1.031	0.0019
0.1348	0.96216	1573	2.96	1.433	-1.431	421	-77.1	1.324	0.0022
0.1538	0.96425	1574	3.22	1.433	-1.480	419	-84.0	1.477	0.0024
0.1951	0.96764	1623	3.74	1.432	-1.482	393	-92.4	1.765	0.0026
0.2666	0.97080	1677	4.48	1.429	-1.221	366	-104	2.104	0.0022
0.3529	0.97191	1720	5.15	1.426	-0.588	347	-104	2.290	0.0016
0.4589	0.97187	1755	5.73	1.422	0.387	334	-95.8	2.276	0.0002
0.5925	0.97236	1771	6.20	1.416	1.511	328	-73.6	2.000	-0.0018
0.7026	0.97458	1764	6.37	1.411	2.022	330	-48.4	1.548	-0.0029
0.8358	0.98016	1766	6.42	1.407	1.824	327	-22.7	0.851	-0.0030

1.0000	0.99170	1788	6.49	1.405	0.000	315	0.0	0.000	0.0000

T = 35 °C

0.0000	0.92761	1408	0.83	1.433	0.000	544	0.0	0.000	0.0000
0.0124	0.93185	1422	0.97	1.433	-0.220	530	-10.6	0.072	0.0002
0.0388	0.93975	1447	1.38	1.432	-0.626	508	-26.7	0.338	0.0008
0.0678	0.94677	1476	1.81	1.432	-0.967	485	-43.3	0.610	0.0012
0.0996	0.95280	1504	2.25	1.432	-1.227	464	-57.1	0.876	0.0017
0.1348	0.95787	1537	2.70	1.431	-1.395	442	-71.2	1.134	0.0020
0.1538	0.95997	1536	2.96	1.430	-1.434	442	-77.2	1.290	0.0021
0.1951	0.96341	1585	3.48	1.430	-1.418	413	-86.7	1.585	0.0022
0.2666	0.96665	1634	4.21	1.427	-1.121	387	-96.8	1.924	0.0019
0.3529	0.96784	1680	4.90	1.424	-0.444	366	-98.9	2.143	0.0010
0.4589	0.96783	1713	5.48	1.419	0.597	352	-89.3	2.144	-0.0003
0.5925	0.96845	1728	5.97	1.413	1.782	346	-65.6	1.905	-0.0021
0.7026	0.97087	1726	6.14	1.409	2.313	346	-41.0	1.474	-0.0031
0.8358	0.97696	1735	6.19	1.405	2.061	340	-16.5	0.796	-0.0032
1.0000	0.98962	1777	6.29	1.403	0.000	320	0.0	0.000	0.0000

T = 40 °C

0.0000	0.92298	1388	0.77	1.431	0.000	562	0.0	0.000	0.0000
0.0124	0.92711	1396	0.90	1.431	-0.203	553	-6.1	0.063	0.0002
0.0388	0.93487	1417	1.23	1.431	-0.581	533	-20.4	0.252	0.0007
0.0678	0.94182	1444	1.64	1.431	-0.898	510	-36.6	0.506	0.0012
0.0996	0.94785	1472	2.06	1.43	-1.139	487	-51.6	0.756	0.0016
0.1348	0.95296	1500	2.49	1.429	-1.290	467	-63.5	0.997	0.0018
0.1538	0.95513	1500	2.71	1.429	-1.324	466	-70.3	1.116	0.0019
0.1951	0.95873	1547	3.21	1.428	-1.302	436	-80.1	1.394	0.0019
0.2666	0.96225	1593	3.94	1.425	-0.996	409	-89.5	1.741	0.0016
0.3529	0.96377	1637	4.62	1.422	-0.314	387	-91.4	1.958	0.0007
0.4589	0.96401	1673	5.21	1.417	0.748	371	-82.7	1.980	-0.0010
0.5925	0.96518	1689	5.73	1.411	1.992	363	-58.1	1.784	-0.0028
0.7026	0.96716	1693	5.93	1.407	2.575	360	-34.4	1.394	-0.0037
0.8358	0.97350	1712	5.99	1.403	2.326	351	-12.8	0.740	-0.0034
1.0000	0.98737	1767	6.13	1.401	0.000	324	0.0	0.000	0.0000

Table 4.9A: Estimated Parameters of Redlich-Kister equation and standard deviation, (σ) for the systems of ammonium-based ILs with DMA at different temperatures.

Y	Systems	T (°C)	a_0	a_1	a_2	σ
V^E(cm^3. mol^{-1})	[TEAH] + DMA					
		25	-14.5902	0.2926	-2.1341	0.003
		30	-14.1193	-0.2876	-0.8690	0.002
		35	-13.849	-0.7207	1.9632	0.002
		40	-13.0551	-0.9145	2.3459	0.003
	[TPAH] + DMA	25	-3.717	11.3412	0.6426	0.002
		30	-3.2822	10.7692	1.8855	0.009
		35	-2.6006	10.5859	2.948	0.004
		40	-1.8828	10.1673	2.7678	0.005
	[TBAH] + DMA	25	2.4983	17.3687	-6.0613	0.003
		30	3.0702	17.9928	-4.1395	0.001
		35	3.9582	19.0154	-3.7149	0.005
		40	4.6265	19.8434	-2.1572	0.005
$\Delta\kappa_s$ (T Pa^{-1})	[TEAH] + DMA					
		25	-376.1649	202.3266	-319.4164	12.18
		30	-404.4534	146.1273	-47.2009	1.54
		35	-357.9242	145.6645	-93.6677	4.68
		40	-360.209	102.18	28.0487	1.31
	[TPAH] + DMA	25	-383.6351	266.6995	-212.2782	6.75
		30	-371.0946	257.8039	-141.267	5.16
		35	-373.641	237.4609	-26.1842	1.76
		40	-359.9592	228.5177	6.7589	0.82
	[TBAH] + DMA	25	-297.2869	358.4178	-495.0387	12.52
		30	-281.1794	340.3383	-408.5993	11.06
		35	-308.4402	342.1789	-136.1855	3.22
		40	-323.661	328.0813	76.2608	3.29
$\Delta\eta$ (mPa. s)	[TEAH] + DMA					
		25	3.1542	-4.5355	2.8857	0.12
		30	3.0507	-4.0877	2.0674	0.10
		35	3.4894	-3.3032	-0.827	0.02
		40	3.1359	-3.0448	-0.6908	0.02
	[TPAH] + DMA	25	5.1464	-4.18	0.0972	0.01
		30	4.88	-3.9032	-0.8645	0.02
		35	4.6876	-3.4393	-2.0951	0 .05
		40	4.1975	-3.1025	-1.8661	0.04

	[TBAH] + DMA	25	9.7654	-4.2248	-0.9426	0.04
		30	9.6127	-3.773	-3.2077	0.10
		35	9.131	-3.1142	-3.9979	0.09
		40	8.4875	-2.4647	-4.3327	0.08
Δn_D	[TEAH] + DMA					
		25	0.0599	-0.0153	0.0107	0.0004
		30	0.0598	-0.0126	-0.0022	0.0003
		35	0.0551	-0.0138	-0.0051	0.0002
		40	0.0506	-0.0125	0.0011	0.0001
	[TPAH] + DMA	25	0.0019	-0.0478	0.0131	0.0004
		30	0.0018	-0.0461	0.0052	0.0002
		35	0.0023	-0.043	-0.0048	0.0001
		40	0.0029	-0.0427	-0.0172	0.0004
	[TBAH] + DMA	25	-0.0015	-0.0302	0.0031	0.0001
		30	-0.0004	-0.0295	-0.0067	0.0002
		35	-0.0021	-0.0288	-0.0061	0.0002
		40	-0.0052	-0.0291	-0.0024	0.0001